THE SPECTRUM OF HIV RELATED NEPHROPATHY IN KWAZULU-NATAL: A PATHOGENETIC APPRAISAL AND IMPACT OF HAART

By

DURAN RAMSURAN

Submitted in partial fulfilment of the requirements for the degree of

DOCTOR OF PHILOSOPHY

in the

Optics and Imaging Centre,

Doris Duke Medical Research Institute,

College of Health Sciences

University of KwaZulu-Natal

Durban

2012

PREFACE

This study represents original work by the author and has not been submitted in any other form to another University. Where use was made of the work of others, it has been duly acknowledged in the text.

The research described in this thesis was carried out in the Optics & Imaging Centre, Nelson R Mandela School of Medicine, University of KwaZulu-Natal, Durban, South Africa under the supervision of Professors T. Naicker and R. Bhimma.

_____
Duran Ramsuran
(Candidate)

_____
Professor Thajasvarie Naicker
(Supervisor)

_____
Professor Rajendra Bhimma
(Co-supervisor)

DECLARATION

I, **Duran Ramsuran** declare that:

(i) The research reported in this dissertation, except where otherwise indicated is my original work.

(ii) This dissertation has not been submitted for any degree or examination at any other university.

(iii) This dissertation does not contain other person's data, pictures, graphs or other information, unless specifically acknowledged as being sourced from other persons.

(iv) This dissertation does not contain other persons writing, unless specifically acknowledged as being sourced from other researchers. Where other sources have been quoted, then:

   a) Their words have been rewritten but the general information attributed them has been referenced.

   b) Where their exact words have been used their writing had been placed inside quotation marks and referenced.

(v) Where I have reproduced a publication of which I am an author, co-author, I have indicated in detail which part of the publication was actually written by myself alone and have fully referenced such publications.

(vi) This dissertation does not contain text, graphics, or tables copied and pasted from the internet, unless specifically acknowledged and the source being detailed in the dissertation and the reference sections.

Signed:_____ Date:_____

DEDICATION

To

My Parents

(Mr and Mrs Ramsuran)

PEER REVIEW PUBLICATIONS AND CONFERENCES PRESENTATIONS

PEER REVIEW JOURNAL ARTICLES:

1. **Ramsuran D**, Bhimma R, Ramdial PK, Naicker E, Adhikari M, Deonarain J, Sing Y and Naicker T (2011). The Spectrum of HIV related nephropathy in children. *Ped Neph*. Manuscript ID pedneph-11-07-0408. (Addendum I)

2. **Ramsuran D**, Naicker T, Dauth T and Moodley J (2012). The role of podocytes in the early detection of pre-eclampsia. *Pregnancy Hypertension- An International Journal of Women's Cardiovascular Health*. 2:(43-47). (Addendum II)

3. Naicker T, **Ramsuran D**, Dauth T and Moodley J (2011). Podocyturia in the early detection of preeclampsia. *Placenta.* 32:9(A89). ISSN 0143-4004. (Addendum III)

JOURNAL ARTICLE HAVE BEEN SUBMITTED: (AWAITING RESPONSE)

1. Naicker T, Dorsamy E, **Ramsuran D**, Burton GJ and Moodley J (2011). The role of apoptosis versus proliferation on trophoblast cell invasion in the placental bed of normotensive and hypertensive pregnancies. Submitted to *Hypertension in Pregnancy*. Manuscript ID LHIP-2011-0054

PEER-REVIEWED CONFERENCE PRESENTATIONS:

1. **Ramsuran D**, Ramdial PK, Bhimma R, Adhikari M and Naicker T (2010). Ultrastructural renal phenotype in paediatric HIV related nephropathy. *48th Annual Conference of the Microscopy Society of Southern Africa (MSSA).* 40:4. ISSN 0250-0418: ISBN 0-620-35056-3

2. **Ramsuran D**, Naicker T, Dauth T, and Moodley J (2010). The role of podocytes in the early detection of pre-eclampsia. *48th Annual Conference of the Microscopy Society of Southern Africa (MSSA).* 40:14. ISSN 0250-0418: ISBN 0-620-35056-3

INTERNATIONAL CONFERENCE PRESENTATIONS:

1. **Ramsuran D**, Bhimma R, Adhikari M, Naicker E, Ramdial PK and Naicker T (2011). Paediatric HIV related nephropathy in KwaZulu-Natal. *31st Annual Conference of Indian Society of Nephrology,* Southern Chapter, Thrissur, India.

2. **Ramsuran D**, Bhimma R, Adhikari M, Naicker E, Ramdial PK and Naicker T (2011). Ultrastructural renal phenotype response in paediatrics in HIV related nephropathy. *31st Annual Conference of Indian Society of Nephrology,* Southern Chapter, Thrissur, India.

3. Naicker T, **Ramsuran D**, Dauth T, and Moodley J (2011). The role of podocytes in the early detection of pre-eclampsia. *31st Annual Conference of Indian Society of Nephrology,* Southern Chapter, Thrissur, India.

4. **Ramsuran D**, Ramdial PK, Bhimma R, Naicker T, Naicker E and Adhikari M (2010). The spectrum of HIV related nephropathy in KwaZulu-Natal, South Africa. *30th Annual Conference of Indian Society of Nephrology*, Southern Chapter, Pondicherry, India.

5. Bhimma R, **Ramsuran D**, Ramdial PK, Naicker T, Naicker E and Adhikari M (2010). HIV Nephropathy in Children in KwaZulu-Natal, South Africa. 15th *Congress of the International Pediatric Nephrology Association.* New York, United States of America (abstract no. O-54).

6. Naicker T, **Ramsuran D**, Bhimma R, Ramdial PK, Winkler C, Ndungu T, Archary M and Adhikari M (2009). HIV related nephropathy. *14th American Society of Nephrology Renal Week*, San Diego, California.

NATIONAL CONFERENCE PRESENTATIONS:

1. **Ramsuran D**, Naicker T, Dauth T and Moodley J (2011). Best method for the detection of podocyturia. *College of Health Sciences Research Symposium 2011*. Nelson R Mandela School of Medicine, UKZN.

2. **Ramsuran D**, Ramdial PK, Bhimma R, Adhikari M, Deonarain J, Sing Y and Naicker T (2010). HIV-related nephropathy in KwaZulu-Natal: is the kidney a reservoir for HIV? *College of Health Sciences Research Symposium 2010.* Nelson R Mandela School of Medicine, UKZN.

ACKNOWLEDGEMENTS

Optics and Imaging Centre, DDMRI, Nelson R Mandela School of Medicine, where the work was carried out;

My parents for always being there for me, your love, encouragement and understanding are immensely appreciated, thank you for believing in me, and for all the sacrifices that you have made over the years so I could get to this point in my life;

My family members, especially my brothers Nedon and Veron for helping me reach this point; I could not have done it without your support, with a special thank you to my sister-in-laws. To my nephew Sarvesh, and niece Nāradi, may this be your inspiration;

Finally, to Shree Krishna for making this possible.

"No child should be born with HIV; no child should be an orphan because of HIV; no child should die due to lack of access to treatment"
Ebube Sylvia Taylor, 2010 United Nations Millennium Development Goals Summit

TABLE OF CONTENTS

LIST OF ABBREVIATIONS

HIV	:	Human Immunodeficiency Virus
HIVRN	:	Human Immunodeficiency Virus Related Nephropathy
HIVAN	:	Human Immunodeficiency Virus Associated Nephropathy
AIDS	:	Acquired Immuno Deficiency Syndrome
HAART	:	Highly Active Antiretroviral Therapy
ESRD	:	End Stage Renal Disease
FSGS	:	Focal Segmental Glomerular Sclerosis
PBMC	:	Peripheral Blood Mononuclear Cell
ACE-I	:	Angiotensin Converting Enzyme Inhibitor
DNA	:	Deoxyribonucleic Acid
RNA	:	Ribonucleic Acid
PCR	:	Polymerase Chain Reaction
CG	:	Collapsing Glomerulopathies
WHO	:	World Health Organization
G	:	Grams
ml	:	Millilitre
ng	:	Nanograms
mg	:	Millgram
Kg	:	Kilogram
µl	:	Microlitre
µm	:	Micron
Kb	:	Kilo basepair
h	:	Hour
Min	:	Minute
CD	:	Cluster of differentiation
°C	:	Degrees Celsius
%	:	Percentage
bp	:	basepair
IALCH	:	Inkosi Albert Luthuli Central Hospital
EM	:	Electron microscopy
IMF	:	Immunofluorescence
LMD	:	Laser Micro-dissection

NIH	:	National Institutes of Health
TBS	:	Tris-buffered saline
PBS	:	Phosphate buffer saline
GBM	:	Glomerular basement membrane
Sec	:	Second
CDK	:	cyclin-dependent kinase
CKIs	:	cyclin-dependent kinase inhibitors
HIVICK	:	HIV Immune complex disease
TEMP	:	Temperature
Viz	:	Namely
Init	:	Initial
Mag	:	Magnification
IgG	:	Immunoglobulin G
L	:	Litres
USA	:	United States of America
RT-PCR	:	Real Time Polymerase Chain Reaction
ER	:	endoplasmic reticulum
FP	:	Foot processes
env	:	Envelope
H_2O	:	Water
dH_2O	:	Distilled water
H&E	:	Haematoxylin & Eosin
Pas	:	Periodic acid-Schiff
gp	:	glycoproteins
MCD	:	Minimal change disease
FITC	:	Fluorescein isothiocyanate
APOL1	:	Apolipoprotein L1
DARC	:	Duffy antigen chemokine receptor
eGFR	:	Estimated Glomerular Filtration Rate

LIST OF FIGURES

LIST OF TABLES

ABSTRACT

Sub-Saharan Africa bears 70% of the global HIV burden with KwaZulu-Natal (KZN) identified as the epicenter of this pandemic. HIV related nephropathy (HIVRN) exceeds any other causes of kidney diseases responsible for end stage renal disease, and has been increasingly recognized as a significant cause of morbidity and mortality. There is nonetheless a general lack of surveillance and reporting for HIVRN exists in this geographical region. Consequentially, the aim of this study was to outline the histopathogical spectrum of HIVRN within KZN. Moreover, from a pathology standpoint, it is important to address whether HIVRN was a direct consequence of viral infection of the renal parenchyma or is it a secondary consequence of systemic infection. Additionally, an evaluation of the efficacy of Highly Active Anti-Retroviral Therapy (HAART) in combination with angiotensin converting enzyme inhibitors (ACE-I) was performed *via* a genetic appraisal of localized replication of HIV-1 in the kidney, ultrastructural review and immunocytochemical expression of a podocyte maturity and proliferation marker pre and post-HAART.

Blood and renal biopsies were obtained from 30 children with HIV related nephropathy pre-HAART, followed-up clinically for a period of 1 year. This cohort formed the post-HAART group. Clinical and demographic data were collated and histopathology, RT-PCR, sequencing, immunocytochemistry and transmission electron microscopy was performed.

The commonest histopathological form of HIVRN in children (n = 30) in KZN was classical focal segmental glomerular sclerosis (FSGS) presented in 13(43.33%); mesangial hypercellularity 10(30%); mesangial, HIV associated nephropathy 3(11%) and minimal change disease 2(6.67%). Post-HAART (n = 9) the predominant pathology was mesangial hypercellularity 5(55.56%); FSGS 3(33.33%) and sclerosing glomerulopathy 1(11.11%). This study also provides data on the efficacy of HAART combined with ACE-I. The immunostaining pattern of synaptopodin, Ki67 and p24 within the glomerulus expressed as a mean field area percentage was significantly down-regulated in the pre-HAART compared to the post-HAART group respectively (1.14 *vs.* 4.47%, p

= 0.0068; 1.01 *vs.*4.68, $p < 0.001$; 4.5% *vs* 1.4%, $p = 0.0035$). The ultrastructural assessment of all biopsies conformed to their pathological appraisal however, features consistent with viral insult were observed. Latent HIV reservoirs were observed within the podocyte cytoplasm but was absent in mesangial or endothelial cells. Real-Time polymerase chain reaction assays provided evidence of HIV-1 within the kidney. Sequence analysis of the C2-C5 region of HIV-1 *env* revealed viral diversity between renal tissue to blood.

In contrast to a collapsing type of FSGS that occurs in adults, the spectrum of paediatric nephropathy in treatment-naive children within KwaZulu-Natal was FSGS with mesangial hypercellularity. Additionally, our study demonstrates podocyte phenotype dysregulation pre-HAART and reconstitution post therapy. Evidence of ultrastructural viral reservoirs within epithelial cells is supported by a genetic appraisal confirming the ubiquitous presence of HIV DNA in renal tissue. Moreover, sequence analysis showed viral evolution and compartmentalization between renal viral reservoirs to blood. Finally, the interplay of viral genes and host response, influenced by genetic background, may contribute to the variable manifestations of HIV-1 infection in the kidney in our paediatric population.

CHAPTER 1

INTRODUCTION

1.1 HIV

The global spread of human immunodeficiency virus (HIV) over the past four decades represents one of the most catastrophic paradigms of the emergence, transmission, and dissemination of a viral genome (Fassin and Schneider, 2003). HIV is a *Retrovirus* that leads to acquired immunodeficiency syndrome (AIDS), a condition in humans in which the immune system begins to fail, leading to life-threatening opportunistic infections (Duesburg, 1988). HIV is transmissible via almost all body fluid including blood, semen, pre-ejaculate, vaginal fluid, or breast milk and can occur as a free virus and/or cell-associated virus (Bhimma, 2007; Osho and Olayinka, 1999).

1.1.1 Epidemiology

The World Health Organization (WHO) estimates that AIDS has killed more than 25 million people since it was first recognized on December 1, 1981 (Kharsany and Karim, 2011). By the end of 2010, globally an estimated 34.0 million (range: 31.6 million–35.2 million) people were living with HIV, with 2.6 million (range: 2.3 million–2.8 million) new HIV infections and 1.8 million (range: 1.6 million–2.1 million) deaths.

Sub-Saharan Africa is home to approximately 10% of the world's population, yet bears a disproportionate burden of the disease, accounting for 70% of the global HIV infections (Figure 1.1); (UNAIDS, 2011). While there has been a decline in the number of new HIV infections, HIV incidence and mortality rates remain unacceptably high, with more than 75% of global AIDS related deaths occurring in this region. Provincial HIV estimates show geographic variations of the epidemic in South Africa whilst highlighting the fact that KwaZulu-Natal represents the highest burden of this infection (UNAIDS, 2011).

According to current estimates, HIV is set to infect 90 million people in Africa, resulting in a minimum estimate of 18 million orphans (UNAIDS, 2011). Antiretroviral treatment reduces both the mortality and morbidity of HIV infection, but routine access to antiretroviral medication is not available in many countries within Africa (Okera *et al*., 2003).

At the end of 2010, a global estimate of 3.4 million [3 000 000–3 800 000] children less than 15 years were living with HIV of which 390 000 [340 000–450 000] represented new infections. AIDS-related causes claimed an estimated 250000 lives of children under 15 years in the same year (Figure 1.2); (UNAIDS, 2011).
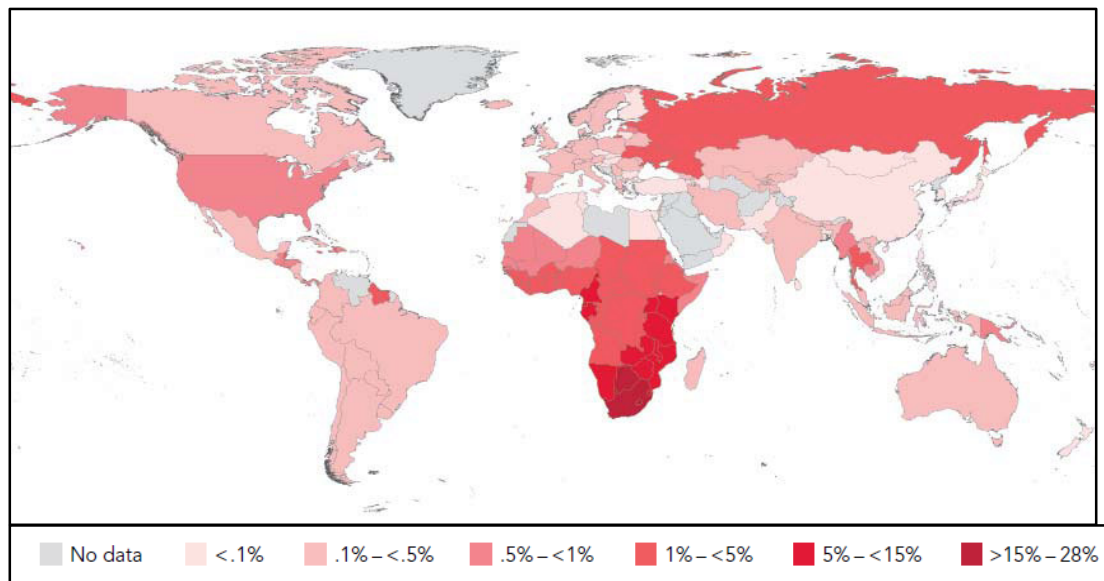
Figure 1.1: World map illustrating intensity of HIV infection. Key indicates severity/percentage of burden (UNAIDS, 2010).
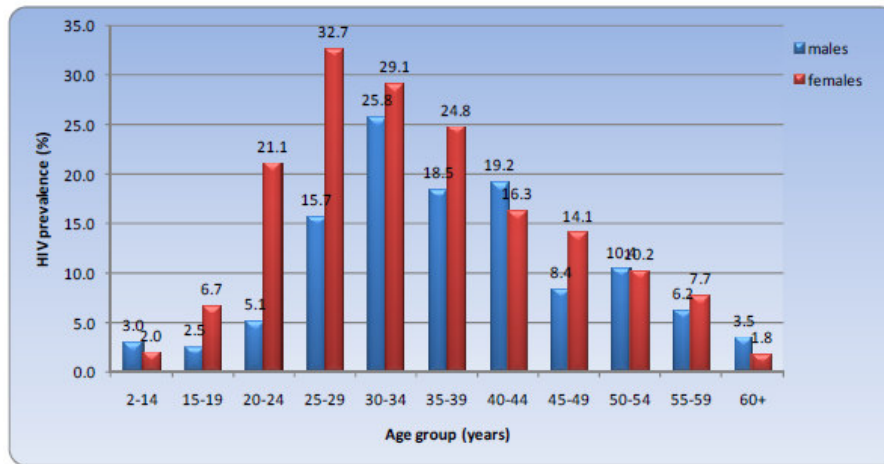
Figure 1.2: Histogram showing estimated HIV prevalence among South Africans, by age and sex (UNAIDS, 2010).

1.1.2 HIV morphology

AIDS was first recognized by Montagnier and Gallo in the early 1980's. AIDS is caused by the human immunodeficiency virus (Kumar *et al*., 2001). This is an enveloped virus (Sun and Wirtz, 2006); the envelope being derived from the host cell membrane as the virus leaves the cell. Inserted into this surface membrane are two glycoproteins - gp120 and gp41. The viral core is composed of a capsid protein (p24) and a matrix protein (p17) that helps maintain viral structure (Chrystie and Almeida, 1988). Within the core are two identical copies of single stranded RNA viral genome and three enzymes, reverse transcriptase, protease and integrase (Figure 1.3); (Gelderblom, 1991).
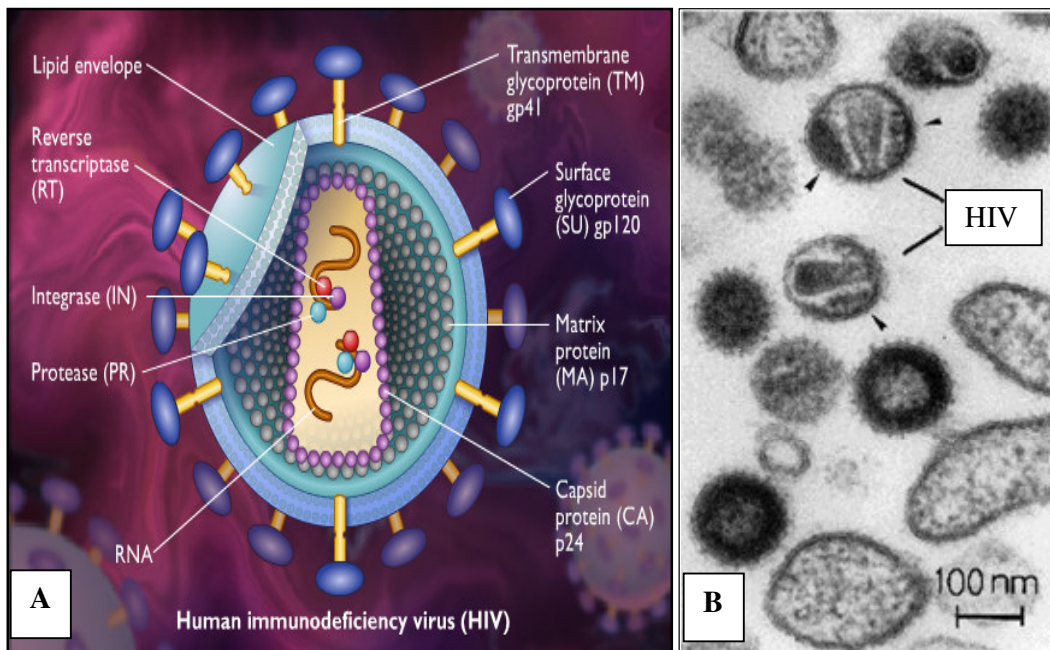
Figure 1.3: **(A).** Schematic diagram of the anatomy of the Human immunodeficiency virus (McGraw, 2008); **(B)** Electronmicrograph of HIV particles using positive contrast enhancement (Gelderblom, 1991).

1.1.3 HIV Replication

To establish infection, HIV must first attach to its host cell (Figure 1.4 - Step 1). Attachment occurs by interaction between gp120 on the surface of the virus and the cluster of differentiation (CD) 4 antigen receptor on the surface of the host cell (Grimwood *et al.*, 1996; Lapham *et al.*, 1996). In addition to the CD4^{+} T cell receptor, there must also be a co-receptor on the host cell (Steffens and Hope, 2004). The co-receptor differs for different host cell types (Doms and Moore, 2000). After attachment, the viral envelope and host cell membrane fuse, resulting in entry of the virus into the cell (Figure 1.4 - Step 2); (Simm *et al*., 1996). Once the RNA is released into the cytoplasm of the host cell, reverse transcriptase makes a DNA copy of the viral RNA genome (Figure 1.4 - Step 3); (Bushman, 2004). As the DNA is being formed, reverse transcriptase degrades the RNA strand (Ichiyama and Yamamoto, 2002). A complementary DNA strand is then added by the reverse transcriptase and the end of the resulting double-stranded DNA segment are joined non-covalently (Pandit and Li, 2004; Trkola *et al.*, 1996). Treatment with

nucleoside analogs or reverse transcriptase inhibitors interferes with these steps (Chan *et al.*, 1998). The resulting circular DNA is then transferred to the nucleus and inserted into the host cell chromosome by the viral integrase enzyme (Figure 1.4 – Step 4); (Heuer and Brown, 1997). The integrated viral DNA is now referred to as proviral DNA (Huang *et al.*, 2006; Stebbing *et al.*, 2004). Following integration, the proviral DNA may remain dormant or, with host cell activation, RNA may be synthesized from the DNA, yielding messenger RNA and viral genome RNA (Figure 1.4 – Step 5); (Appel, 2007; Gallo *et al.*, 2003). Viral messenger RNA is translated, yielding viral enzymes and structural proteins (Nelson *et al.*, 2001). Some of the functional proteins are formed by cleavage of a long poly-protein by the enzyme, protease (Liu *et al.*, 1999). Protease inhibitors interfere with this step (Barisoni *et al.*, 1999; Reeves *et al.*, 2002). Gp41 and gp120 are inserted into the host cell membrane and the structural proteins surround the viral RNA to form the core (Figure 1.4 – Step 6); (Melikyan *et al.*, 2000). Finally, the virion is released by budding (Figure 1.4 - Step7).
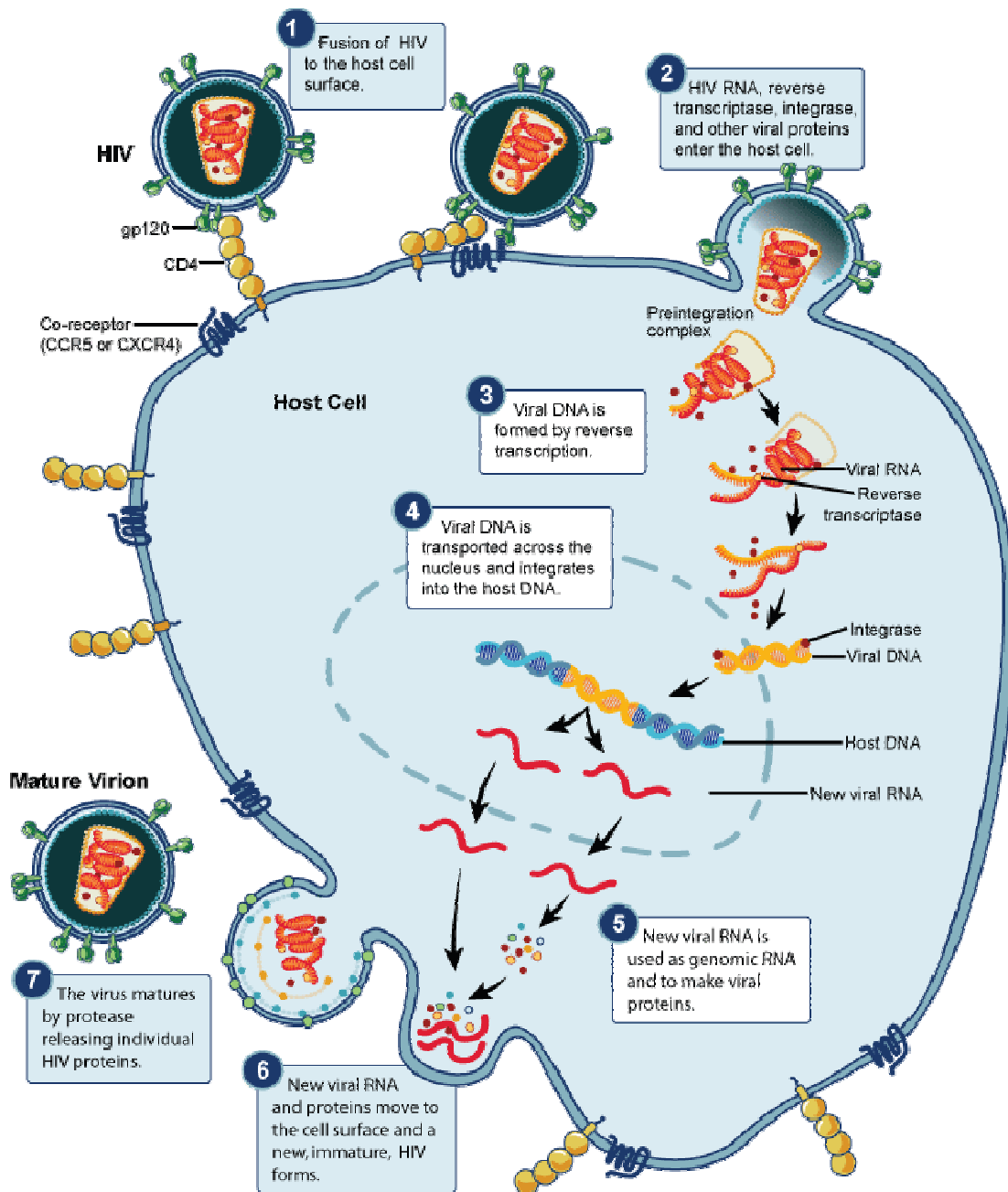
Figure 1.4: The replication cycle of a human immunodeficiency virus (NIAID, 2010). Steps 1-7 indicate viral entry, replication and budding.

1.1.4 Effect on host immune response

HIV primarily infects vital cells in the human immune system such as helper T cells, macrophage and dendritic cells (Varbanov et al., 2006). HIV infection leads to low levels of CD4$^+$ T cells through three main mechanisms: firstly, direct viral killing of infected cells; secondly, increased rates of apoptosis in infected cells; and thirdly, killing of infected CD4$^+$ T cell by CD8 cytotoxic lymphocytes that recognize infected cells (Brest et $al.$, 2004; Eggers and Kimmel, 2004; Izzedine et $al.$, 1999; Paranjape, 2005).

Two types of blood tests are routinely used to monitor HIV-infected people. One of these tests, which counts the number of CD4$^+$ T cells, assesses the status of the immune system (Connolly et $al.$, 1995; Peraldi et $al.$, 1999) whilst the other determines the viral load, by directly measuring the amount of virus in the system (Varbanov et $al.$, 2006).

In individuals not infected with HIV, the CD4$^+$ T cell count in the blood is normally above 500 cells per cubic milliliter (mm^3) of blood (Mannucci et $al.$, 1994). HIV-infected people generally not at risk for complications unless their CD4$^+$ T cell count is < 200 cells/mm^3 (Mannucci et al., 1994). A declining CD4$^+$ T cell count indicates that the HIV disease is advancing. In addition, CD4$^+$ T cell counts aid in determining the appropriate treatment according to the stage of the disease (Goldsmith et al., 1991). The viral load predicts whether or not the CD4$^+$ T cell count will decline in the coming months (Fagard et al., 2005).

When CD4$^+$ T cell numbers decline below a critical level, cell-mediated immunity is lost, and the body becomes progressively more susceptible to opportunistic infections as shown in Figure 1.5. The viral load increases over time, as the HIV virus is replicating, therefore

making the virus more abundant, and further infecting helper T cells, consequently decreasing the CD4$^+$ T cell count (Mackewicz *et al*., 2000). If untreated, eventually most HIV-infected individuals develop AIDS and die of opportunistic infection (Lal and Sengupta, 1994).
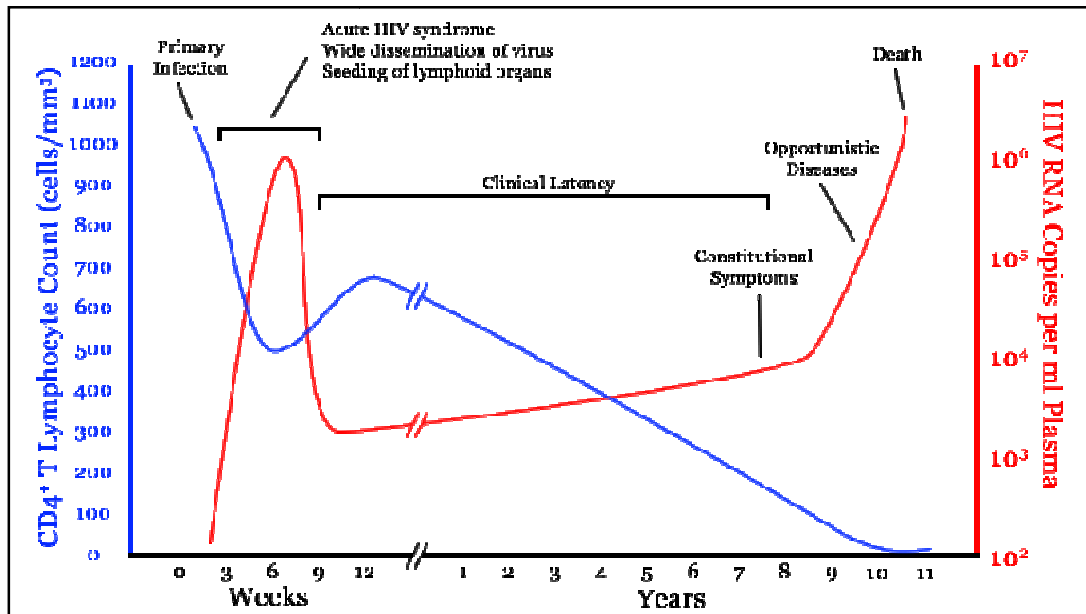
Figure 1.5: Graph illustrating the different stages, CD4$^+$ T cell and viral load over time from primary infection to death (Sigve, 2008).

1.2 NORMAL KIDNEY

1.2.1 Function

The primary role of the kidney is to maintain water and electrolyte homeostasis in the body (Kurokawa, 1993). This is achieved by filtration of blood plasma and excretion of toxic metabolic waste products in the urine (Verkman *et al.*, 1995). The kidneys regulates the osmotic concentration of the blood plasma thereby ensuring the osmotic regulation of all other body fluids (Dorup, 1990).

1.2.2 Normal morphology

The urinary system consists of two kidneys, two ureters, the urinary bladder, and a urethra. The total blood volume of the body is filtered through the kidneys about 300 times/day (Rebouche, 2004). The urine produced is conducted via the ureters to the bladder where it is temporally stored prior to being voided to the outside *via* the urethra (Trump, 1970).

1.2.3 Nephron

The nephron, the functional unit of the kidney selectively filters molecules from blood plasma to form a filtrate (Figure 1.6); (Zuo *et al.*, 2006). It is also involved in the selective re-absorption of water and other essential molecules from the filtrate, thereby leaving behind excess and waste material to be excreted as urine (Hayashi, 1998; Verkman *et al.*, 1995). The nephron is composed of two important components, renal tubule and renal corpuscle, each with very specific functions (Burkitt *et al.*, 1993).
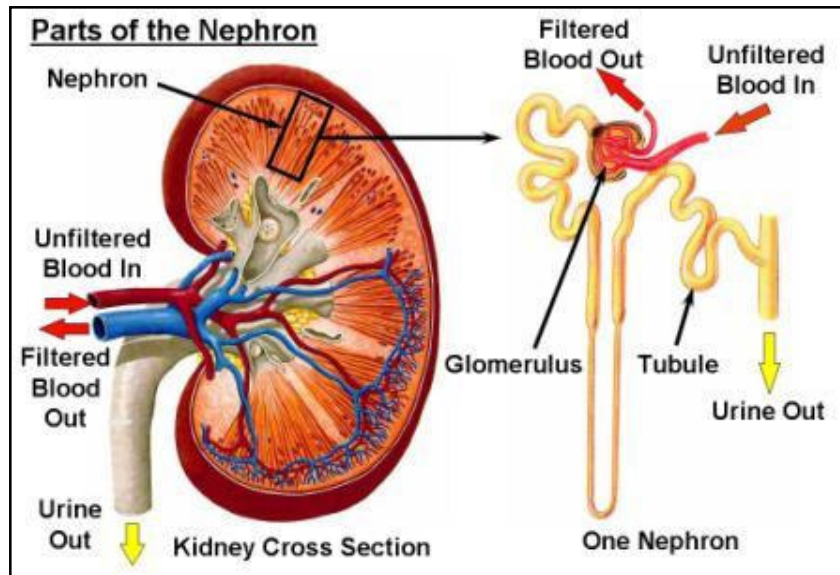
Figure 1.6: Schematic diagram of cross section of kidney linking structure to function. Direction of blood flow and filtration in the nephron is amplified (Falk, 2008).

1.2.3.1 Renal tubule

The primary function of the renal tubule is ultrafiltration and selective re-absorption of water and inorganic ions from the glomerular filtrate (Berglund and Lotspeich, 1956; Verkman *et al.*, 1995). The renal tubule has a convoluted shape divided into four distinct histo-physiological regions (Morel, 1999) *viz.*,

a. proximal convoluted tubule - is lined by tall cuboidal epithelial cells with a brush border that is compliant with it role of re-absorption of approximately 75% of sugar, sodium and chloride ions, and water from the glomerular filtrate (Baum and Quigley, 1998; Matsuo *et al.*, 1986).

b. loop of Henle - is a hairpin bend lined by stratified squamous epithelium whose main purpose is re-absorption of water and ions achieved by the counter current multiplier system (Hogg and Kokko, 1979; Wareing and Green, 1994).

c. distal convoluted tubule - is lined with simple cuboidal cells and is responsible for the active regulation of potassium, sodium, calcium, and pH (Maurer *et al.*, 2004; Urreizti *et al.*, 2007).

11

d. Collecting tubules - exit into the pelvicalyceal system and serve to concentrate urine by passive re-absorption of water into the medullary interstitium following the osmotic gradient created by the loops of Henle (Imai *et al.*, 1987; Sands, 2003; Tenstad *et al.*, 2001).

1.2.3.2 Renal corpuscle

The renal corpuscle functions as the initial filtering component for the plasma (Lacy *et al.*, 1987). It is a formed by the combination of two structures, the Bowman's capsule and the glomerulus (Ojeda *et al.*, 2003).

1.2.3.2.1 The Bowman's capsule

The Bowman's capsule is a cup-shaped structure surrounding a tuft of capillaries, the glomerulus (Boucher *et al.*, 1987). It is lined by simple squamous epithelial cells referred to as the parietal layer whilst each capillary is lined by a layer of visceral epithelial cells (Khedun *et al.*, 1997).

1.2.3.2.2 The glomerulus

Blood enters the glomerulus via the afferent arteriole, passes through the tuft of capillaries and then drains out *via* the efferent arteriole (Kosaka and Kosaka, 2005). The latter maintains a pressure gradient (Bruggeman *et al.*, 2000; Nochy *et al.*, 1993b) in the glomerulus, thereby contributing to the process of ultrafiltration where fluids and soluble materials in the blood are forced out of the capillaries and into the Bowman's space (Figure 1.7); (Honda, 1984). The rate at which blood is filtered through all of the glomeruli, and thus the measure of the overall renal function, is the glomerular filtration rate (GFR)

(Thomas and Huber, 2006). Blood is filtered *via* the filtration barrier which consists of three components *viz*:

a. Fenestrated endothelium with 50-100nm fenestrations. This luminal surface is negatively charged (Khedun *et al.*, 1997).

b. Glomerular basement membrane (340nm) is made up of three zones, lamina densa, rara interna, and externa (Vogler *et al.*, 1999). The structural meshwork of collagen and other matrix proteins of the lamina densa separates molecules on their basis of size and shape whilst the lamina rara externa and interna repels negatively charged molecules (Bertolatus, 1990; Brenner *et al.*, 1978).

c. Podocyte layer – discussed in 3.2.1.
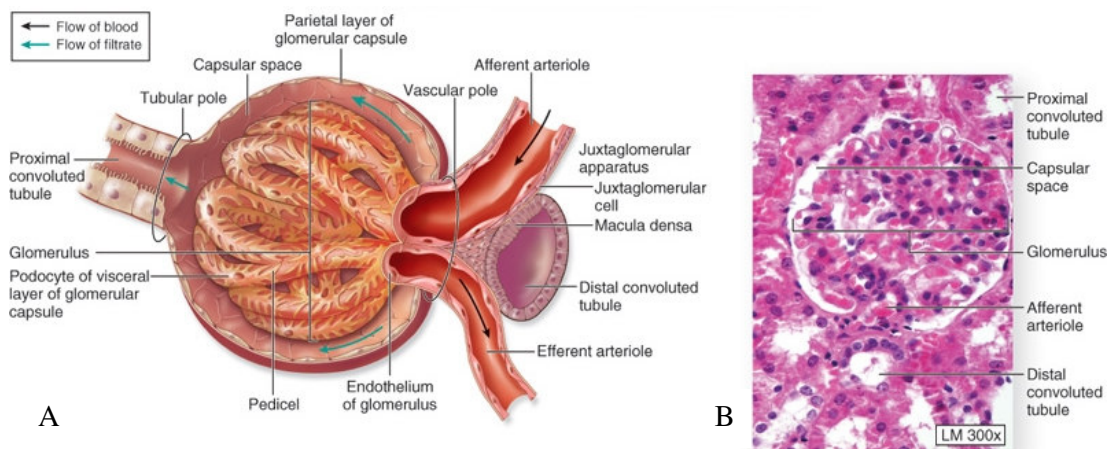
Figure 1.7: (A). Schematic Cross section of glomerulus, showing the flow of blood and filtrate. **(B)**. H&E stained section depicting normal glomeruli and tubules Adapted from McGraw-Hall (McGraw, 2008).

1.2.3.2.3 Podocytes

Podocytes also known as visceral epithelial cells (Hamano *et al.*, 2002; Levidiotis and Power, 2005) are highly specialized cells essential to the ultrafiltration of blood, with the subsequent extraction of urine, the retention of protein, as well as in maintaining a massive filtration surface (Khedun *et al.*, 1997; Pitts and Van Thiel, 1986; Sladen and Landry, 2000). The large cell body sends out major primary processes that further ramify into

13

secondary processes (foot processes/pedicels) (Figure 1.8); (Somlo and Mundel, 2000).

Adjacent foot processes interdigitate with each other forming a direct contact with the urinary aspect of the glomerular basement membrane (GBM) (Nochy *et al*., 1993a). The uniform gaps (25nm) between adjacent foot processes are referred to as the filtration slit (Caulfield and Farquhar, 1974). Adjacent foot processes are linked by a diaphragm (4nm) (Caulfield and Farquhar, 1974). Large macromolecules such as serum albumin and gamma globulin remain in the bloodstream. Small molecules such as water, glucose and ionic salts are able to pass through the slit diaphragms and form an ultrafiltrate (Kawachi *et al.*, 2006; Moeller and Holzman, 2006).
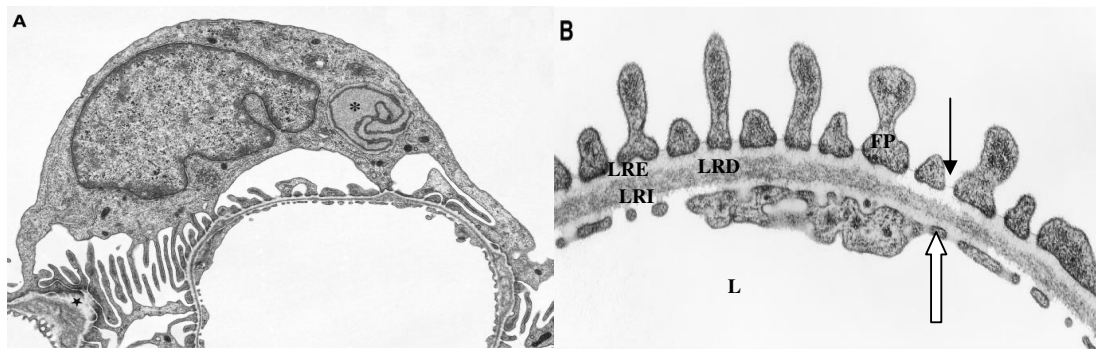
Figure 1.8: **(A)**. Low-power electron micrograph illustrating podocyte and the glomerular filtering apparatus. **(B)**. High-power electron micrograph depicting glomerular basement membrane layers *viz.*, lamina rara densa (LRD) opposed by lamina rara interna (LRI) and externa (LRE). Note foot processes (FP), slit diaphragm (arrow) and fenestrated endothelial cells (open arrow) lining the capillary loop (L).
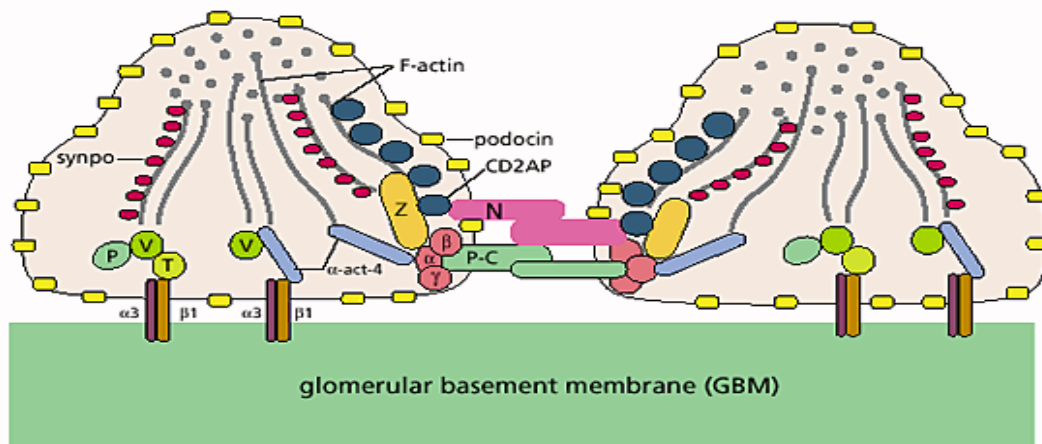
Figure 1.9: Molecular anatomy of the podocyte foot process cytoskeleton consisting of actin, myosin-II, α-actinin-4, talin, vinculin and synaptopodin that is connected to the GBM via α3β1 integrins. The actin cytoskeleton is linked to the slit diaphragm components, nephrin and P-cadherin, via CD2AP, Z complex and α-, β-, γ-catenin. Note nephrin (N); P-cadherin (P-C); α-catenin(α); β-catenin (β); γ-catenin (γ); ZO-1 (Z); 3-integrin (3); 1−integrin (1); vinculin (V); talin (T); paxillin (P); α-actinin-4 (α-act-4); synaptopodin (synpo) (Somlo and Mundel, 2000).

The function of podocytes is primarily based on its cytoarchitecture (Smoyer *et al*., 1997). The cytoskeleton of foot processes contain a dynamic highly ordered parallel contractile system comprised of actin, myosin-II, α-actinin-4, and synaptopodin that is connected to the GBM via α3β1integrins (Figure 1.9); (Somlo and Mundel, 2000). This actin filament organization of the cytoskeleton is integrated with different signal-transduction pathways from the cytosolic matrix, GBM interface, the slit diaphragm and the cell surface (Ichimura *et al.*, 2003; Lahdenkari *et al.*, 2005; Patrakka *et al.*, 2002).

Foot processes are defined by three membrane domains:

i) apical membrane domain-links the actin cytoskeleton, making it the common denominator in podocyte function and dysfunction (Kerjaschki, 2001)

ii) slit diaphragm protein complex, and

iii) basal membrane domain or sole plate (Kerjaschki, 2001).

The actin bundles are linked to the slit diaphragm complex through several scaffolding proteins such as actinin (Arias *et al*., 2009), CD2AP (Yuan *et al*., 2002), densin (Oh *et al*., 2004), nephrin (Arias *et al*., 2009), Nck (Yanagida-Asanuma *et al*., 2007) and ZO-1 (Mundel *et al.*, 1997b; Schnabel *et al.*, 1990). Disruption with any of the three foot process domains would lead to a reorganization of the parallel actin contractile bundles into an irregular network, hence a collapse of the cytoskeleton with the resultant foot process effacement and subsequent proteinuria (Faul *et al.*, 2007; Yanagida-Asanuma *et al.*, 2007).

Mutations affecting several podocyte proteins cause disruption of the filtration barrier by rearrangement of the highly dynamic podocyte actin cytoskeleton (Ramsuran *et al.*, 2011b; Tryggvason *et al.*, 2006) (Addendum II). Proteins regulating the plasticity of the podocyte actin cytoskeleton are therefore of critical importance for sustained kidney barrier function (Ramsuran *et al.*, 2011b; Tryggvason *et al.*, 2004) (Addendum II).

1.2.3.2.3.1 Synaptopodin

Synaptopodin is the founding member of a novel class of proline-rich actin-associated proteins highly expressed in telencephalic dendrites and renal podocytes (Mundel *et al*., 1991). It regulates the actin-binding activity of α-actinin in the highly dynamic cell compartments of podocytes (Mundel *et al*., 1997a). At the protein level, two isomers exist with synpo-long been expressed in the kidney, whereas synpo-short is expressed in the brain (Figure 1.10); (Asanuma *et al*., 2005).

Synaptopodin is found on chromosome 5 location 5q33.1. It has two isoforms, *viz*:

1. Isoform A- This variant represents the longer transcript consisting of 903 amino acids.

2. Isoform B- This variant uses an alternate splice site in the coding region which results in an early stop codon, compared to isoform A. The resulting protein (isoform B) has a shorter, distinct C-terminus and consists of 685 amino acids (Mundel and Reiser, 1997).
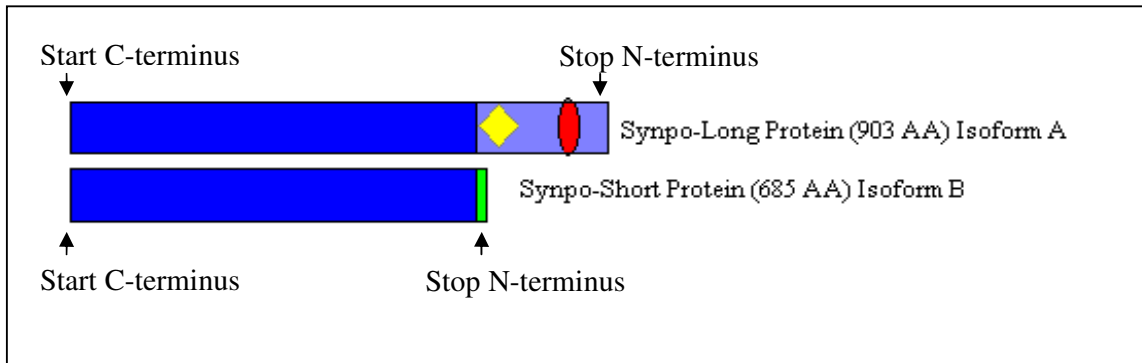
Figure 1.10: Comparison of Synpo-long and Synpo-short isoform expression. The blue box shows the first 670 AA that are shared between both isoforms; the purple box shows amino acid 671–903 corresponding to the Synpo-alt fragment of Synpo-long. Synpo-alt contains a LPPPP motif (yellow) for ENA/VASP binding and a PPRPF motif (red) for homer binding (Asanuma *et al*., 2005).

Synaptopodin is essential for the maintenance of the integrity of the actin cytoskeleton and for the regulation of podocyte cell migration (Asanuma *et al*., 2006). Cell behaviour, is mediated by the Rho family of small GTPases (RhoA, Rac1 and Cdc42). Synaptopodin, is a novel regulator of RhoA signalling and cell migration in podocytes via induction of stress fibres by competitive blocking of Smurf1-mediated ubiquitination of RhoA, thereby preventing the targeting of RhoA for proteasomal degradation (Denamur *et al*., 2000). Furthermore, gene silencing of synaptopodin in podocytes causes the loss of stress fibres and the formation of aberrant non-polarized filopodia and impairment of cell migration (Yanagida-Asanuma *et al*., 2007). Consequently, this impairment is correlated with loss of synaptopodin and ensued severity of proteinuria. Reduced expression of synaptopodin is associated with poor response to steroid therapy in glomerulosclerosis (Hirakawa *et al*., 2006).

1.3 PODOCYTE CELL CYCLE

The cell-division cycle is a series of events that takes place in a eukaryotic cell leading to its replication (Boye and Nordstrom, 2003; Nurse, 1991). It consists of four different phases *viz.*, G_1, S, G_2 and M phase (Figure 1.11); (Dewey and Humphrey, 1963). Activation of each phase is dependent on the proper progression and completion of the previous phase. Cells that have temporarily stopped dividing are said to have entered a state of quiescence called G_0 phase (Barisoni *et al.*, 2000b).
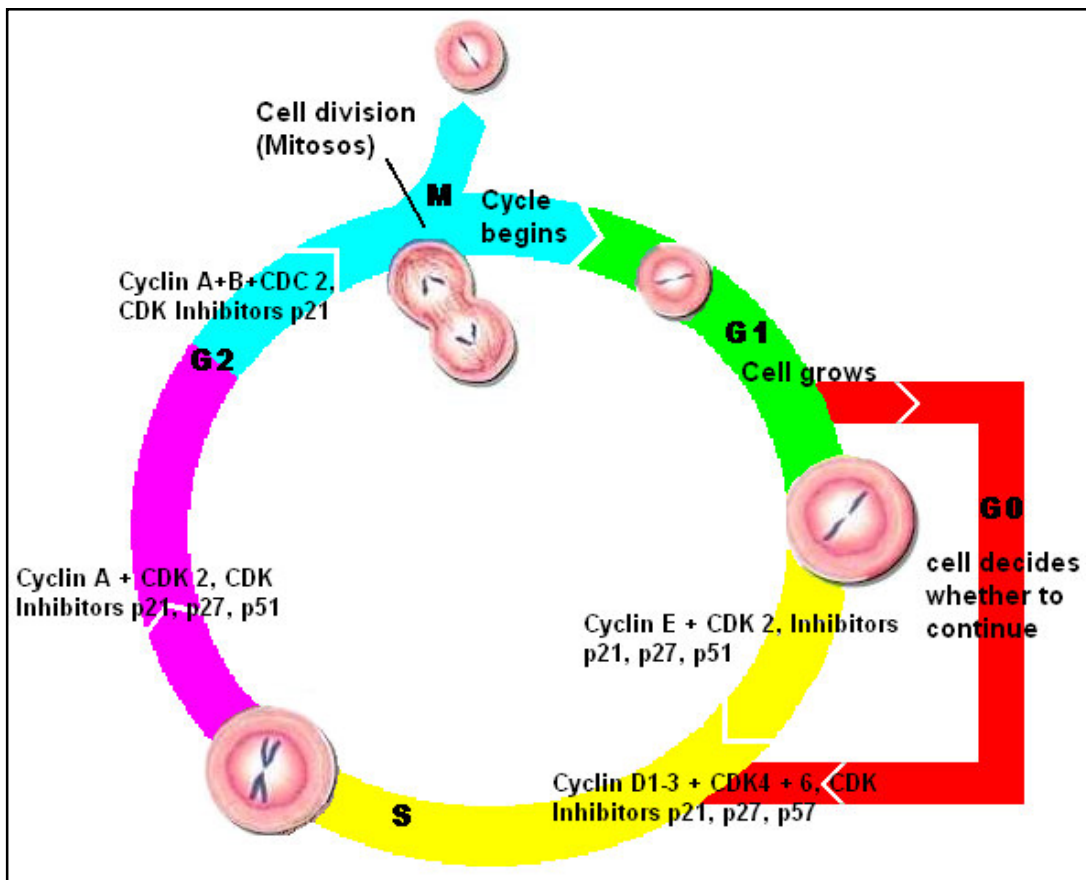
Figure 1.11: Podocyte phenotype dysregulation-a complete series of events from one cell division to the next. It is usually divided into the phase when DNA is replicated (S phase), the phase when the cell actually divides into two cells (M phase), the two intervening gap phases (G1 and G2), and a quiescence phase (G0). adapted from (David, 1999).

The cell cycle progression is regulated by cyclin and cyclin-dependent kinase (CDK) complexes (Measday *et al.*, 1994) (Figure 1.11). CDK activity is controlled by cyclin-

dependent kinase inhibitors (CKIs) (Baghdassarian and Ffrench, 1996). Each step in the cell cycle is initiated and controlled by a specific set of cyclins, CDKs, and CKIs. However, p27 and p57, can inhibit cyclin-CDK complexes (Pines, 1997). Entry into the cell cycle can have three consequences *viz.*, cell proliferation, cellular hypertrophy, and cellular apoptosis (George *et al.*, 2003).

Systematic analysis of the cell cycle regulatory molecules in podocytes have revealed a tight control of cell cycle quiescence, in sharp contrast to the proliferative capacity of the neighbouring mesangial cells (Marshall and Shankland, 2006; Ng *et al.*, 1998). Podocytes enters the cell cycle at the G_1 phase (Figure 1.11) – however their growth at this phase of the cycle is mainly due to the presences of cyclin D and E (Wang *et al.*, 2005). Mature non-proliferative podocytes enter the quiescent G_0 state from G_1 and may remain quiescent/growth-arrested expressing cyclin-dependent kinase inhibitors. These cells are terminally differentiated and express maturity markers such as synaptopodin and Wilm's tumour (Conaldi *et al.*, 2002; Saleem *et al.*, 2002).

1.3.1 Podocyte proliferation

Cell proliferation is defined as the rapid multiplication of a cell (Truong *et al.*, 1996). The Ki-67 protein located on chromosome 10q26.2 is a cellular marker for proliferation expressed in all active phases of the cell cycle (G_1, S, G_2 phase and mitosis) (Figure 1.11), but is absent from the quiescent cells (G_0) (Winking *et al.*, 2004). During interphase, the Ki-67 antigen can be exclusively detected within the cell nucleus, whereas in mitosis most of the protein is relocated to the surface of the chromosomes (Noel *et al.*, 2006; Winking *et al.*, 2004).

The ability of podocytes to proliferate depends on their state of differentiation (Barisoni *et al.*, 2000b). During glomerulogenesis, the immature podocyte precursor cells originate from the metanephric mesenchyme which undergoes marked proliferation. However, as podocytes mature they exit the cell cycle stop proliferating and becomes terminally differentiated thereby acquiring a phenotype that is quiescent (Barisoni *et al.*, 2000b; Saleem *et al.*, 2002). Normal terminally differentiated podocytes express regulatory proteins (CKI p27, p57 and Cyclin D1), indicating that they have entered the cell cycle, completed the DNA synthesis in S phase, and are ready for G2 phase in the cell cycle.

1.4 GLOMERULAR DISORDERS

Glomerular disorders is termed "Nephropathy" which originates form the Greek word "nephros" meaning kidney and "patho" meaning disease (Takata *et al.*, 2000). Therefore, the name nephropathy refers to any damage or disease of the kidney (Hiura *et al.*, 2006).

Histological evidence supports genetic data indicating podocyte dysfunction in glomerular disease (Naicker *et al.*, 2006). An early event is the loss of integrity of foot processes and the slit diaphragm, leading to foot-process fusion, altering the filtration barrier with resultant protein in the urine (proteinuria) and blood in the urine (haematuria) (Figure 1.12; (Bhimma *et al.*, 2008; Lai *et al.*, 2007; Tapia *et al.*, 2008). Alternatively, foot process effacement may be a result of dysfunction of one of the molecular players in the signal-transduction pathway (Kawachi *et al.*, 2006). If these early structural changes are not reversed it, ultimately leads to the development of glomerulosclerosis and to end stage renal disease (ESRD) (Jarad *et al.*, 2006).
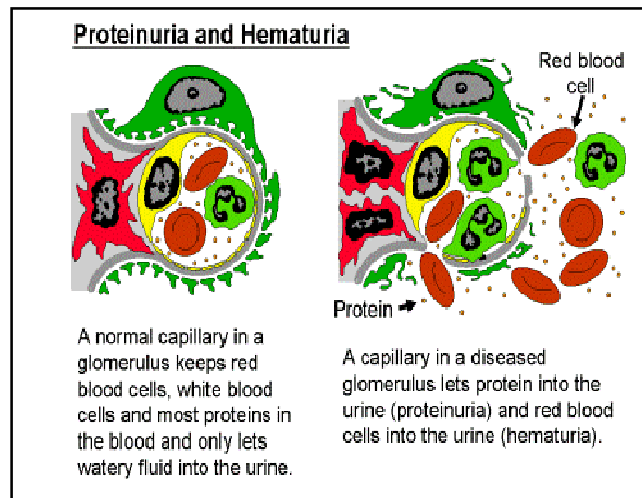
Figure 1.12: A schematic representation of a typical functioning glomeruli versus a diseased glomeruli presentation with proteinuria and hematuria (Falk, 2008).

1.4.1 Spectrum of glomerular disorders

The histopathological spectrum of glomerular disorders that can cause nephrotic syndrome are highlighted below:

1.4.1.1 Minimal Change

Minimal change disease (MCD) is characterised by foot process effacement (Figure 1.13) and loss of the normal charge barrier such that albumin leaks out and proteinuria ensues (Han *et al*., 2006b). The glomerulus appears normal under the light microscope (Moeller and Holzman, 2006). Most cases of MCD are idiopathic, whilst secondary sources of aetiology may be drugs, cancer, viral and allergens (Lahdenkari *et al*., 2004).
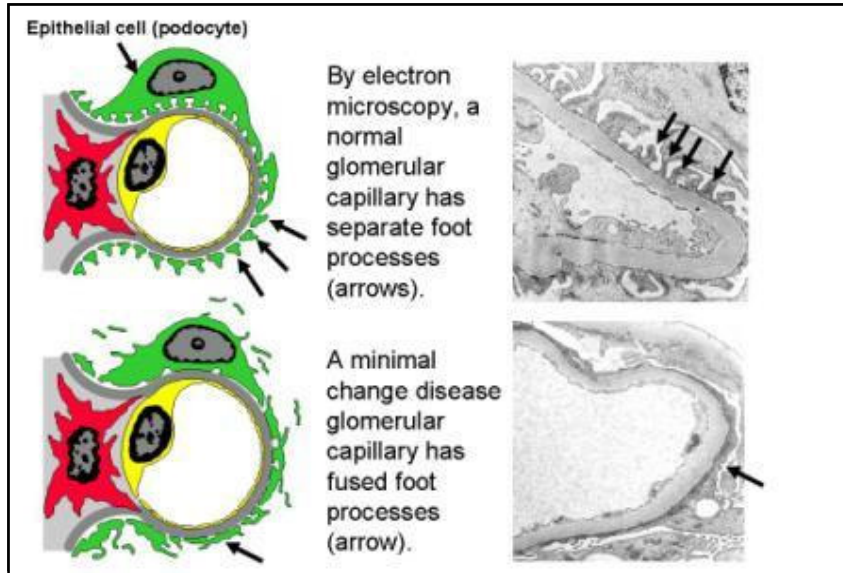
Figure 1.13: Schematic and corresponding EM graph illustrating (top) normal capillary loop and foot processes (arrow). (bottom) fused/effaced foot processes (arrow) as observed in Minimal Change Disease's (Falk, 2008).

1.4.1.2 Focal segmental glomerulosclerosis

Focal segmental glomerulosclerosis (FSGS) indicates that some (focal) segments (segmental) of the kidney filters (glomeruli) are scarred (sclerosis) (Figure 1.14); (Kriz, 2003). It is the direct common form of nephrotic syndrome in children and adolescents, leads to end stage kidney disease (Smeets *et al.*, 2006). In contrast to MCD, patients with FSGS are more likely to have a form of non-selective proteinuria, hematuria, progression to chronic renal failure, and poor response to corticosteroid therapy (Bolton and Abdel-Rahman, 2001).

The pathogenesis of FSGS may be idiopathic, or it can be associated with several aetiological agents including HIV (Dijkman *et al.*, 2006; Tucker, 2002). Clinical presentation of HIVAN include moderate to nephrotic range proteinuria (loss of large amount of protein in the urine), oedema (retention of water - weight gain), hypoalbuminemia (albumin in blood serum are abnormally low), hypertension (blood pressure is chronically elevated) and ultrasound findings of large, highly echogenic kidneys.(Schrier *et al.*, 1981; Wyatt *et al.*, 2008).
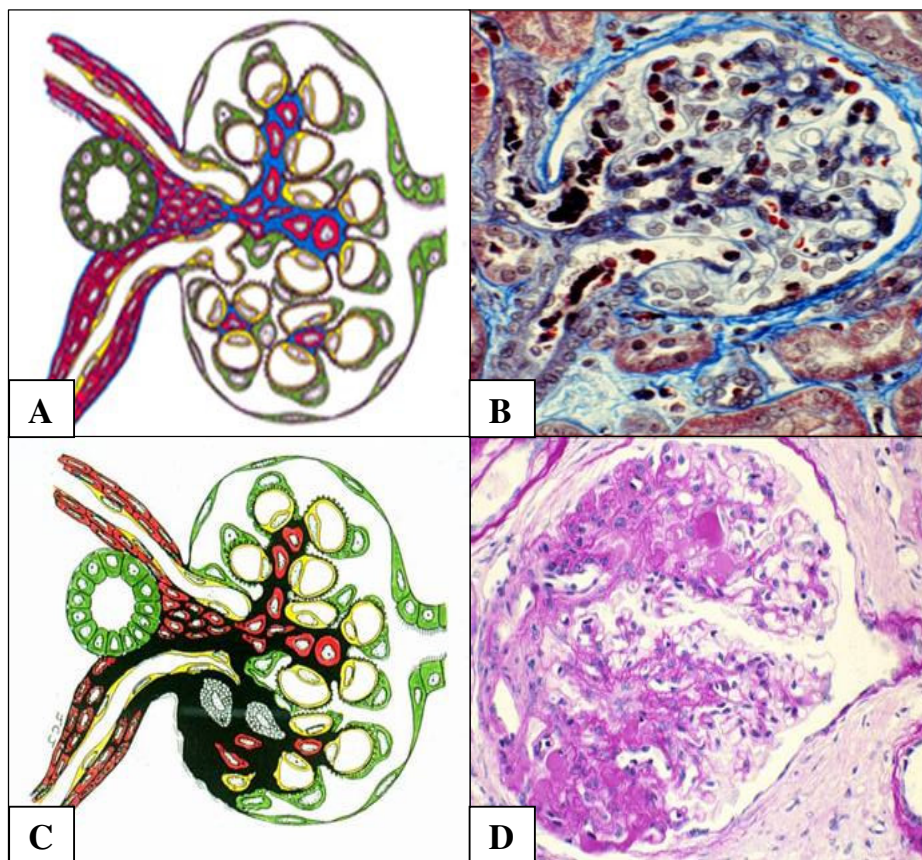
Figure 1.14: Schematic and light micrograph of cross-section of **A & B**: normal glomeruli; **C & D** glomeruli with focal segmental glomerulosclerosis. (Falk, 2008).

1.4.1.3 Membranous glomerulopathy

In membranous glomerulopathy, the GBM is thickened (Figure 1.15) due to the accumulation of immune complexes in the walls of glomerular capillaries between the basement membrane and the podocyte (O'Regan, 1979; Sheerin *et al.*, 2006). Antibodies

bind to target molecules (antigens) (Figure 1.15); (Abrahamson, 1987; Caulfield and Farquhar, 1974) with the resultant immune complex formation that disturbs glomerular filtration hence proteins leak into the urine (proteinuria) (Brasile *et al*., 1997). In most patients, the source of the antigens in the immune complexes is idiopathic, however, in some patients, it comes from an infectious micro-organism. Occasionally, the antigen is an auto-antigen, for e.g., in patients with membranous glomerulopathy secondary to an auto-immune disease such as systemic lupus erythematosus (Jennette and Falk, 1997).
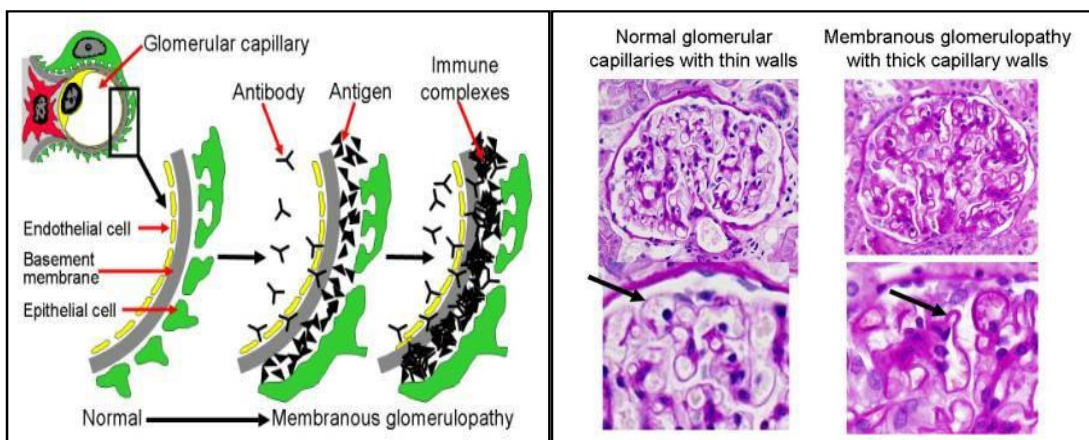
Figure 1.15: Schematic illustration of the process of normal accumulation of immune complexes (antibodies that are attached to antigens) within glomerular capillary walls of membranous glomerulopathy and light micrographs indicating thickened (arrows) capillary walls (Falk, 2008).

1.4.1.4 IgA nephropathy

IgA nephropathy (also known as IgA nephritis, IgAN, *Berger's disease* and synpharyngitic glomerulonephritis) is the commonest type of glomerulonephritis in the world (D'Amico, 1987). It is characterized by diffuse deposition of the IgA antibody in the mesangium (Hernandez *et al.*, 1997; Suzuki *et al.*, 2003; Yoshikawa *et al.*, 1994). Henoch-Schönlein purpura is the most common disease associated with glomerular IgA deposits, considered by many to be a systemic form of IgA nephropathy (Figure 1.16); (Vogler *et al*., 1999).
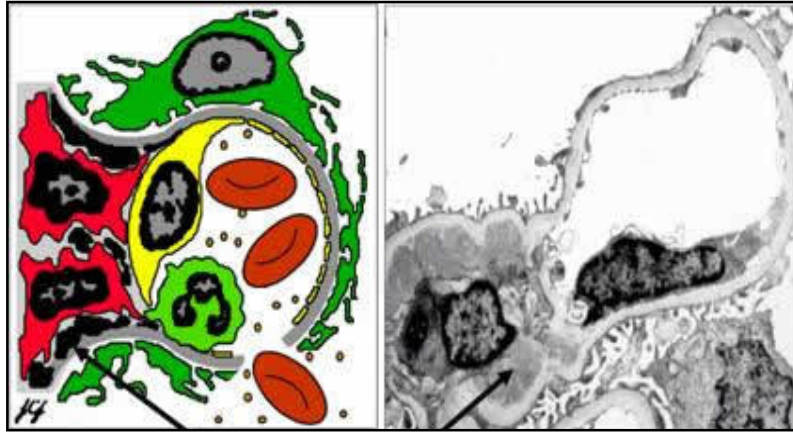
Figure 1.16: Schematic and electron micrograph showing immune complex deposition within the mesangium (arrows) (Falk, 2008).

1.4.1.5 Diabetic Glomerulosclerosis

Diabetic nephropathy t is characterised by diffuse or nodular glomerulosclerosis, afferent and efferent hyaline arteriolosclerosis, and tubule-interstitial fibrosis and atrophy (Alsaad and Herzenberg, 2007). It is a major cause of ESRD (Markowitz *et al*., 2002).

1.4.1.6 HIV related nephropathy

Renal disease associated with AIDS was first reported in 1984 (Gardenswartz *et al*., 1984). Today HIV related renal diseases is considered the third leading cause of ESRD (Szczech, 2001). The etiological role of the virus in these pathologies is unknown (Symeonidou *et al*., 2008). It has been show that renal disease is more common in HIV infected patients with a CD4$^+$ T cell < 200 cells/µL(Gerntholz *et al.*, 2006; Symeonidou *et al.*, 2008). Majority of HIV-1 seropositive patients at some point during their illness, develop renal impairment ranging from minor transient electrolyte imbalance to ESRD (Symeonidou *et al*., 2008). HIV-1 seropositive patients progress rapidly (6-8 wks) to ESRD with a mortality-rate approaching 100% within 6 months of diagnosis (Moro *et al*., 2007).

The most common histologic lesion occurring in these patients is HIV associated nephropathy (HIVAN) (Kimmel *et al.*, 2003). This lesion demonstrates collapsing type FSGS with proliferation of tubulo-epithelial cells (Gerntholz *et al.*, 2006). Studies by Han *et al* (2006a), demonstrate that in South Africa, HIVAN is the commonest biopsy finding occurring in adult patients with HIV infection and is characterized by mesangial hyperplasia, variants of FSGS and with microcystic transformation of renal tubules (Figure 1.17);.
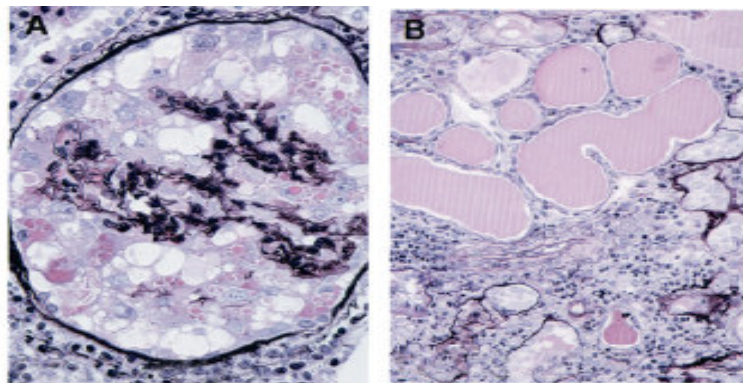
Figure 1.17: Human HIV-associated nephropathy: **(A).** A glomerulus shows global collapse of capillary lumina. The glomerular basement membranes are wrinkled and folded, and the urinary space is occupied by proliferating podocytes forming pseudocrescents. Numerous protein reabsorption droplets are present in the podocyte cytoplasm; **(B).** Tubulointerstitial damage includes interstitial fibrosis with inflammation, tubular atrophy, and microcysts. Eosinophilic casts are present in the dilated tubular lumina (Kimmel *et al.*, 2003).

Another variant, the histologic pattern of HIV Immune complex disease (HIVICK) involves immune deposition within the mesangial and paramesangial regions with concomitant (Figure 1.18), overlap of the tubulo-interstitial changes that occur in classic 'HIVAN' (Gerntholz *et al.*, 2006).
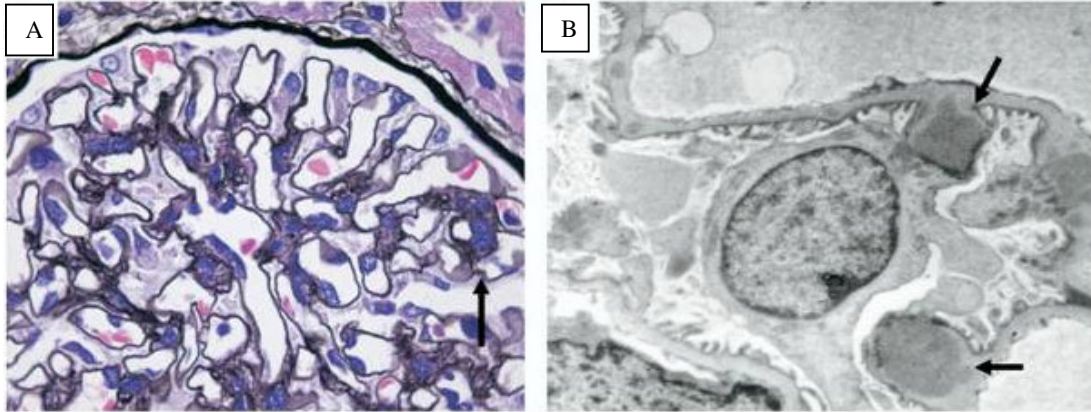
Figure 1.18: **(A)** Light microscopy renal section from a child with HIVICK showing mesangial prominence. The glomerular tuft is lobulated with double contours of the glomerular basement membrane (black arrow) (Jones methenamine silver stain). **(B)** Transmission electron microscopy from a glomerular capillary in a child with HIVICK. The black arrows show subepithelial deposits (Pakasa and Binda, 2011).

Other variants, such as HIV associated thrombotic microangiopathies (TMA) resulting from hemolytic uremic syndrome (HUS) is believed to be triggered by endothelial cell dysfunction as a consequence of viral proteins (Kimmel *et al*., 2003).

HIV related nephropathy can also result from the adverse effects of HIV treatment regiments (Prins *et al*., 2005). An example of HAART-related renal disease was reported by Symeonidou and co-workers in 2008 due to the use of a protease inhibitor (indinavir) implicated in forming renal calculi. Additionally, a direct renal tubular toxicity is associated with antiretroviral agents, such as the nucleotide analog tenofovir (Symeonidou *et al*., 2008). Furthermore, patients with HIV disease are at risk for developing pre-renal azotemia due to volume depletion as a result of salt wasting, poor nutrition, nausea and/or vomiting (Moro *et al*., 2007).

HIV related nephropathy primarily occurs in Black patients, suggesting a genetic predisposition to the disease (Choi *et al.*, 2007b; Moore and Doms, 2000). A recent study (Kopp *et al*., (2008) using mapping by admixture linkage disequilibrium identified MYH9 as a genetic variant that pre-disposes to HIV associated FSGS and additionally showed

27

strong association of African chromosomal ancestry with FSGS in African Americans. This racial discrepancy in susceptibility to HIV-related nephropathy (HIVRN) has been reported in studies from the USA, France and Brazil (Kopp and Winkler, 2003). Although the vast majority of infected patients reside in sub-Saharan Africa (approximately 75%), there is paucity of data from this continent (Gerntholz *et al.*, 2006). In the USA, African Americans represent approximately 65% of all children with HIV-1 infection or AIDS of which 40% experience an increased prevalence of renal complications (Klotman, 1999; Ray *et al.*, 2004; Winston *et al.*, 1999).

Ray *et al.*, (2004) suggested that HIV-1 infection *per se* was capable of inducing HIVAN in children and that HIVAN in children progressed at a slower rate when compared with adults with HIVAN. HIVAN occurs more frequently in males than in females, with a male-to-female ratio of 10:1 (Moro *et al.*, 2007).

Over the past 28 years despite a substantial advancement in understanding the aetiology, natural history and drug therapy for the spectrum of HIVRN, renal biopsy remains the gold standard for the identifying the disease pattern (Gerntholz *et al.*, 2006).

1.4.1.6.1 Spectrum of HIVRN in South Africa

Despite the large burden of HIV-1 disease in Africa, there have been no substantial reports of HIV-related kidney disease. Africa represents a true opportunity for refining our understanding of the epidemiology of HIV-related renal diseases (Cohen and Kimmel, 2007). If the US data for HIVAN was extrapolated to Africa, between 0.9 and 3.1 million people would be predicted to have HIV related diseases (Naicker *et al*., 2006). These figures predict an unprecedented and possibly underestimated burden of chronic kidney

disease in Africa. Naicker *et al*., (2006) suggest that the low socioeconomic conditions in South Africa contributes to the low prevalence of reported HIV related diseases as many patients demise before reaching ESRD.

A study by Gerntholtz *et al*., (2006) looks at the spectrum of 99 adult patients with HIVRN from South Africa (Fig 1.19 A). Ramsuran *et al*., (2011a) outlines the spectrum of HIV-1 related kidney diseases of children in South Africa (Fig 1.19 B); (Addendum I). Although collapsing glomerulopathy is thought to be the most common form of chronic kidney disease in adults of African descent who are HIV positive, it accounts for only about a quarter of the histological spectrum of disease seen in HIV positive children in our region. This conforms to reports from other regions in South Africa where HIVAN accounted for less than a third of all adult patients and 11.5% of all children with HIV-related nephropathy (Gerntholz *et al.*, 2006; Kala U *et al.*, 2007). Additionally a study by Cachat (1998) showed that in children of African American descent focal and segmental glomerulosclerosis occur in contrast to those of European ancestry (Caucasian) were mesangial hyperplasia, rarely with IgA nephropathy predominate.
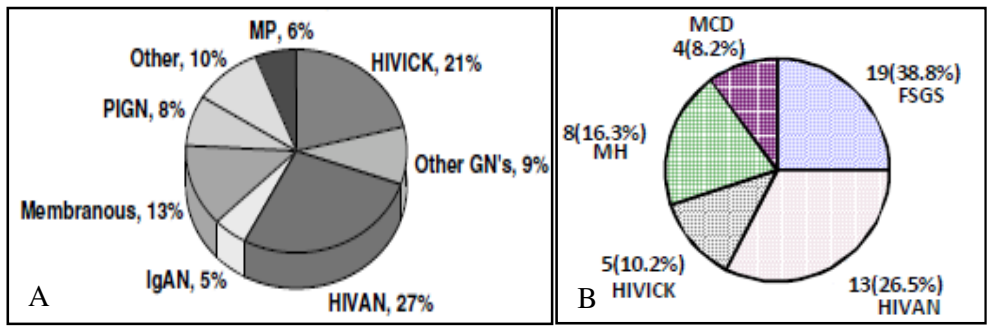
Figure 1.19: Piechart comparing HIVRN adults **(A)** with children **(B)** in South Africa. HIVICK: immune complex deposition disease; other GN's: other glomerulonephritides; HIVAN: collapsing nephropathy; IgAN: IgA nephropathy; PIGN: post-infectious glomerulonephritis; other: other (non-glomerulonephritic) renal disease; MP: mesangial proliferative glomerulonephritis; FSGS: focal glomerulosclerosis; and min change: minimal change (MCD), and MH: mesangial hypercellularity.

1.4.1.6.2 Pediatric HIVRN

At the beginning of the HIV epidemic, childhood HIVAN was first reported in African American children from the United States of America (Barre-Sinoussi *et al.*, 1983; Fauci, 1999; Pardo *et al.*, 1987). The finding of HIVAN in children provided evidence that HIV-1 virions *per se* was capable of inducing renal disease independently of other confounding variables that are present in HIV-infected adults such as heroin abuse (Ray *et al*., 2004). However, unlike adults, many children with HIV and kidney disease did not develop collapsing glomerulopathy. In children, the unique microscopic feature of HIVAN is defined as the presence of classical FSGS with or without mesangial hyperplasia in combination with microcystic tubular dilatation and interstitial inflammation (Fauci, 1999; Mitsuya *et al.*, 1985). However, mesangial proliferative lesions secondary to immune complex deposits have also been identified in some HIV-infected children with HIVAN (Fauci, 1999; Mitsuya *et al.*, 1985; Ray, 2009). Thus the clinicopathological spectrum of childhood HIVAN has been revised (Ray, 2009).

Although Sub Sarhan Africa is the epicentre of HIV there have been no substantial reports of HIVRN in children. It has been estimated that of the 2.1 million HIV-infected children under 15 years of age living in sub-Saharan Africa, approximately 300 000 children without access to antiretroviral therapy could develop HIVAN (McCulloch and Ray, 2008). These figures predict an unprecedented and possibly underestimated burden of HIV renal disease in children in Africa (Gerntholz *et al.*, 2006; Naicker *et al.*, 2006).

1.4.1.6.3 Podocytes in HIVRN

An escape of the podocyte from the cell cycle blockade results in a disruption of glomerular architecture followed by a rapid decline of renal function. This is demonstrated by the deleterious course of collapsing focal glomerulosclerosis pathology and persistent proteinuria of HIV nephropathy (Kiryluk *et al.*, 2007; Klotman, 1999).

HIV-1 protein expression, *Tat*, *Nef* and *Vpr* have been implicated in podocyte dysfunction and phenotypical change (Lu *et al.*, 2007). More specifically, the regulatory protein *Tat* and the 2 accessory proteins *Vpr* and *Nef* have been linked to the pathogenesis of HIVAN. *Vpr* transports cytoplasmic viral DNA into Nucleus and *Tat* is essential for HIV infection and replication whilst *Nef* protects cell from dying. *Tat* and/or *Vpr* have also been reported to alter differentiation genes, whereas *Nef* induces proliferation (Figure 1.20); (Sunamoto *et al.*, 2003).
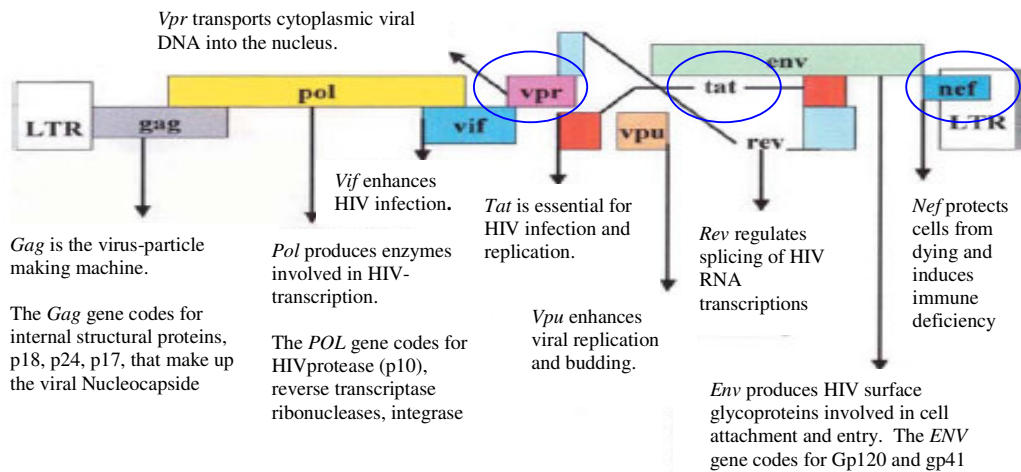
Figure 1.20: Organization of the HIV-1 genome, the function of each protein is outlined. Vpr, tat nef have been linked to HIVRN (Sunamoto *et al.*, 2003).

Podocytes are injured in many forms of glomerular disease, including disease that are immune mediated (membrane glomerulopathy), toxin associated (puromycin aminonucleoside model of minimal change nephropathy), metabolic (diabetes), and

hemodynamic (glomerular hyper-filtration) (Barisoni *et al.*, 2000a; Ichikawa and Fogo, 1996; Remuzzi *et al.*, 1997; Wharram *et al.*, 2005).

However, under pathological conditions, podocytes de-differentiate, re-entering the cell cycle and proliferating, therefore detecting the Ki-67 antigen (Barisoni *et al.*, 2000b; Ferrara, 2004). Ki67 is a constituent of compact chromatin hence is vital for cell proliferation. Exceptions to this rule are conditions of collapsing glomerulopathies, including HIVAN, where podocytes undergo a dysregulation of their differentiated phenotype and proliferate (Barisoni *et al.*, 2000a; Mundel and Shankland, 1999; Shankland, 1999).

In most glomerular diseases, podocytes may undergo DNA synthesis and mitosis, but not in cytokinesis (Marshall and Shankland, 2006; Nagata *et al.*, 2003; Shankland, 1999). Failure to replicate leads to an inappropriate response of podocytes to injury resulting in progressive glomerulosclerosis (Barisoni *et al.*, 2000b; Ihalmo *et al.*, 2007).

1.5 HIV MOLECULAR EXPRESSION IN HIVRN

As eluded to in 1.1.3 viral RNA enters the infected cell via receptors where reverse transcription occurs to synthesize complementary circular DNA. This is then inserted into the host cell chromosome by the viral integrase enzyme; the integrated viral DNA is now referred to as proviral DNA (Gibellini *et al*., 2004). HIV-1 RNA is considered to be an effective marker to predict the level of HIV expression (Gibellini *et al.*, 2004; Katzenstein, 2003; Vitone *et al.*, 2005).

HIV-1 proviral DNA represents viral reservoirs whereas HIV-1 RNA represents viral replication (Desire *et al.*, 2001; Gibellini *et al.*, 2004). Proviral HIV-1 DNA has been measured in Peripheral blood mononuclear cells (PBMC) as well as within lymphoid tissue biopsy specimens (Desire *et al*., 2001).

A study using transgenic murine models by Salifu (2010), presented one of the most persuasive evidence to show a direct role of HIV-1 in the development of HIV renal disease. It demonstrated latent viral reservoirs within renal glomerular and tubular epithelial cells, supporting the theory that epithelial cells like podocytes may transcytose viral particles despite their lack of HIV-1 receptors (Sagar *et al.*, 2004; Salifu. M, 2010). Further research should be attributed to monitoring the interplay between proviral load and treatment which offers substantial therapeutic information, as the surrogate marker HIV RNA can drop below the detectable limits (Desire *et al.*, 2001; McCutchan *et al.*, 2000; Nora *et al.*, 2008).

Envelope protein is essential for virus entry as it seeks out specific receptors for entry into CD4^{+} T cell. To be successful against the immune system the *env* protein mutates frequently (Zhang *et al*., 1993), causing nucleotide substitutions in HIV-1 envelope gene as characterized by a high non-synonymous/ synonymous substitution ratio compared with other regions of the viral genome (Sagar *et al*., 2004). The most striking changes in diversity occur in the envelope glycoproteins by modest increases in nucleotide sequence diversity (Nora *et al*., 2008). HIV-1 can result in infection of the new host with multiple viruses expressing genetically diverse *env* sequences (McCutchan *et al.*, 2000; Nora *et al.*, 2008).

1.6 TREATMENT OF HIVRN

1.6.1 Highly Active Antiretroviral Therapy

The development of a multi-drug combination therapy (Highly Active Antiretroviral Therapy - HAART) for treatment of HIV in 2006 transformed this catastrophic illness of AIDS to a more manageable chronic illness (Delaney M, 2006). The WHO guidelines considers HIVAN as stage four (severe symptoms; Addendum IV), for disease progression, which is an immediate initiation of HAART, regardless of CD4$^+$ T cell count (Kaufman *et al*., 2010). No standard therapy for HIVAN has been developed but HAART has been shown to retard the progression of renal disease in persons with HIVAN (Herman and Klotman, 2003; Moro *et al.*, 2007). South Africa's HIV epidemic remains the largest in the world with an increasing number of HIV infected patients accessing HAART. With a an increasing total number of people living with HIV in South Africa; it reached an estimated 5.6 million [5 400 000 – 5 800 000] in 2010, of which only 1 389 865 people were receiving HAART, by the end of 2010 (UNAIDS, 2011).

However, the long term effects of HAART may be complicated by direct nephrotoxicity or by metabolic disorders that are associated with the development of kidney disease, such as hypertension and diabetes (Wyatt and Klotman, 2007).

1.6.2 Angiotensin-converting enzyme inhibitor

It has been suggested that renal recovery and histological improvement may be possible following the initiation of HAART with an adjunctive therapy of ACE inhibitors (Wyatt and Klotman, 2007). The exact pharmacology of this salubrious drug is unknown. In HIVAN there is an up regulation of circulating transforming growth factor-β which is

thought to contributes to the pathology (Bhimma, 2007). ACE-I has been shown to reduce the production of transforming growth factor-β (Choi *et al*., 2007a).

1.6.3 Corticosteroids

Studies have shown steroids have a beneficial effect when treating HIVAN, by improving renal function and proteinuria. Steroids are considered second line therapy, with ACE-I being the first line of therapy for HIVAN patients, as it has only short term benefits (Choi *et al*., 2007a).

1.6.4 Dialysis

In the pre-HAART era, HIVAN patients with ESRD demised soon after initiating dialysis, (Bhimma, 2007; Choi *et al.*, 2007a).

1.6.5 Kidney transplantation

Transplantation is not standard of care for HIVAN patients within South Africa. The immunosuppression of HIVAN may increase the risk of opportunistic infections, factors contributing to increased morbidity and/or mortality (Bhimma, 2007; Choi *et al.*, 2007a).

1.7 AIMS OF THE STUDY

1.7.1 The primary aims of this study were:

1. Compare the immunoexpression of podocyte cytoskeleton proteins (synaptopodin) as well as the proliferation marker (Ki67) pre and post-HAART treatment.

2. To provide evidence for localized replication of HIV-1 in the kidney and the existence of a renal viral reservoirs using polymerase chain reaction assays.

3. To provide ultrastructural architectural differences between pre and post treatment whilst at the same time identifying renal viral reservoirs.

1.7.2 Secondary Objectives and Secondary Endpoints:

1. Determine the efficacy of HAART combined with ACE-I in patients with HIV and nephropathy.

2. Outline the spectrum of HIV-related nephropathies in KwaZulu-Natal.

1.7.3 The hypothesis tested:

a. The loss of synaptopodin and the proliferation of podocytes are reversible events following HAART therapy.

b. Glomerular and tubular epithelial cells are a source of latent viral reservoirs in HIV positive patients.

CHAPTER 2

MATERIALS AND METHODS

2.1 ETHICAL APPROVAL AND PATIENT CONSENT

This prospective study was conducted at the Optics & Imaging Centre, Doris Duke Medical Research Institute (PG Reference Number PG030/07; Addendum V), Inkosi Albert Luthuli Central Hospital (IALCH) and King Edward VIII Hospital (KEH) in Durban, South Africa. For this study, ethical approval was obtained from the Biomedical Research Ethics Committee, Nelson R. Mandela School of Medicine, University of KwaZulu-Natal (Reference Number BF149/07; Addendum VI). Permission to conduct research was granted by the Hospital Managers at IALCH (Addendum VII) and KEH (Addendum VIII). Informed consent was obtained from all parents/guardians of children participating in the study (example of Doc used; Addendum IX). Familial consent was sort for control brain tissue obtained at post mortem (Addendum X).

2.2 STUDY POPULATION

Patients were managed in accordance with the institutional guidelines for their kidney disease and HIV was managed according to the standard of care used by the Department of Health, KwaZulu-Natal. Demographics findings were recorded in all patients. Clinical examination, patient care and follow-up of patients were performed by a trained senior paediatric nephrologist at the Renal Units in IALCH and KEH.

The targeted study population included children with HIVRN (N = 30 patients) *viz.*,

    (i)   Pre-Highly Active Anti-Retroviral Therapy (HAART) (N = 30 samples).

    (ii) Post-HAART (N = 30 samples).

All patients within the pre-HAART group were followed-up clinically for a period of 12 months. This cohort formed the post-HAART group.

2.2.1 Inclusion Criteria for Study Group

(i)   all patients with HIV infection (all stages of HIV infection) and evidence of nephropathy as evident by persistent proteinuria*;

(ii) informed written consent from the parent/guardian together with informed assent from children >8 years;

(iii) patients eligible for ARV therapy according to standard of care utilised by the Department of Health in KwaZulu-Natal.

* Persistent proteinuria is defined as urinary dipstick finding of 1+ or more proteinuria on two or more occasions in the absence of fever and a protein-to-creatinine ratio, (each measured in mg/dL using a random, early morning urine sample) of ≥ 0.2 with or without the presence of haematuria on urine microscopy.

2.2.2 Exclusion Criteria for Pre-HAART Group

(i) patients with transient proteinuria and HIV infection.

(ii) failure to obtain informed written informed consent and/or assent in a child >8 years of age.

(iii) patients with congenital abnormalities of the renal tract with HIV infection.

(iv) patients with bleeding diatheses who cannot undergo renal biopsy.

(v) non South African patients.

2.3 RENAL BIOPSY

A complete aseptic technique was used to obtain biopsy material, *viz.*, gowns, masks, gloves, etc. The skin was disinfected using chlorhexidine and povodine iodine. Land marks used were the lumbar vertebral spinous processes, the iliac crest, twelfth rib, the guadratus lumborum and the spinal extensor muscles. An in-house ultrasound scan was

performed by a qualified radiologist to obtain the size of the kidney, position of the lower pole and the depth of the lower pole of the kidney from skin surface. The patient was sedated with pethidne (1mg/kg; maximum dose 100mg) and midazolam (0.3-0.6mg/kg; maximum dose 15mg). If this was not sufficient to obtain adequate sedation, ketamine 1mg/kg diluted was added to the sedation. A 16 guage needle was used to explore the kidney depth after infiltration with 10cc (cubic centimetres) of 2% lignocaine used as a local anaesthetic. The needle was advanced until resistance of the renal capsule was encountered and the depth and position confirmed under ultrasound guidance. The scout needle was confirmed to be in kidney parenchyma when the needle oscillated with respiration. Once the site, path and depth of the scout needle was confirmed to be in the lower pole, it was removed. A 16-18 gauge tru-cut needle (QuickCore; Wilson-Cook Medical, NC) was used to biopsy the kidney under ultrasound guidance. The biopsy material was removed with a sterile forceps and placed on a microscope slide. A drop of saline was used to prevent the kidney biopsy material from drying. Three cores of tissue were obtained and part of the core was placed in a sterile tube snap frozen in liquid nitrogen for laser micro-dissection, polymerase chain reaction (PCR) and sequencing. The remaining 3 cores were stored in 4% glutaraldehyde, 5% formal saline and Mitchel's medium respectively and transported to the Department of Anatomical Pathology Laboratory (IALCH) for routine light microscopy, immunofluorescence and electron microscopy. Finally the biopsy area was cleaned and sterilized, OpSite spray (Zhejiang Top-Medical, Medical Dressing Co., Ltd. China) was used as an aqua film dressing, and a pressure dressing was applied to prevent further bleeding. A post-biopsy ultrasound was done to detect the presence of a haematoma. During the biopsy the patient's oxygen saturation was monitored. Pulse, blood pressure and electrocardiograph monitoring was carried out using an automated Welch Alan monitoring machine.

Post-biopsy monitoring was continued for 24 hours in the ward and if there was any evidence of frank haematuria or pallor the patient was subjected to a repeat ultrasound to check for evidence of an expanding hematoma.If bleeding did not stop within 48 hours or the patient became severely anaemic or haemodynamically unstable, an embolisation of the bleeding vessel was done by the radiologist using angiography.

Hypertension was controlled in patients using angiotensin converting enzyme (enalapril 0.3-0.5mg/kg). Diuretic therapy (hydrochlorothiazide and spironolactone) was used initially for control of oedema in patients with nephrotic syndrome and for control of hypertension in combination with angiotensin converting enzyme.

2.4 BLOOD ANALYSIS

Prior to biopsy, peripheral venous blood samples were obtained by venipuncture and collected in commercially available tubes containing a strong anti-coagulant *viz.*, ethylene diamine tetra-acetic acid (EDTA; Becton Dickinson).

The samples were then analysed and subjected to the tests below:

      2.4.1 CD4$^+$ T cell count and Viral Load

      2.4.2 Blood DNA extraction

      2.4.3 HIV Proviral DNA Quantification

      2.4.4 Sequence Diversity Analyses

2.4.1 Measurement of plasma viral load and CD4$^+$ T cell counts:

PBMC and plasma were isolated by density gradient centrifugation at 1000 rpm (Heraeus Megafuge 1.0R) for 10 min at room temperature.

i) **Viral load -** Quantification of plasma HIV-1 RNA was made by using the automated ultrasensitive (lower detection limit 50 copies/ml) COBAS Amplicor/Ampli Prep HIV-1 Monitor Test V1.5 (Roche Molecular Systems Inc., New Jersey, USA) as per manufacturer's instructions.

ii) **CD4$^+$ T cell -** A cluster of differentiation (CD) cells from PBMCs were enumerated by using the Multi-test kit (CD4/CD3/CD8/CD45) on a four parameter FACS Calibre flow cytometer (Becton Dickinson, New Jersey, USA).

2.4.2 Blood DNA extraction

DNA was extracted from buffy coats using the QIAamp DNA Mini kit (Qiagen, Santa Clarita, CA, USA) according to the manufacturer's instructions (Figure 2.1). DNA was quantified on the spectrophotometer NanoDrop 2000 (Thermo Scientific, Fermentas Canada Inc., Burlington, Ontario) to determine the quantity and quality of extracted DNA.

Lyse: 200μl of the lysed sample was loaded on the column membrane.

Bind

Wash (Buffer AW1): The column was then washed which allowed the DNA to bind in during centrifugation.

Wash (Buffer AW2): Protein and other contaminants will not bind to the membrane, due to the salt and pH conditions of the lysate buffer, and will therefore prevent downstream inhibition of PCR.

Elute: Finally purified DNA was eluted.

Figure 2.1: An overview of the QIAGEN QIAamp DNA Blood Mini Spin kit procedure for DNA extraction from buffy coat samples (Adapted from QIAGEN, 2003).

2.4.3 HIV Proviral DNA Quantification

A modified method of Desire *et al*., (2001) involving real time PCR technology was used for proviral load quantification. The LightCycler® 480 (Roche Molecular Systems, New Jersey, USA) was used for PCR amplification, acquisition and data analysis.

The PCR primers were selected to optimize HIV-1 subtype C *gag* sequence amplification, following earlier studies that suggest that this genetic subtype is the predominant virus in Southern Africa (Novitsky *et al*., 2001). The sequence of the forward and reverse primers were p24-F1 (5'-CAAGCAGCCATGCAAATGTT-3') and 330L (5'-GGTACTAGTAGTTCCTGC TAT-3') respectively. The primers ALB-S (5'-GCTGTCATCTCTCTTGTGGGCTGT-3') and ALB-AS (5'-AAACTCATGGGAGCTGCTGGTT-3') were used to quantify the human albumin gene. All samples, controls and standards were run in duplicate and the average value was used to compute HIV and albumin copy number. A standard curve for HIV and albumin was accepted with slopes ranging between -4.52 and -3.91 and when the coefficient of correlation (r^2) was >0.986.

Albumin DNA was quantified to determine the level of DNA input, to normalize for variation in buffy coat cell differences and for differences in DNA extraction. The normalized value of HIV proviral load was calculated as HIV DNA copy number/albumin DNA copy number multiplied by $2X10^6$ cells. The 8E5 cell line (American Type Culture Collection., Manassas, USA), was cultured by incubation horizontally at 37ºC in a 5% CO_2 in air atmosphere using RPMI-1640 medium (Sigma-Aldrich Corporation, MO) with 10% fetal bovine serum. The 8E5 cell line, a T lymphoblastoid cell line that contained a single

defective genome copy of HIV-LAV (lymphadenopathy-associated virus) per cell, was used as a positive control for each run and for the generation of a standard curve.

2.4.4 Sequence Diversity Analyses

Genomic DNA was extracted directly from PBMCs and kidney biopsy cells using the QIAamp Blood kit (Qiagen, Chatsworth, CA). Thereafter, the Expand High Fidelity PCR kit (Roche Molecular Systems, New Jersey, USA) was used to amplify a 957 base pair (bp) C2-C5 fragment of the *env* gene by using a nested PCR reaction protocol. In the first round reaction the forward primers was vpu232 (TGCTCCTTGGGATATTGATGA) while the reverse primers was p131 (AGCCAGGACTCTTGCCTGGAGCT). Five µL of the first round reaction product was subjected to a second round of amplification, with primers Bstq2+ (CCAATTCCTATACATTATTGTGC) and 1556 (CCATAGTGCTTCCTGCTGCTCCTAAGAACCCAA). Ten picomoles of each primer were used per PCR reaction. The cycling conditions for both amplifications consisted of initial activation at 95°C for 10 mins, followed by 39 cycles of 95°C for 15 sec, 58°C for 30 sec and 72°C for 1 min with a final extension at 72°C for 7 mins. To minimize re-sampling bias and to gain an understanding of the extent of diversity within the samples, three independent PCR reactions were performed for each sample at each time point (pre and post-HAART in PBMCs and kidney tissue) using identical PCR conditions. These PCR products were run on a 1% agarose gel at 100 Volts for 2 h to confirm the amplification of the 957 bp C2-C5 fragment by electrophoresis on an Enduro-power supplier (Labnet International Inc, New Jersey, USA). The desired band was then cut from the gel to ensure a greater probability that no other products were carried onto sequencing. The gel purification was performed utilizing the GE Healthcare kit (Table 2.1; GE Healthcare Life Sciences, Buckinghamshire, UK).

Table 2.1: Procedure for gel purification.

STEPS	METHOD	TEMP	TIME
1	PCR products run on a 1% gel at 100 Volts	24°C	2 h
2	Excise band of interest	24°C	
3	500µl Capture buffer type 3	60°C	5 mins
4	Add sample mix to GFX MicroSpin™ column and collection tube	24°C	1 min
5	Centrifuge @ 10000rpm (discarded flow through)	24°C	30 sec
6	500 µl wash buffer type 1	24°C	30 sec
7	Centrifuge @ 10000rpm (discarded flow collection tube)	24°C	30 sec
8	20µl elution buffer type 4	24°C	1 min
9	Centrifuge @ 12000rpm (retain flow through)	24°C	1 min
10	Run on a gel with a low DNA mass ladder (Invitrogen Corporation, Carlsbad, California, USA) and Molecular Weight Marker (1kb O'gene ruler, Thermo Scientific, Fermentas Canada Inc. Canada, Ontario)	24°C	2 h

2.4.5 Sequencing and Sequence Analysis

2.4.5.1 Cloning

The gel purified PCR products of specific segments of DNA with a single deoxyadenosine (A) to the 3' end complemented to the 3' deoxythymidine (T) of the PCR 2.1-Topo vector (Invitrogen Corporation, Carlsbad, California, USA), was then transformed into competent cells by the protocol outlined in Table 2.2.

Table 2.2: Procedure for cloning PCR products into a PCR 2.1-Topo vector.

STEPS	METHOD	TEMP	TIME
1	Ligation: H$_2$O = 1µl Vector = 1µl Salt = 1µl DNA (10ng/µl) = 3µl	24°C	30 min
2	Transform: 3µl ligation to competent *E. coli* One Shot® Mach1™	On ice	30 min
3	Heat shock	42°C On ice	30 sec 2 min
4	250µl Super Optimal broth with Catabolite (S.O.C) medium	37°C	5 h
5	100µl cell mixture plated on X-gal, ampicillin	37°C	overnight
6	TBE (growth medium) was inoculated with white colonies	37°C	overnight
7	Cultures were pelleted @ 12000 rpm	24°C	2 min

2.4.5.2 Plasmid isolation

This procedure was used to extract plasmid DNA, GeneJET^{TM} (Thermo scientific, Fermentas Canada Inc. Canada, Ontario) from bacterial cell suspensions, as per manufacturer's protocol. It is based on a silica membrane technology that utilises a spin column to selectively bind DNA molecules using high salt concentration and then washed to remove contaminants. Purified plasmid DNA was then eluted using the plasmid mini preparation as outlined in Table 2.3.

Table 2.3: Procedure for plasmid isolation.

STEPS	METHOD	TEMP	TIME
1	To pelleted cells, 250µl of resuspension solution- vortex	24°C	15 sec
2	250µl lysis solution, invert tube 4-6 times	24°C	15 sec
3	350µl of neutralization solution, invert tube 4-6 times	24°C	15 sec
4	Centrifuge @ 12000rpm	24°C	5 min
5	Transfer supernatant to GeneJET^{TM} spin column, Centrifuge @ 12000rpm	24°C	1 min
6	Wash column: 500µl wash solution - Centrifuge @ 12000rpm -Repeat	24°C	1 min
7	Empty column - Centrifuge @ 12000rpm	24°C	1 min
8	50µl Elution buffer – incubate – Centrifuge @ 12000rpm	24°C	4 min
9	Ran a 1% gel at 100 Volts	24°C	2 h
10	Spectrophotometer - NanoDrop 2000 (Thermo scientific, Fermentas Canada Inc. Canada, Burlington, Ontario)	24°C	

2.4.5.3 Sequencing

Sequencing of the plasmid inserts was performed using Big Dye chemistry fluorescence-based cycle sequencing reaction mechanism on an ABI Prism 3130xl Genetic Analyzer (Table 2.4; Applied Biosystems, Foster city, California, USA). In this system double-stranded DNA templates were sequenced from PCR fragments. For each sample, 3 clones were sequenced using with primers Bstq2+ (CCAATTCCTATACATTATTGTGC), 1556 (CCATAGTGCTTCCTGCTGCTCCTAAGAACCCAA) and ES8 (CACTTCTCCATTTGTCCC).

Table 2.4: Procedure for fluorescence-based sequencing reaction.

STEPS	METHOD	TEMP	TIME
1	Primer (1.6µM) = 2µl Big Dye = 0.4µl buffer = 2µl H2O = 5µl Template (150ng)	96°C 96°C 50°C 60°C 4°C	1 min ⎫ 1 10 sec ⎫ 5 sec ⎬ 35 4 min ⎭ ∞
2	1µl 125mM EDTA pH8.0	24°C	
3	26µl (1µl of 3M NaOAc pH5.2 + 25µl 100% ethanol)	24°C	
4	Centrifuge at 3000 X g	24°C	20 min
5	Invert to dry plate	24°C	5 mins
6	35µl cold 70% ethanol	24°C	30 sec
7	Centrifuge at 3000 X g	24°C	5 mins
8	Dry	50°C	5 min
9	10µl formamide, vortex	24°C	15 sec
10	Denature	95°C 4°C	3 mins 3 mins

2.4.5.4 Sequence Analysis

Individual contiguous sequences were assembled and edited using the Sequencher 5.0 software program (Gene Codes Corporation, Ann Arbor, Michigan). Multiple sequence alignment were done on the Mafft online server (http://align.bmr.kyushu-u.ac.jp/mafft/online/server/). The pairwise distances of nucleotide alignment was computed by DNADist (University of Washington, USA) with the Kimura two-parameter model. The neighbour-joining tree and bootstrap values were generated using Mega Version 5.05 (Biodesign Institute, Tempe, USA). Highlighter plots were generated by Highlighter at www.hiv.lanl.gov, a visualization tool of aligned nucleotides sequences that highlights nucleotide polymorphisms.

2.5 KIDNEY BIOPSY

Percutaneous renal biopsies were performed by a paediatric nephrologist under ultrasound guidance at IALCH using a trucut biopsy needle. Three biopsy cores were obtained from each patient, divided and distributed as shown in Figure 2.2.
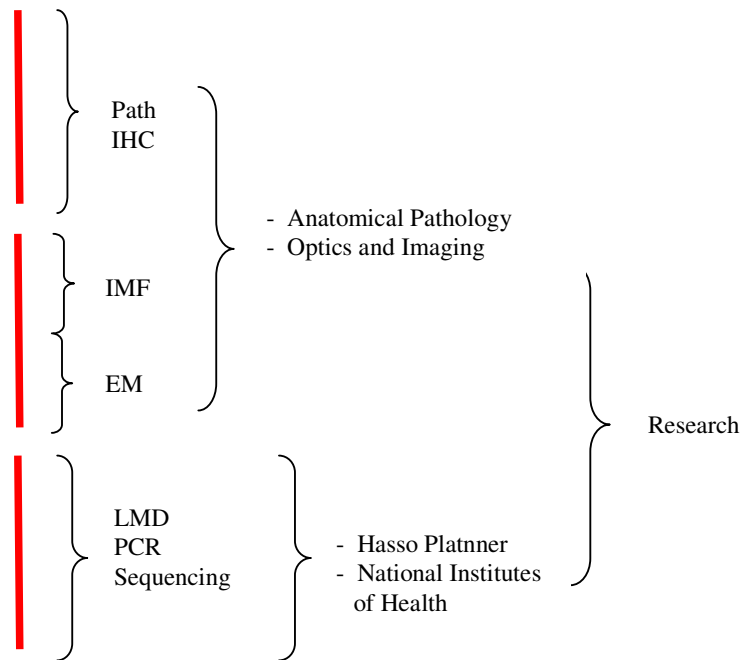
Figure 2.2: Schematic diagram showing the three biopsy cores, their division and distribution for specialised assessment viz., electron microscopy (EM, Anatomical Pathology); immunofluorescence (IMF, Anatomical Pathology); laser micro-dissection (LMD, National Institutes of Health, US); evaluation of latent viral reservoirs and architecture (EM, Optics & Imaging Centre); immunohistochemistry (IHC, Optics & Imaging Centre) and genetic analysis (PCR and sequencing, Hasso Platnner).

All renal biopsy material were evaluated by a senior pathologist experienced in interpretation of percutaneous renal biopsy at the Department of Anatomical Pathology, National Health Laboratory Service, IALCH. Post biopsy, the patient was followed-up bi-monthly for a period of one year whilst on HAART and ACE-I. At the end of this period a second biopsy was performed. The time frame of 12–14 months follow-up was stringently adhered to and a standard procedure.

2.5.1 Histopathology

2.5.1.1 Fixation and tissue processing

Biopsies were immediately immersed in 5% formal saline (41% formaldehyde / 0.9% NaCl, 1:8 v/v) – dilute formaldehyde (35%, Saarchem, SA) 1:7 in 0.9% NaCl and fixed at RT for 12 h. Samples were orientated and placed in tissue cassettes. These were then dehydrated through a series of ethanol (99% ethanol, Saarchem, SA), cleared with xylene (AR, Saarchem, SA) and infiltrated with paraffin wax (Paraplast Plus, Sherwood Medical, St Louis, USA) in an automatic tissue processor (Excelsior ES, Thermo scientific, Fermentas Canada Inc., Burlington, Ontario). Biopsies were then embedded in cassettes and polymerised at 60°C. The automated schedule of steps outlining this procedure (Table 2.5) was carried out by the Department of Anatomical Pathology, National Health Laboratory Service, IALCH. The processed tissue was then embedded using a Leica EG 1160 embedding station (Leica Biosystems, Newcastle Upon Tyne, UK).

Table 2.5: Fixation, dehydration and embedding schedule for light microscopy.

PROCESS	METHOD	TEMP	TIME
Fixation	10% buffered formal saline	24°C	1 h
	10% buffered formal saline	24°C	1 h
Dehydration	SVR (95% ethanol)	24°C	1 h
	SVR (95% ethanol)	24°C	1 h
	SVR (95% ethanol)	24°C	1 h
	absolute ethanol	24°C	1 h
	absolute ethanol	24°C	1 h
	absolute ethanol	24°C	1 h
Clearing	xylene	24°C	1 h
	xylene	24°C	1 h
Vacuum infiltration	paraffin wax 1	60°C	2 h
	paraffin wax 2	60°C	2 h

51

2.5.1.2 Microtomy

Sections (2µm) were cut on a Leica microtome RM2135 (Leica Biosystems, Newcastle Upon Tyne, UK). They were floated in a water bath and picked onto slides for staining.

2.5.1.3 Haematoxylin & Eosin (H&E); Periodic acid Schiff reaction (PAS), Masson's trichrome, Miller's Elastic and Silver Methenamine staining

For each biopsy, one section was cut and stained according to an outlined protocol for H&E (Table 2.6); PAS reaction (Table 2.7); Masson's Trichrome (Table 2.8) and Miller's Elastic stain (Table 2.9). In addition, 1 µm sections were cut for Silver Methenamine staining as outlined in Table 2.10.

Table 2.6: Procedure for H&E staining.

STEPS	METHOD	TIME
1	Dewax – xylene	2 x 5 min
2	Rehydrate – absolute ethanol	2 x 1 min
3	Rehydrate – 90% ethanol	1 min
4	Rehydrate – 70% ethanol	1 min
5	Rehydrate – water	1 min
6	Mayer's Haematoxylin (Addendum XI)	5 min
7	Blue – rinse in running tap water	5 min
8	0.5% alcoholic eosin (Addendum XI)	2 min
9	Rinse quickly by immersing slides in 95% ethanol	30 sec
10	Dehydrate - Absolute Alcohol	2 x 1 min
11	Dehydrate – Xylene	1 min
12	Mount in DPX	

Table 2.7: Procedure for PAS staining.

STEPS	METHOD	TIME
1	Dewax – xylene	2 x 5 min
2	Rehydrate – absolute ethanol	2 x 1 min
3	Rehydrate – 90% ethanol	1 min
4	Rehydrate – 70% ethanol	1 min
5	Rehydrate – water	1 min
6	1% Periodic Acid	10 min
7	Rinse in running water	30 sec
8	Schiff reagents (BDH Laboratory Supplies, England)	15 min
9	Running tap water	5 min
10	Mayer's Haematoxylin (Addendum XI)	2 min
11	Blue in running tap water	2 min
12	2% Orange-G (KGaA 64271, Merck, Germany) in 5% Phosphotungstic acid	1 dip
13	Rinse in running tap water	2 min
14	Dehydrate - Absolute alcohol	2 x 1 min
15	Dehydrate – Xylene	1 min
16	Mount in DPX	

Table 2.8: Procedure for Masson's Trichome staining.

STEPS	METHOD	TIME
1	Dewax – xylene	2 x 5 min
2	Rehydrate – absolute ethanol	2 x 1 min
3	Rehydrate – 90% ethanol	1 min
4	Rehydrate – 70% ethanol	1 min
5	Rehydrate – water	1 min
6	Weigert's Iron Haematoxylin (Addendum XI)	10 min
7	Rinse in running tap water	30 sec
8	1% Acid Alcohol	
9	Wash in distilled water	1 min
10	Biebrich scarlet-acid fuchsin (Addendum XI)	3 min
11	Rinse in distilled water	
12	5% Phosphotungstic Acid	10 min
13	1% Light Green SF yellowish soln (Merck, Germany)	
14	Rinse in distilled water	
15	Dehydrate - Absolute alcohol	2 x 1 min
16	Dehydrate – Xylene	1 min
17	Mount in DPX	

Table 2.9: Procedure for Miller's Elastic staining.

STEPS	METHOD	TIME
1	Dewax – xylene	2 x 5 min
2	Rehydrate – absolute ethanol	2 x 1 min
3	Rehydrate – 90% ethanol	1 min
4	Rehydrate – 70% ethanol	1 min
5	Rehydrate – water	1 min
6	0.5% Potassium permanganate (Addendum XI)	5 min
7	Rinse well	
8	1% Oxalic Acid solution	*
9	Rinse in running water	
10	Rinse in 70% Alcohol	5 min
11	Elastic stain (Addendum XI)	1 h
12	Rinse in 70% Alcohol	
13	Rinse in running water	
14	Counterstain with Van Gieson	5 min
15	Dehydrate through alcohol	
16	Clear in xylene	2 min
17	Mount in DPX	

* Treat until sections appear white macroscopically

Table 2.10: Procedure for Silver methenamine staining.

STEPS	METHOD	TIME
1	Dewax – xylene	2 x 5 min
2	Rehydrate – absolute ethanol	2 x 1 min
3	Rehydrate – 90% ethanol and 70% ethanol	1 min
4	Rehydrate – water	1 min
5	Lugol's iodine (Kanchem cc, Durban, SA)	5 min
6	Rinse in running water	30 sec
7	Coplin jar containing ammonia-Alcohol solution	30 min
8	Rinse in running water	5 min
9	Distilled water	1 min
10	1% periodic acid solution	15 min
11	Rinse in distilled water	30 sec
12	0.5% thiosemicarbazide	5 min
13	Rinse in distilled water	3 x 2 min
14	Pre-heated Methenamine-silver solution (Addendum XI) - 60ºC	60 min
15	Rinse in distilled water	2 min
16	0.2% Gold Chloride	2 min
17	Rinse in distilled water	2 min
18	5% Sodium thiosulphate	2 min
19	Rinse in distilled water	2 min
20	Mayer's Haematoxylin (Addendum XI)	5 min
21	Rinse in distilled water	2 min
22	Lithium carbonate solution	
23	Rinse in distilled water	2 min
24	Eosin	3 min
25	Rinse in distilled water	2 min
26	Dehydrate - Absolute alcohol	2 x 1 min
27	Clear in xylene	2 min
28	Mount in DPX	

2.5.1.2 Immunofluorescent staining

The biopsy core in Mitchel's medium (Vaughn-Jones *et al*., 1995) was washed with phosphate buffered saline (PBS) (30min). This core was subsequently embedded on a cryostat chuck using Cryo-Optimal Cutting Temperature (OCT) compound. 7µm sections were cut onto poly-1-lysine coated slides. The sections were subsequently washed in PBS for 10mins, prior to incubation in conjugates using a direct immunolabelling technique as follows; FITC-conjugated polyclonal rabbit anti-human Immunoglobulin A (IgA), FITC-conjugated rabbit anti-human Immunoglobulin G (IgG), FITC-conjugated polyclonal rabbit anti-human Immunoglobulin M (IgM), Cytochrome P450 Polyclonal Antibody (MFO), FITC-conjugated polyclonal rabbit anti-human Fibrinogen (1:80) and FITC-conjugated polyclonal rabbit anti-human Complement 1(C1q), 3(C3c), 4(C4c)(4:80) (Dako, Denmark, UK) for 30mins in the dark. Thereafter slides were washed in PBS, and coverslipped with Kaiser's glycerol jelly as the mountant.

2.5.2 Transmission electron microscopy

2.5.2.1 Fixation and tissue processing

Biopsies were immediately immersed into 4% glutaraldehyde for 24 h at 4°C. The specimen was then diced into 1 mm^3 cubes immersed into 0.2M sodium cacodylate, pH 7.2 maintained at 4°C prior to a dehydration protocol. Final dehydration was performed by incubation in propylene oxide with subsequent infiltration, polymerization and embedding in Araldite CY212 epoxy resin embedding kit (Electron Microscopy Services, USA) in polythene capsules (size 00, BEEM) for 48 h at 60°C (Table 2.11).

Table 2.11: Processing schedule for electron microscopy.

PROCESS	METHOD	TEMP	TIME
Fixation	4% glutaraldehyde fixative (Addendum XI)	4°C	24 h
Wash	0.2 M sodium cacodylate buffer (pH 7.2) (Addendum XI)	20°C	10 min
Wash	0.2 M sodium cacodylate buffer (pH 7.2)	20°C	10 min
Fixation/Contrast	1% osmium tetroxide (0.2M NaCacodylate buffer) (Addendum XI)	4°C	1 h
Wash	0.2 M sodium cacodylate buffer (pH 7.2)	20°C	10 min
Wash	0.2 M sodium cacodylate buffer (pH 7.2)	20°C	10 min
Dehydration	70% ethanol	20°C	30 min
Dehydration	90% ethanol	20°C	30 min
Dehydration	100% ethanol	20°C	30 min
Dehydration	100% ethanol	20°C	30 min
Intermediate	propylene oxide (1,2-epoxypropane)	20°C	30 min
Infiltration	propylene oxide : Araldite epoxy resin (1:1) (Addendum XI)	20°C	30 min
Infiltration	Araldite epoxy resin	60°C	1 h
Infiltration	Araldite epoxy resin	60°C	1 h
Polymerisation	Araldite epoxy resin	60°C	48 h

2.5.2.2 Ultramicrotomy

Semi-thin (1 μm) sections were cut using glass knives on a Leica R ultramicrotome (Leica Biosystems, Newcastle Upon Tyne, UK). Sections were collected onto glass slides, heat-fixed, stained with 1% toluidine blue (Addendum XI) and examined with a Leica DMLS light microscope (Leica Biosystems, Newcastle Upon Tyne, UK). Fields of interest (always included glomeruli) were selected and located on the block face, and the block trimmed to produce a "mesa" with a trapezoidal shape. Ultrathin sections (50-60 nm) were cut, collected onto uncoated copper 200 mesh grids and stained with potassium permanganate, saturated ethanolic uranyl acetate and Reynold's lead citrate solution for 3 min (Reynolds, 1963).

2.5.2.3 Transmission electron microscopy evaluation

Diagnosis of the spectrum of pathology in the study cohort was performed at IALCH using the Joel 1010 transmission electron microscope linked to a MegaView III cooled camera. The ultrathin stained sections were evaluated by a pathologist and the results extrapolated to make the final diagnosis.

Thereafter, identification of latent viral reservoirs and assessment of other pathological changes of the biopsy core both pre and post-HAART was performed at the Optic and Imaging Centre. Sections were viewed on the Jeol 1011 transmission electron microscope. Images were digitally archived by a MegaView III camera interfaced to an ITEM Software Imaging System program.

2.5.3 Imunohistochemistry

Two µm paraffin embedded sections were collected on poly-1-lysine coated slides and immunostained using a NovoLink Max Polymer Detection kit (Table 2.12; Leica Biosystems, Newcastle Upon Tyne, United Kingdom).

2.5.3.1 Rabbit Anti-Human Syno Antibody

Anti-Synaptopodin antibody was an affinity isolated antibody produced in rabbit and reactive to human. Specificity was performed by protein array targeting PrEST protein and Western blotting (Horinouchi *et al.*, 2003).

2.5.3.2 Mouse Anti-Human Immunodeficiency Virus Antibody

This was a monoclonal mouse anti-human immunodeficiency virus antibody targeting the band corresponding to the viral core protein p24 and the band corresponding to the precursor protein pr55. Its isotype is IgG1 kappa and clone: Kal-1 (Kaluza *et al.*, 1992).

2.5.3.3 Mouse anti human Ki67 antibody

The monoclonal anti human-Ki67 antibody is a recombinant peptide corresponding to a 1002 bp Ki67 cDNA fragment reacting with a nuclear protein in proliferating cells (Gerdes). The isotype is IgG1 kappa and its clone: MIB-1 (Key *et al.*, 1993).

Table 2.12: Procedure for imunohistochemical staining.

PROCESS	METHOD	TIME
Rehydration	3 x Xylene	3 min
	3 x 100% Ethanol	2 min
	95%, 80%, 70% Ethanol	2 min
	Rehydrate in running tap water	10 min
	Rinse in dH$_2$O	2 min
Endogenous peroxidase quenching	3% H$_2$O$_2$	15 min
Wash	Wash in running tap water	10 min
	Rinse in dH$_2$O	2 min
Antigen retrieval	Microwave on 570W in 0.01M Citric Buffer pH 6	30 min
Block	Peroxidase Block	5 min
	2 x TBS	5 min
	Protein block	5 min
	2 x TBS	5 min
Primary antibody	mouse anti-human Ki67 antibody *(1/100) rabbit anti-human synaptopodin antibody *(1/50) mouse anti-human immunodeficiency virus p24 antibody *(1/10)	120 min
Wash	2 x TBS	5 min
Link	NovoLink Polymer	30 min
Wash	2 x TBS	5 min
Chromogen	DAB	5 min
Wash	Rinse slide in water	5 min
Nuclei stain	Hematoxylin	5min
Dehydration	Rinse in dH2O	5 min
	95%, 80%, 70% Ethanol	2 min
	3 x 100% Ethanol	2 min
	3 x Xylene	3 min
Mountant	DPX	

*Ki67 - Monoclonal mouse anti-human, clone MIB-1, Dako, Denmark, UK.
*Synaptopodin - Rabbit anti-Synpo, Sigma-Aldrich Corporation, MO.
*p24 - Monoclonal mouse anti-human immunodeficiency Virus p24, clone Kal-1, Dako, Denmark, UK.

Slides were then viewed on the Zeiss AxioScope A1 and captured on the Zeiss AxioCam ICC3 system image analyses was performed using the AxioVision 4.8.2 software (Carl Zeiss Pty Ltd, Germany).

2.5.4 Laser Microdissection

Laser capture microdissection is a method for isolating specific cells of interest from microscopic regions of tissues. Glomeruli, arteriole and tubules were microdissected using an Arcturus Pixcell II at the NIH Molecular Pathology Laboratory, SAIC-Frederick/NCI-Frederick, USA.

The biopsy tissue was snap frozen in liquid nitrogen. The frozen tissue was then sectioned using a cryostat and collected onto a slide. The area of interest was identified as targets for isolation and subsequently orientated so that it was in the centre of the field of view; it was then microdissected by means of a laser. The dissected sample then via gravity drops into a capture device. The microdissection process did not alter or damage the morphology and chemistry of the sample collected.

2.5.5 Tissue DNA extraction

DNA was extracted from the epithelial cells using the QIAamp DNA mini kit (Qiagen, Chatsworth, CA). Initially, the epithelial cells were placed in an eppendorf tube and ruptured using a hand held rotor-stator homogenizer TissueRuptor (Qiagen, Chatsworth, CA) for approximately 20 sec at maximum speed with plastic disposable probes to ensure sterility of the sample. Similarly, the DNA extraction, HIV proviral DNA quantification and sequence diversity analyses was performed on blood samples as indicated in sub-heading 2.4.2, 2.4.3 and 2.4.4.

2.6 STATISTICAL ANALYSIS

SPSS version 18 (SPSS Inc., Chicago, Illinois) was used to analyse the data. A statistical significant level was set at alpha equal 0.05. Descriptive statistics was performed for all data. Categorical variables were presented in frequency tables (No. and %). Numeric data were presented by mean, median, standard deviation, minimum, maximum, range, Quartile 1, Quartile 3 and IQR as appropriate.

Inferential statistics regarding categorical data were by means of Pearson Chi-square test (or Fischer Exact test where appropriate) to determine trends. In the case of comparing means of numeric continuous data, paired t-tests were performed. An equivalent non-parametric test was performed where data were not normally distributed.

CHAPTER 3

RESULTS

3.1 PATIENT POPULATION

3.1.1 Pre-HAART Group

A total of 30 HIV infected children presented with persistent proteinuria (pre-HAART). In keeping with the demographic profile of the local HIV epidemic in the Durban Functional Region in South Africa, 28(93.3%) of the children were Black African and 2(6.7%) were of mixed ancestory; 17(56.7%) were males and 13(43.3%) were females. The average age at presentation was 76 months (range: 10 – 159) with 12(40%); younger then 5yrs. All 30 children underwent kidney biopsy and all were commenced on anti-retroviral therapy post kidney biopsy. The demographic profile and source of referral to IALCH is shown in Table 3.1.

3.1.2 Post-HAART Group

Only 20(66.67%) childrenwere followed up for a mean period of 12 months (range: 5 - 17); 7(23.33%) died and 3(10%) were lost to follow-up, post commencement of HAART. The demographic profile for this group was 18(90%) Black African and 2(10%) children of mixed ancestory; 10(50%) were males and 10(50%) females with an average age of 81.3 months (range: 18 - 141). Nine children returned for a repeat biopsy after an average period of 12 months. Seven children demised during the follow up period, 9 were lost to follow-up, and 5 refused a repeat biopsy. Of these 9 children (repeat biopsy), 7(77.8%) were Black African and 2(22.2%) children of mixed ancestry; 5(55.6%) were males and 4(44.4%) females with an average age of 98.7 months (range: 22 - 153).

Table 3.1: Demographics of Referral Source of children with HIV related nephrophaty.

		Pre-HAART	
		Number	Percentage
Population Group:	Black	28	93.3
	Coloured	2	6.7
Gender:	Female	13	43.3
	Male	17	56.7
Mean Age:	Months	30	98.7
Referral Source:	Greys Hospital	7	23.3
	King Edward VIII Hospital	10	33.3
	Mahatma Gandhi Memorial Hospital	2	6.7
	Ngwelezane Hospital	1	3.3
	Prince Mshiyeni Memorial Hospital	8	26.7
	Port Shepstone Hospital	1	3.3
	Stanger Hospital	1	3.3
	Total	30	100.0

3.1.3 Clinical data of Pre-HAART Group

The clinical data for the pre-HAART group is outlined in Table 3.2. Twelve (40%) children had severe range proteinuria, 12(40%) moderate and 6(20%) presented with mild proteinuria. Microscopic haematuria was present in 15(50%) children together with proteinuria. Of the twelve (40%) children presenting with nephrotic syndrome only 2 had anasarca. Five (16.7%) children had hypertension on initial presentation. The mean systolic blood pressure on initial presentation was 108±8 mmHg and diastolic blood pressure of 64±9 mmHg.

All children had growth retardation at initial presentation. Other co-morbidities included 2(6.67%) children with gastroenteritis, 1(3%) bronchopneumonia, 1(3.33%) child had *Pneumocystis jiroveci pneumonia*, 12(40%) pulmonary *Mycobacterium tuberculosis* infection and 1(3%) child had chicken pox. None had evidence of urinary tract infection. None of the children had co-existing infections with cytomegalovirus, Epstein Barr virus, parvo virus, herpes simplex virus and hepatitis A, B, and C. Two (6.67%) had generalised

lymphadenopathy, 2(6.67%) chronic lung disease, 2(6.67%) cardiac disease (cardiomyopathy or myocarditis) and 1(3%) child had marasmus.

All patients had haematological abnormalities on initial presentation; 20(66.7%) had anaemia, 12(40%) leucocytosis and 5(16.7%) had thrombocytopenia. Biochemical hepatitis was present in 8(26.7%) children. On initial presentation, 1(3.3%) child had hypocomplementaemia (low C3 and/or C4), 9(30%) hypercholesterolaemia and all had hypergammaglobulinaemia. Biochemical abnormalities present in 22(73.3%) children included: 5(16.7%) children with hyponatraemia, 5(16.7%) hypokalaemia, 2(6.7%) hyperchloraemia, 4(13.3%) hypocalcaemia, and 4(13.3%) having hypophosphataemia. Ten (33.3%) children on initial presentation had systemic acidosis based on a low serum bicarbonate level (<22μmol/L).

Ultrasonography was performed on all children prior to biopsy and showed increased echogencity in 7(23.3%) and an increase in kidney size above the mean corrected for height in 8(26.7%).

Fourteen (46.67%) children had Stage II to V chronic kidney disease on initial presentation: 2(7%) Stage II disease, 3(10%) Stage III disease, 5(17%) Stage IV and 4(13%) children had end stage kidney disease (Stage V).

The mean CD4 count in 19 children done at initial presentation in was 403 cells/μL (range: 28 - 793) and the mean viral load was 232161 copies/μL (range: 19 – 2900000). Seven (23.3%) had a CD4 count less than 350 cells/μL and in 9(30%) children the viral load was greater than 1000 copies/μL.

3.1.4 Histopathological spectrum of HIVRN in Pre-HAART

A histopathological spectrum of 30 HIVRN children who underwent kidney biopsy is shown in Figure 3.1. The commonest histopathological form of HIVRN in children in KwaZulu-Natal was classical FSGS present in 13(43.33%) (Figure 3.2 - 3.4); followed by mesangial hypercellularity 10(30%) (Figure 3.5 -3.7); HIVAN 3(11%) (Figure 3.8 -3.12) and MCD 2(6.67%) (Figure 3.13 - 3.14).
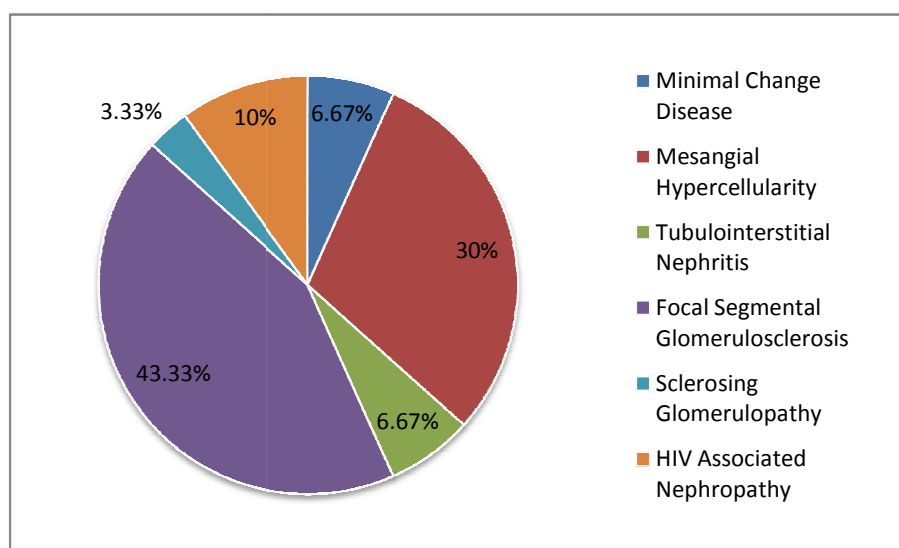
Figure 3.1: Histopathological spectrum of pre-HAART children with HIV-related nephropathy.

3.1.5 Treatment

HIV treatment given was based on the Department of Health guidelines for the Province of KwaZulu-Natal. Additional therapy included angiotensin converting enzyme antagonists, diuretics in those children with oedema and/or persistent hypertension and vitamin supplementation. Child with chronic kidney disease stage III or more had correction of acid base balance, electrolytes and dietary reduction of protein in accordance with K/DOQI guidelines used as anti-renal failure therapy. None of the patients were managed with renal replacement therapy. None of the patients on HAART were resistant to first line anti-retroviral therapy.
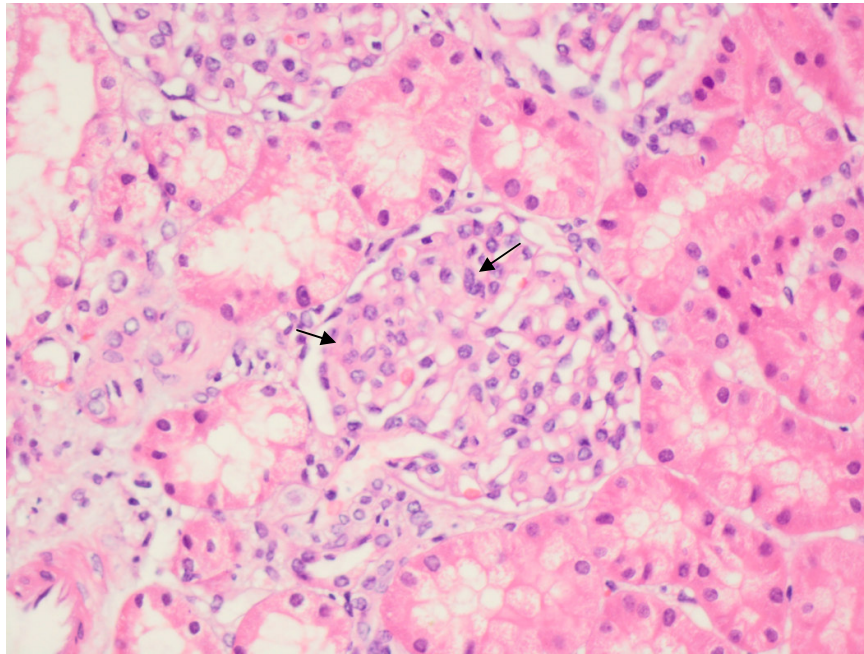
Figure 3.2: Light micrograph of Haematoxylin & Eosin stained section showing an increase in mesangial cells (arrows) in a segmental distribution.
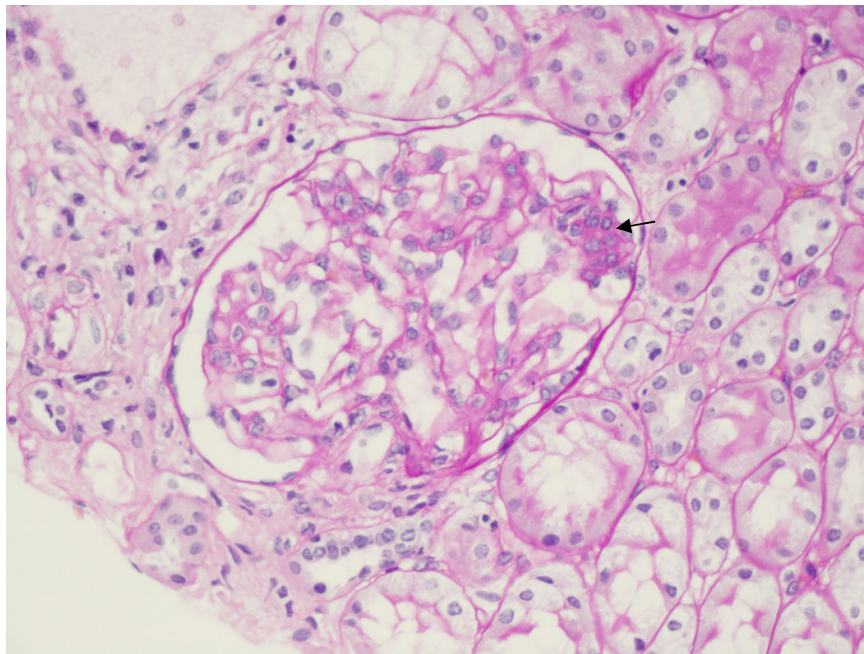
Figure 3.3: Light micrograph of Periodic acid-Schiff stain showing segmental mesangial hypercellularity (arrow).
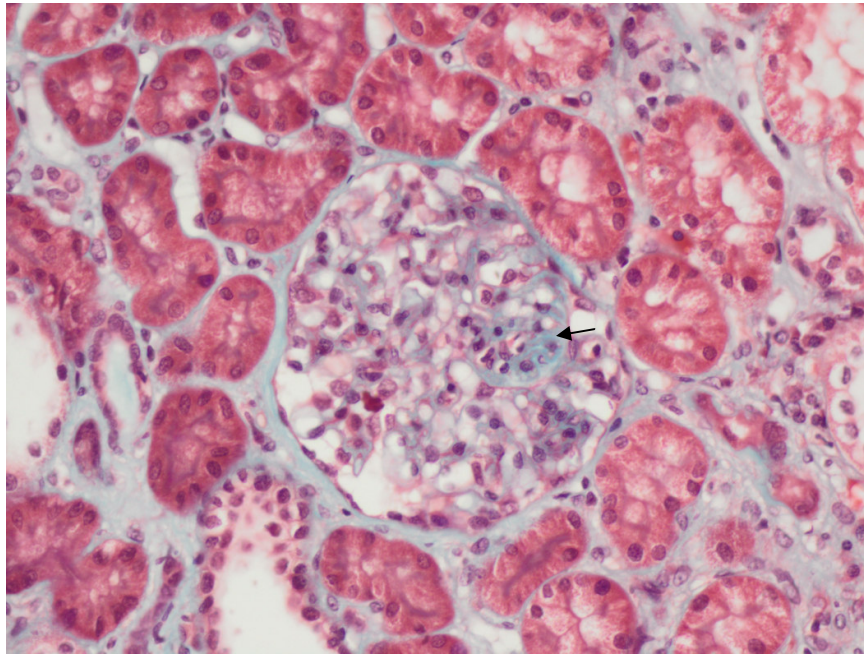
Figure 3.4: Light micrograph of stain Masson's trichrome illustrating mesangium increase (arrow).
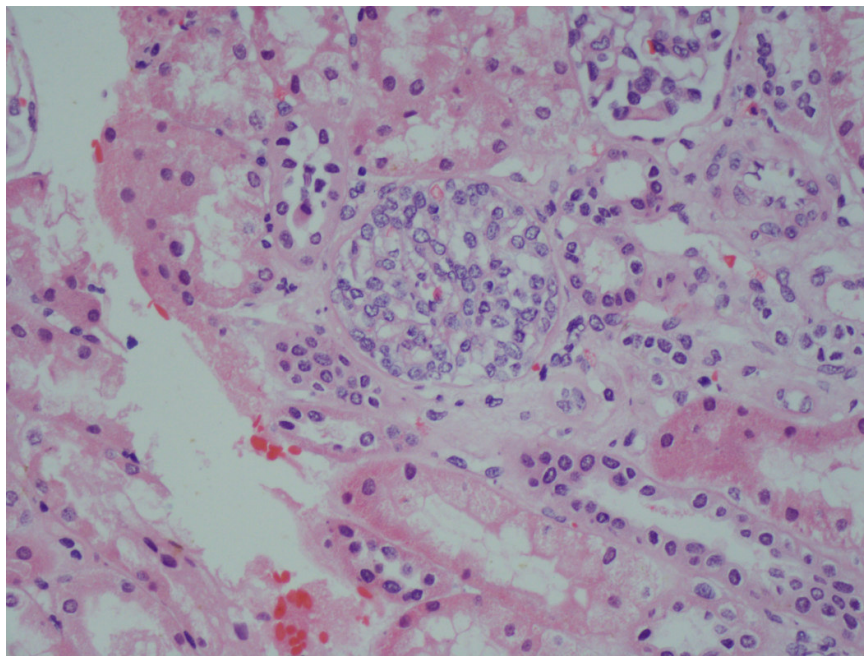
Figure 3.5: Light micrograph of Haematoxylin & Eosin stained section depicting mesangial hypercellularity of glomeruli.
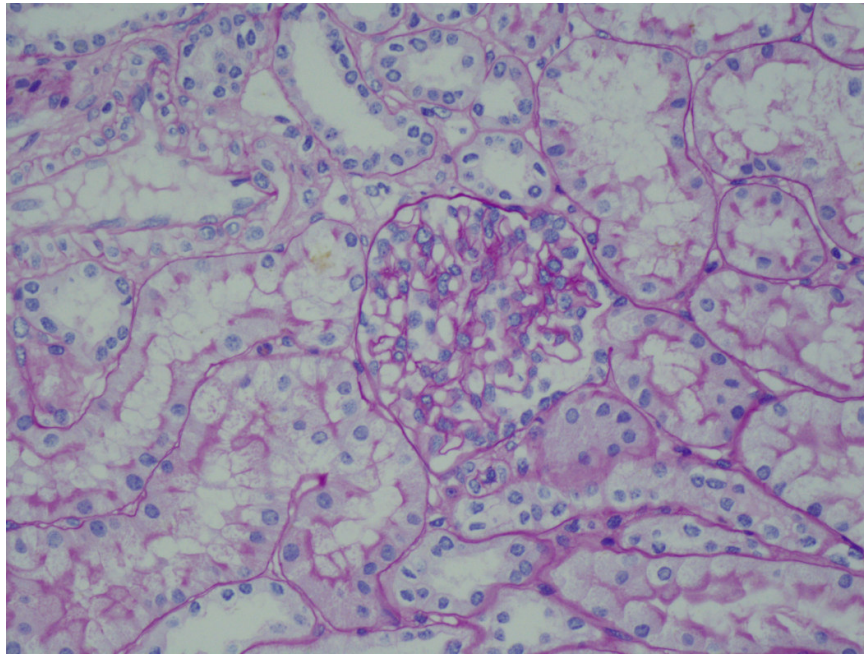
Figure 3.6: Light micrograph of Periodic acid-Schiff stained section depicting segmental mesangial hypercellularity.
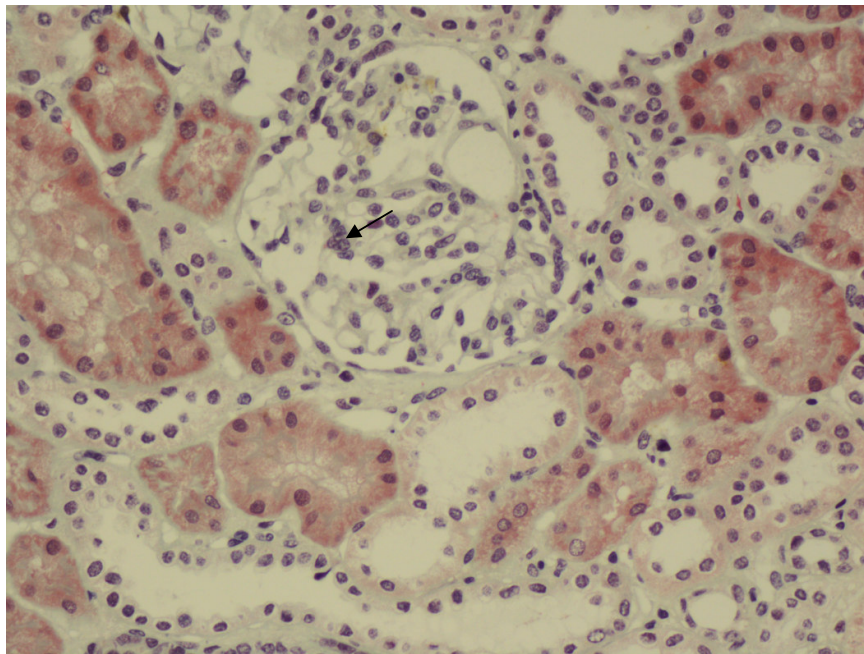
Figure 3.7: Light micrograph of Masson's trichrome stained section illustrating focal mesangial hypercellularity (arrow).
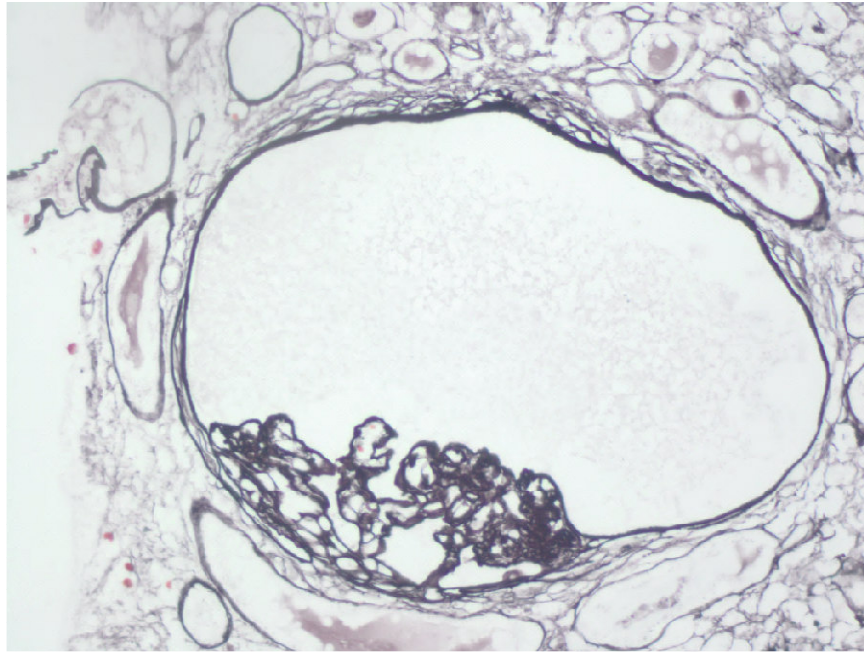
Figure 3.8: Light micrograph of Methenamine stained section illustrating extensive glomerular tuft collapse with pseudocresent absence.
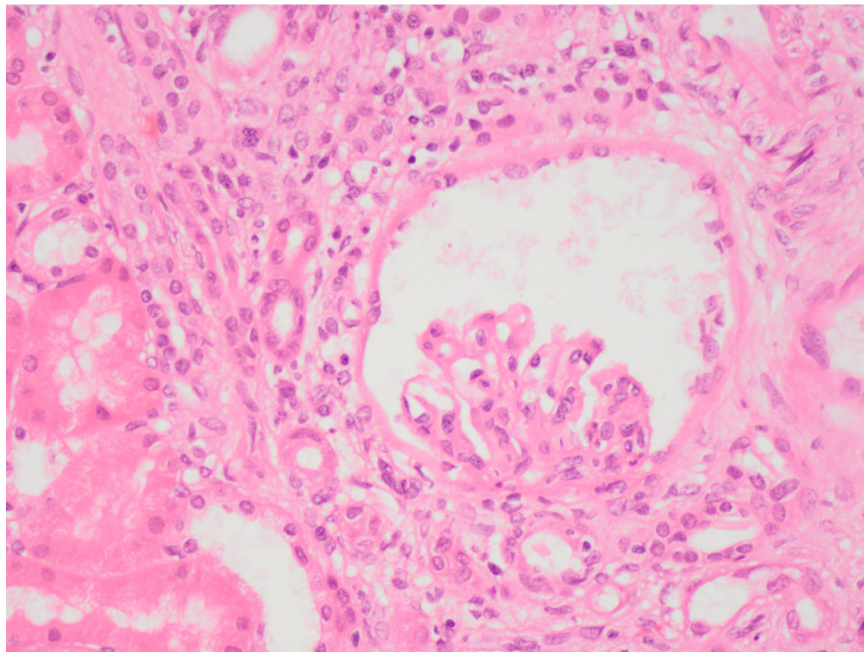
Figure 3.9: Light micrograph of Haematoxylin & Eosin stained section showing collapse of glomerular capillaries.
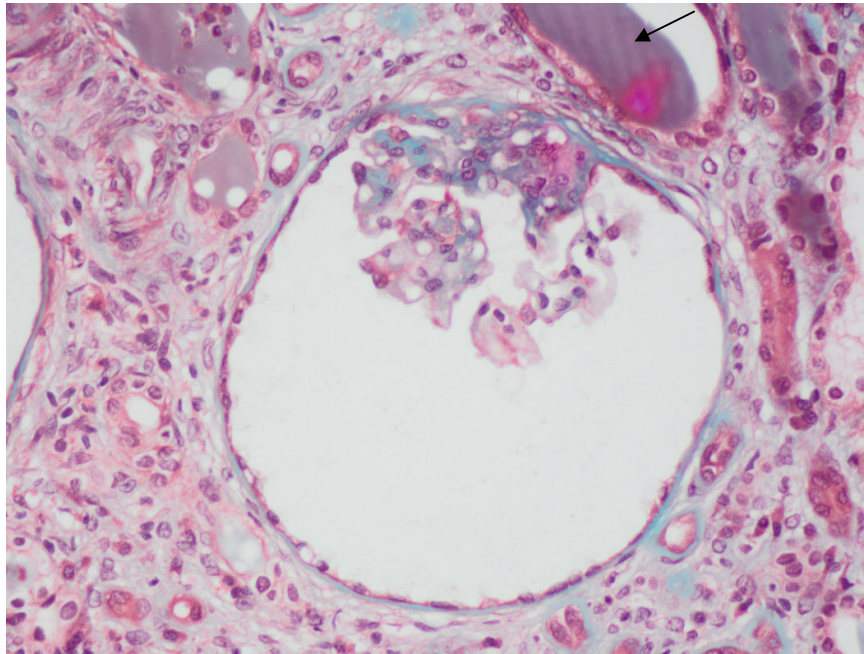
Figure 3.10: Light micrograph of Masson's trichrome stained section showing the collapsing glomerulopathy. Note tubular cast (arrow).
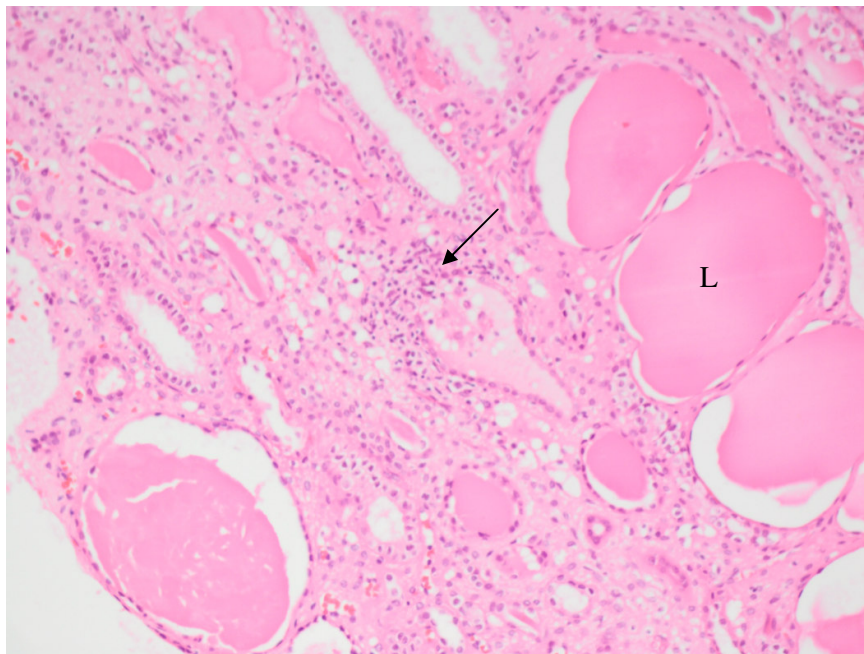
Figure 3.11: Light micrograph of Haematoxylin & Eosin stain showing dilated tubular lumina (L) with eosinophilic casts. Note tubular-interstitial inflammation (arrow).
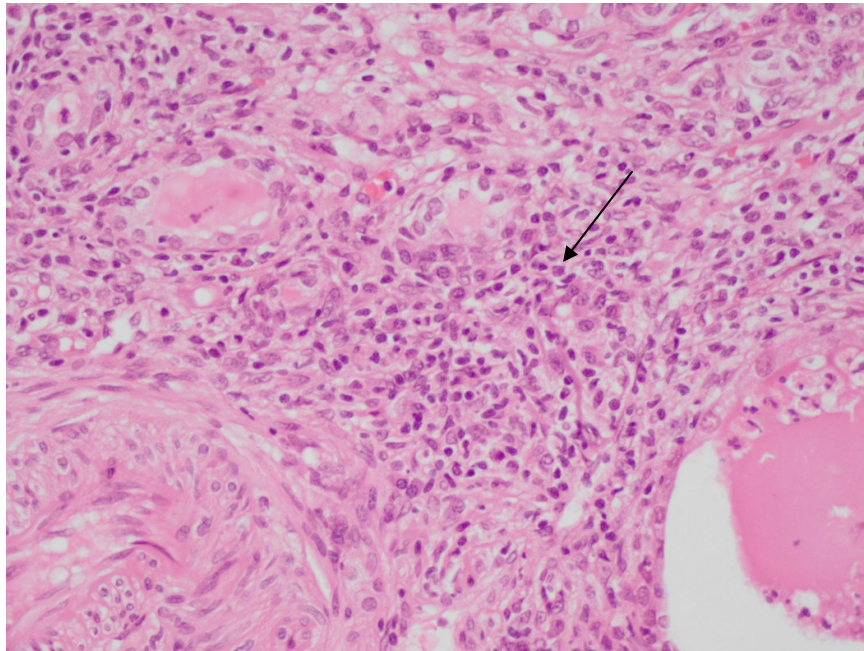
Figure 3.12: Light micrograph of Haematoxylin & Eosin stained section depicting polymorphonuclear lymphocytes in tubular-interstitium (arrow).
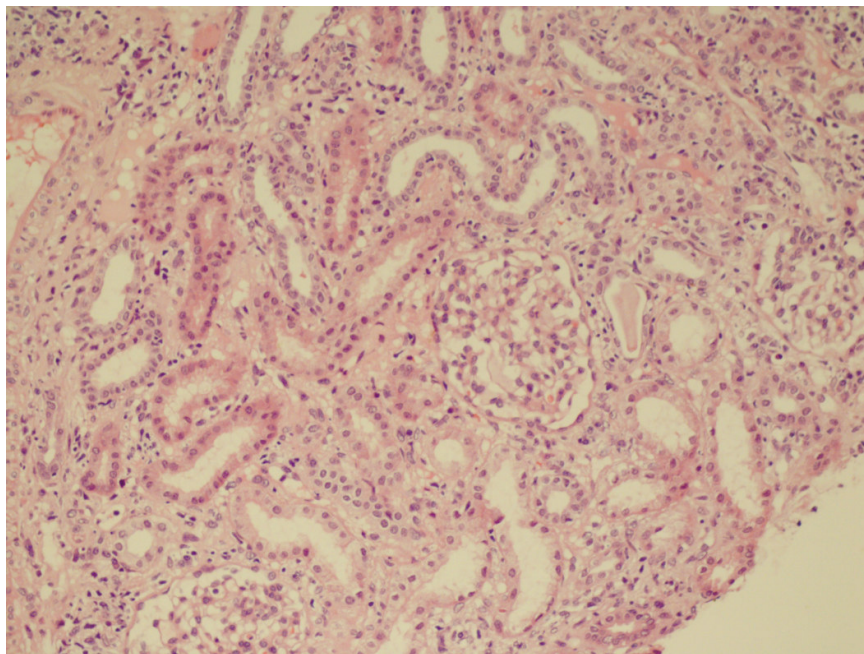
Figure 3.13: Light micrograph of Haematoxylin & Eosin stain normal appearing glomeruli.
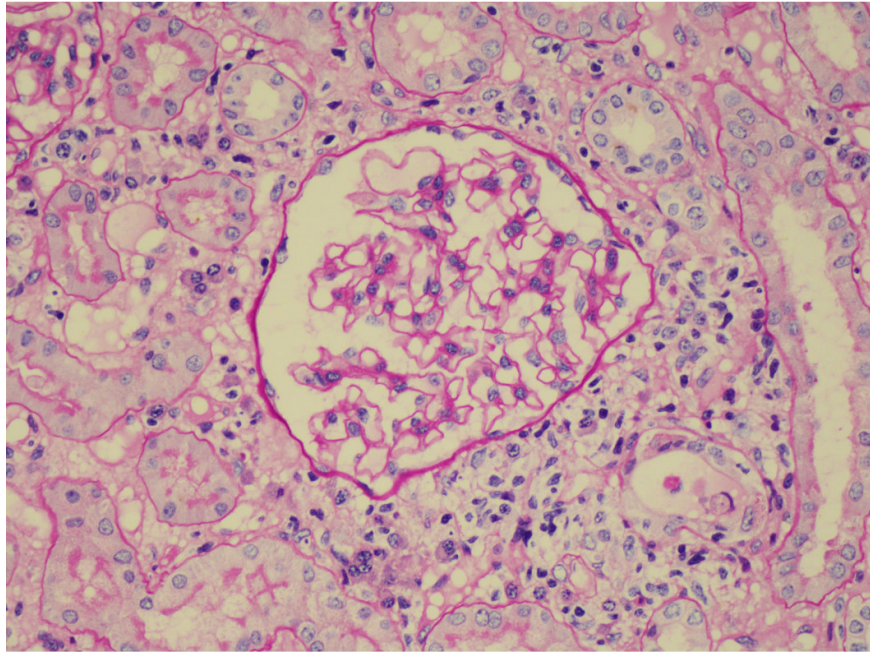
Figure 3.14: Light micrograph of Periodic acid-Schiff stained section glomeruli with MCD.

3.1.6 Clinical data of Post-HAART Group

The clinical data for this group is outlined in Table 3.2. None of the children post-HAART presented with persistent hypertension. The mean systolic blood pressure was 114±7 mmHg and diastolic blood pressure was 66±8 mmHg.

At the last hospital visit 13(65%) had total abrogation of proteinuria following treatment, 3(15%) had mild range proteinuria. Four (13.3%) children who failed to respond to treatment had progressive deterioration of renal function despite treatment and at the last hospital visit 1(5%) child was in end stage kidney disease with a blood urea of 33.4 mmol/L and serum creatinine of 694 μmol/L. All 16 children with complete remission, and mild proteinuria on follow-up had preservation of their renal function

Fourteen (70%) patients had haematological abnormalities in the post-HAART group; 4(20%) had anaemia, 9(45%) leucocytosis and 1(5%) had thrombocytopenia. Biochemical hepatitis was present in 1(5%) child. Post-HAART no child had hypocomplementaemia, 2(10%) hypercholesterolaemia and 4(20%) hypergammaglobulinaemia. Electrolyte abnormalities were present in 4(20%) children and included: 2(10%) hyponatraemia, 1(5%) hyperchloraemia, 1(5%) hypocalcaemia. Two (10%) had mild persistent systemic acidosis (HCO_3: 18 - 22 mmol/L) despite correction. None of the children had hypophosphataemia or hypokalaemia.

Ultrasonography showed 1(5%) child had increased echogencity in the post-HAART group and 2(10%) children had an increased kidney size above the mean corrected for height.

On last hospital visit 7(35%) children had Stage II to V chronic kidney disease: 3(15%) Stage II disease, 2(10%) Stage III disease, 1(5%) Stage IV and 1(5%) child had end stage kidney disease (Stage V). Of the fourteen children pre-HAART that had chronic kidney disease following HAART 3(21.4%) of the children in the post HAART group had improvement in their kidney function.

On the last recorded follow-up visit the mean CD4 count was 540 cells/µL (range: 181 - 793) and mean viral load 55273 copies/µL (range: 19 - 977011).

Table 3.2: Comparison of children Pre and Post-HAART with HIV related nephropathy.

Test	Pre-HAART (N = 30)			Post-HAART (N = 20)			P Value	Post-Biopsy (N = 9)			P Value
	Mean	Range or %	Std Dev(σ)	Mean	Range or %	Std Dev(σ)		Mean	Range or %	Std Dev(σ)	
Clinical:											
Age (months)	75	(5 – 158)	49	81.3	(18 – 141)	41	0.070	98.7	(22 – 153)	49	0.091
Weight (kg)	19.38	(4.80 -44.10)	9.50	22	(7 – 50)	11	0.007	21.7	(9 – 37)	8.9	0.014
Height (cm)	110	(30 – 151)	28	123	(36 – 153)	30	0.638	107	(36 – 153)	32.5	0.983
Body Surface Area (m^2)	0.76	(0.27 – 1.36)	0.28	0.81	(0.33 – 1.46)	0.30	0.062	0.79	(0.33 – 1.22)	0.28	0.062
Oedema	2	(1 – 3)	2	2	(1 – 2)	2	0.000	0	0	0	0.023
Stunted	10	33%	-	9	45%	-	0.000	4	45%	-	0.422
Wasting	6	20%	-	1	5%	-	0.154	1	11.1%	-	0.366
Blood Pressure:											
Systolic (mmHg)	108	(87 – 174)	8	114	(81 – 191)	7	0.781	111	(82 – 123)	8	0.458
Diastolic (mmHg)	64	(41 – 90)	9	66	(32 – 135)	9	0.829	59	(50 – 78)	7	0.695
Urine Dipstick:											
pH	5	(5 – 6)	3	6	(5 – 6)	3	0.324	5.75	(5 – 8)	1.16	0.405
SG	1020	(1010 – 1020)	5.2	1015	(1010 – 1020)	5	0.408	1020	(1010 – 1030)	5.3	0.227
Leucocytes	0	(0 – 0)	0	1	(0 – 3)	2	1.000	0	(0 – 0)	0	1.000
Nitrites	0	(0 – 0)	0	0	(0 – 0)	0	1.000	0	(0 – 0)	0	1.000
Blood	1	(1 – 3)	2	1	(0 – 3)	1	0.036	0.5	(1 – 4)	1.33	0.178
Protein	2	(1 – 4)	1	1	(1 – 2)	1	1.000	0.1	(0 – 1)	0.33	0.003
Extrarenal opportunistic infections											
Acute gastroenteritis	2	67%	-	0	0%	-		0	0%	-	
Chickenpox	1	3%	-	0	0%	-	0.0187	0	0%	-	0.012
Chronic lung disease	2	7%	-	0	0%	-	(t-test)	0	0%	-	(t-test)
bronchcopneumonia	1	3%	-	0	0%	-		0	0%	-	
Pulmonary tuberculosis	12	40%	-	0	0%	-		0	0%	-	
Haematology											
Haemoglobin (g/dL)	9.5	(4.8 - 14.0)	2.3	11	(7 - 13)	2	0.369	10.8	(7 - 13)	2.1	0.436
Platelets (x10^9/L)	300.60	(105 – 482)	173.91	360	(25 - 714)	159	0.632	362	(276 - 459)	94	0.647
White Cell Count (x10^9/L)	8	(5.14 – 12.74)	11	8.36	(6.23 - 11.33)	8.60	0.651	7.2	(5 - 10)	27	0.802

3.1.7 Comparison of children Pre-HAART *vs.* Post-HAART

Persistent proteinuria significantly decreased in the post-HAART group with only 3(15%) children having mild range proteinuria ($p = 0.003$). On initial presentation (pre-HAART) 15(50%) children had microscopic haematuria following treatment and 12 (60%) children did not present with microscopic haematuria. However, 3 children with persistent mild range protein had microscopic haematuria. None of the children post-HAART presented with persistent hypertension ($p < 0.0001$). Co-morbid manifestations of HIV-1 present in 5(16.6%) children pre-HAART e.g. (generalised lymphadenopathy, cardiac disease and marasmic) was not present in any of the children in the post-HAART group. Pre-HAART all children had growth retardation at initial presentation and following appropriate treatment 2(10%) children attained linear growth above the 3rd centile corrected for age and sex after an average of 12 months.

Haematological abnormalities were present in all of the children pre-HAART and in 14(70%) children post-HAART: [20(66.7%) *vs.* 4(20%) $p < 0.0001$] had anaemia, [12(40%) *vs.* 9(45%) $p = 0.0819$] leucocytosis and [5(16.7%) *vs.* 1(5%) $p = 0.0161$] had thrombocytopenia. A biochemical hepatitis was present in 8(26.7%) children pre-HAART and in 1(5%) child post-HAART ($p = 0.0002$). One (3.3%) child in the pre-HAART group presented with hypocomplementaemia but this corrected to normal post-HAART. Hypercholesterolaemia in the pre-HAART *vs.* post-HAART group significantly decreased [9(30%) *vs.* 2(10%) $p = 0.0007$] as did hypergammaglobulinaemia [30(100%) *vs.* 4(20%) $p < 0.0001$].

Comparison of electrolyte abnormalities in the pre *vs.* post-HAART groups showed differences for the following: hyponatraemia [5(16.7%) *vs.* 2(10%) $p = 0.016$],

hypokalaemia [5(16.7%) *vs.* 0(0%) $p < 0.05$] and hypophosphataemia [4(13.3%) *vs.* 0(0%) $p < 0.05$]. No differences in the groups were noted for hyperchloraemia [2(6.7%) *vs.* 1(5%) $p = 0.181$] and hypocalcaemia [4(13.3%) *vs.* 1(5%) $p = 0.057$]. Systemic acidosis was present in 10(33.3%) children pre-HAART *vs.* 2(10%) children post-HAART showing a significant improvement ($p = 0.0002$).

Ultrasonography was performed on all patients prior to biopsy and on comparison there were a significant differences with regard to increased echogencity pre *vs.* post-HAART (7 *vs.* 1; $p = 0.001$) and increase in kidney size above the mean corrected for height (8 *vs.* 2; $p = 0.0025$). Figure 3.15-3.16 shows the ultrasound of a child pre and post-HAART respectively.

Chronic kidney disease staging for pre *vs.* post-HAART was as follows: Stage II [2(7%) *vs.* 3(15%); p = 0.422], Stage III [3(10%) *vs.* 2(10%); p = 0.422], Stage IV [5(17%) *vs.* 1(5%); p = 0.016], and [4(13%) *vs.* 1(5%); p = 0.057], children had end stage kidney disease (Stage V).

The mean CD4 count at initial presentation (pre-HAART) was 403 cells/µL (range: 28 - 793) and the mean viral load was 232161 copy/µL (range: 19 – 2900000). In the post-HAART group at last hospital visit the mean CD4 count increased to 540 cells/µL (range: 181 - 793) and mean viral load decreased to 55273 copy/µL (range: 19 - 977011). On comparison of both these parameters at initial presentation and last recorded follow-up visit there were no statistically significant difference ($p = 0.168$ and $p = 0.767$ respectively).
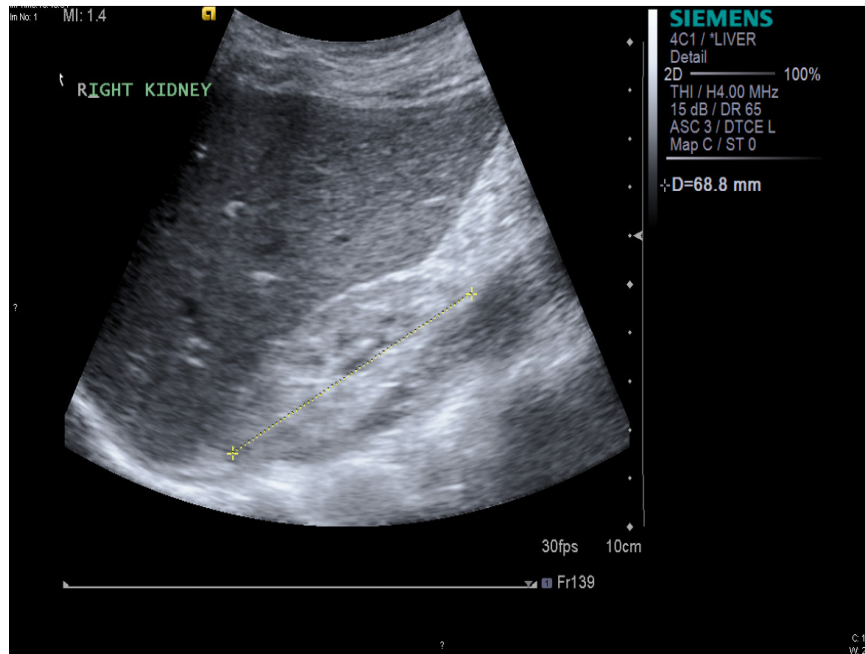
Figure 3.15: Ultrasound image of the right kidney from a patient with HIV infection pre-HAART; the kidney measured 68.8mm.
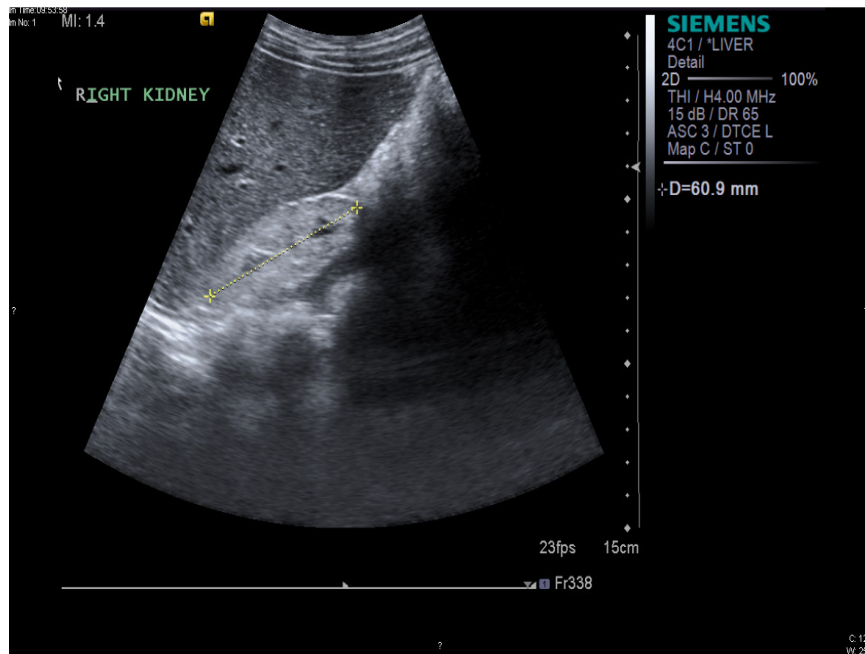
Figure 3.16: Ultrasound image of the same kidney (Figure 3.1) one year later *ie*., post -HAART; the kidney measured 60.9mm.

3.1.8 Histopathological spectrum of HIVRN in Post-HAART biopsy group

Nine children returned post-HAART and re-consented for repeat biopsy. The histopathological spectrum of post-HAART is illustrated in Figure 3.17 in which the commonest microscopic finding was mesangial hypercellularity present in 55.56% of children; 33.33% having FSGS and 11.11% sclerosing glomerulopathy.
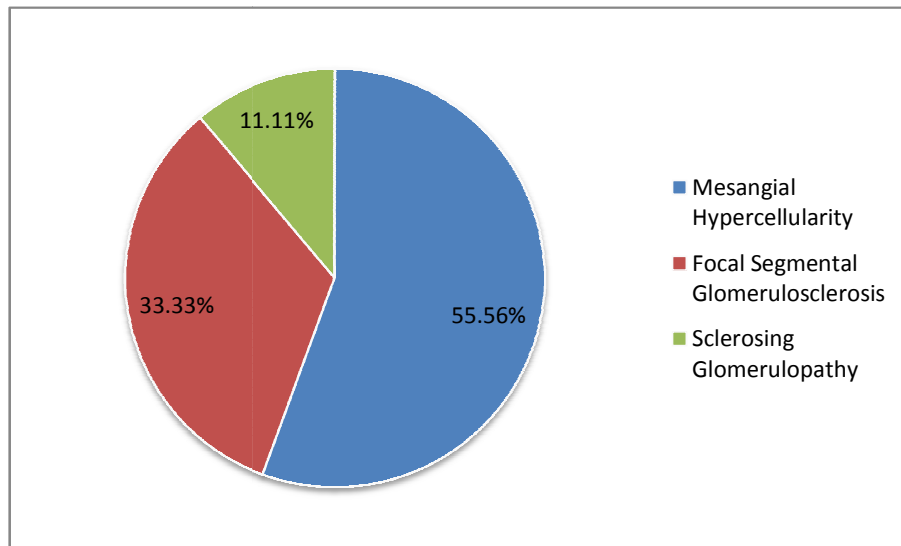
Figure 3.17: Histopathological spectrum of post -HAART children with HIV-related nephropathy.

3.1.9 Comparison of matched Pre-HAART Biopsy *vs.* Post-HAART Biopsy

Comparison of the histopathological spectrum of children pre and post-HAART (9 children) showed a difference in histopathology in only two children, one child with tubulointerstitial nephritis on post biopsy was found to have mesangial hypercellularity and another with MCD was found to have mesangial hypercellularity.

3.2 SYNAPTOPODIN, KI67 AND P24 IMMUNOREACTIVITY

3.2.1 Pre-HAART Synaptopodin

Human brain tissue served as the positive control displaying immunoprecipitation within telencephalic dendrites (Figure 3.18). Replacement of anti-synaptopodin antibody with a non-immune sera of the same IgG class produced no immunoreaction (negative control; Figure 3.19). Similarly, replacement of the antibody with Tris buffered saline (TBS) produced no immune reaction. Anti-synaptopodin antibody was immunolocalised within glomerular podocytes in the pre-HAART group (Figure 3.20 - 3.21). Tubular distribution of synaptopodin was absent.

3.2.2 Post-HAART Synaptopodin

The immunolocalisation of synaptopodin was similar to the pre-HAART group. Immunoreactivity was observed within glomerular podocytes (Figure 3.22 - 3.23) but absent in tubules.

3.2.3 Morphometric image analysis of synaptopodin Pre *vs.* Post-HAART

The immunostaining pattern of synaptopodin within the glomerulus expressed as a mean field area percentage was significantly down-regulated in the pre-HAART compared to the post-HAART group (1.14 *vs.* 4.47%; p= 0.0068; Figure 3.24). The mean field intensity of the staining reaction within the pre-HAART group compared to the post-HAART group was 1025 (range: 628 - 1221) *vs.* 685 densitometric unit (range: 167 – 1003; p<0.0001; Figure 3.24).
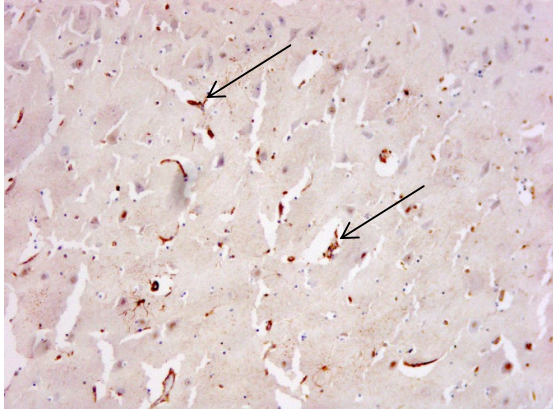
Figure 3.18: Positive control - telencephalic dendrites (arrow). Init Mag X 20.
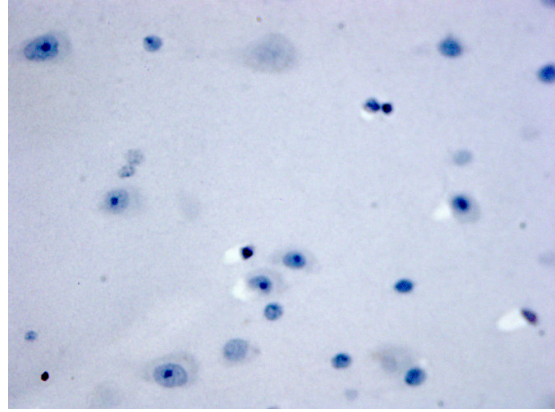
Figure 3.19: Negative control - telencephalic dendrites. Init Mag X 100.
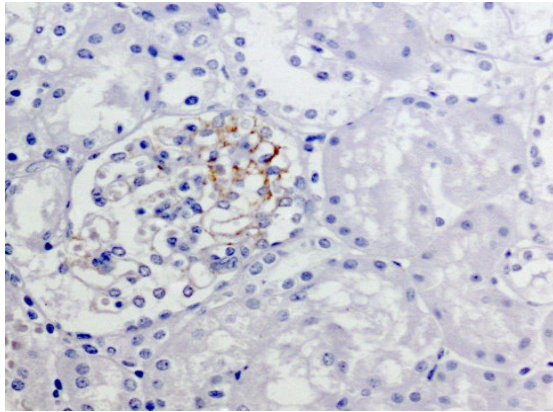
Figure 3.20: Pre-HAART - segmental glomerular immunoreactivity of synaptopodin. Init Mag X 40.
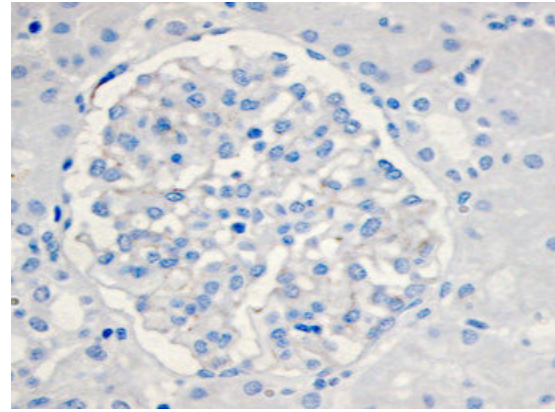
Figure 3.21: Pre-HAART - Mild to absent immunoreactivity of synaptopodin. Init Mag X 40.
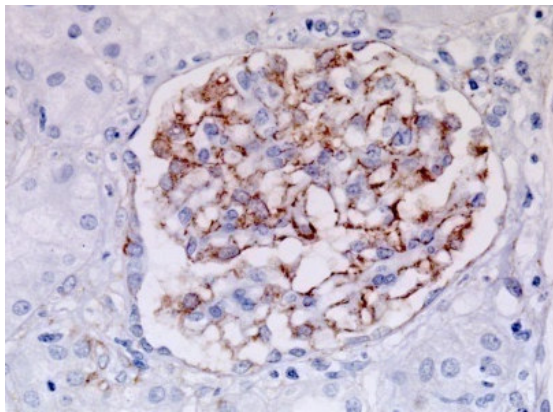
Figure 3.22: Post-HAART – globally diffuse immunoreactivity of synaptopodin within podocytes. Init Mag X 40.
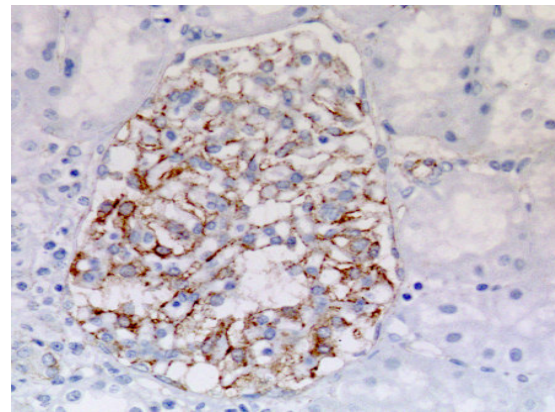
Figure 3.23: Post-HAART - globally diffuse immunoreactivity of synaptopodin within podocytes. Init Mag X 40.
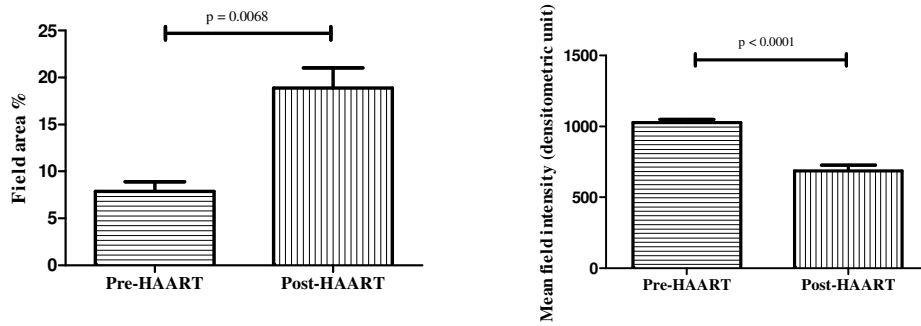
Figure 3.24: Histogram illustrating glomerular mean field area and intensity distribution of synaptopodin.

3.2.4 Pre- HAART Ki67

Ki-67, a nuclear cell cycle protein was expressed within the U87 human glioblastoma cell line and served as the positive control (Figure 3.25). An additional positive control from a patient with a hind gut carcinoma produced positive reactivity within proliferating cells (Figure 3.26). Replacement of the primary antibody with an low immune serum of the same IgG class in the U87 human glioblastoma cell line was non-reactive (negative control; Figure 3.27). In the pre HAART group, Ki67 immunoreactivity was observed within focal and segmental glomerular proliferating visceral epithelial cells/podocytes (Figure 3.28) as well as within parietal epithelial cells (Figure 3.29) and occasionally within tubular epithelial cells (Figure 3.30).

3.2.5 Post-HAART Ki67

There was an absence of Ki-67 immmunoreactivity within the glomerular and tubular cells (Figure 3.31 - 3.32).

3.2.6 Morphometric image analysis of Ki67 Pre *vs.* Post-HAART

The immunoreactivity of Ki-67 within the glomerulus expressed as a mean field area percentage was significantly down-regulated in the post-HAART group (1.01 *vs.*4.68; $p < 0.001$; Figure 3.33). The mean field intensity of the staining reaction expressed as a densitometric unit was similar in the pre-HAART group compared to the post-HAART 1162 (range: 657 - 1312) *vs.* 1116 (range: 1015 - 1229); ($p = 0.1278$; Figure 3.33).
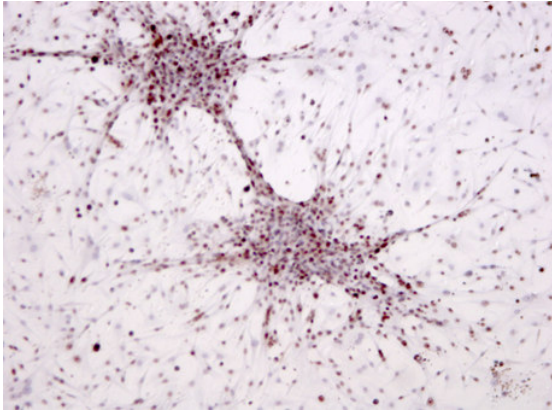
Figure 3.25: U87 glioblastoma cell line - positive control (NIH, Washington DC, USA). Init Mag X 10.
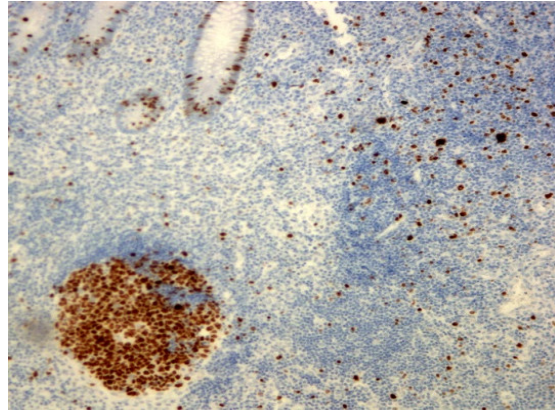
Figure 3.26: Hind gut carinnoma - positive control. Init Mag X 10.
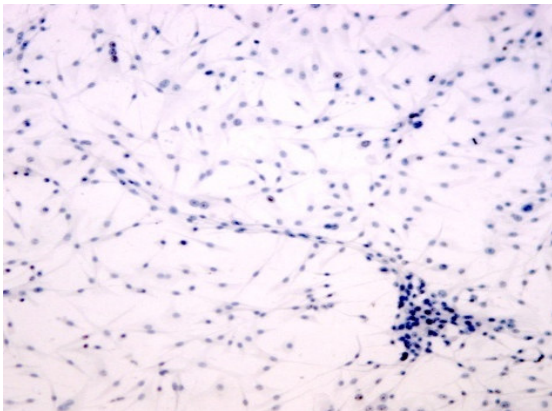
Figure 3.27: U87 human glioblastomacell line - Negative control. Init Mag X 10.
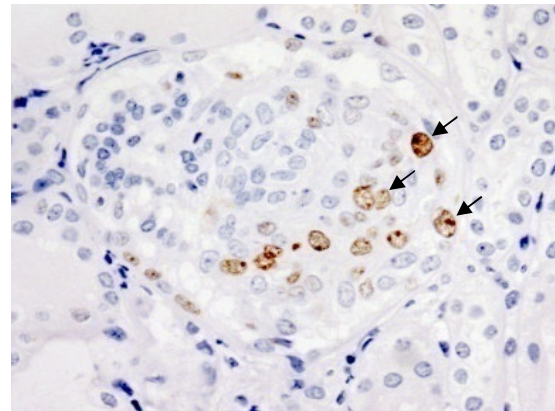
Figure 3.28: Pre-HAART - Ki67 antibody staining the specific tubular epithelial cells (brown). Init Mag X 40.
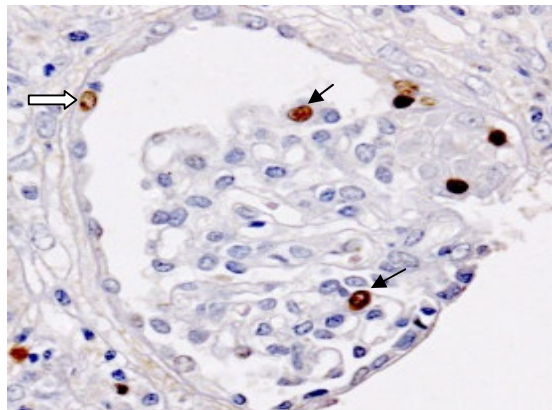
Figure 3.29: Pre-HAART - Ki67 immuno-precipitation within parietal (open arrow) and visceral epithelial cells (arrows). Init Mag X 40.
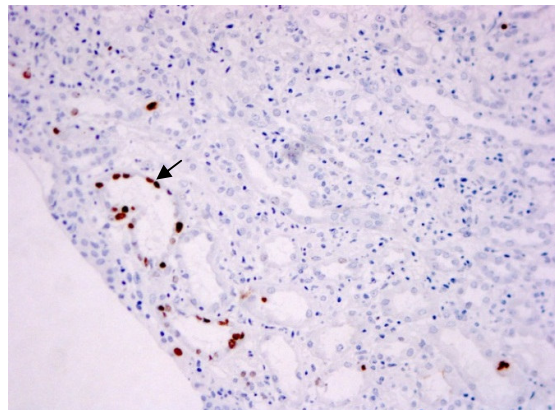
Figure 3.30: Ki67 immunoprecipitation within distal tubular epithelial cells (brown). Init Mag X 20.
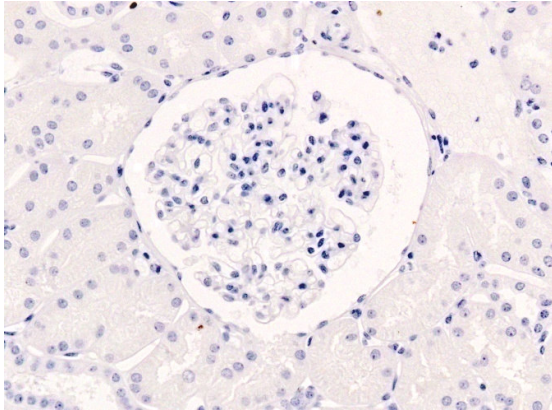
Figure 3.31: Post-HAART - Absence of Ki67 immunoreactivity. Init Mag X 40.
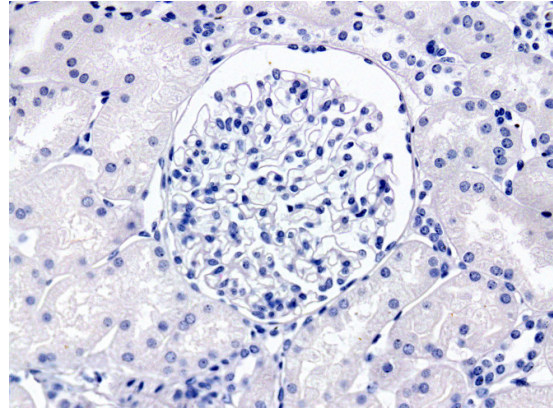
Figure 3.32: Post-HAART - Absence of Ki67 immunoreactivity. Init Mag X 40.
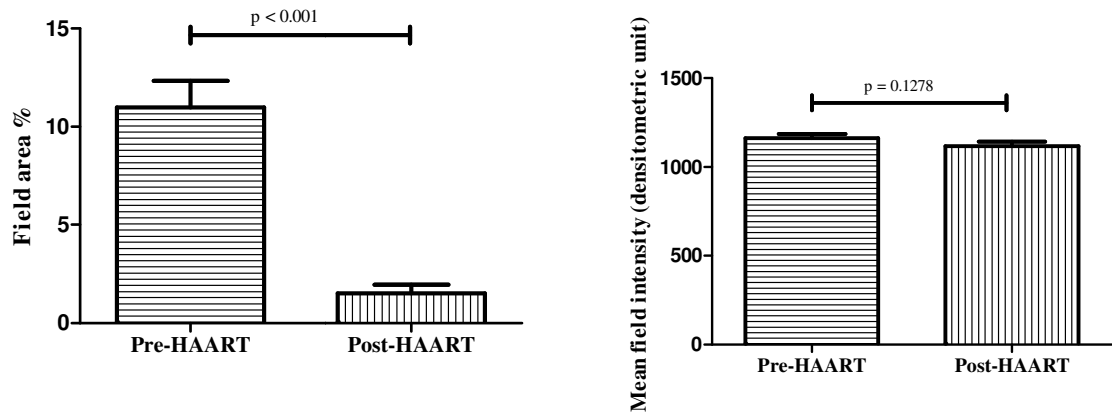
Figure 3.33: Histogram illustrating glomerular mean field area and intensity distribution of Ki67.

3.2.7 Pre-HAART p24

Sections of HIV infected lymph nodes were used as a positive control (Figure 3.34). Replacement of the primary antibody with non-immune serum of the same IgG class revealed an absence of immunoreactivity (Figure 3.35; negative control). A punctate distribution of the p24 HIV-1 viral core protein was observed within epithelial cells of glomeruli and tubules (Figure 3.36 – 3.37). Additionally, immunoprecipitation was noted within lymphocytes.

3.2.8 Post-HAART p24

Weak to nil immunprecipitation was obscured in podocytes (Figure 3.38 – 3.39).

3.2.9 Morphometric image analysis of p24 Pre *vs.* Post-HAART

In the post-HAART group, the mean field area percentage of p24 immunoreactivity in the glomerulus was significantly down regulated compared to the pre-HAART group (1.4 *vs.* 4.5%; p = 0.0035; Figure 3.40). The mean intensity of staining expressed as a densitometric unit was 1116 (range: 847 - 1315) in the pre-HAART group and 854 (range: 854 - 1319) in the post-HAART group (p= 0.2473; Figure 3.40).
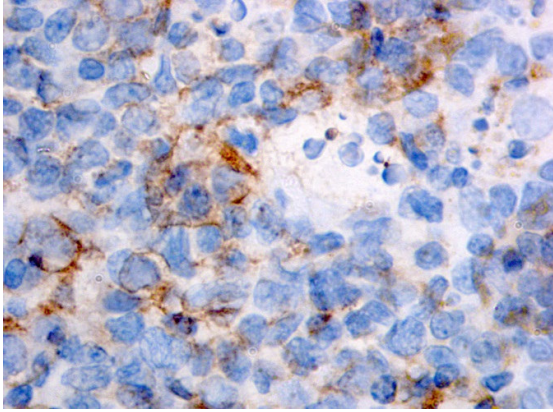
Figure 3.34: Lymph node negative control. Init Mag X 100.
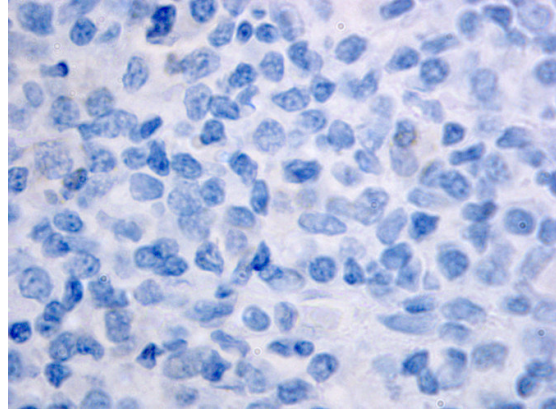
Figure 3.35: Lymph node negative control. Init Mag X 100.
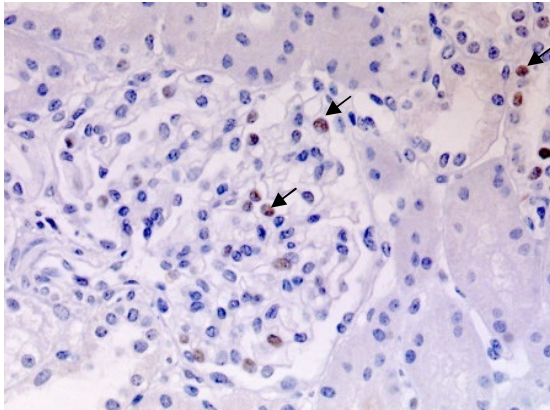
Figure 3.36: Pre-HAART - p24 immunoreactivity within the glomeruli and tubular cells (arrows). Init Mag X 20.
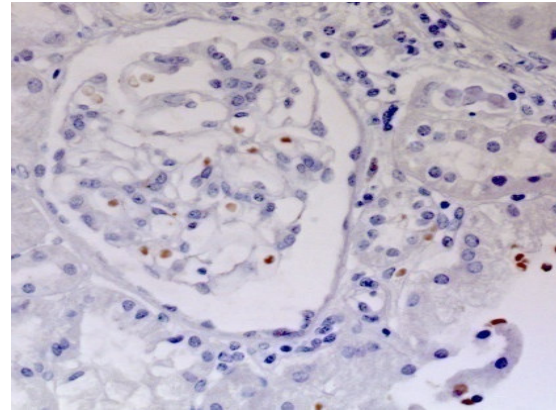
Figure 3.37: Pre-HAART - p24 immunoreactivity within the epithelials cells of glomerulus. Init Mag X 40.
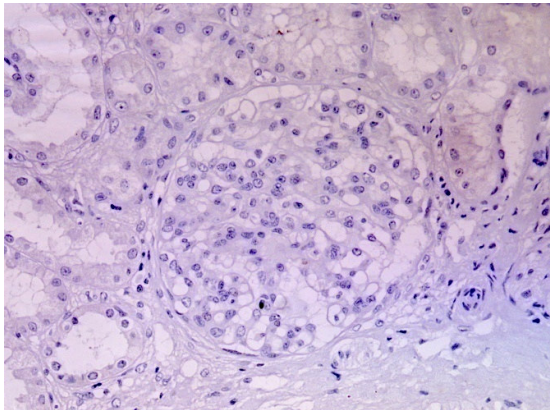
Figure 3.38: Post-HAART - absence of p24 immunoreactivity within renal biopsy. Init Mag X 40.
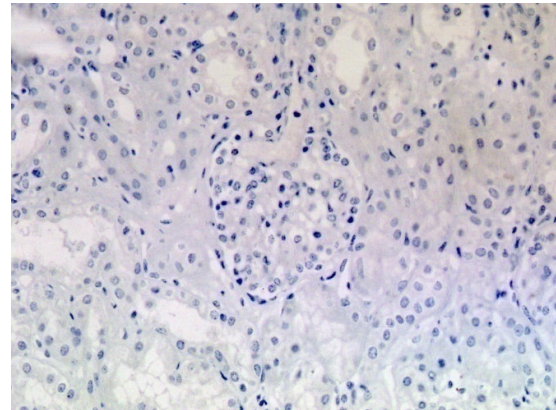
Figure 3.39: Post-HAART - weak p24 immunoreactivity within renal biopsy. Init Mag X 40.
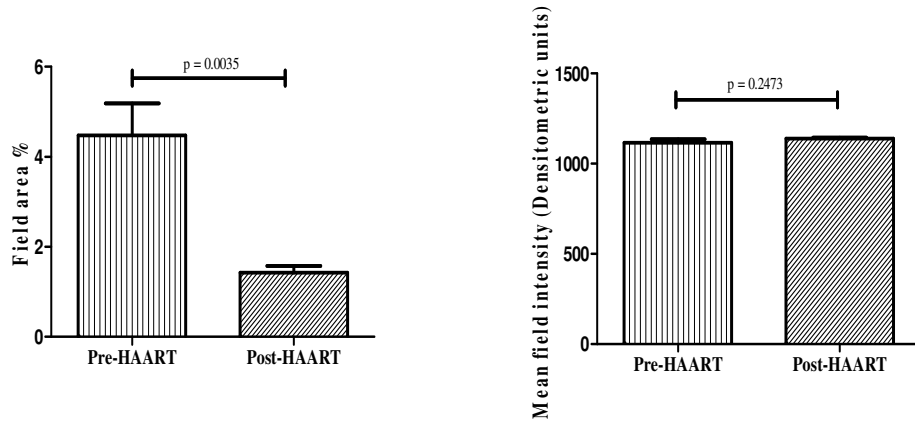
Figure 3.40: Histogram illustrating glomerular mean field area and intensity distribution of p24.
.

3.3 ULTRASTRUCTURAL ARCHITECTURAL MORPHOLOGY

3.3.1 Pre-HAART

The ultrastructural assessment of all biopsies conformed to their pathological appraisal. Electron dense deposits consistent with immune complex glomerulonephritis were found within the mesangium or along the peripheral glomerular capillary wall in subendothelial or epimembranous locations. Segmental capillary collapse was also noted.

The GBM was opposed by the foot processes on the urinary aspect and by fenestrated endothelium on the capillary luminal aspect (Figure 3.41). It consisted of an electron dense lamina densa flanked by an electron lucent lamina rara externae and internae on the epithelial and endothelial sides respectively. "Frilling" or irregular contouring of the endothelial aspect of the GBM was frequently observed (Figure 3.42). In addition, double contouring/tramlining of the basement membrane was evident (Figure 3.43). Periodically banded striated electron dense fibrils resembling fibrin and was noted within the lamina densa (Figure 3.44). Immune deposits occurred on the sub epithelial (Figure 3.45) and sub-endothelial aspect (Figure 3.46).

A dysregulated phenotype of visceral epithelial was observed with podocytes effacement varying in severity from focal (Figure 3.47), segmental (Figure 3.48) and diffuse. Subcellularly podocytes displayed pathological features such as mitochondrial stress, swollen/dilated pools of cisternal type endoplasmic reticulum (ER), and cytoplasmic vacuolation. Mitochondrial swelling with peripherally displaced disorientated and disintegrating cristae was frequently observed. Dilatation and vesiculation of the cisternae of rough endoplasmic reticulum was recurrent with the formation of ER pools (Figure 3.49). The contents of these discrete pools contained moderately electron dense secretory

products. Dilated golgi stacks were observed. Centrioles were identified (Figure 3.50). Intra-cytoplasmic fatty degeneration and occurrence of markedly electron dense lipid droplets was observed (Figure 3.51). Nuclear envelope thickening, proliferation and crenation were prominent (Figure 3.52). Vacuolation was noted (Figure 3.53). Subepithelial deposits associated with a basement membrane reaction resulting in a "ball in cup" appearance were observed (Figure 3.54). A relatively undifferentiated podocyte cytoplasm was occasionally observed (Figure 3.55). The plasmalemma of podocytes displayed microvillous extensions (Figure 3.56). Podocytes proliferation and apoptosis were observed.

Mostly, cell bodies of endothelial cells lining capillary loops appeared normal whilst their cytoplasm was fenestrated (Figure 3.57). Intracytoplasmic microtubular reticular structures were frequently observed (Figure 3.58). Due to electron opacity of the microtubules, the microtubular lumen was not discernible and randomly orientated in a reticular fashion. The mesangial extracellular matrix was increased (Figure 3.59). Mesangial cell proliferation varied from focal (Figure 3.60), segmental and diffuse.

Proliferation of parietal epithelial cells with crescent formation was evident (Figure 3.61). Capsular adhesions of parietal epithelial cells to visceral epithelial cells were noted (Figure 3.62). Occasionally, the Bowmans capsule was denuded of parietal epithelial cells (Figure 3.63). Glomerular sclerosis varied in severity from focal (Figure 3.64), segmental and diffuse (Figure 3.65). Proteinaceous casts were observed within proximal (Figure 3.66) and distal tubules (Figure 3.67). Interstitial inflammatory infiltration was noted (Figure 3.68).
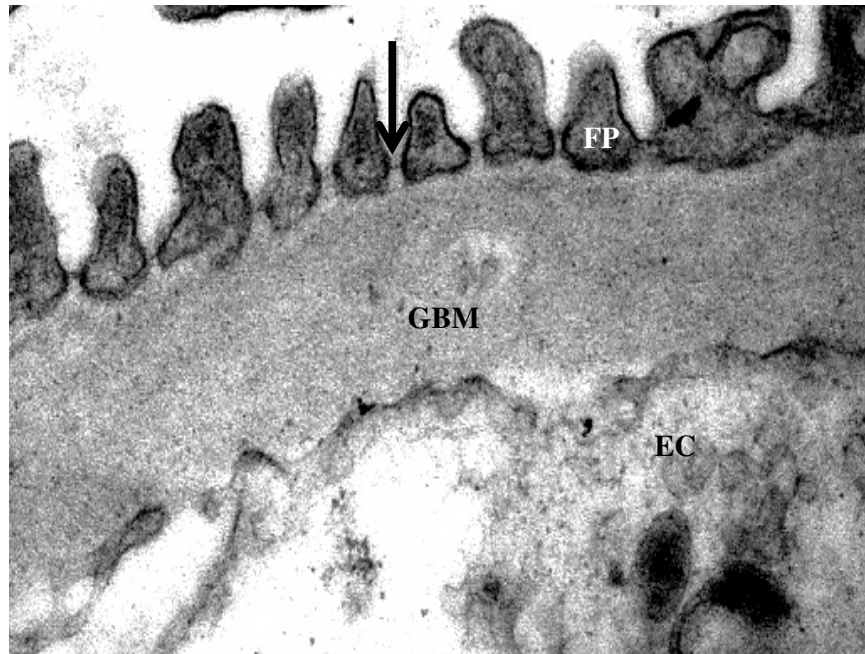
Figure 3.41: Electron micrograph illustrating the glomerular filter viz., foot processes (FP) lining the glomerular basement membrane (GBM) and endothelial cell (EC). Note slit diaphragm between foot processes (arrow). Init Mag X 40000.
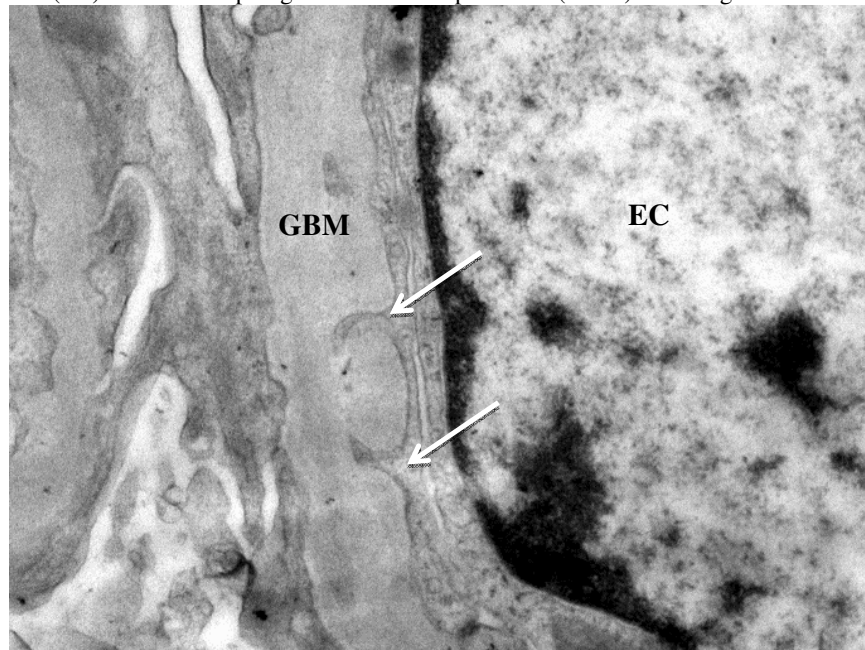
Figure 3.42: Electron micrograph depicting contouring or frilling (arrow) of the lamina rara interna of the GBM. Note endothelial cell (EC). Init Mag X 25000.
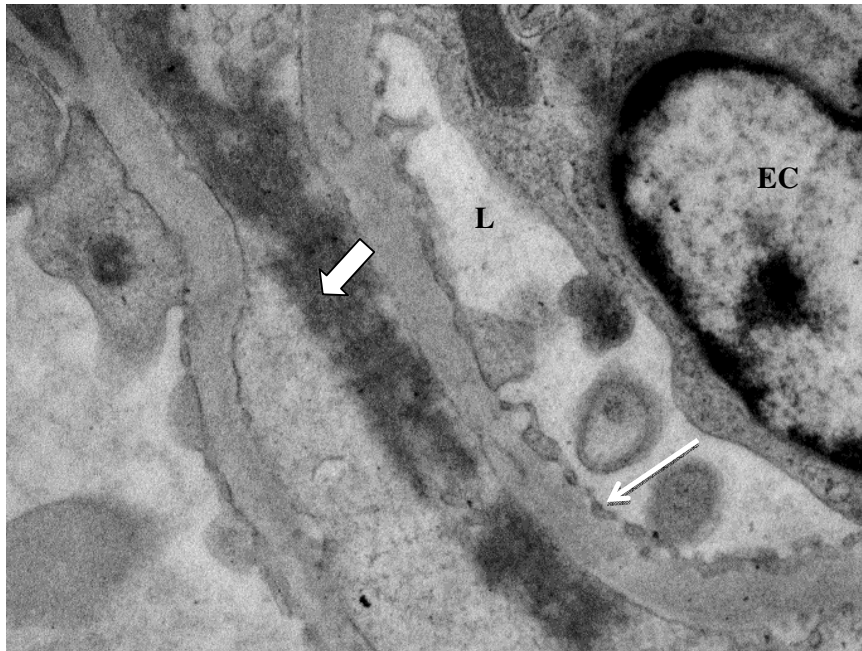
Figure 3.43: Electron micrograph depicting two opposing GBM interfaced with electron dense deposits (open arrow). Cap lumen (L), endothelial cell body (EC) and fenestrations (arrow). Init Mag X 12000.
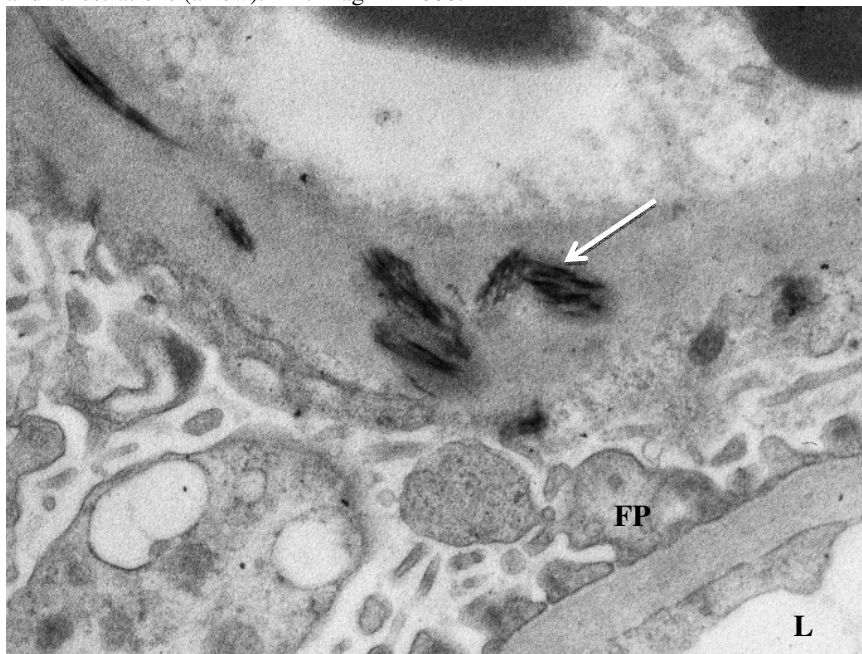
Figure 3.44: Electron micrograph illustrating GBM with fibrin (arrowed) within the lamina rara densa. Foot processes (FP) and cap lumen (L). Init Mag X 20000.
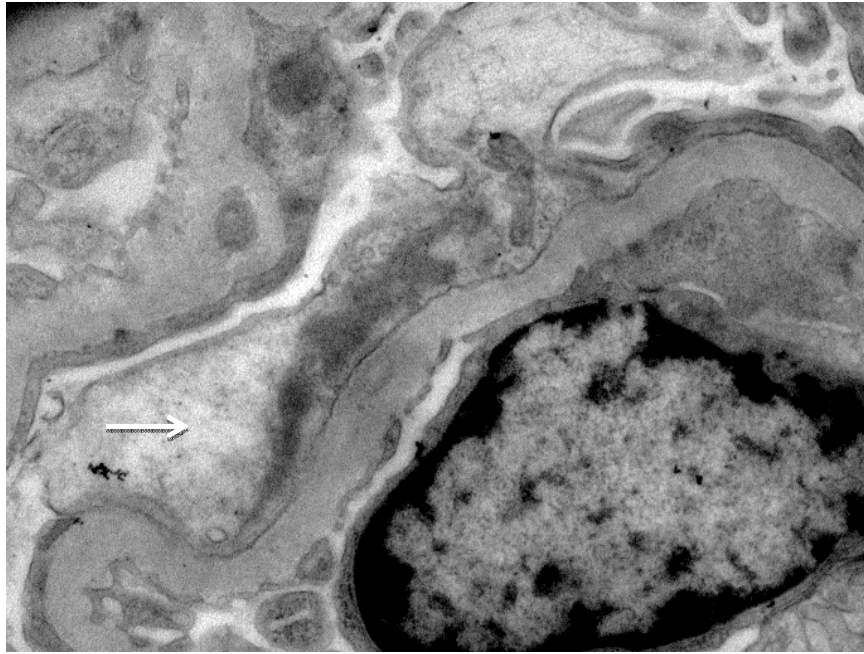
Figure 3.45: EM graph illustrating focal effacement of foot processes (arrow) with epithelial dense deposits. Init Mag X 20000.
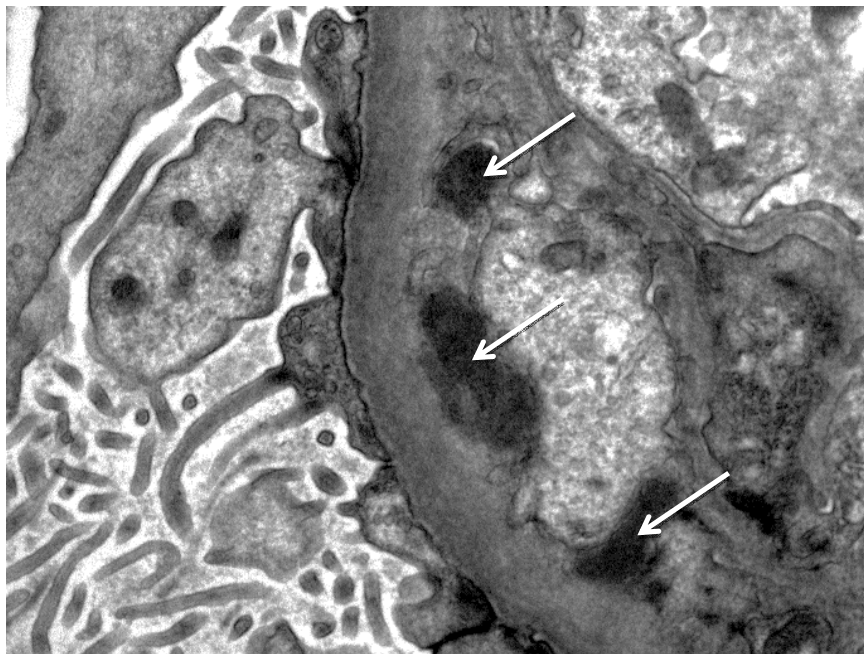
Figure 3.46: EM graph showing sub endothelial immune deposits (arrow). Note also microvillous (MV) transformation of podocytes. Init Mag X 20000.
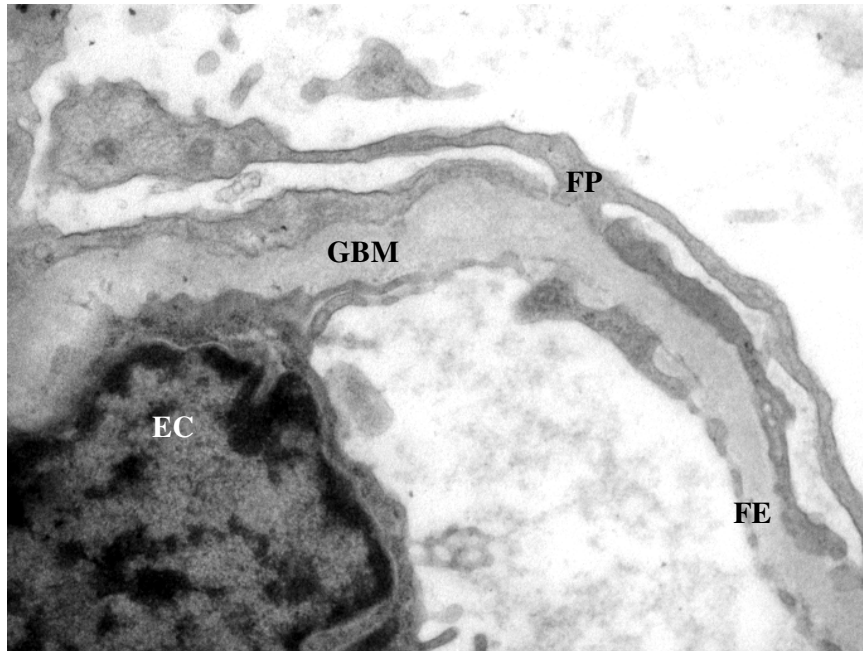
Figure 3.47: Electron micrograph illustrating glomerular basement membrane (GBM) with focal effacement of the foot process (FP). Note endothelial cell (EC) and fenestrated endothelium (FE). Init Mag X 12000.
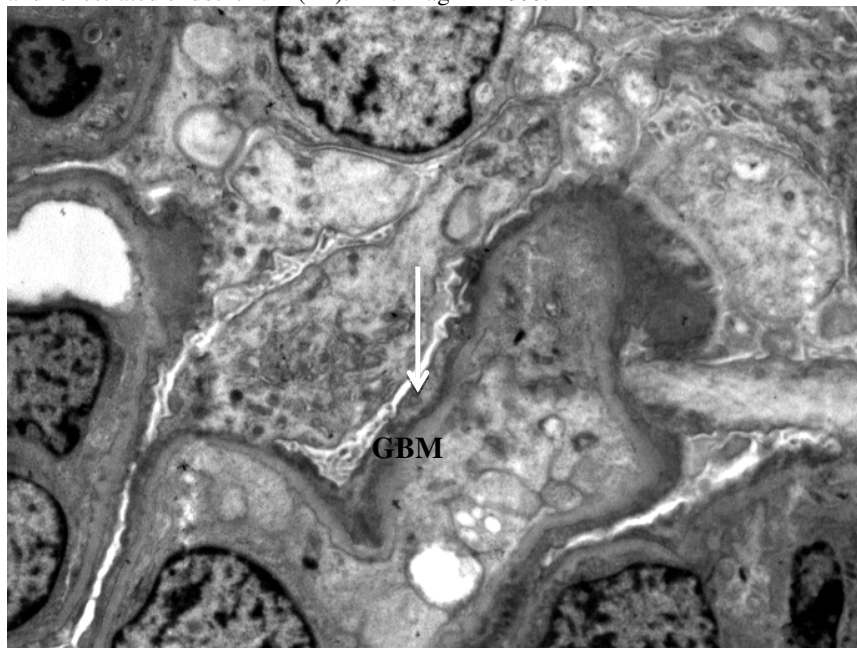
Figure 3.48: Electron micrograph illustrating glomerular basement membrane (GBM) with segmental podocytes effacement. Init Mag X 8000.
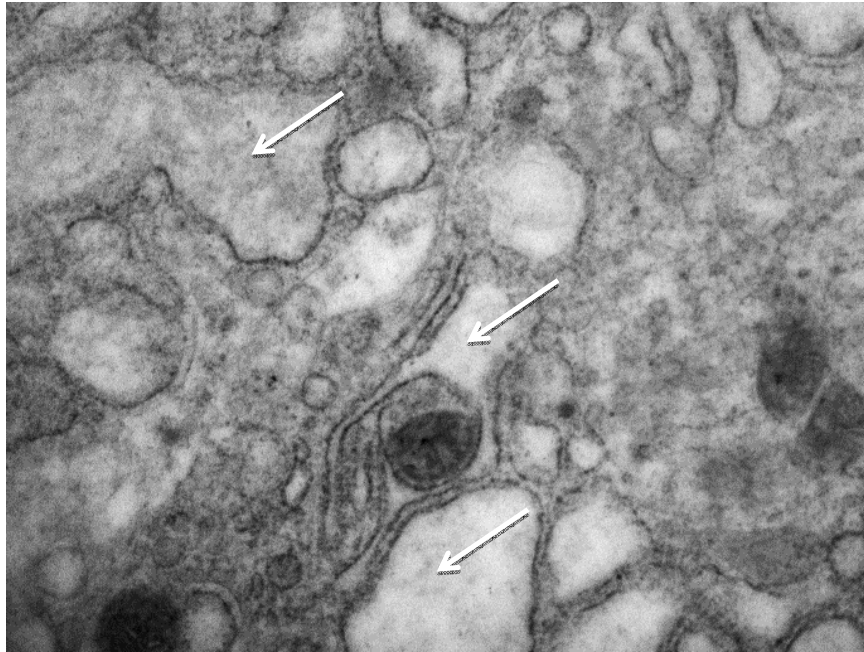
Figure 3.49: Electron micrograph illustrating cisternal pools of dilated endoplasmic reticulum (arrow). Init Mag X 25000.
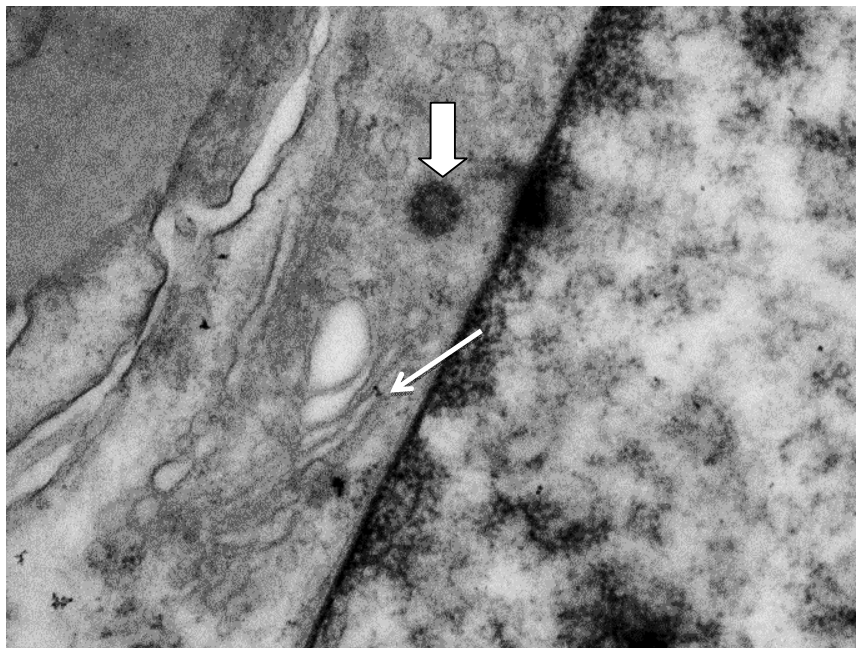
Figure 3.50: Electron micrograph showing dilated golgi stacks (arrow) with centrioles (open arrow). Init Mag X 25000.
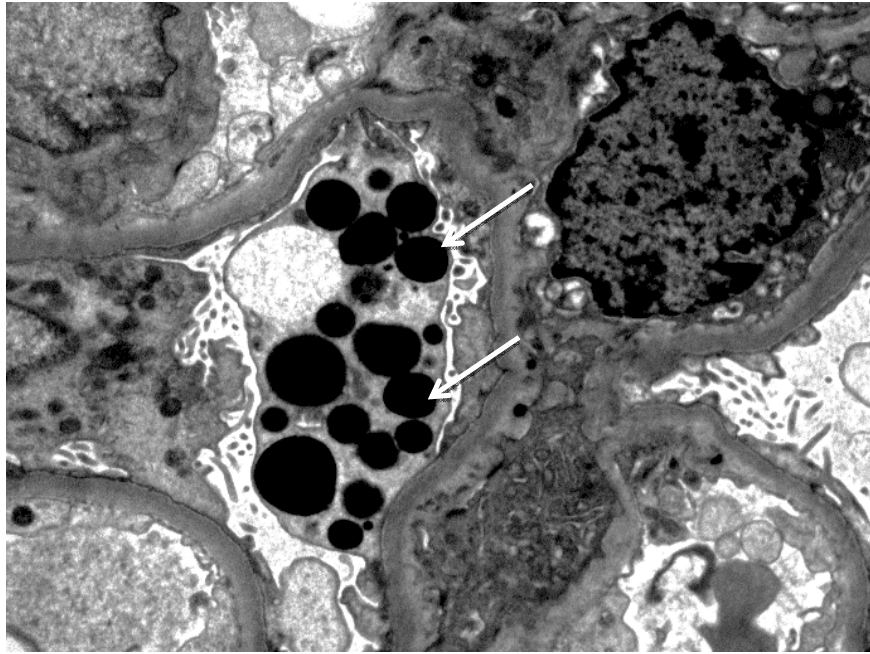
Figure 3.51: Electron micrograph showing lipid (arrow) distention within podocyte cytoplasm. Note frilling of GBM. Init Mag X 8000.
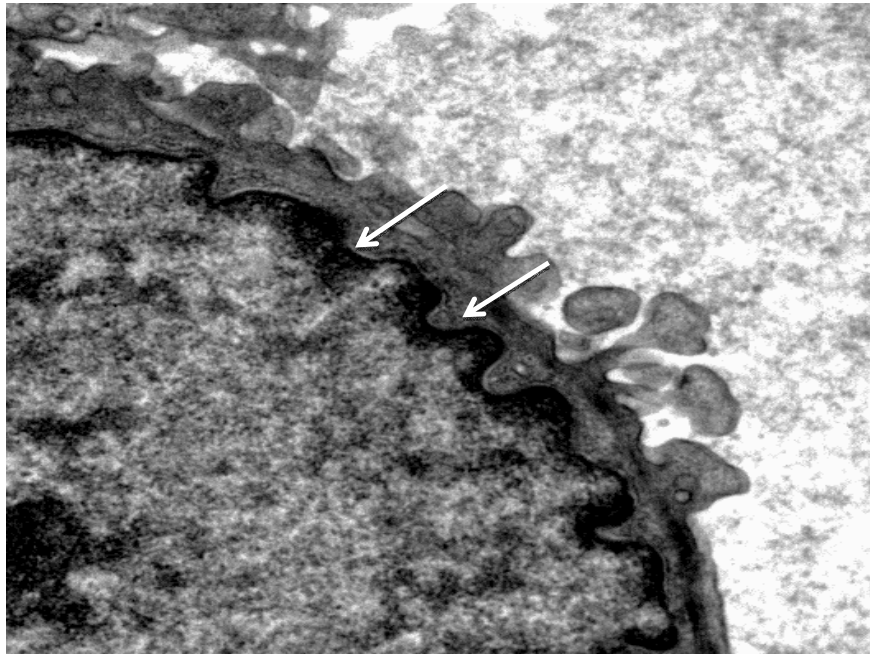
Figure 3.52: Electron micrograph demonstrating podocyte nucleo lemmal crenation (arrows). Init Mag X 25000.

Figure 3.53: Electron micrograph illustrating vacuolation (V) within a podocyte cell body. Note cap lumen (L) Init Mag X 10000.
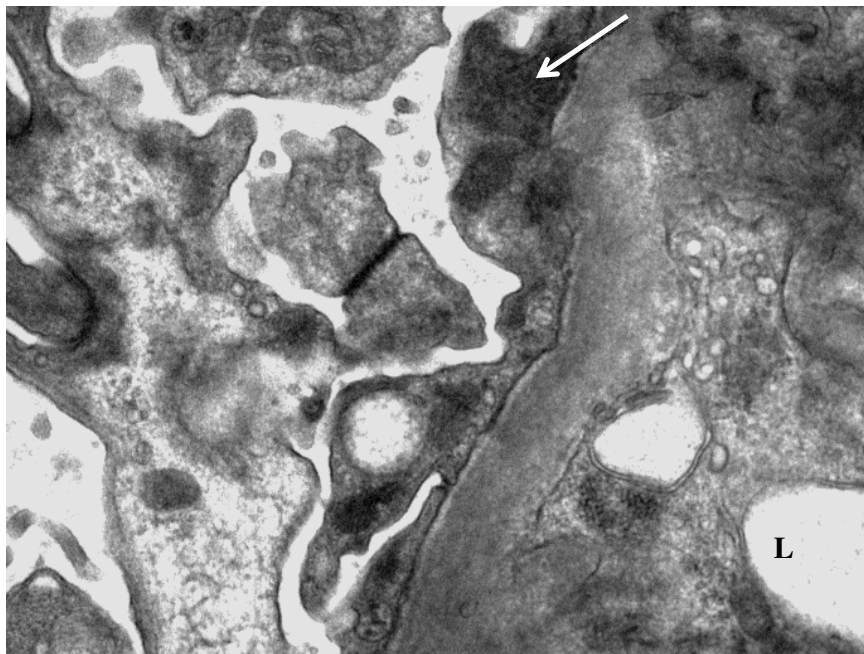
Figure 3.54: Electron micrograph showing "ball and cup" (arrow) appearance of immune deposits within the podocyte. Note cap lumen (L). Init Mag X 30000.
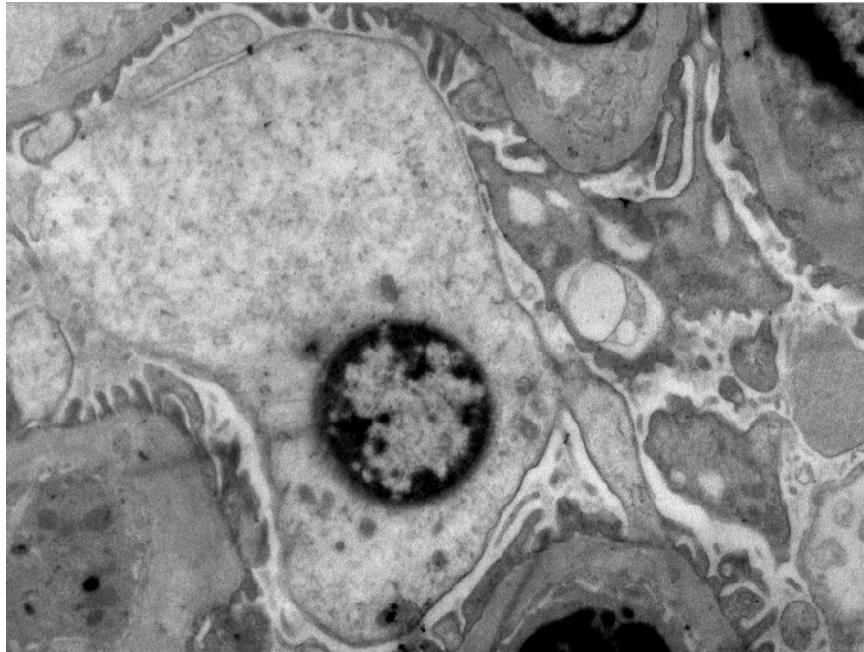
Figure 3.55: Electron micrograph showing an undifferentiated podocyte cytoplasm. Init Mag X 10000.
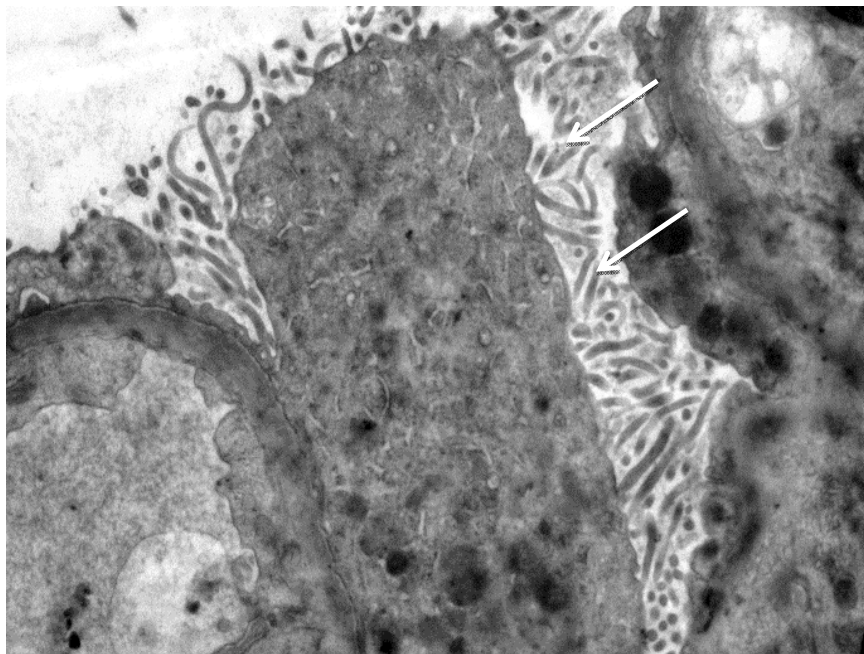
Figure 3.56: Electron micrograph demonstrating podocyte microvillous profusion (arrow). Init Mag X 10000.
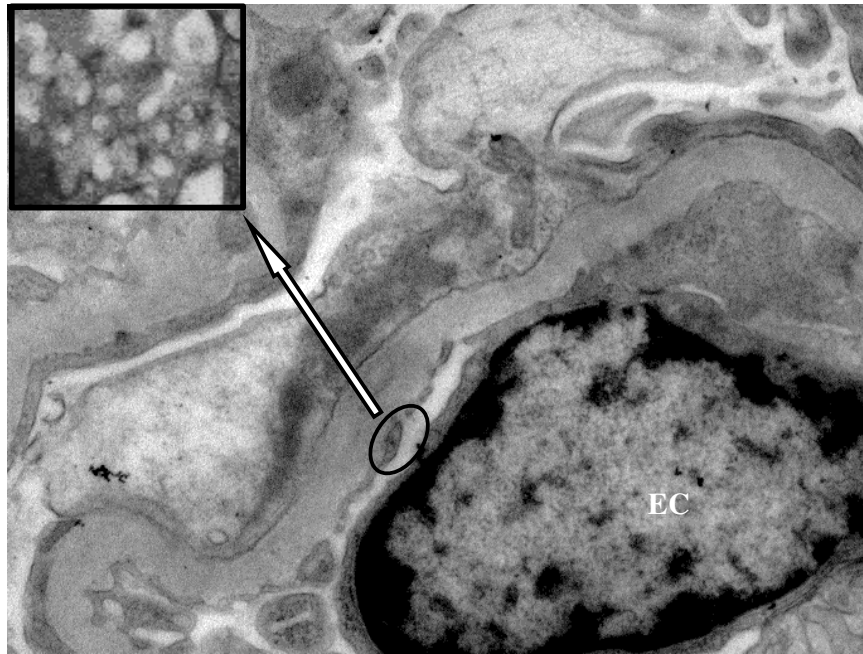
Figure 3.57: Electron micrograph illustrating endothelial cell body (EC) and fenestrations (arrow). Inset illustrates cross-cut fenestrations. Init Mag X 10000.
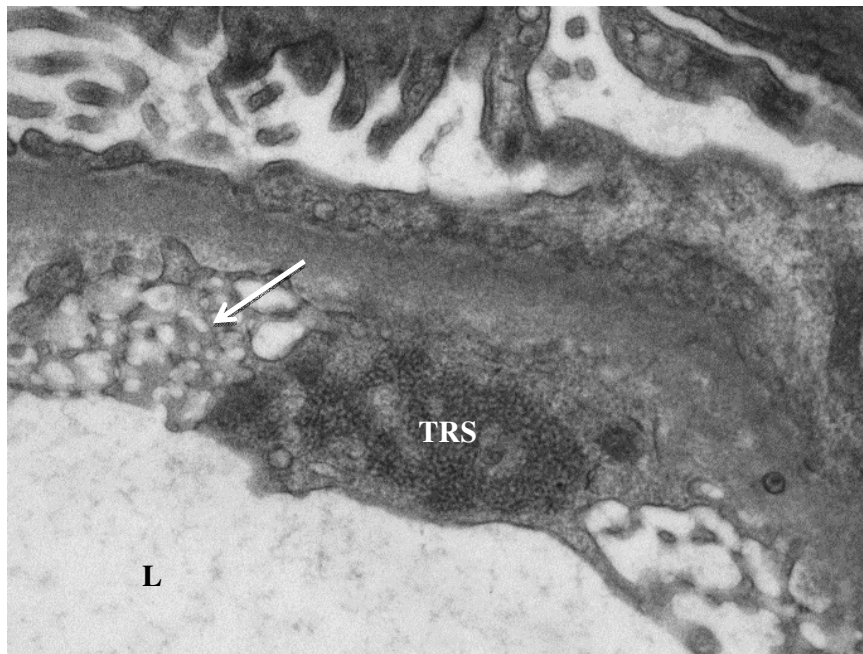
Figure 3.58: Electron micrograph depicting tubular reticular structure (TRS) within an endothelial cell. Note cross-cut endothelial fenestrations (arrow) and cap lumen (L). Init Mag X 25000.
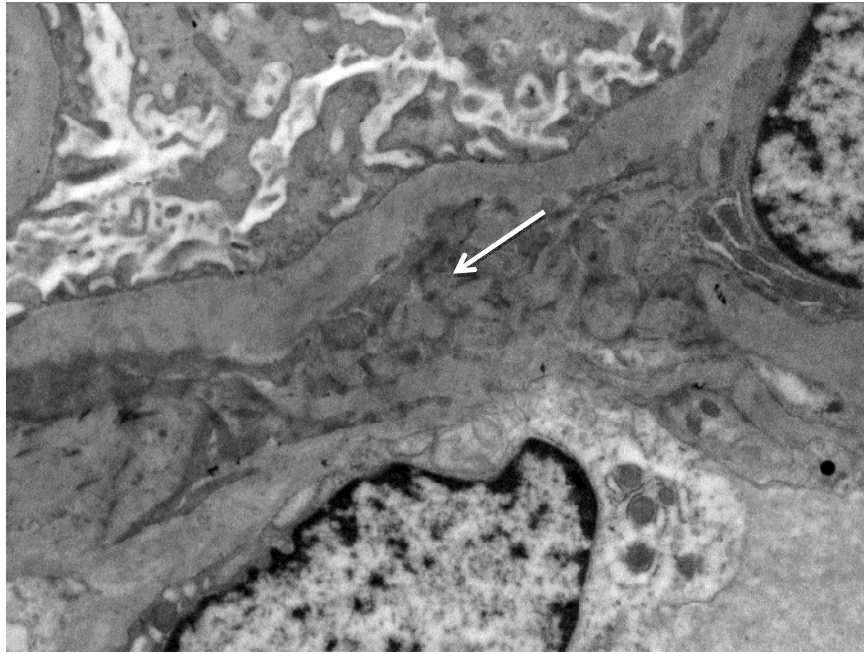
Figure 3.59: Electron micrograph showing mesangial matrix extension (arrow). Init Mag X 10000.
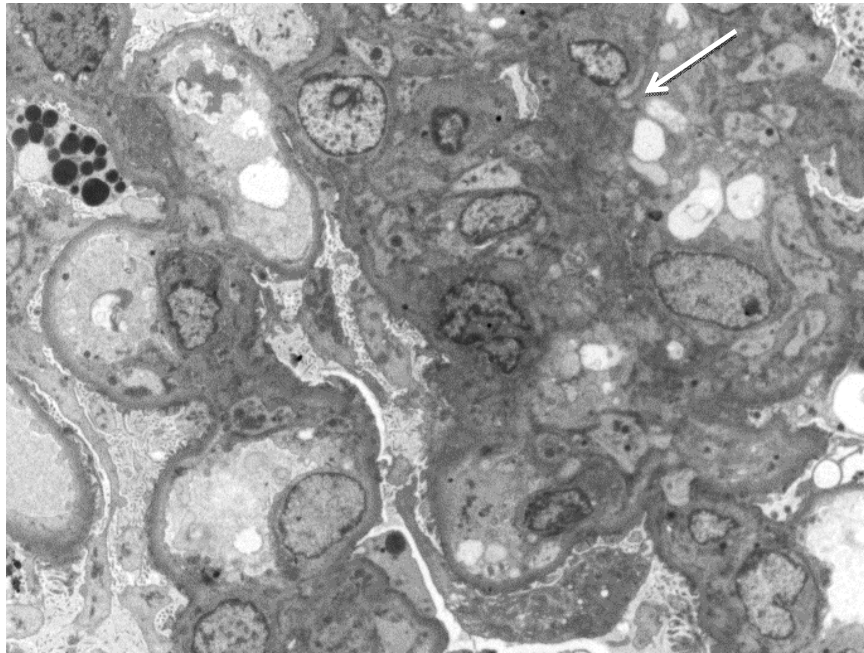
Figure 3.60: Electron micrograph showing focal mesangial cell proliferation (arrow). Init Mag X 2500.
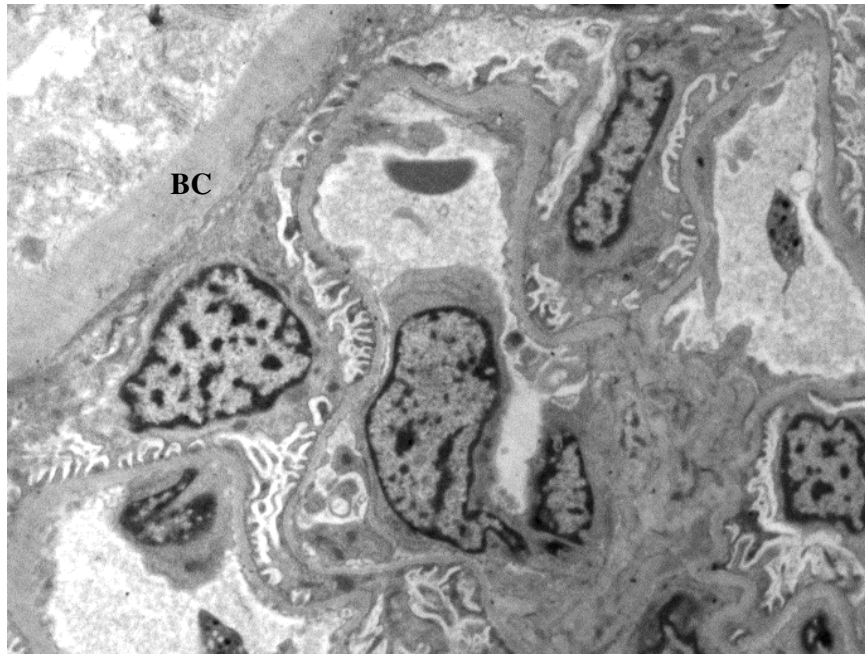
Figure 3.61: Electron micrograph showing crescent formation and occlusion of Bowman's capsule (BC). Init Mag X 5000.
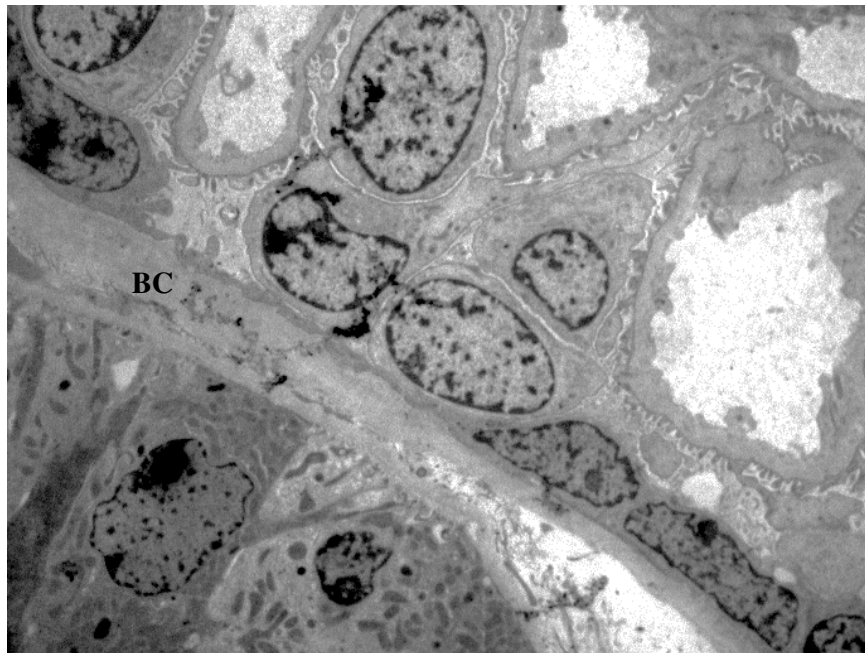
Figure 3.62: Electron micrograph illustrating visceral and parietal epithelial cell adhesion with occlusion of Bowman's space. Note Bowman's capsule (BC). Init Mag X 4000.
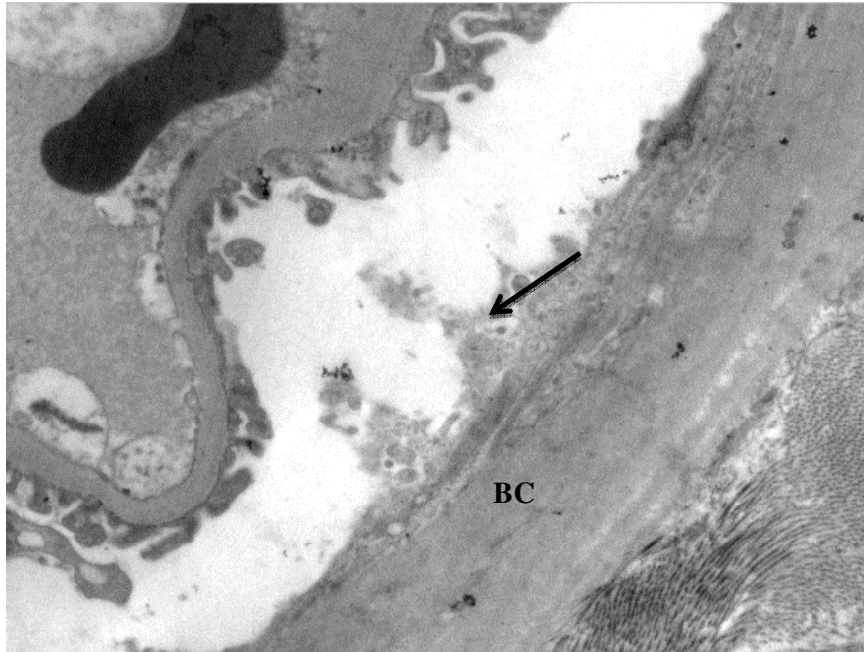
Figure 3.63: Electron micrograph illustrating Bowman's capsule (BC) denuded of parietal epithelial lining (arrow). Init Mag X 10000.

Figure 3.64: Electron micrograph showing incomplete glomerular sclerosis. Init Mag X 6000.
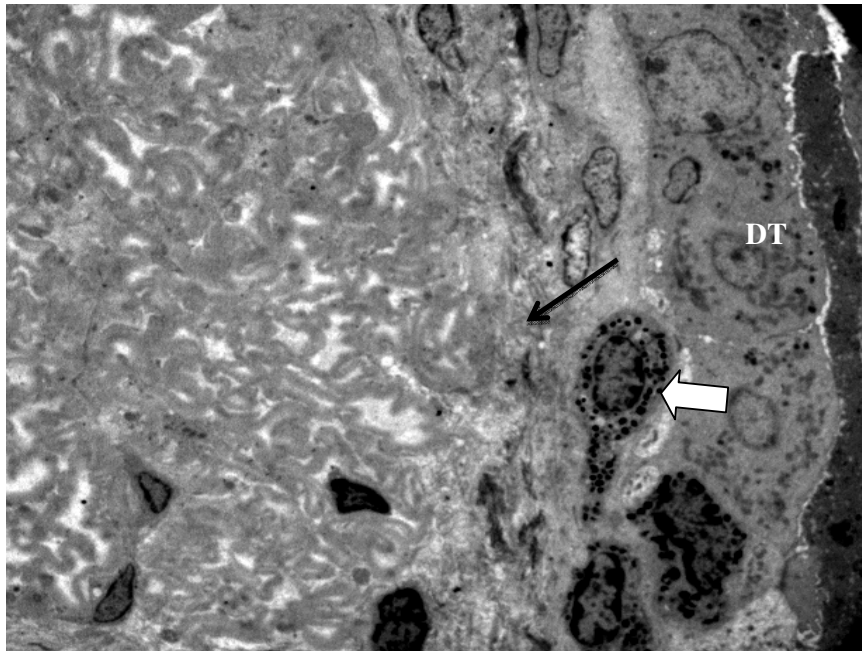
Figure 3.65: Electron micrograph illustrating diffuse glomerular sclerosis. Note capsule (arrow), interstitial inflammatory infiltrate (open arrow) and distal tubular epithelial cells (DT). Init Mag X 2500.
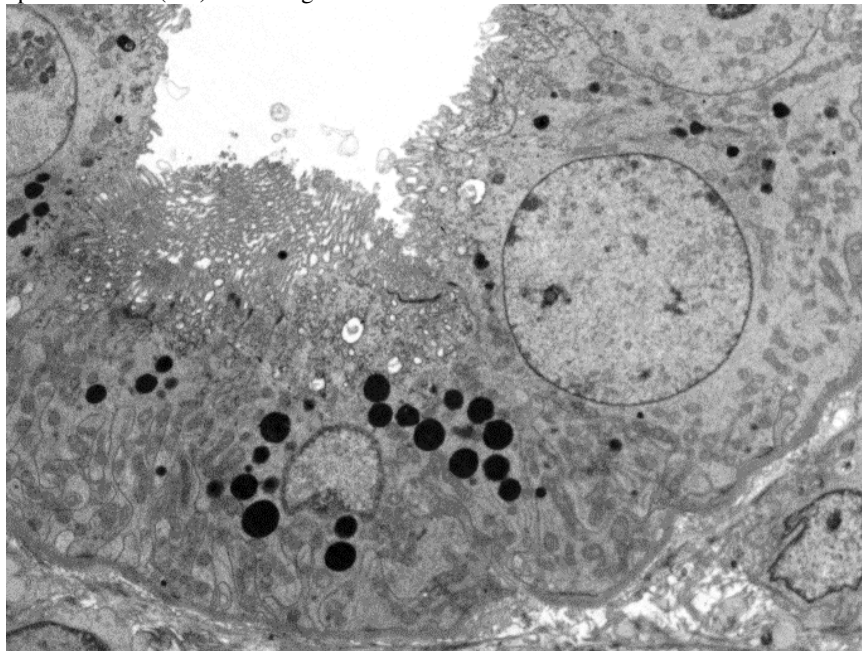
Figure 3.66: Electron micrograph showing normal appearance of proximal tubular cells. Init Mag X 4000.
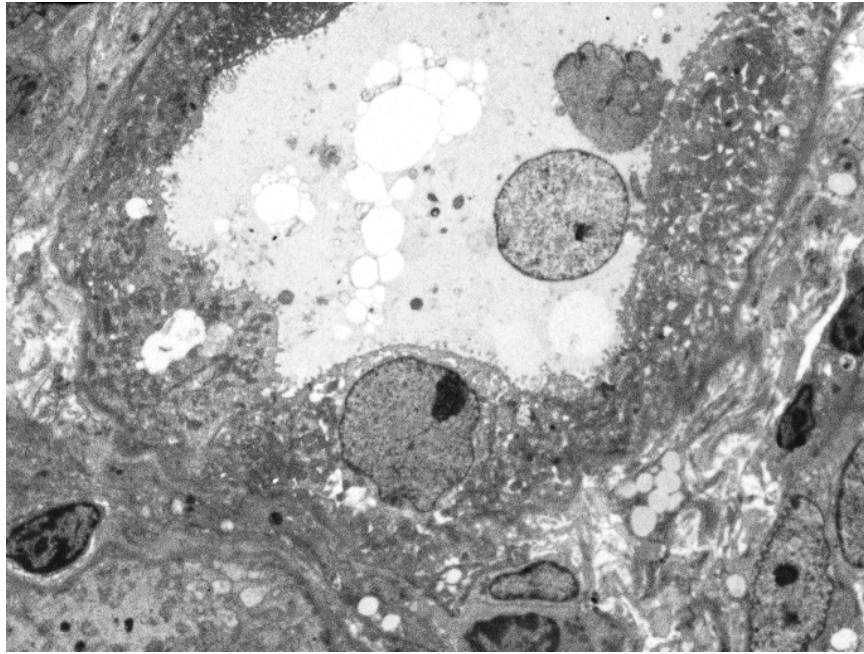
Figure 3.67: Electron micrograph of distal tubular cells with mild cast inclusion within lumen. Init Mag X 3000.
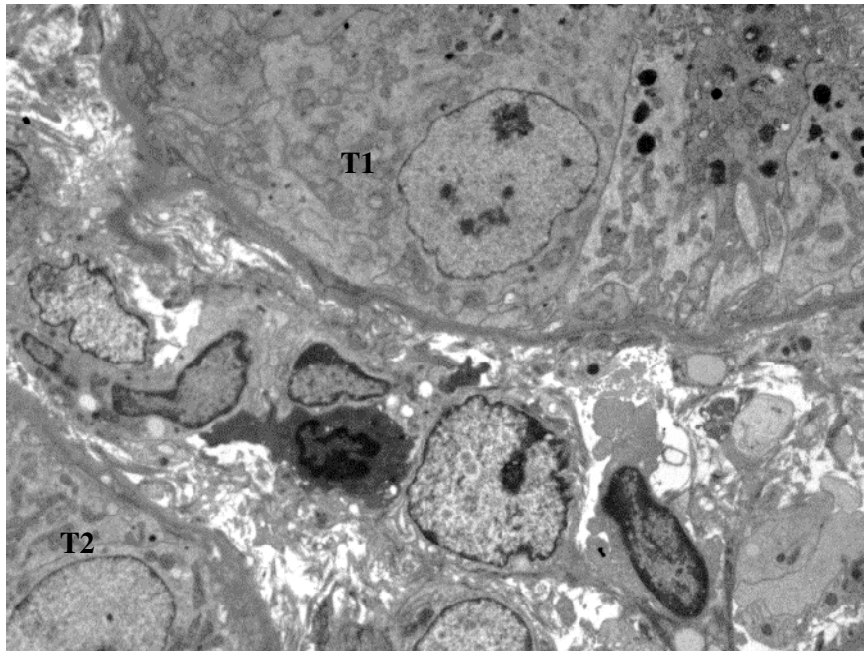
Figure 3.68: Electron micrograph depicting interstitial inflammatory infiltrate between tubules (T1 and T2). Init Mag X 4000.

3.3.2 Post-HAART

A qualitative ultrastructural assessment of the biopsies conformed to their pathological appraisal.

"Frilling" or irregular contouring of the endothelial aspect of the GBM was noted (Figure 3.69). Immune deposits occurred on the sub epithelial (Figure 3.69) or sub-endothelial aspect.

The phenotype of visceral epithelial cells was improved (Figure 3.70) occurring sometimes with focal (Figure 3.71) and segmental effacement. Subcellularly, podocytes displayed minimal mitochondrial and endoplasmic stress features (Figure 3.72).

Endothelial cells lining capillary loops appeared normal with fenestrations (Figure 3.71).

Mesangial cell proliferation varied from focal (Figure 3.73) and segmental (Figure 3.74) Mesangial matric increase was noted (Figure 3.75).

The parietal epithelial cells lining the Bowmans capsule were occasionally found to adhere to visceral epithelial cells with an occlusion of the Bowmans space (Figure 3.75 - 3.77). Glomerular sclerosis was observed (Figure 3.78).

The proximal (Figure 3.79) and distal tubular lumen were often filled with proteinaceous casts. The renal interstitium displayed inflammatory infiltration of polymorphonuclear lymphocytes cells.
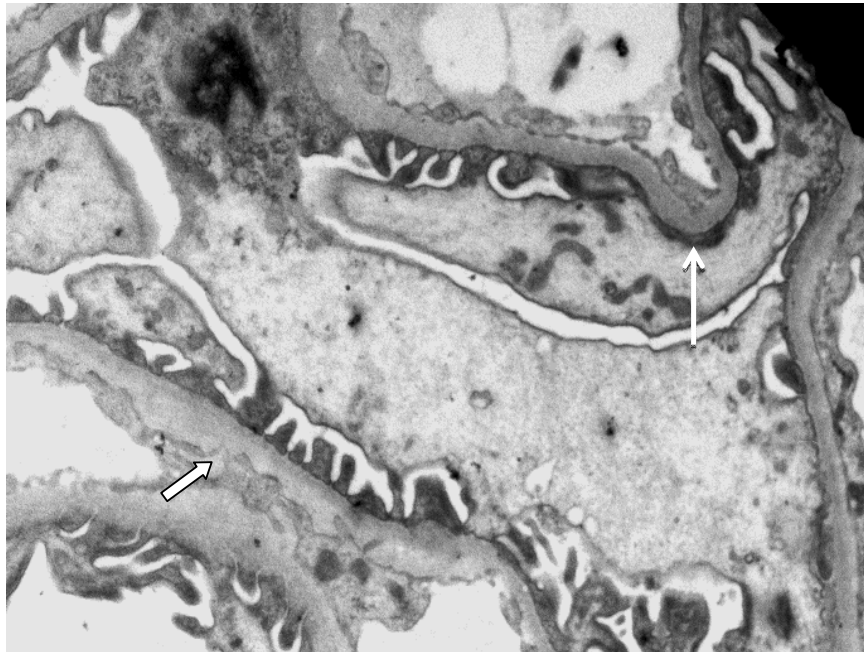
Figure 3.69: Electron micrograph illustrating focal frilling (open arrow) of the GBM. Note foot process effacement and sub epithelial cell deposits (arrow). Init Mag X 12000.
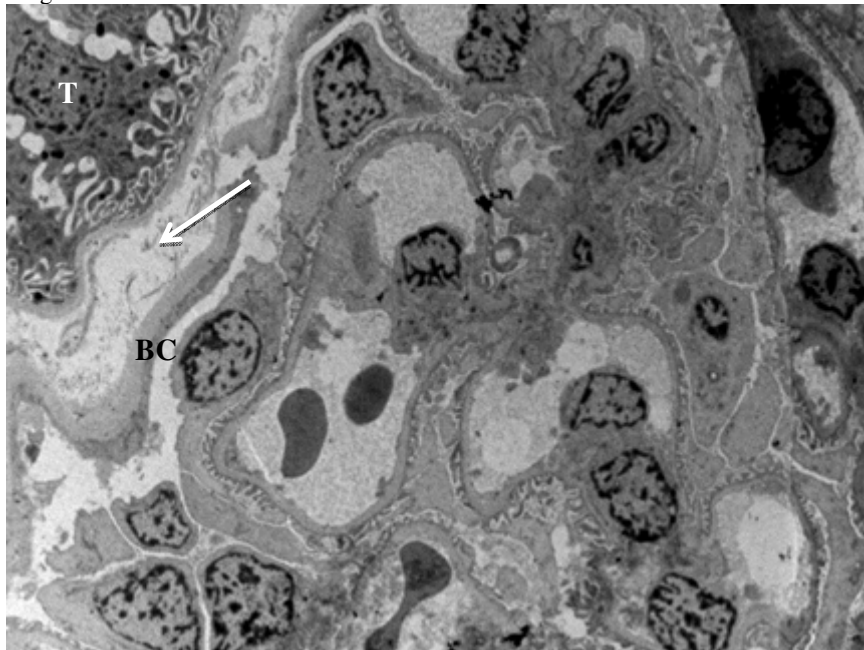
Figure 3.70: Electron micrograph showing normal appearance of podocytes. Note tubule (T), Bowman's capsule (BC) and interstitium (arrow). Init Mag X 2500.
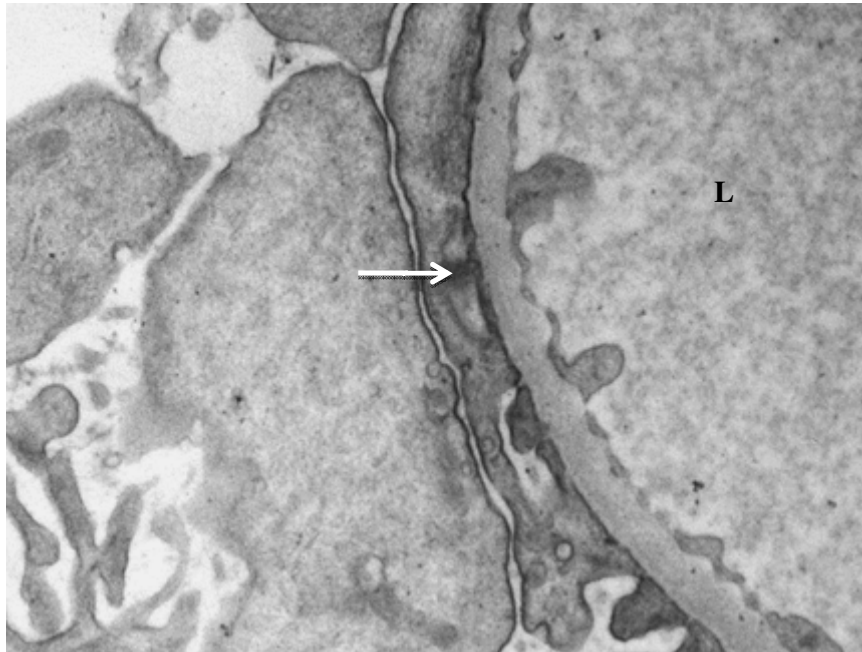
Figure 3.71: Electron micrograph depicting focal effacement of foot processes (arrow). Note cap lumen (L). Init Mag X 12000.
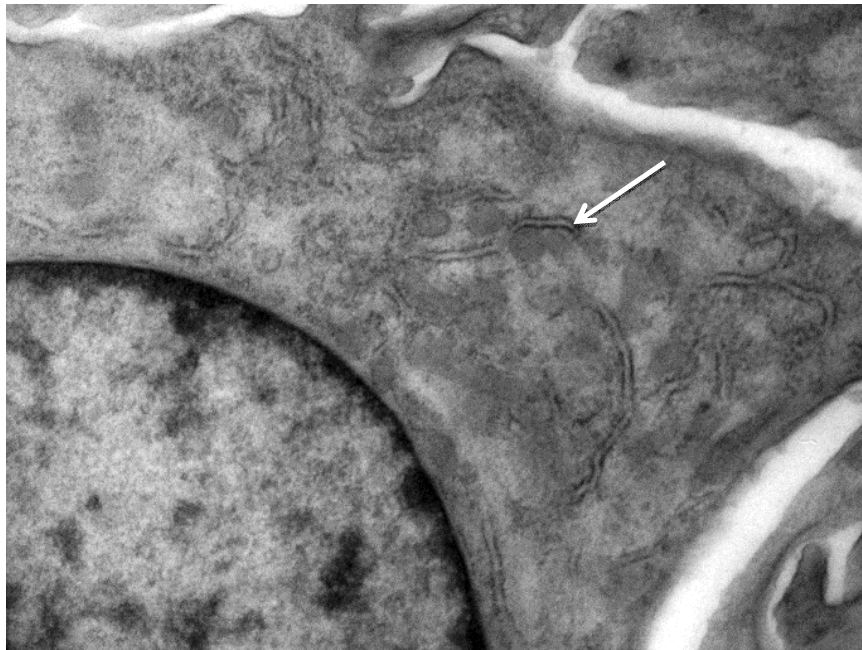
Figure 3.72: Electron micrograph showing undilated endoplasmic reticulum (ER) (arrow). Init Mag X 25000.
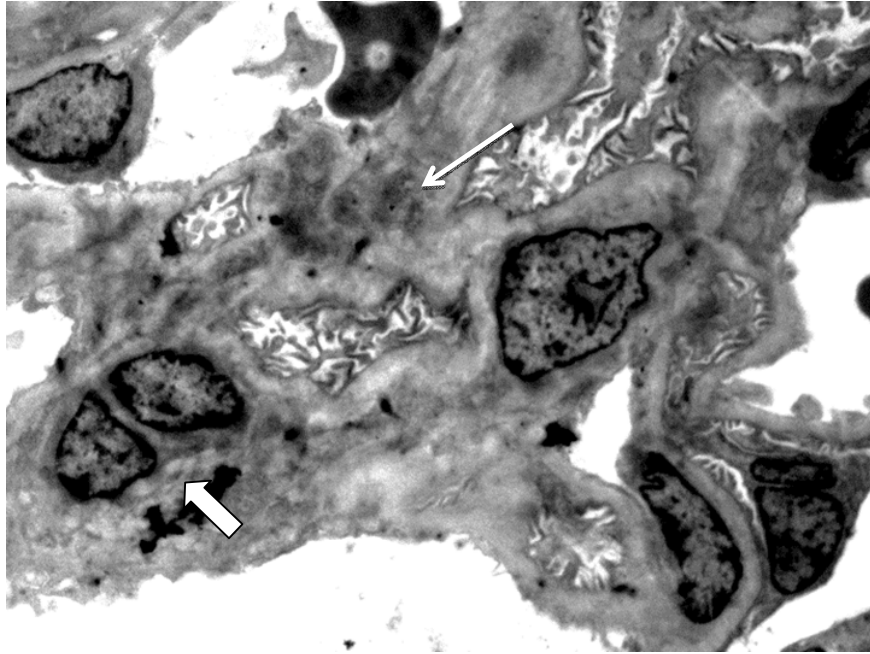
Figure 3.73: Electron micrograph showing mesangial matrix increase (arrow) and focal mesangial cell increase (open arrow). Init Mag X 4000.
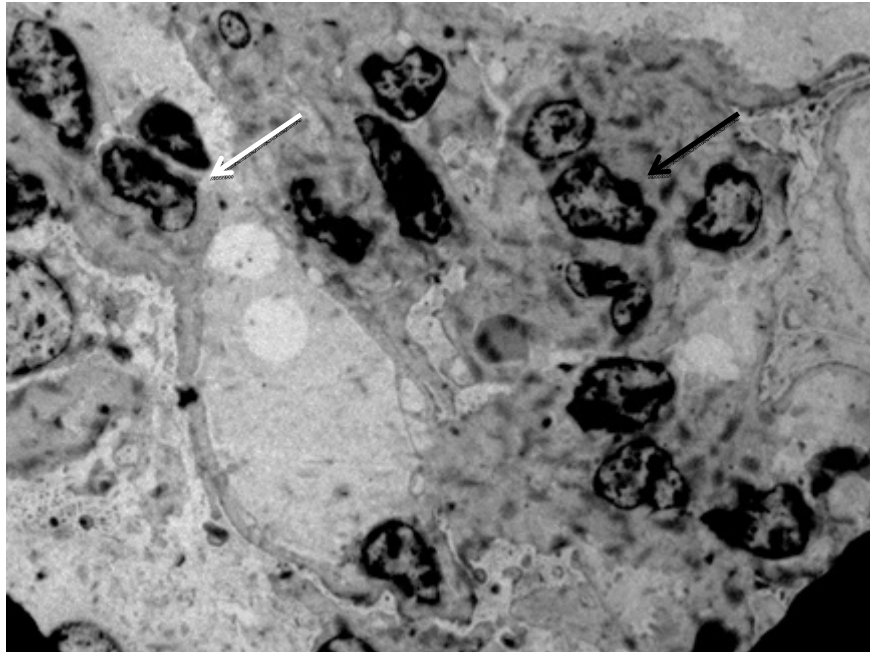
Figure 3.74: Electron micrograph illustrating mesangial cell proliferation (arrow). Init Mag X 3000.
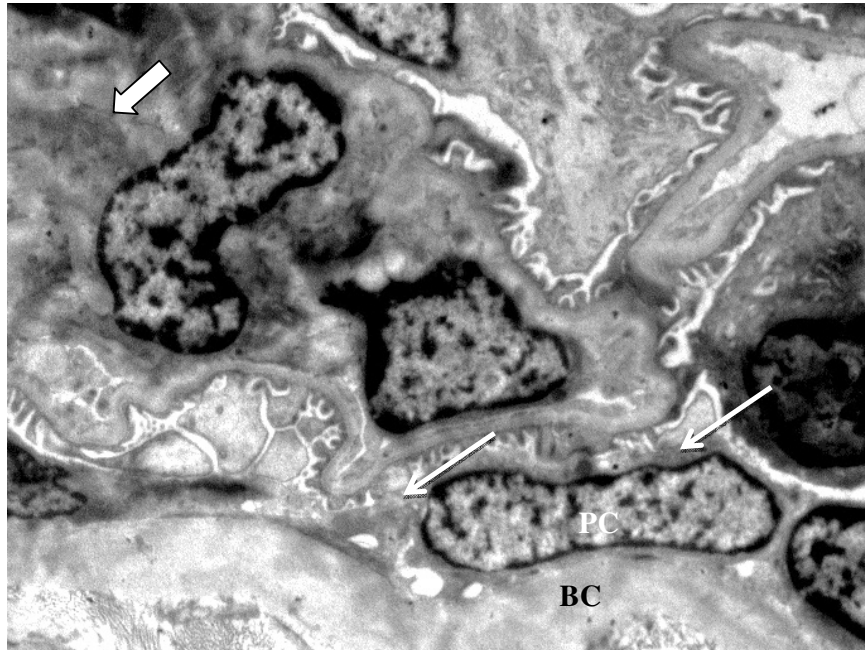
Figure 3.75: Electron micrograph illustrating mesangial matrix (open arrow) and adhesion (arrow) of visceral epithelial cells to parietal cell (PC) lining the Bowman's capsule (BC). Adhesion of BC and podocyte. Init Mag X 6000.
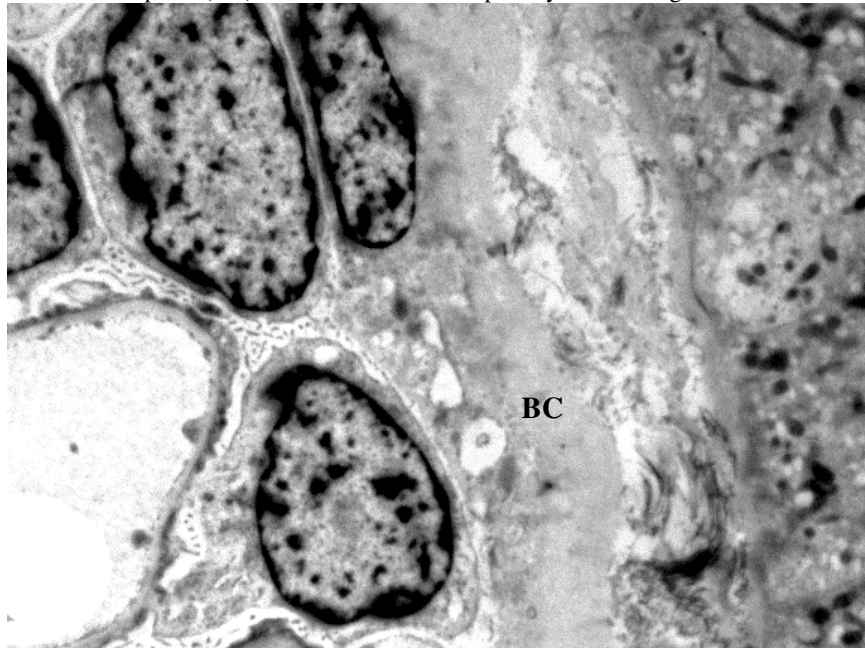
Figure 3.76: Electron micrograph depicting occlusion of Bowman' space. Bowmans capsule (BC). Init Mag X 6000.
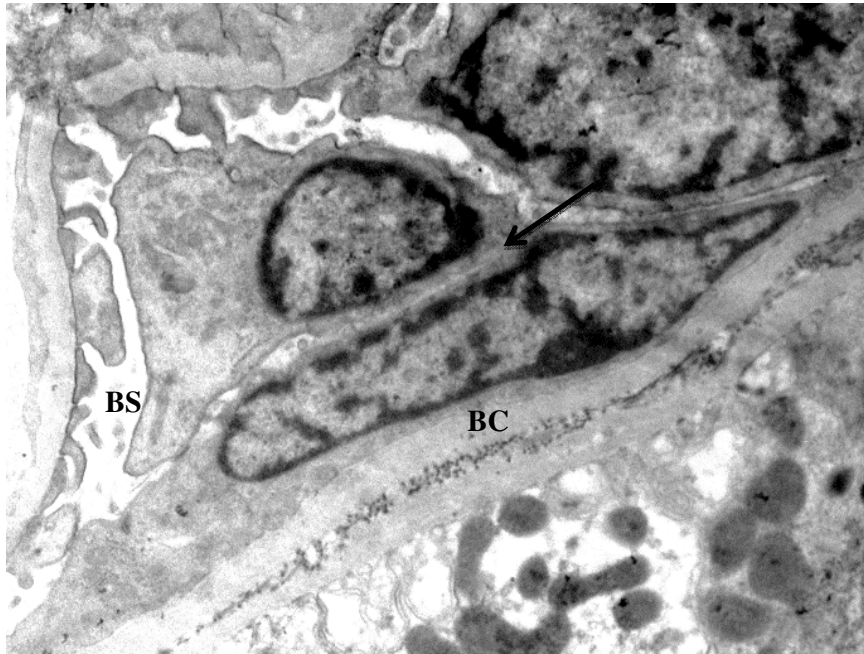
Figure 3.77: Electron micrograph illustrating podocyte adherent to parietal cell (arrow). Note Bowman's space (BS) and capsule (BC). Init Mag X 12000.
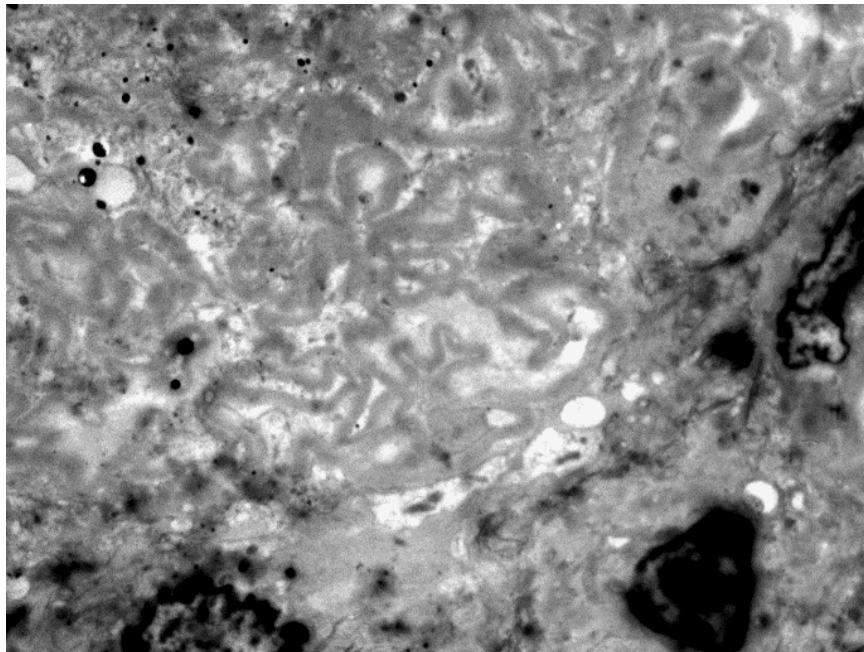
Figure 3.78: Electron micrograph showing part of a sclerosed glomeruli. Init Mag X 5000.
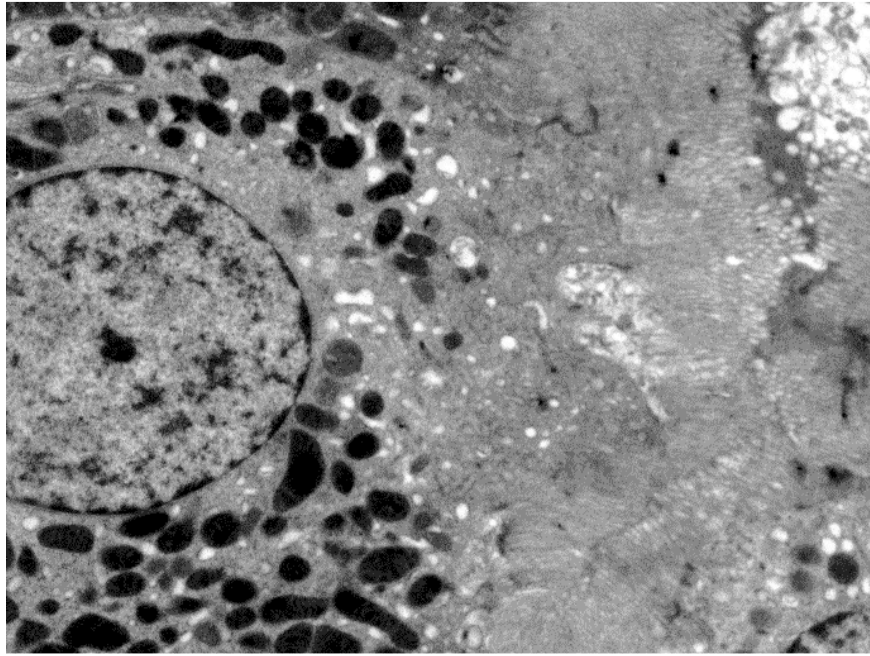
Figure 3.79: Electron micrograph showing proximal tubular cells. Init Mag X 8000.

3.4 IDENTIFICATION OF RENAL VIRAL RESERVOIRS

3.4.1 Ultrastructural

3.4.1.1 Pre-HAART

Latent HIV reservoirs were observed within the podocyte cytoplasm. HIV was identified on morphology and size (Figure 3.80 - 3.81). HIV-1 particles were not noted in glomerular mesangial or endothelial cells.
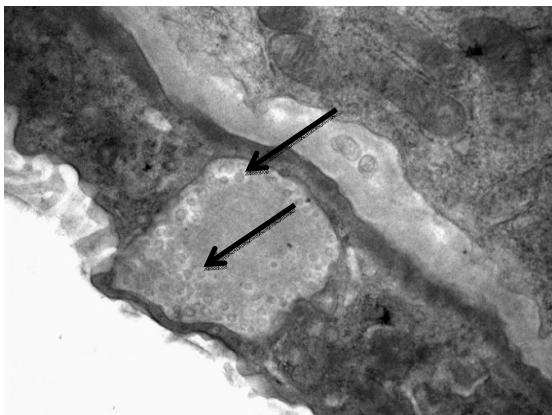
Figure 3.80: Low power electron micrograph depicting HIV-like particles (arrows) sequestered within an endocytic compartment of a podocyte. Init Mag X 30 000.
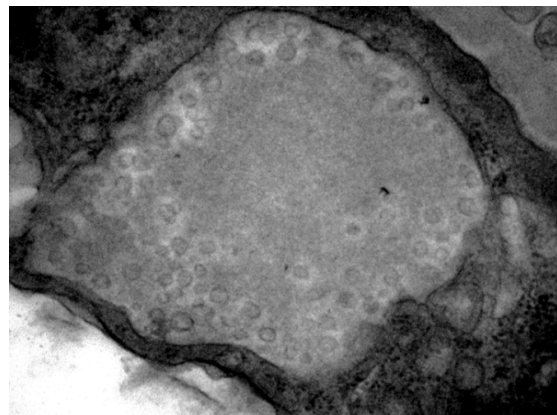
Figure 3.81: Higher power electron micrograph of 3.80. Init Mag X 60 000.

3.4.1.2 Post-HAART

Within the post-HAART biopsy core, no latent HIV reservoirs were observed.

3.4.2 HIV proviral DNA quantification

Real-Time polymerase chain reaction assays (RT-PCR) provided evidence of HIV-1 within the kidney. Two standard curves were created using, albumin (to determine the level of input DNA) and *gag* (HIV copy number).

3.4.2.1 Albumin

A dilution series of albmiun amplicon was used as standard template for the amplification using the SYBR Green dye reaction (Figure 3.82). Melting curves for the albmiun gene are shown in Figure 3.83.
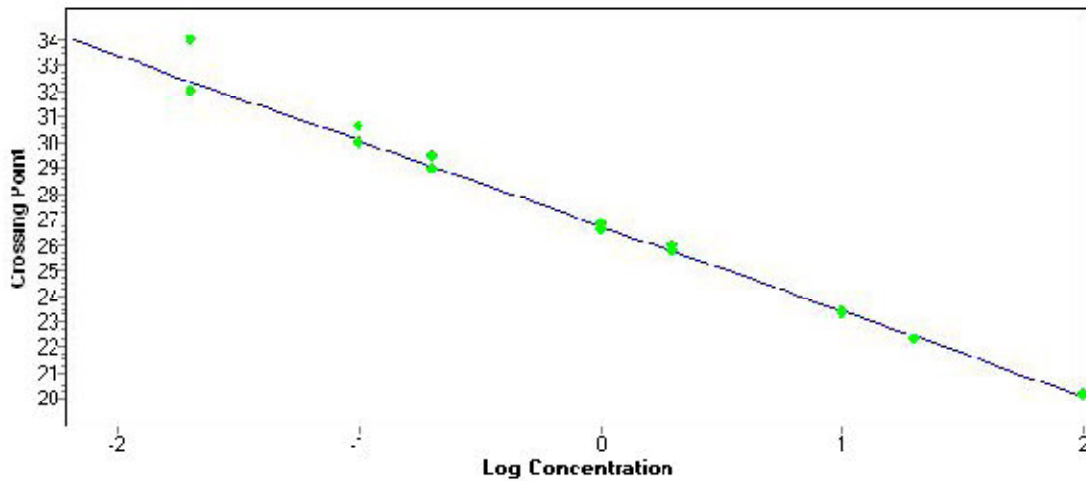
Figure 3.82: The standard curve for albumin derived from the crossing points (cycle numbers) of each standard plotted against the logarithmic concentration.
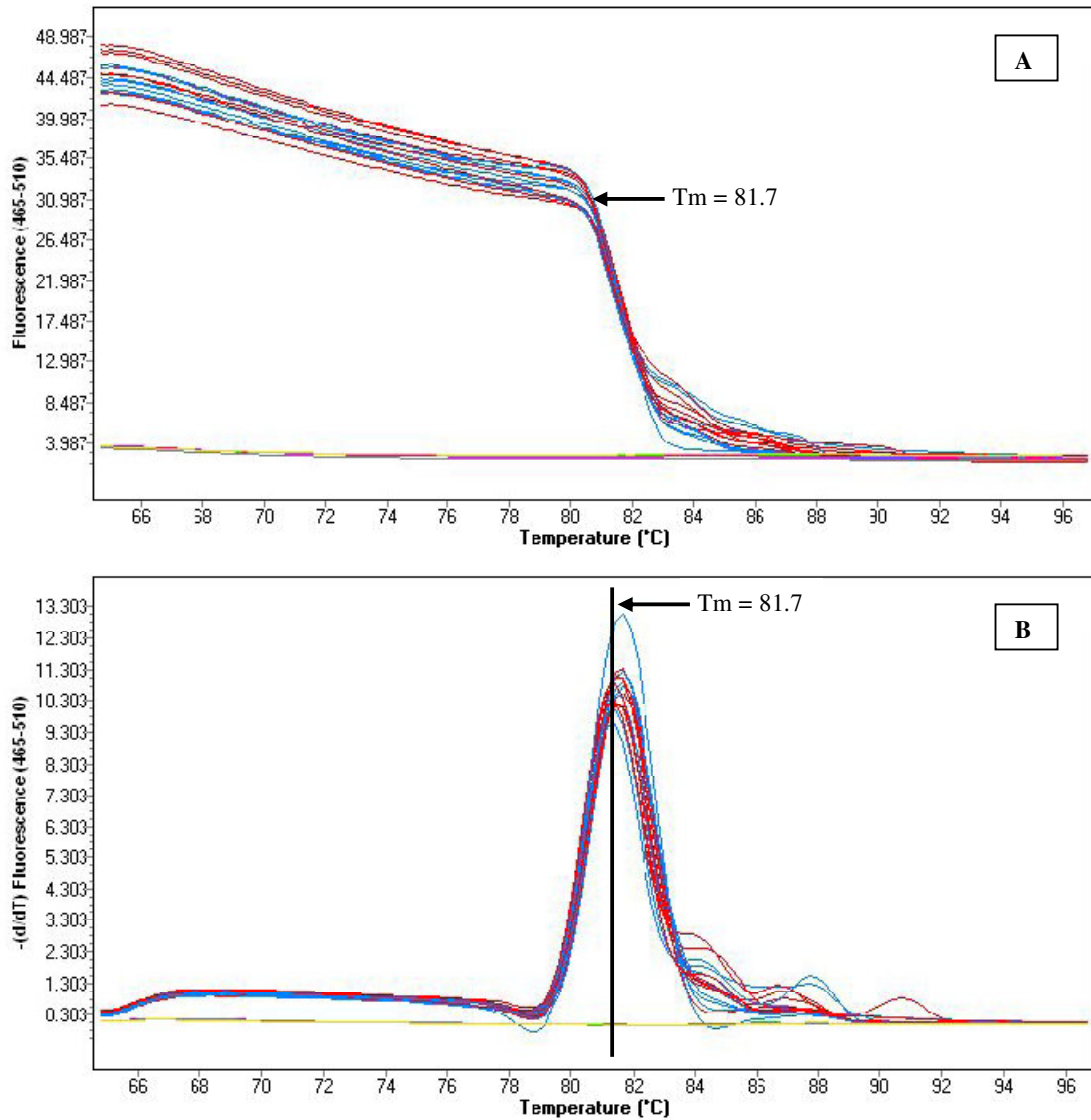
Figure 3.83: **(A).** Melting curves for albumin amplification products. **(B).** The melting peaks of the albumin amplification product. The melting temperature (Tm) of the gene product is shown by the arrow.

3.4.2.2 *Gag*

A stand curve was created utilizing the 8E5 cell line, which contained a single defective genome copy of HIV per cell (Figure 3.84). Melting curves for the *gag* gene are shown in Figure 3.85.
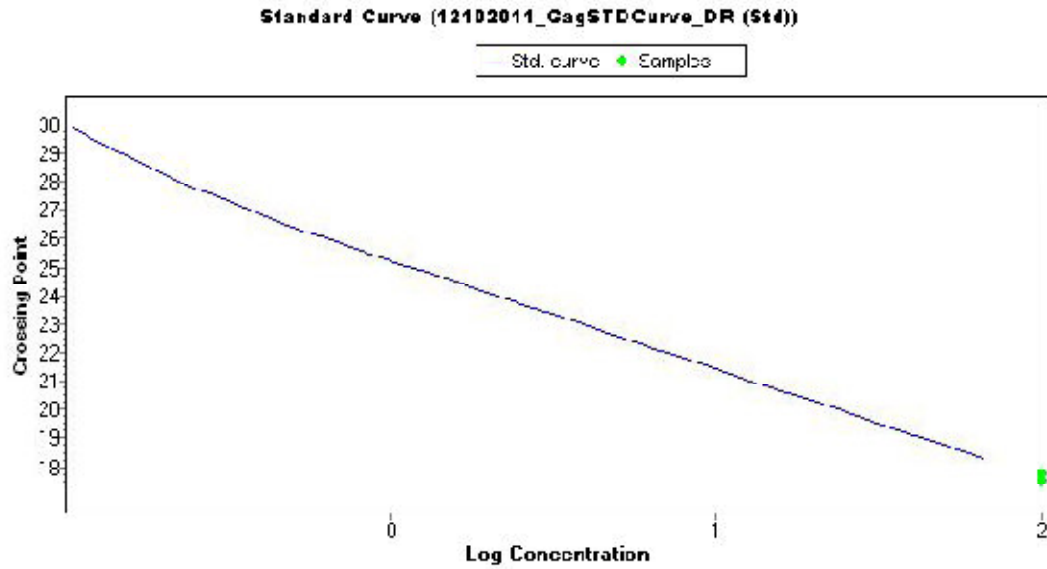
Figure 3.84: The standard curve for *gag* derived from the crossing points (cycle numbers) of each standard plotted against the logarithmic concentration.
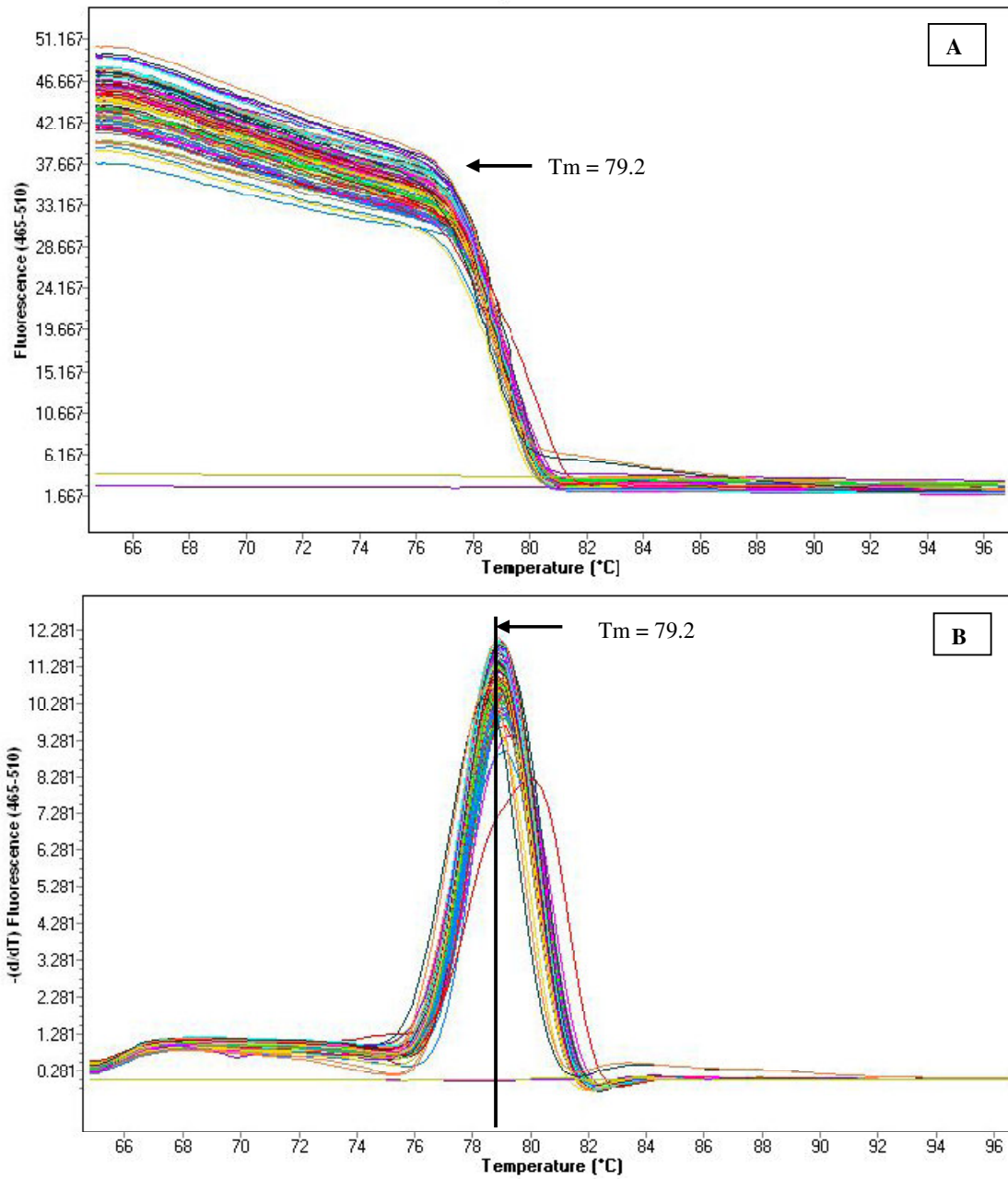
Figure 3.85: (A). Melting curves for *gag* amplification products. (B). The melting peaks of the *gag* amplification product. The melting temperature (Tm) of the gene product is shown by the arrow.

3.4.2.3 Verification of PCR specificity

Real time PCR products of a positive and negative control as well as samples were verified using by a 1% agarose gel which was run for 1h30 at 100 Volts. Specific amplification of proviral DNA viz., *gag* was indicated by the presence of a 95 bp band (Figure 3.86).

L1 – 1kb O'gene molecular weight marker
L2 – Sample
L3 – Sample
L4 – Sample
L5 – Sample
L6 – Sample
L7 – Positive control (8E5 cells)
L8 – Positive control (8E5 cells)
L9 – Negative control (dH$_2$O)
L10 – Negative control (dH$_2$O)
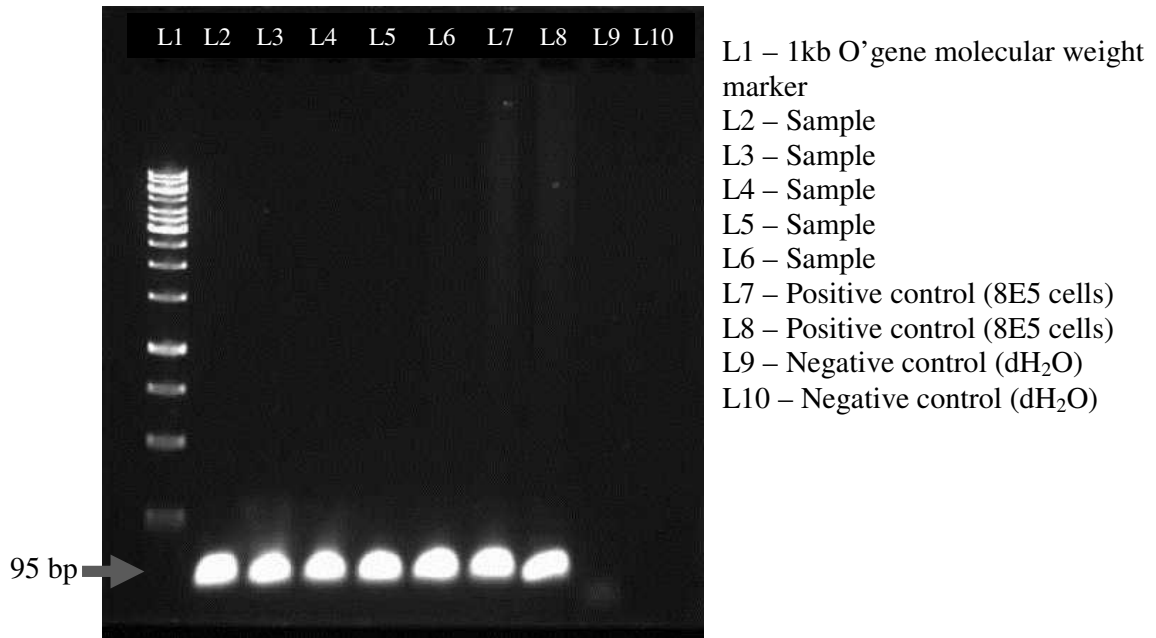
Figure 3.86: Validation of PCR specificity on a 1% (w/v) agarose gel. Amplified products of *gag* are shown by the presence of a 95bp product.

3.4.2.4 Calculated expression levels of proviral DNA

HIV-1 proviral load levels was dissimilar amongst the different areas of the kidney that were laser micro-dissected *viz.*, glomeruli (2.14), tubules (1.95), arterioles (2.86) and whole biopsy core (-0.38) (Figure 3.87). The proviral load differed significantly between the glomerulus, tubules and arterioles *vs.* the whole biopsy ($p < 0.0001$). The proviral load expression was the highest within the arterioles followed by the glomeruli. There was no significant difference of the proviral load between tubules and arterioles ($p < 0.05$).

Our results revealed a statistically significant elevated level of proviral DNA in whole kidney biopsy compared to PBMCs (0.53 *vs.* -0.92; $p < 0.0005$; Figure 3.88). The proviral load of the post-HAART patients (n = 9) that were biopsied was significantly lower when compared to their matched pre-HAART sample (-1.34 *vs.* 0.73; $p < 0.02$; Figure 3.89). A few of the follow up patients real time assay were below the detectable levels of the real time machine. Using the standard curve created the threshold was shown to be 0.2ng/ml.

The proviral DNA level of the biopsy was significantly different to the blood of the pre-HAART (n = 30; $p < 0.0001$) unlike the biopsy *vs.* the blood levels in the post-HAART group (n = 9; $p < 0.05$; Figure 3.90).

Furthermore, we compared proviral DNA load pre and post-HAART in the 9 children undergoing repeat biopsy groups; biopsy (0.53 *vs.* -1.34) and blood (-0.92 *vs.* 0.53; Figure 3.90). Finally, we compared the pre *vs.* post-proviral DNA level (-0.08 *vs.* 0.67) to the pre *vs.* post-CD4 count (2.58 *vs.* 2.67) and pre *vs.* post-Viral load (3.87 *vs.* 3.45; Figure 3.91). The correlation graph (D) showed the relationship between Viral load and proviral DNA to CD4 count. The pre viral load and post viral load showed a positive and negative correlation to CD4 respectively.
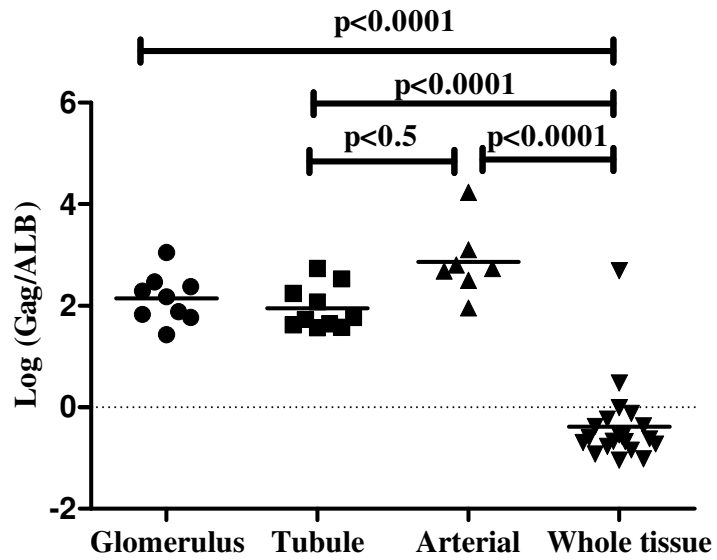
Figure 3.87: Scatterplot of proviral DNA of the whole tissue, and the laser micro-dissected glomeruli, tubules and arterioles within the pre-HAART group.
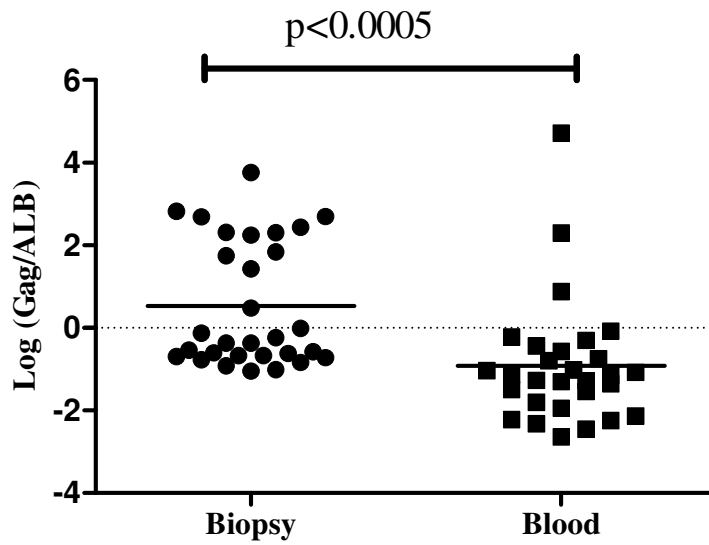
Figure 3.88: Scatterplot of proviral DNA in the biopsy *vs.* blood within the pre-HAART group.
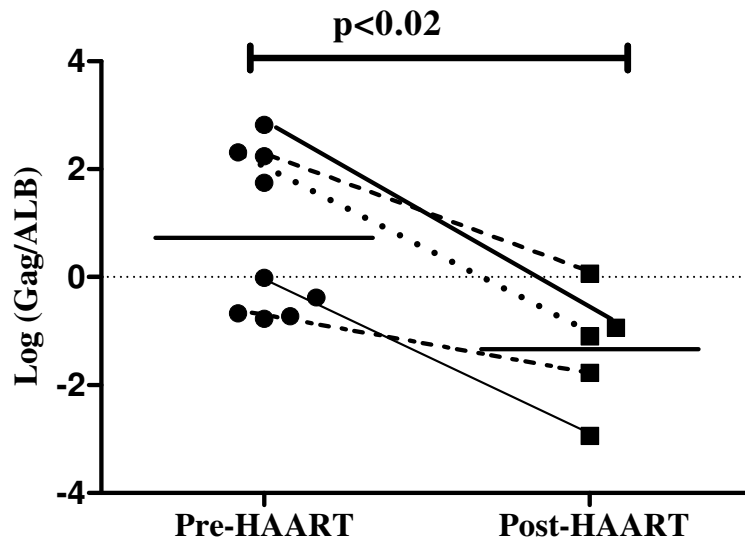
Figure 3.89: A line plot of proviral DNA from blood obtained for patients that were biopsied in the post-HAART group and matched with their pre-HAART counterpart.
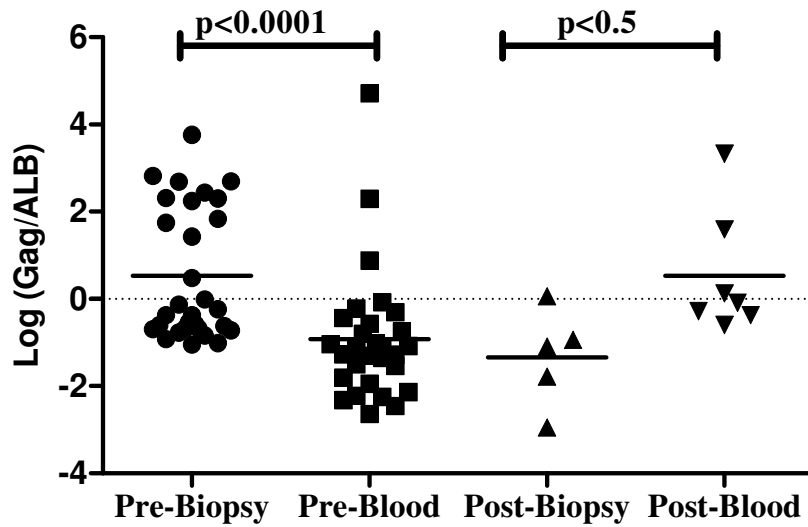
Figure 3.90: A scatterplot of proviral DNA of biopsy and blood compared between pre-HAART and post-HAART.
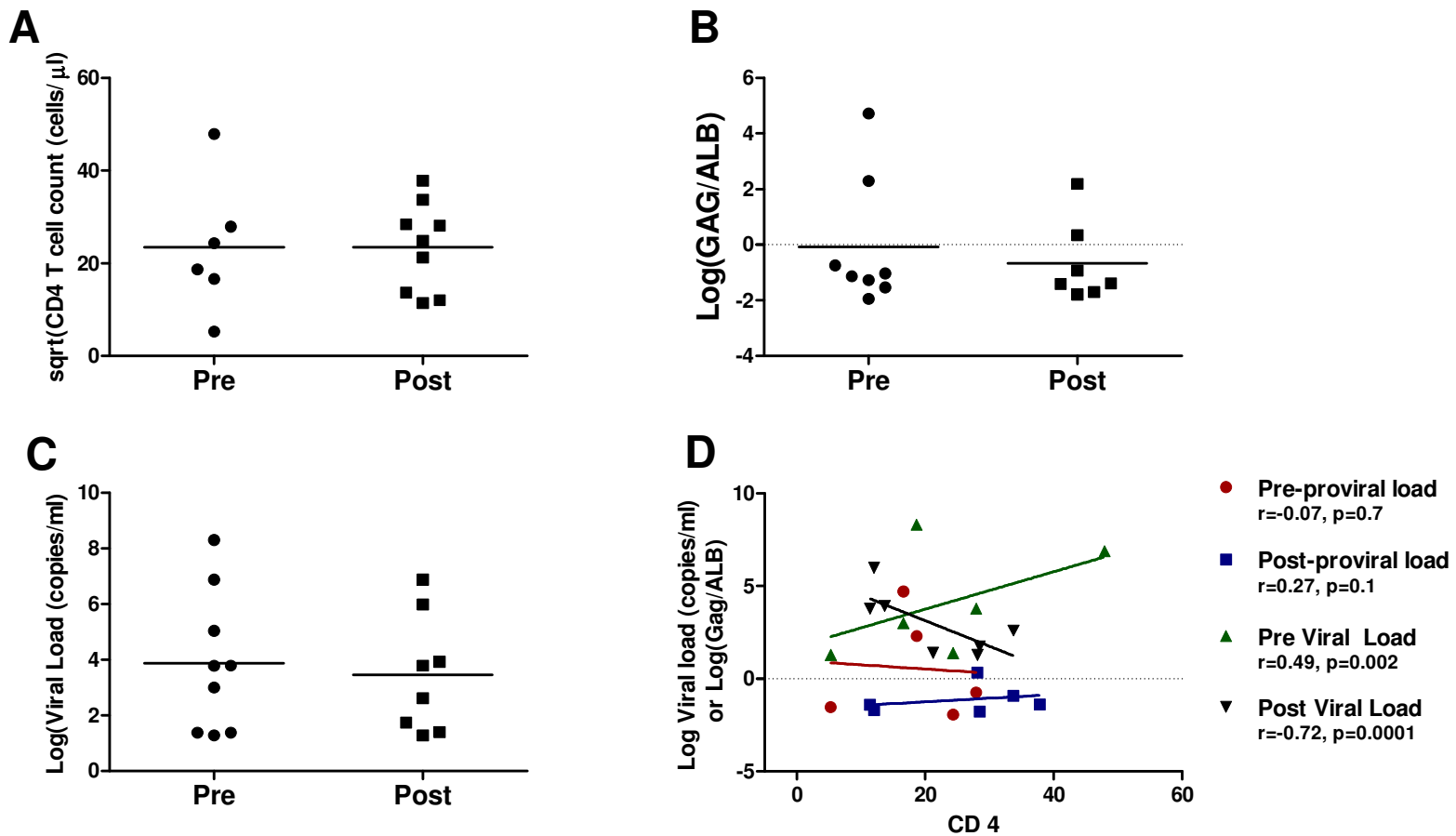
Figure 3.91: (A). Scatterplot comparing the square root of CD4 T cells between the pre *vs.* post-HAART groups. **(B).** Scattergram comparing the log transformation of the HIV proviral DNA between the pre *vs.* post-HAART groups. **(C).** Scatterplot of the log transformation of viral load between the pre-HAART and post-HAART groups. **(D).** A correlation graph showing the relationship between A, B and C.

3.5 SEQUENCE DIVERSITY ANALYSES

3.5.1 Confirmation of Envelope PCR

Extracted DNA was subjected to nested PCR of C2-C5 fragment of the *env* gene reaction and analysed on a 1% (w/v) agarose gel to verify successful amplification. A representative agarose gel pattern of C2-C5 fragment DNA sample is shown in Figure 3.92. Successfully nested PCR from HIVRN samples was confirmed by the presence of 957Kb DNA bands.

L1 L2 L3

L1 – 1kb O'gene molecular weight marker
L2 – Negative control (dH$_2$O)
L3 – Sample

1Kb

≈ 957Kb
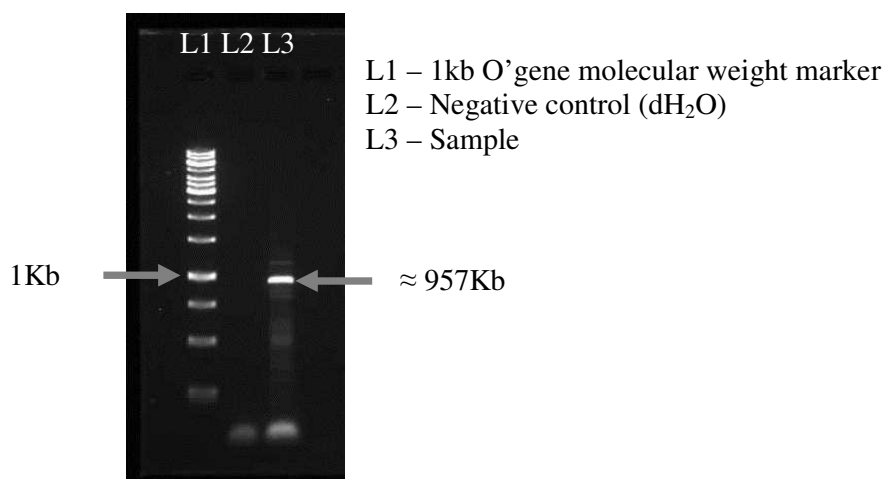
Figure 3.92: Micrograph of an agarose gel illustrating amplification of C2-C5 fragment of the *env* gene as shown by the presence of a 957 bp product.

Ligation of the amplified product into a topo 2.1 vector (Invitrogen) resulted in clonal constructs. The presence of the insert in white colonies was determined by performing colony PCR using specific primers and restriction analysis. Colonies containing inserts were utilized for sequencing. The schematic diagram below shows the actual arrangement of the inserted PCR product within the plasmid (Figure 3.93).
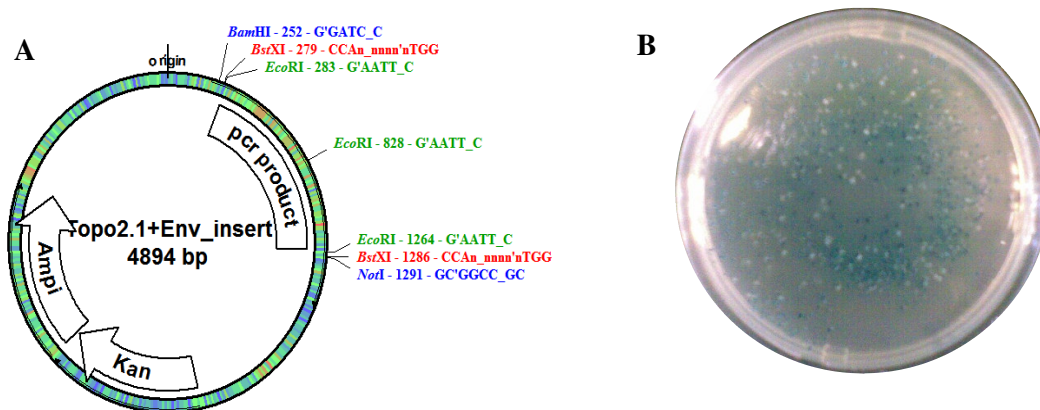
Figure 3.93: (A). Graphic representation of PCR insert within the Topo2.1 vector. **(B).** Photograph of a X-gal, ampicillin agar plate illustrating blue and white colonies.

3.5.2 Phylogenetic analysis biopsy *vs.* blood

The representative Highlighter plots for the envelope region shown in Figure. 3.94, comparing the mutations acquired and lost between biopsy *vs.* blood. A phylogenetic tree generated showed the distinguishing differences between the HIV-1 *env* DNA extracted from blood *vs.* biopsy (Figure 3.95).
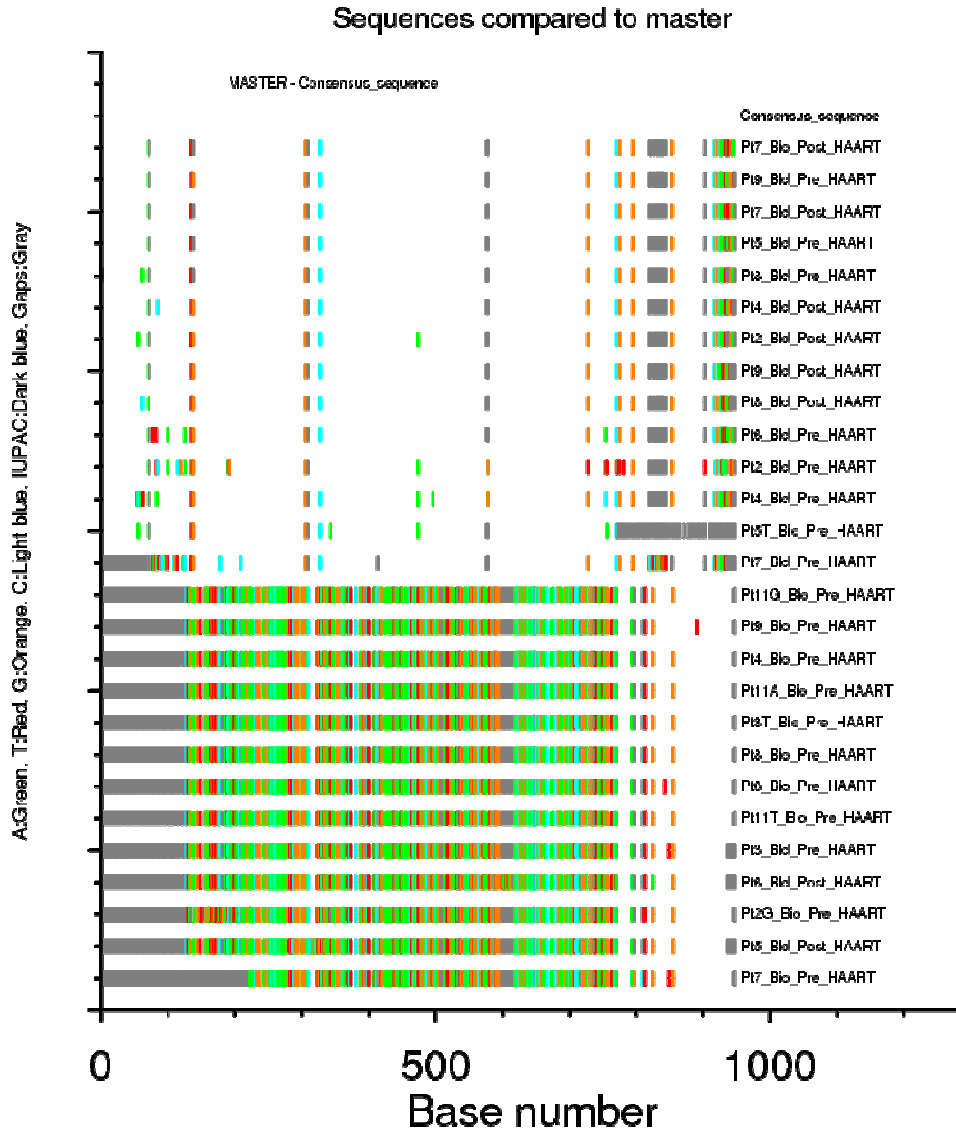
Figure 3.94: Highlighter plot depicting mutations found in *env* region of blood *vs.* biopsy.
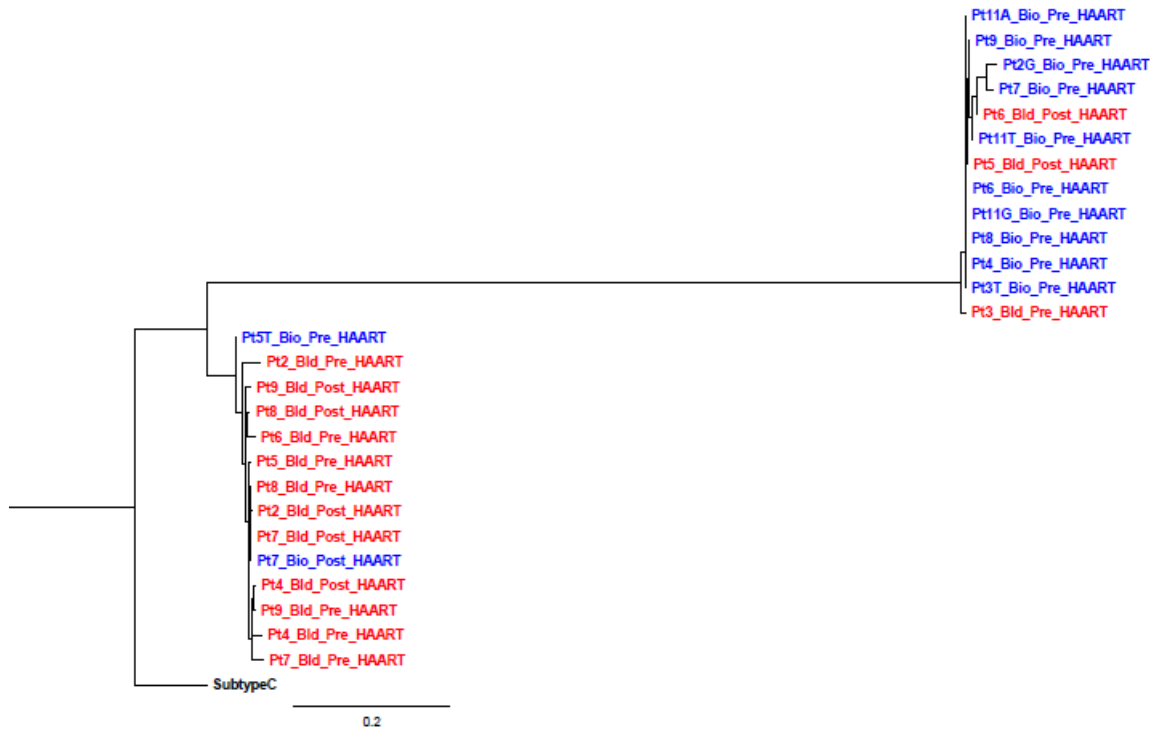
Figure 3.95: Phylogenetic analysis of HIV-1 *env* sequences C2-C5 region comparing blood (Bld) *vs.* biopsy (Bio). Sequences were rooted using representative South African HIV-1 subtype C sequence from Los Alamos database accession number HQ615983.

3.5.3 Phylogenetic analysis Pre *vs.* Post-HAART

The Highlighter Plots showed that before and after treatment mutations are gained and lost with an equal frequency (Figure 3.96). Furthermore, our results showed silent and non-silent mutations within *env* comparing pre *vs.* post-HAART (Figure 3.97). Finally a representative tree comparing pre to post-HAART (Figure 3.98).
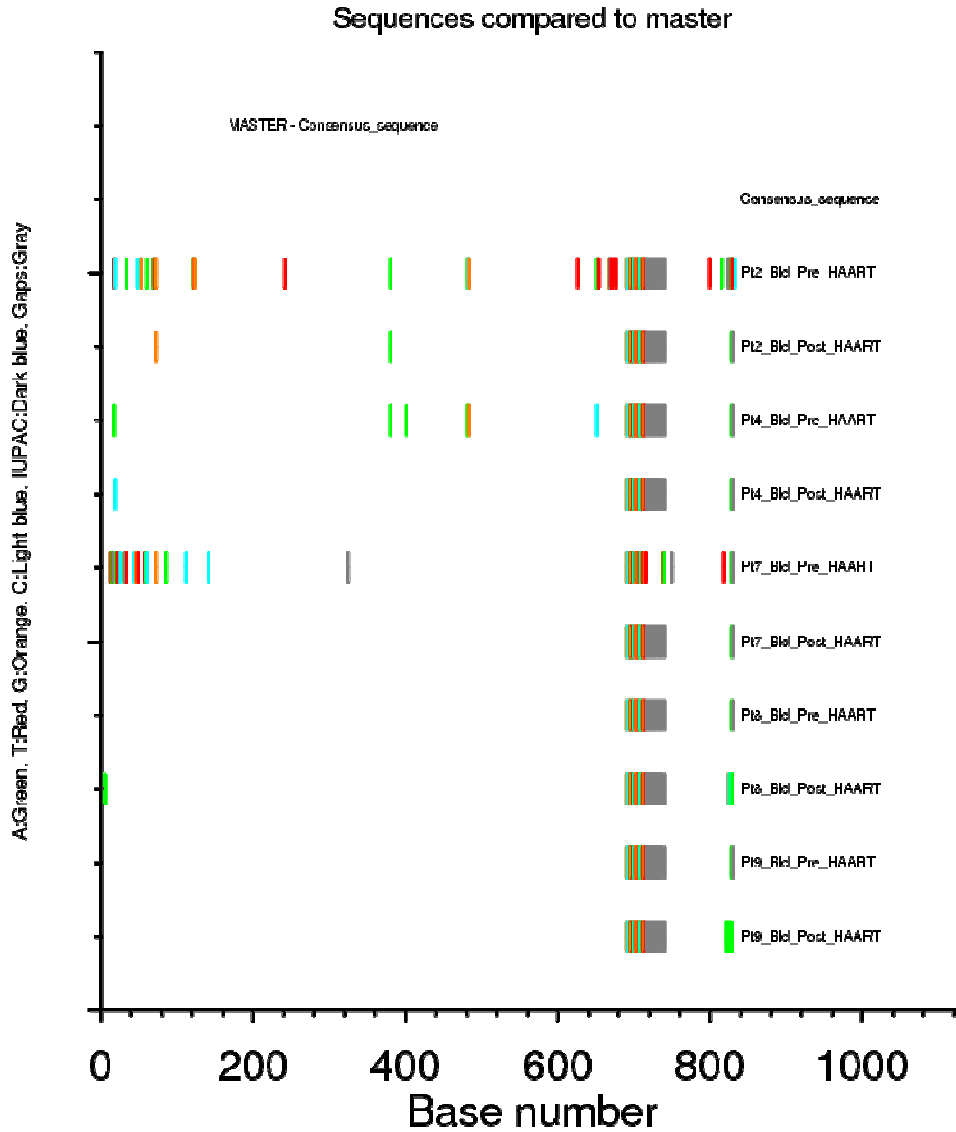
Figure 3.96: Highlighter plot depicting the positions and identities of nucleotide polymorhism insertions and deletions across the *env* region from blood (Bld) samples for pre *vs.* post-HAART analysis.
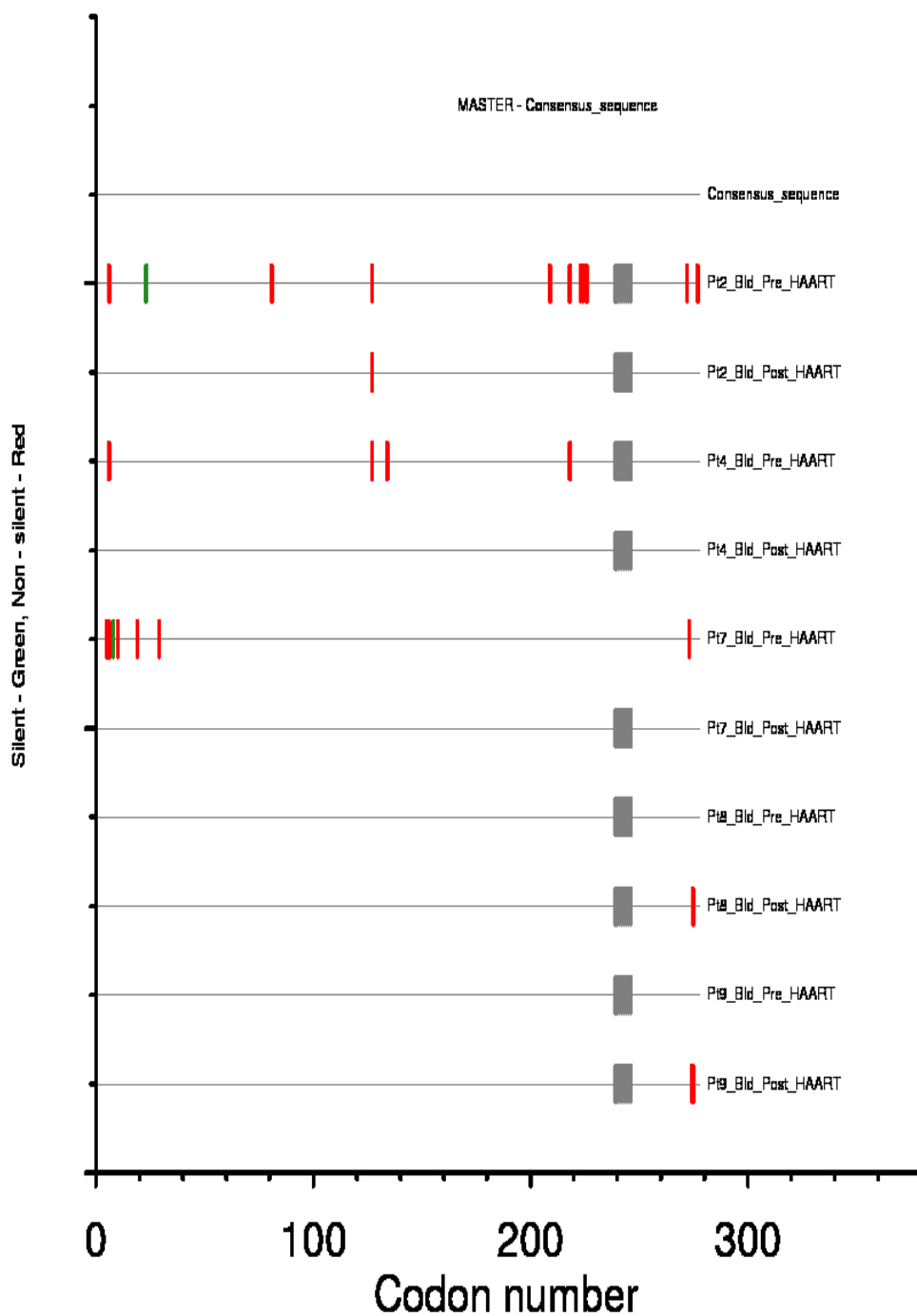
Figure 3.97: Highlighter plot depicting silent and non-silent mutations within the *env* gene from blood (Bld) for pre *vs.* post-HAART.
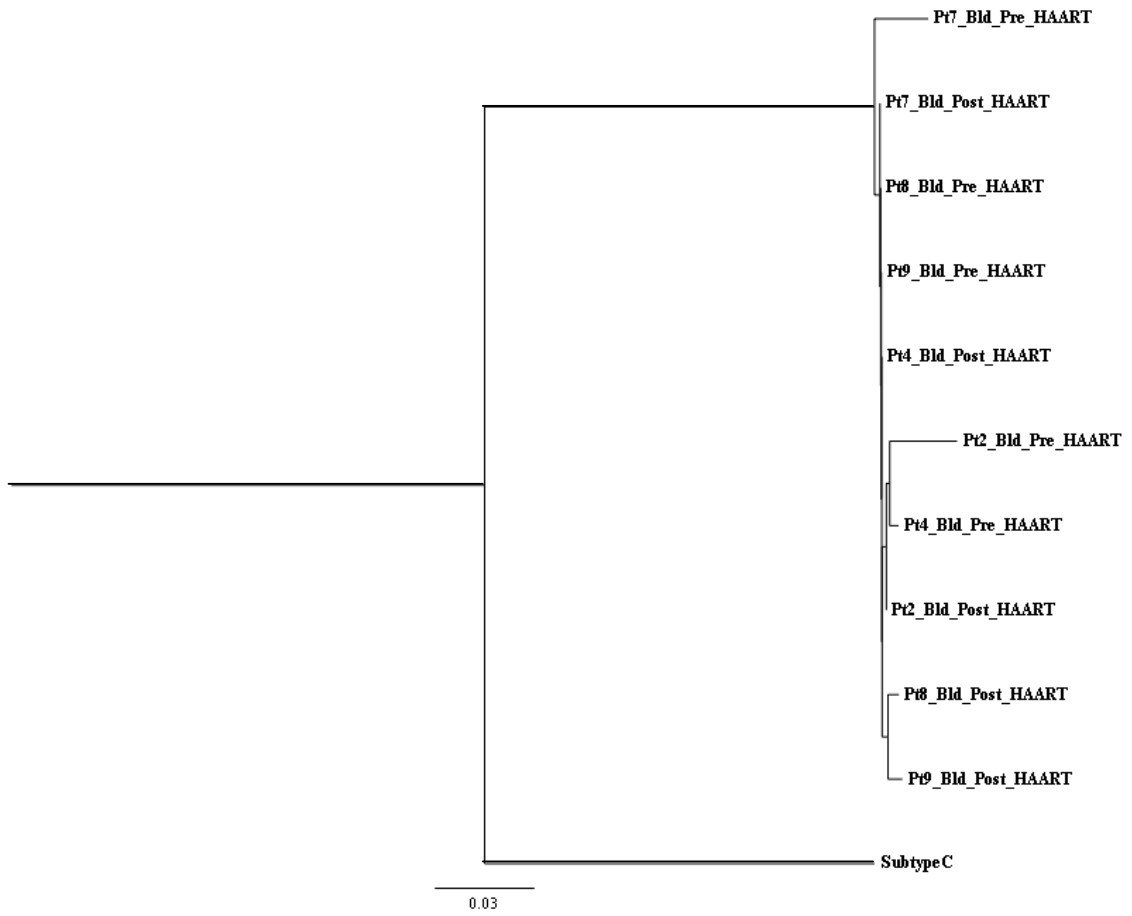
Figure 3.98: Phylogenetic analysis of HIV-1 *env* sequences C2-C5 region comparing pre *vs.* post-HAART blood (Bld). Sequences were rooted using representative South African HIV-1 subtype C sequence from Los Alamos database accession number HQ615983.

CHAPTER 4

DISCUSSION

Sub-Saharan Africa has just over 10% of the world's population, yet it bears 70% of the burden of the HIV epidemic with approximately 25.4 million people being infected by the virus. KwaZulu-Natal is the epicenter of this pandemic. Renal disease has become an increasingly prevalent entity in HIV-infected patients; therefore KwaZulu-Natal is faced with a challenge that is approaching epidemic proportions with HIV related renal disease being a major cause of morbidity and mortality. Nonetheless, a general lack of surveillance and reporting for renal disease in HIV-positive patients exists in this geographical region.

Rao *et al.*, (1987) divided the HIV-1-associated renal parenchymal diseases into four groups: (1) acute tubular dysfunction with electrolyte fluid abnormalities and/or renal failure caused by infections and nephrotoxic drugs; (2) HIV glomerulopathies related to immunological abnormalities (IgA nephropathy, lupus-like syndromes, and HIV-associated immune complex renal disease); (3) HIV-associated thrombotic microangiopathies, including atypical forms of the hemolytic uremic syndrome; and (4) HIV-1-associated nephropathy (HIVAN) (Connor *et al.*, 1988; Strauss *et al.*, 1989; Turner *et al.*, 1997).

In the early 1980s, soon after the onset of the HIV/AIDS epidemic, nephropathy was increasingly recognized to be associated with HIV infection. HIVAN is characterized by a collapsing glomerulopathy with collapse of glomerular capillary structures and a hyperplasia of podocytes, microcystic transformation of renal tubules, and concomitant interstitial inflammation and fibrosis. To-date it is estimated that about 10% of HIV-

infected patients develop HIVAN worldwide (Han *et al.*, 2006a; Valeri and Neusy, 1991). However, it appears that this prevalence is influenced by the type of study (whether autopsy or biopsy based) and the demographics of the HIV-infected population.

A study by Lascure *et al.*, (2011) showed HIVAN decreased over time, while FSGS emerged as the most common cause of glomerular diseases (46.9%) in HIV-infected individuals in the period 2004 - 2007. This study showed that HIV related nephropathy exceeds any other cause of kidney disease responsible for end stage renal disease, and has been increasingly recognized as a significant cause of morbidity and mortality (Lescure *et al.*, 2011).

Unfortunately there is also a paucity of data of HIVRN from Africa. The true prevalence of childhood HIVRN is also unknown for Africa. Consequentially, this alarming reality emphasis the importance of outlining the spectrum of HIV related nephropathies within this geographical epicenter of the global HIV pandemic as well as evaluating the efficacy of HAART in combination with ACE-I in our population. Moreover, from a pathology standpoint, it is important to address whether HIV related nephropathy is a direct consequence of viral infection of the renal parenchyma or is it a secondary consequence of systemic infection.

It is interesting to note that Black patients have a relative risk of 51.1% compared to White patients for developing end-stage renal disease from AIDS or an AIDS-defining diagnosis (Bhimma, 2007; Kimmel *et al.*, 2003). This increased burden of chronic kidney disease, particularly end-stage kidney diseases in populations of African ancestry has been largely unexplained. A review of over 200 patients with HIV-associated nephropathy in the USA

found that 90% were Black and 70% male (Bourgoignie, 1990; D'Agati and Appel, 1997). This predominance among Black African Americans and males is striking if one considers that in the United States, HIV infection is three times more common among Whites than Blacks with a preponderance of males being infected (Bourgoignie, 1990). Also, it is important to remember the low incidence of HIVAN in Europe presumably reflects the region's small Black population (Barbiano di Belgiojoso *et al.*, 1990; Baumelou *et al.*, 1989; Burger *et al.*, 1989).

Using the United States Renal Data System, Ahuja *et al.*, (2004) report that of 7732 patients with HIVAN only 60 were classified as children, of which 88% were Black and there was an equal distribution in terms of gender. Other studies have reported a male gender preponderance in HIV related nephropathy (Anochie *et al.*, 2008), a finding supported in this study in which 56.7% were males.

Strauss *et al.*, (1993) and others have reported a prevalence of 10-15% HIVAN of approximately in HIV infected children of which 95% were African American (Connor *et al.*, 1988; Ingulli *et al.*, 1991; Ray *et al.*, 1998; Ray *et al.*, 2004; Strauss *et al.*, 1989). There is a high prevalence of the duffy antigen chemokine receptor (DARC) promoter polymorphism in the Black race (Hadley and Peiper, 1997; Ray *et al.*, 2004), and previous studies have shown that HIV-1 binds to *DARC* (Lachgar *et al.*, 1998). Additionally, genetic variation at the *MYH9* locus substantially explains the increased burden of FSGS and hypertensive end-stage kidney disease among African Americans (Kopp *et al.*, 2008). In a recent study a major source of genetic risk for African American patients with end stage kidney disease and FSGS was localized to apolipoprotein L1 (ApoL1), 14kb from *MYH9*. This study also showed the effect of carrying two *APOL1* risk alleles accounted

for 18% of FSGS and 35% of HIVAN which implies that eliminating this genetic variation will reduce FSGS and HIVAN by 67% (Kopp *et al.*, 2011).

In contrast to most studies that believe HIVAN is a late manifestation of HIV infection (Ahuja *et al.*, 2004; Anochie *et al.*, 2008; Ray *et al.*, 1998; Ross *et al.*, 2000; Winston *et al.*, 1999), recent studies have reported HIVAN as an early manifestation of HIV infection (Anochie *et al.*, 2008; Burns *et al.*, 1997; Ramsuran *et al.*, 2011a). It is plausible to assume HIVRN is a early manifestation of HIV infection from our study since the occurrence of HIV infection in the youngest patient recruited in our cohort was 10 months, and 12(40%) were younger then 5yrs, supporting this hypothesis.

This study is part of the largest paediatric cohort in Africa that followed-up HIV-infected children for 1 year (pre and post-HAART). It outlines the spectrum of paediatric nephropathy in treatment-naïve children in KwaZulu-Natal as being FSGS (43.3%), mesangial hypercellularity (30%), HIVAN (10%), tubulointerstitial nephritis (6.67%), minimal change (6.67%) and sclerosing glomerulopathy (3.3%). This spectrum contrasts to the adult chronic kidney disease population in which HIVAN was shown to be the most common form of chronic kidney disease. In a previous South African study performed on adult patients from the same centre, HIVAN was also found to occur in 83.3% of all patients who were biopsied (Han *et al.*, 2006a).

Whereas collapsing FSGS (HIVAN) is the predominant lesion in adult HIV-infected patients undergoing renal biopsy, this is not the case in children in the United States (Bourgoignie, 1990). Data from diverse geographic regions of the United States suggest that lesions other than FSGS, such as mild mesangial proliferative forms of

glomerulopathy and immune-mediated glomerulonephritis, are more frequent in children than adult patients with HIV infection (D'Agati and Appel, 1997; Strauss *et al.*, 1993). However, in one of the largest reported series of children with HIVRN in Africa to-date, the most frequent histological form of the disease in Black children was the classic form of FSGS accounting for 37.3% of all cases of children who underwent kidney biopsy (Ramsuran *et al.*, 2011a). This study, a sub-group of the latter study cohort, also reports a predominance of FSGS (43%).

The absence of HIVICK in our study may be due to the fact that most of the children recruited in this study were of African origin. According to previous studies, HIVICK has a racial distribution occurring predominantly (80%) in patients of Caucasian origin, particularly drug abusers (Lescure *et al.*, 2011). Although HIVICK a 'lupus-like' picture is absent in our cohort of children, it accounts for approximately a quarter of HIV-related kidney diseases in Black adults from Johannesburg, South Africa (Gerntholz *et al.*, 2006). The explanation provided by Gerntholz *et al.*, for this high incidence of HIVICK as in HIV-infected patients there are often large amounts of circulating antigen associated with a polyclonal antibody response. This could lead to the formation of immune complexes, either in the circulation or in situ in the kidney itself. The concomitant activation of inflammatory mediators would then result in secondary renal damage in a manner analogous to lupus nephritis (Gerntholz *et al.*, 2006). However the low incidence of HIVICK in children in our cohort of patients did not support this hypothesis.

In a Miami-based caucasian population of HIV-infected adults with glomerular disease, 17% had a mild forms of focal glomerulosclerosis, 75% had diffuse mesangial hyperplasia, and none had severe FSGS (Bourgoignie, 1990). Whilst the latter study fails to supports

our histopathological finding, the spectrum of HIVAN seen in Caribbean and American Blacks, in which 55% had severe focal sclerosis, 9% had mild focal sclerosis, and only 27% had diffuse mesangial hyperplasia (Cohen, 1990).

Other histological forms of HIVRN, such as membranous nephropathy and IgA nephropathy were absent in children in our study. This could be due to IgA nephropathy being a rare disease in people of Black African origin (Gerntholz *et al.*, 2006; Kimmel *et al.*, 1992) and the small sample size in this study. However in a study in adults from South Africa 13% had membranous nephropathy and 5% IgA nephropathy (Gerntholz *et al.*, 2006)

In this study we found that oedema and hypertension occurred at a lower incidence in children post-HAART which is in accordance with reports from adult patients (Cochat *et al.*, 2009; Herman and Klotman, 2003). The low incidence of these clinical findings on initial presentation may hide the presence of nephropathy. The possible explanation for the absence of these two clinical findings is that these patients have salt-losing nephropathy, which accounts for the normal blood pressure, and the high oncotic pressure contributed by the marked hypergammaglobulinaemia that prevents the development of oedema (Klotman, 1999; Ramsuran *et al.*, 2011a). Also, the lack of oedema and hypertension in these children despite the presence of heavy proteinuria may mask the presence of nephropathy (Klotman, 1999; Ramsuran *et al.*, 2011a).

Electrolyte disorders in patients with AIDS can have multiple and variable causes. Other studies have reported hyponatremia as the most common electrolyte abnormality in majority of their patients (Bourgoignie, 1990; Cusano *et al.*, 1989; Seney *et al.*, 1989;

Tang *et al.*, 1988). In this study hyponatremia was noted in 5(16.7%) patients at initial visit, on follow-up only 2(10%) patients remained hyponatremic following treatment.

Hyperkalemia has been reported in 16% of patients with AIDS (Seney *et al*., 1989). This increased serum potassium may be the consequence of Addison's disease, or it can result from hyperreninemia (Bourgoignie, 1990). In our study 5(16.7%) patients presented with hyperkalemia, but reverted to normal at follow-up showing significant difference between pre and post-HAART groups. All five children had chronic kidney disease stage II-V, with one child having ESRD.

Mild to moderate hypocalcemia, generally associated with hypoalbuminemia affects the majority of AIDS infected patients (Seney *et al.*, 1989; Vaziri *et al.*, 1985). The hypoalbuminemia however does not always fully account for the hypocalcemia (Seney *et al.*, 1989; Vaziri *et al.*, 1985). Four (13.3%) presented with hypocalcemia at initial presentation, but only three resolved on follow-up. This child's eGFR decreased to 27(m/s/m^2/min) on follow-up and the child developed hypocalcemia following correction of metabolic acidosis.

The largest reported series of imaging findings in HIV nephropathy identified new sonographic findings of advanced HIV-associated nephropathy involving decreased corticomedullary definition, decreased renal sinus fat, parenchymal heterogeneity and cortical echogenic bands and a globular appearance (Bourgoignie, 1989). In our study, ultrasonographic examination of the kidneys revealed enlarged kidneys in only 40% of the pre-HAART group compared to 10% of the post-HAART group. Kidneys in patients with HIVRN have being reported to be either normal-sized or enlarged and size does not

correlate with the degree of proteinuria (Bourgoignie, 1989). Thus enlarged kidney size is not a sensitive marker of HIVRN in our children. However, Post-HAART there was a statistically significant decrease in kidney size and echogenicity, which is in accordance with reports from adult patients

Renal dysfunction is an important complication of advanced HIV infection in Africa. In our study we showed that in 12 children the eGFR were stabilized, 3 deteriorated and 5 improved post-HAART. Thus HAART in combination with ACEI treatment has been shown to ameliorate renal function in children with HIVRN. However, studies carried out amongst adults with advanced HIV disease in rural Uganda showed improved renal function over 2 years on HAART (Peters *et al.*, 2008). Given a longer period of follow-up it is possible that a larger proportion of children may show improvement in their renal function in our study.

The combination of collapsing FSGS and extensive renal tubular injury is thought to be specific to HIVAN although previous studies have shown both adults and children not infected with HIV-1 can develop similar lesions (Ray *et al.*, 2004; Singh *et al.*, 2000; Vivette, 2003). Thus, it is tempting to speculate that infectious agents other than HIV-1 may be involved in the pathogenesis of collapsing FSGS. Several studies have investigated the role of *Mycoplasma fermentans*, the polyomavirus simian virus 40, and parvovirus B19 with inconclusive results (Kimmel *et al.*, 2003; Moudgil *et al.*, 2001; Ray *et al.*, 2004). In our study we had very low incidence of opportunist infections.

The survival of HIV-infected children after the development of clinical nephropathy is reported to be dismal (Ingulli *et al.*, 1991; Rajpoot *et al.*, 1996; Ray *et al.*, 1998; Strauss *et*

al., 1989). Some studies noted that HIVAN progresses to ESRD at a very rapid rate, varying from weeks to months (Ahuja *et al.*, 2004; Pardo *et al.*, 1984; Rao *et al.*, 1984). However, Strauss *et al*., (1993) and Ray *et al*., (2004) noted a less fulminant course in children compared with adults. In this study, overall patient survival at 1 year follow-up (post-HAART) was 76%. Laradi *et al*., (1998) demonstrated lower patient survival at 0.5, 1 and 3 yr to be 73 ± 5, 55 ± 6, and $38 \pm 7\%$, respectively. The 7 patients that demised in our study were predominantly non-renal related causes, suggesting that in this new era of HIV therapy survival rates have considerably improved. Laradi *et al*., (1998) suggests that the only reliable predictor of patient survival is the intensity of immunodeficiency.

Our study has shown the beneficial effects of HAART in combination with ACE-I in managing patients with HIVRN. All patients recruited pre-HAART presented with varying degrees of proteinuria, with 40% in the nephrotic range. Post-HAART only 15% of patient's had mild degrees of proteinura and it is possible that with a longer follow-up period this 15% may also attain remission.

Whilst the ultrastructural examination of human biopsies are of great value in general pathology, they are essential to the interpretation of renal biopsies. This is the first study to perform a comprehensive evaluation of the ultrastructural pathology of children with HIV related glomerulo-nephropathy in Africa. Additionally, electron microscopy may add to and confirm molecular analyses.

Consistent with FSGS, the incidence of tubular reticular structures were frequently noted within endothelial cells lining glomerulo-capillary loops. Tubuloreticular inclusions have

previously been noted within the cytoplasm of glomerular and other vascular endothelial cell of HIV–associated FSGS (Cohen and Nast, 1988; D'Agati and Appel, 1997).

Cellular immune factors have been implicated in renal pathology. Interstitial inflammatory infiltration was frequently observed in our study. HIV-associated FSGS and immune complex disease, is also characterised with a dense interstitial inflammatory infiltrate (Cohen and Nast, 1988; D'Agati and Appel, 1997; Rao *et al.*, 1984). Since different immune cell populations characterize the latter conditions, a cellular influence on phenotypic expression may be involved. Furthermore, this rich inflammatory cell milieu supports direct viral entry into renal epithelial cells via trans-infection by phagocytosis of released virus or perhaps during direct leucocyte-to-renal cell contact (Bruggeman and Nelson, 2009; Wu and Kewalramani, 2006).

Podocytes, the specialized epithelial cells that form the final filtration barrier of the glomerulus, are one of the primary cell types infected by HIV-1 (Barisoni *et al.*, 1999; Winston *et al.*, 2001). HIVAN is associated with podocyte effacement and loss of cytoskeletal structure on electron microscopy (Barisoni *et al.*, 1999). Accumulating evidence indicates that podocyte damage triggers progression of glomerular deterioration that leads to glomerular sclerosis (Zuo *et al.*, 2006).

Moreover, podocytes are terminally differentiated cells that normally cannot proliferate. They do not change their phenotype in response to injury, however, there are experimental data showing that podocyte can change their phenotype and proliferate in experimental crescentic glomerulonephritis and HIV nephropathy.

Podocyte hyperplasia (pseudocresent formation) as typically observed in adults with collapsing glomerulopathies was also noted in our pediatric cohort. Thorner *et al.*, (2008) have indicated that proliferating podocytes may initiate the formation of and populate true glomerular crescents (Bruggeman and Nelson, 2009). In our pre-HAART group proliferation of parietal epithelial cells with adhesions to visceral epithelium and crescent formation was evident.

In this study, the podocyte cytopathic features noted included ER stress, lipid distention and mitochondrial oedema which are direct causes of viral insult. It may be plausible to hypothesize that the observation of dilated pools of cisternal type ER in the podocyte cytoplasm may be attributed to ER stress. An increasing amount of literature supports the hypothesis that viruses like other ER stress signals may induce membrane proliferation through the activation of specific components of the Unfolded Protein Response (Kaufman, 2002; Umareddy *et al.*, 2007). This response alleviates stress by stimulating protein folding and degradation in the ER and down-regulating overall protein synthesis, finally decreasing viral replication. Additionally, the Unfolded Protein Response may account for the mitochondrial oedema and nucleolemmal crenation observed in this study. Furthermore, HIV-1 infection has been shown to induce alteration of cellular lipids (Raulin, 2002). The observation of distention/accumulation of lipid droplets within podocytes in the pre-HAART group may hence be viral induced.

Moreover, the occurrence of podocyte vacuolation in this study may also be attributed to viral presence (Henics and Wheatley, 1999). Induction of cytoplasmic vacuoles by viruses have been described previously (Henics and Wheatley, 1999). This finding lends credence to the assumption that the HIV-1 presence induces cellular vacuolation.

Mesangial proliferation was prominent. Mesangial cells have been shown to express HIV-1 receptor and co-receptors (Bruggeman and Nelson, 2009). However, in our study, HIV-1 was not observed in glomerulo-mesangial and endothelial cells. These findings are supported by (Cohen *et al.*, 1989; Kimmel *et al.*, 1993a; Marras *et al.*, 2002). Additionally, reports on the infection of mesangial cells in vitro are inconclusive whilst endothelial cells are CD4 and co-receptor negative (Bruggeman and Nelson, 2009). This study does not report transcytosis or evidence of direct replication within endothelial and mesangial cells.

Subepithelial deposits in relation to the GBM, resulting in a "ball-in-cup" reaction pattern was noted. This form of immune-complex-mediated glomerulopathy is thought to represent a distinctive form of HIV associated glomerulo-nephropathy (Naicker *et al.*, 2007). The irregular contouring of the GBM as frequently observed within both pre and post-HAART group is a frequent pathological observation associated with nephropathy.

Fibrin is an important mediator of glomerular injury and is pivotal in crescent formation in glomerulonephritis (Holdsworth *et al.*, 1979; Thomson *et al.*, 1975). The ability of macrophages to initiate intraglomerular fibrin deposition in association with augmented levels of glomerular procoagulant acitivity has recently been demonstrated in a passively induced model of experimental glomerulonephritis (Tipping and Holdsworth, 1986). The occurrence of fibrin deposition within the GBM as noted in this study may be linked to a temporal relationship between macrophage accumulation and glomerular fibrin deposition (Holdsworth and Tipping, 1985).

Podocytes have several functions; the slit diaphragm complements the glomerular filtration barrier by limiting molecules based on their size, charge and shape (Naicker *et al.*, 1997). Additionally they lay down and remodel the GBM with structural functions maintaining capillary loop structure against the ballooning force of hydrostatic pressure and contractile force of mesangial cells (Kimmel *et al.*, 2003). FSGS is a disorder of podocyte depletion (Barisoni *et al.*, 1999). In contrast, HIVAN is manifested by abnormal extensive proliferation of podocytes, cells that are normally terminally differentiated. Recent results showed that HIV can directly infect the podocyte, and a series of interrelated pathways leads to loss of the differentiated phenotype with extensive proliferation and resultant glomerular collapse (Bostrom and Freedman, 2010; Papeta *et al.*, 2009).

In this study, we evaluated renal epithelial proliferation and dedifferentiation using immunohistochemistry analysis performed on specific cell type markers; Ki67 and synaptopodin which was evaluated pre and post-HAART. Additionally, we demonstrated viral core protein, p24 in renal biopsies pre and post-HAART.

Classically, HIV entry is into cells are receptor mediated epithelial cells are CD4 negative, hence an unrecognized site of HIV-1 infection. However it has been shown that other epithelial cells such as cervical epithelial cells may harbor HIV-1 (Barisoni *et al.*, 2000b), Additionally, murine models support the latter findings (Salifu. M, 2010). This study conclusively demonstrates HIV-1 viral core proteins within glomerular and tubular epithelial cells. The mean field area percentages of these proteins were statistically significant in the pre-HAART group compared to the post-HAART group. A direct translation implies efficacy of HAART over a 1 year period in reducing viral reservoirs.

144

Our results show weak immunoreactivity of synaptopodin, an actin based cytoskeleton podocyte proteinin pre-HAART group. Following a year of HAART the mean field area percentage of synaptopodin was upregulated indicating reconstitution of the initial podocyte effacement. Previous studies have implicated HIV-1 proteins such as *Tat*, *Nef* and *Vpr* in podocyte dysfunction and phenotype change. The latter finding is supported by our p24 immunolabelling and evidence of viral reservoirs by electron microscopy. The introduction of HAART and ACE-I as the combination prophylaxis in this study, proved to be immensely efficient in glomerular structural and functional reconstitution.

In this study, the cell cycle protein, Ki67 was statistically, higher in the pre-HAART group compared to the post-HAART group (1.01 *vs.* 4.68; $p < 0.001$). This epithelial proliferation in the pre-HAART group was expected as the spectrum consisted of majority (84%) of proliferative glomerular disorders *viz.*, HIVAN, FSGS and mesangial hypercellularity. The down regulation of this antibody in the post-HAART group is indicative of the efficiency of the combination therapy of HAART and ACE-I.

In (1989), Cohen *et al.*, reported the presence of HIV RNA in podocytes by *in situ* hybridization . These findings were corroborated by the microdissection studies of Kimmel *et al.*, (1993a). However, a failure to replicate these studies using in situ hybridization, the inability to demonstrate the presence of viral peptides in renal parenchymal cells by immunohistochemistry, and the inability to demonstrate appropriate receptors for viral entry on renal parenchymal cells was reported (Cohen *et al.*, 1989). This study provides evidence for localized replication of HIV-1 in the kidney and the existence of a renal viral reservoir using polymerase chain reaction assays and transmission electron microscopy.

Proviral integrated HIV-1 DNA genomes induce productive replication via the transcription of viral RNA genome defining the spread of HIV-1 virions (Skalka, 1999). Both HIV-1 proviral DNA and plasma RNA detection denotes two basic targets to monitor the viral reservoir and viral replication respectively (Clementi *et al.*, 1996; Yilmaz, 2001). It is important to note that the detection of HIV-1 proviral DNA in PBMCs is an important diagnostic marker in the evaluation of HIV-1 of newborns of HIV-1 seropositive women (Yilmaz, 2001).

Proviral HIV-1 DNA is also a useful indicator for detecting viral reservoirs. Our results demonstrate proviral quantification of HIV-1 DNA in PBMCs and biopsy tissue using simple SYBR green based real time assay. This assay successfully amplified/detected proviral DNA from different laser micro-dissected epithelial cells within the kidney and from PBMCs. HIV-1 proviral DNA were elevated in biopsy tissue as compared to PBMCs. Likewise, Gibellini *et al*., (2004) and Popper *et al*., (2000), report a higher proviral load in tissue compared to blood. Additionally, in our study HIV-1 proviral DNA expression within glomeruli were higher than tubules and whole biopsy tissue. It is possible that the low proviral DNA yield within whole biopsy tissue is due to dilution attributed to an admixture of cell types.

Additionally, this study shows a decrease of HIV-1 DNA content post-HAART compared to pre-HAART. Gibellini *et al* (2004) report analogous data. Thus, despite the major effect HAART has in decreasing proviral DNA (as observed in this study), it was not successful in eradicating the total proviral load. Hence the SYBR green PCR technique is useful for monitoring HIV-1 DNA contaminated cells in infected patients receiving

HAART, since HIV-1 reservoir infection formed during the primary infection and highly resistant to therapy is one of the major obstacles to eradication of infection.

Since proviral DNA has been simultaneously amplified and quantified in patients that had an absence of detectable plasma viremia, HIV-1 proviral DNA count may be a potential biomarker identifying latent viral reservoirs and determining the impact/efficacy of HAART. In contrast to a report by Gibellini *et al.*, (2004), there was no correlation between proviral DNA *vs.* viral load. However, there was a statistically significant correlation between the CD4+ T cell count (post-HAART) *vs.* proviral DNA (post-HAART).

We showed the ubiquitous presence of HIV DNA in renal tissue of HIV-infected patients whilst other studies are limited to the localization of HIV-1 messenger RNA in renal tissue, specifically glomerular and tubular epithelial cells (Bruggeman *et al.*, 2000; Kimmel *et al.*, 2003; Ross and Klotman, 2002; Winston *et al.*, 2001). From these results one can conclude that HIV-1 proviral DNA load represents the infection reservoir in epithelial cells within the kidney and plays a pivotal role in immune surveillance escape. Winston *et al.*, (2001) demonstrated viral transcripts in renal epithelial cells in patients on HAART that is similar to a report of the persistence of spliced and unspliced HIV-1 mRNA in PBMCs in such patients. These results suggest that renal epithelial cells may be a persistent reservoir of HIV-1 RNA transcription and that any interruption in therapy could lead to the rapid formation of infectious virions (Ho and Zhang, 2000).

In this study, RT-PCR provided evidence of HIV-1 within the kidney, specifically by amplification of proviral DNA *viz.*, *gag*. Since renal epithelial cells lack CD4, HIV-1 has

exploited receptor mediated entry thereby utilising unconventional mechanisms to cross the epithelium. The ultrastructural and genetic evidence provided in this study supports the theory of a non-receptor mediated HIV-1 trafficking across renal epithelial cells. It is important to note that no replication occurs within the epithelial cell however, endocytic trafficking of the virus from apical to basal pole of the cell occur. Previous studies have shown that non-lymphoid cells may be exploited as a means of virus trafficking rather than a means of replication (Bruggeman and Nelson, 2009).

The lipid composition of the apical epithelial membrane exhibits unique features. It contains Gal Cer, a monohexosylceramide which is markedly enriched at the apical surface of epithelial cells (Alfsen *et al.*, 2001; Simons and van Meer, 1988). Transient lateral assemblies of these glycosphingolipids are stabilized by cholesterol and they participate in the establishment of microdomains referred to as rafts, which act as platforms for endocytosis (Brown and London, 1998; Rietveld and Simons, 1998) and transcytosis (Hansen *et al.*, 1999; Verkade *et al.*, 2000). Gal Cer is thought to act as gp120 epithelial cell receptor thereby facilitating movement of HIV-1 across the epithelium (Bhat *et al.*, 1993; Yahi *et al.*, 1992).

The subunit of beta-integrins of intercellular adhesion molecule-grabbing non-integrin, expressed by cervical epithelium binds to gp120 on fibronectin coated virions thereby facilitating viral entry (Hladik and McElrath, 2008). A direct extrapolation of these findings to our study may be linked to the glomerular fibrin deposition and to the fibronectin content of the GBM, all of which probably enable gp120 binding.

The GBM consists of type IV collagen, structural glycoproteins and proteoglycans rich in heparin sulphate proteoglycans. Interactions of HIV-1 gp120 with transmembrane heparin sulphate proteoglycans (especially syndecan-1 and syndecan-2) expressed by epithelial cells can also contribute to HIV-1 attachment and entry (Bobardt *et al.*, 2007). Given that Arg298 is critical for HIV-1 binding to syndecans (de Parseval *et al.*, 2005), HIV-1 exploits syndecans (syndecan-1 and syndecan-2) to facilitate its adsorption onto the epithelium (Bobardt *et al.*, 2007).

HIV infection of the kidney has been etiologically related to the development of nephropathy (Bruggeman *et al.*, 1997; Winston *et al.*, 2001). The expression of viral genes alone, may induce HIVAN, whereas virus production or immune responses to viral proteins *viz.*, *Nef*, *Vpr* and *Tat* might be required to induce HIVICK (Bruggeman and Nelson, 2009; Dickie *et al.*, 1991). HIVAN is mostly owing to direct viral infiltration of renal cells (Bruggeman *et al.*, 1997; Kimmel *et al.*, 1993b; Marras *et al.*, 2002). This study shows direct evidence of HIV-1 sequestration within endocytic compartments of glomerular visceral epithelial cells supporting the hypothesis that the kidney could serve as a latent viral reservoir for HIV-1. HIV-1 nucleic acids have been shown to be present in both the non-lymphoid and lymphoid renal compartments of patients diagnosed with HIVAN (Bruggeman *et al.*, 2000; Cohen *et al.*, 1989; Kimmel *et al.*, 1993a). Renal epithelial cells, however, do not normally express T cell surface glycoprotein CD4, CCR5, or CXCR-4 hence the route by which HIV-1 enters these cells is poorly understood (Eitner *et al.*, 1998; Eitner *et al.*, 2000; Grone *et al.*, 2002; Segerer *et al.*, 1999). Non receptor mediated entry of HIV-1 is facilitated via interaction of epithelial cells with the HIV-1 surface envelope glycoprotein subunit gp120 which foster transcytosis (Bomsel, 1997).

Raft microdomains are involved in endocytosis via caveolae like structures and subsequent transcytosis of HIV-1 across epithelial cells (Kaushic, 2011; Nazli *et al.*, 2010).

Many of the previously reported studies focusing on plasma and PBMC sequences derived from HIV-1 do not accurately describe the full scope of HIV infection within the tissue compartments (Lerner *et al.,* 2011). As viral persistence is attributed to viral latency in cellular reservoirs, ongoing replication or poor drug penetration, leads to viral sanctuaries, despite the major benefits of HAART in the eradication of HIV-1 (Bull *et al.*, 2009; Chun *et al.*, 1997; Finzi *et al.*, 1999; Lerner *et al.*, 2011; Zhang *et al.*, 2000).

Central to current theories regarding viral pathogenesis and the immune response to infection, is understanding the nature of sequence change (or viral diversity), dynamics and spread within the HIV-1 genome. Previous studies comparing published sequences have shown that the *gag* and *pol* genes are more highly conserved than *env* (Simmonds *et al.,* 1990).

The hypervariable regions of *env* not only are polymorphic in sequence but in many cases also differ in length (Alizon *et al.*, 1986; Hahn *et al.*, 1986; Simmonds *et al.*, 1990; Starcich *et al.*, 1986). This study compared viral sequences of the C2-C5 region of HIV-1 *env* from epithelial cells to those of PBMC pre and post-HAART. We found that the sequence diversity of *env* varied in our study cohort. However, there has been no satisfactory explanation of the high rates of mutation in localized regions of the *env* gene. It could be argued that the cause is simply a lack of functional constraints which might limit the amount of variation in regions such as the CD4 binding site (Cordonnier *et al.*, 1989; Lasky *et al.*, 1987).

As expected no HIV-1 quasispecies were found as this study was performed in children. Analysis of *env* sequences derived from both blood and biopsy tissue were found to yield relatively homogeneous populations respectively. However, there were two different sequences for circulating virus (blood) and latent virus (biopsy) signifying compartmentalization. In recent studies, compartmentalization of genital tract compared to blood of HIV-1 sequences has been observed in 50 to 75% patients (Bull *et al.*, 2009; Coombs *et al.*, 1998; Delwart *et al.*, 1998; Ellerbrock *et al.*, 2001; Gupta *et al.*, 2000).

HAART inhibits HIV-1 replication to the extent that plasma viremia levels fall below the detectable amounts of HIV-1 RNA copies (<50 copies/ml). Desire *et al.,* (2001) showed a decline in viral load to undetectable levels with the use of HAART, but later the same patients with a "clean" behavior progress to a high viral load, as if re-infected. A study by Lerner *et al.,* (2011) reported that HIV infected patients that strictly adhere to HAART have uniformly low genomic diversity within the early established and persistence viral reservoirs. These findings are in agreement with our results of a low diversity viral population post-HAART. Highlighter plot analysis indicated that the few mutations observed within the post-HAART group were found to be synonymous mutations. Additionally, there were no significant HIV sequence diversity between glomeruli, arterioles and tubules.

A plausible hypothesis for this occurrence is that the latent virus has undergone mutations hence has a different sequence, thereby escaping HAART and later re-infecting the patient. Therefore this study demonstrates the potential significance of early initiation of HAART

in controlling viral diversification. The viral mutation may arise from immune suppression pressures exacerbated by the immature immune system of the child.

Proviral sequence diversity is important in determining whether unique viruses evolve within the epithelial cells is particularly relevant to developing an effective vaccine and interventions to reduce HIV-1 transmission. In addition, further studies are warranted to investigate mechanisms producing monotypic viral reservoirs that have been established early in infection within epithelial cells, and more importantly to determine whether the proliferation of cells with provirus sustain HIV-1 persistence despite the effect of HAART and incomplete immune restoration (Bull *et al.,* 2009).

In conclusion, this study classified the spectrum of paediatric nephropathy in treatment-naïve children within KwaZulu-Natal (in descending rank) as being FSGS, mesangial hypercellularity, HIVAN, tubulointerstitial nephritis, minimal change and sclerosing glomerulopathy. Notably, in the HAART era this spectrum was marginally altered. Additionally, our study demonstrates podocyte phenotype dysregulation pre-HAART with loss of differentiation markers and increased proliferation and reconstitution post antiretroviral and angiotensin converting enzyme inhibiting therapy. Evidence of ultrastructural viral reservoirs within epithelial cells is supported by a genetic appraisal confirming the ubiquitous presence of HIV DNA in renal tissue. Moreover, sequence analysis showed viral evolution and compartmentalization between renal viral reservoirs to PBMCs. Finally, the interplay of viral genes and host response, influenced by genetic background, may contribute to the variable manifestations of HIV-1 infection in the kidney in our paediatric population.

REFERENCES

Abrahamson, D. R. (1987). Structure and development of the glomerular capillary wall and basement membrane. *Am J Physiol* 253, F783-94.

Ahuja, T. S., Abbott, K. C., Pack, L. and Kuo, Y. F. (2004). HIV-associated nephropathy and end-stage renal disease in children in the United States. *Pediatr Nephrol* 19, 808-11.

Alfsen, A., Iniguez, P., Bouguyon, E. and Bomsel, M. (2001). Secretory IgA specific for a conserved epitope on gp41 envelope glycoprotein inhibits epithelial transcytosis of HIV-1. *J Immunol* 166, 6257-65.

Alizon, M., Wain-Hobson, S., Montagnier, L. and Sonigo, P. (1986). Genetic variability of the AIDS virus: nucleotide sequence analysis of two isolates from African patients. *Cell* 46, 63-74.

Alsaad, K. O. and Herzenberg, A. M. (2007). Distinguishing diabetic nephropathy from other causes of glomerulosclerosis: an update. *J Clin Pathol* 60, 18-26.

Anochie, I. C., Eke, F. U. and Okpere, A. N. (2008). Human immunodeficiency virus-associated nephropathy (HIVAN) in Nigerian children. *Pediatr Nephrol* 23, 117-22.

Appel, G. (2007). Viral infections and the kidney: HIV, hepatitis B, and hepatitis C. *Cleve Clin J Med* 74, 353-60.

Arias, L. F., Vieco, B. E. and Arteta, A. A. (2009). Expression of nephrin, podocin and a-actinine-4 in renal tissue of patients with proteinuria. *Nefrologia* 29, 569-75.

Asanuma, K., Kim, K., Oh, J., Giardino, L., Chabanis, S., Faul, C., Reiser, J. and Mundel, P. (2005). Synaptopodin regulates the actin-bundling activity of alpha-actinin in an isoform-specific manner. *J Clin Invest* 115, 1188-98.

Asanuma, K., Yanagida-Asanuma, E., Faul, C., Tomino, Y., Kim, K. and Mundel, P. (2006). Synaptopodin orchestrates actin organization and cell motility via regulation of RhoA signalling. *Nat Cell Biol* 8, 485-91.

Baghdassarian, N. and Ffrench, M. (1996). Cyclin-dependent kinase inhibitors (CKIs) and hematological malignancies. *Hematol Cell Ther* 38, 313-23.

Barbiano di Belgiojoso, G., Genderini, A., Vago, L., Parravicini, C., Bertoli, S. and Landriani, N. (1990). Absence of HIV antigens in renal tissue from patients with HIV-associated nephropathy. *Nephrol Dial Transplant* 5, 489-92.

Barisoni, L., Bruggeman, L. A., Mundel, P., D'Agati, V. D. and Klotman, P. E. (2000a). HIV-1 induces renal epithelial dedifferentiation in a transgenic model of HIV-associated nephropathy. *Kidney Int* 58, 173-81.

Barisoni, L., Kriz, W., Mundel, P. and D'Agati, V. (1999). The dysregulated podocyte phenotype: a novel concept in the pathogenesis of collapsing idiopathic focal segmental glomerulosclerosis and HIV-associated nephropathy. *J Am Soc Nephrol* 10, 51-61.

Barisoni, L., Mokrzycki, M., Sablay, L., Nagata, M., Yamase, H. and Mundel, P. (2000b). Podocyte cell cycle regulation and proliferation in collapsing glomerulopathies. *Kidney Int* 58, 137-43.

Barre-Sinoussi, F., Chermann, J. C., Rey, F., Nugeyre, M. T., Chamaret, S., Gruest, J., Dauguet, C., Axler-Blin, C., Vezinet-Brun, F., Rouzioux, C. et al. (1983). Isolation of a T-lymphotropic retrovirus from a patient at risk for acquired immune deficiency syndrome (AIDS). *Science* 220, 868-71.

Baum, M. and Quigley, R. (1998). Inhibition of proximal convoluted tubule transport by dopamine. *Kidney Int* 54, 1593-600.

Baumelou, A., Assogba, V., Beaufils, H., Hinglais, N., Ben Hmida, M., Christin, S., Eugene, M., Deray and Jacobs, C. (1989). Pathologie renale associee a l'infection a virus VIH et au syndrome d' immunodeficience acquise. . *Seminaires d ' Uro-Nephro!ogie*, 42-49.

Berglund, F. and Lotspeich, W. D. (1956). Renal tubular reabsorption of inorganic sulfate in the dog, as affected by glomerular filtration rate and sodium chloride. *Am J Physiol* 185, 533-8.

Bertolatus, J. A. (1990). Affinity cytochemical labeling of glomerular basement membrane anionic sites using specific biotinylation and colloidal gold probes. *J Histochem Cytochem* 38, 377-84.

Bhat, S., Mettus, R. V., Reddy, E. P., Ugen, K. E., Srikanthan, V., Williams, W. V. and Weiner, D. B. (1993). The galactosyl ceramide/sulfatide receptor binding region of HIV-1 gp120 maps to amino acids 206-275. *AIDS Res Hum Retroviruses* 9, 175-81.

Bhimma, R. (2007). HIV and Renal Disease in Children. Avaiable in http://www.hivinchildren.org/Treatment_issues/hiv_renaldisease.asp Accessed [5 December 2011], vol. 2011 (ed.: HIV in Children [serial online].

Bhimma, R., Adhikari, M., Asharam, K. and Connolly, C. (2008). The spectrum of chronic kidney disease (stages 2-5) in KwaZulu-Natal, South Africa. *Pediatr Nephrol* 23, 1841-6.

Bobardt, M. D., Chatterji, U., Selvarajah, S., Van der Schueren, B., David, G., Kahn, B. and Gallay, P. A. (2007). Cell-free human immunodeficiency virus type 1 transcytosis through primary genital epithelial cells. *J Virol* 81, 395-405.

Bolton, W. K. and Abdel-Rahman, E. (2001). Pathogenesis of focal glomerulosclerosis. *Nephron* 88, 6-13.

Bomsel, M. (1997). Transcytosis of infectious human immunodeficiency virus across a tight human epithelial cell line barrier. *Nat Med* 3, 42-7.

Bostrom, M. A. and Freedman, B. I. (2010). The spectrum of MYH9-associated nephropathy. *Clin J Am Soc Nephrol* 5, 1107-13.

Boucher, A., Droz, D., Adafer, E. and Noel, L. H. (1987). Relationship between the integrity of Bowman's capsule and the composition of cellular crescents in human crescentic glomerulonephritis. *Lab Invest* 56, 526-33.

Bourgoignie, J. J. (1989). Acquired immunodeficiency syndrome (AIDS) — Related renal disease. *Journal of Molecular Medicine* 67, 889-894.

Bourgoignie, J. J. (1990). Renal complications of human immunodeficiency virus type 1. *Kidney Int* 37, 1571-84.

Boye, E. and Nordstrom, K. (2003). Coupling the cell cycle to cell growth. *EMBO Rep* 4, 757-60.

Brasile, L., Green, E. and Haisch, C. (1997). Ex vivo resuscitation of kidneys after postmortem warm ischemia. *ASAIO J* 43, M427-30.

Brenner, B. M., Hostetter, T. H. and Humes, H. D. (1978). Glomerular permselectivity: barrier function based on discrimination of molecular size and charge. *Am J Physiol* 234, F455-60.

Brest, P., Betis, F., Cuburu, N., Selva, E., Herrant, M., Servin, A., Auberger, P. and Hofman, P. (2004). Increased rate of apoptosis and diminished phagocytic ability of human neutrophils infected with Afa/Dr diffusely adhering Escherichia coli strains. *Infect Immun* 72, 5741-9.

Brown, D. A. and London, E. (1998). Functions of lipid rafts in biological membranes. *Annu Rev Cell Dev Biol* 14, 111-36.

Bruggeman, L. A., Dikman, S., Meng, C., Quaggin, S. E., Coffman, T. M. and Klotman, P. E. (1997). Nephropathy in human immunodeficiency virus-1 transgenic mice is due to renal transgene expression. *J Clin Invest* 100, 84-92.

Bruggeman, L. A. and Nelson, P. J. (2009). Controversies in the pathogenesis of HIV-associated renal diseases. *Nat Rev Nephrol* 5, 574-81.

Bruggeman, L. A., Ross, M. D., Tanji, N., Cara, A., Dikman, S., Gordon, R. E., Burns, G. C., D'Agati, V. D., Winston, J. A., Klotman, M. E. et al. (2000). Renal epithelium is a previously unrecognized site of HIV-1 infection. *J Am Soc Nephrol* 11, 2079-87.

Bull, M., Learn, G., Genowati, I., McKernan, J., Hitti, J., Lockhart, D., Tapia, K., Holte, S., Dragavon, J., Coombs, R. et al. (2009). Compartmentalization of HIV-1 within the female genital tract is due to monotypic and low-diversity variants not distinct viral populations. *PLoS One* 4, e7122.

Burger, H. R., Kriemler, S. and Mihatsch, M. (1989). Oibr es em AIDS nephropathie? Resultate von 210 autopsie fallen [Abstract]. . *Nierenund Hochdruck-Krankeiten* 6, 379.

Burkitt, G. H., Young, B. and Heath, W. J. (1993). Wheater's Functional Histology. New york: Timothy Home

Burns, G. C., Paul, S. K., Toth, I. R. and Sivak, S. L. (1997). Effect of angiotensin-converting enzyme inhibition in HIV-associated nephropathy. *J Am Soc Nephrol* 8, 1140-6.

Bushman, F. (2004). Gene regulation: selfish elements make a mark. *Nature* 429, 253-5.

Cachat, F., Cheseaux, J. J. and Guignard, J. P. (1998). HIV-associated nephropathy in children. *Arch Pediatr* 5, 1353-8.

Caulfield, J. P. and Farquhar, M. G. (1974). The permeability of glomerular capillaries to graded dextrans. Identification of the basement membrane as the primary filtration barrier. *J Cell Biol* 63, 883-903.

Chan, D. C., Chutkowski, C. T. and Kim, P. S. (1998). Evidence that a prominent cavity in the coiled coil of HIV type 1 gp41 is an attractive drug target. . *Proc Natl Acad Sci USA* 95, 15613-15617.

Choi, A. I., O'Hare, A. M. and Rodriguez, R. A. (2007a). Update on HIV-associated Nephropathy. *Nephrology* 5.

Choi, A. I., Rodriguez, R. A., Bacchetti, P., Bertenthal, D., Volberding, P. A. and O'Hare, A. M. (2007b). Racial differences in end-stage renal disease rates in HIV infection versus diabetes. *J Am Soc Nephrol* 18, 2968-74.

Chrystie, I. L. and Almeida, J. D. (1988). The morphology of human immunodeficiency virus (HIV) by negative staining. *J Med Virol* 25, 281-8.

Chun, T. W., Carruth, L., Finzi, D., Shen, X., DiGiuseppe, J. A., Taylor, H., Hermankova, M., Chadwick, K., Margolick, J., Quinn, T. C. et al. (1997). Quantification of latent tissue reservoirs and total body viral load in HIV-1 infection. *Nature* 387, 183-8.

Clementi, M., Menzo, S., Bagnarelli, P., Valenza, A., Paolucci, S., Sampaolesi, R., Manzin, A. and Varaldo, P. E. (1996). Clinical use of quantitative molecular methods in studying human immunodeficiency virus type 1 infection. *Clin Microbiol Rev* 9, 135-47.

Cochat, P., Mourani, C., Exantus, J., Bourquia, A., Martinez-Pico, M., Adonis-Koffy, L. and Bacchetta, J. (2009). [Pediatric nephrology in developing countries]. *Med Trop (Mars)* 69, 543-7.

Cohen, A. H. (1990). HIV-associated nephropathy: Racial difference in severity of renal damage [Abstract]. *J Am Soc Nephrol* 1, 305.

Cohen, A. H. and Nast, C. C. (1988). HIV-associated nephropathy. A unique combined glomerular, tubular, and interstitial lesion. *Mod Pathol* 1, 87-97.

Cohen, A. H., Sun, N. C., Shapshak, P. and Imagawa, D. T. (1989). Demonstration of human immunodeficiency virus in renal epithelium in HIV-associated nephropathy. *Mod Pathol* 2, 125-8.

Cohen, S. D. and Kimmel, P. L. (2007). HIV-associated renal diseases in Africa a desperate need for additional study. *Nephrol Dial Transplant* 22, 2116-9.

Conaldi, P. G., Bottelli, A., Baj, A., Serra, C., Fiore, L., Federico, G., Bussolati, B. and Camussi, G. (2002). Human immunodeficiency virus-1 tat induces hyperproliferation and dysregulation of renal glomerular epithelial cells. *Am J Pathol* 161, 53-61.

Connolly, J. O., Weston, C. E. and Hendry, B. M. (1995). HIV-associated renal disease in London hospitals. *QJM* 88, 627-34.

Connor, E., Gupta, S., Joshi, V., DiCarlo, F., Offenberger, J., Minnefor, A., Uy, C., Oleske, J. and Ende, N. (1988). Acquired immunodeficiency syndrome-associated renal disease in children. *J Pediatr* 113, 39-44.

Coombs, R. W., Speck, C. E., Hughes, J. P., Lee, W., Sampoleo, R., Ross, S. O., Dragavon, J., Peterson, G., Hooton, T. M., Collier, A. C. et al. (1998). Association between culturable human immunodeficiency virus type 1 (HIV-1) in semen and HIV-1 RNA levels in semen and blood: evidence for compartmentalization of HIV-1 between semen and blood. *J Infect Dis* 177, 320-30.

Cordonnier, A., Montagnier, L. and Emerman, M. (1989). Single amino-acid changes in HIV envelope affect viral tropism and receptor binding. *Nature* 340, 571-4.

Cusano, A. J., Siegal, F. P. and Maesaka, J. K. (1989). Hyponatremia in AIDSand ARC (abstract). *Kidney Int* 35, 215.

D'Agati, V. and Appel, G. B. (1997). HIV infection and the kidney. *J Am Soc Nephrol* 8, 138-52.

D'Amico, G. (1987). The commonest glomerulonephritis in the world: IgA nephropathy. *Q J Med* 64, 709-27.

David. (1999). The Worlds of David Darling. Avaiable in http://www.daviddarling.info/images/cell_cycle.jpg [Accessed 12 July 2008], vol. 2008 (ed.

de Parseval, A., Bobardt, M. D., Chatterji, A., Chatterji, U., Elder, J. H., David, G., Zolla-Pazner, S., Farzan, M., Lee, T. H. and Gallay, P. A. (2005). A highly conserved arginine in gp120 governs HIV-1 binding to both syndecans and CCR5 via sulfated motifs. *J Biol Chem* 280, 39493-504.

Delaney M. (2006). History of HAART – the true story of how effective multi-drug therapy was developed for treatment of HIV disease. *Retrovirology* 3, S1-S6.

Delwart, E. L., Mullins, J. I., Gupta, P., Learn, G. H., Jr., Holodniy, M., Katzenstein, D., Walker, B. D. and Singh, M. K. (1998). Human immunodeficiency virus type 1 populations in blood and semen. *J Virol* 72, 617-23.

Denamur, E., Bocquet, N., Baudouin, V., Da Silva, F., Veitia, R., Peuchmaur, M., Elion, J., Gubler, M. C., Fellous, M., Niaudet, P. et al. (2000). WT1 splice-site mutations are rarely associated with primary steroid-resistant focal and segmental glomerulosclerosis. *Kidney Int* 57, 1868-72.

Desire, N., Dehee, A., Schneider, V., Jacomet, C., Goujon, C., Girard, P. M., Rozenbaum, W. and Nicolas, J. C. (2001). Quantification of human immunodeficiency virus type 1 proviral load by a TaqMan real-time PCR assay. *J Clin Microbiol* 39, 1303-10.

Dewey, W. C. and Humphrey, R. M. (1963). Survival of mammalian cells irradiated in different phases of the life-cycle as examined by autoradiography. *Nature* 198, 1063-6.

Dickie, P., Felser, J., Eckhaus, M., Bryant, J., Silver, J., Marinos, N. and Notkins, A. L. (1991). HIV-associated nephropathy in transgenic mice expressing HIV-1 genes. *Virology* 185, 109-19.

Dijkman, H. B., Weening, J. J., Smeets, B., Verrijp, K. C., van Kuppevelt, T. H., Assmann, K. K., Steenbergen, E. J. and Wetzels, J. F. (2006). Proliferating cells in HIV and pamidronate-associated collapsing focal segmental glomerulosclerosis are parietal epithelial cells. *Kidney Int* 70, 338-44.

Doms, R. W. and Moore, J. P. (2000). HIV-1 membrane fusion: targets of opportunity. *J Cell Biol* 151, F9-14.

Dorup, J. (1990). Ultrastructure of the distal nephron. An analysis of structure-function relationships in distal nephron segments of the kidney. *Dan Med Bull* 37, 502-6.

Duesburg, H. P. (1988). Human immunodeficiency virus and acquired immunodeficiency syndrome: Correlation but not causation. *Proc. Nati. Acad. Sci.* 86, 755-764.

Eggers, P. W. and Kimmel, P. L. (2004). Is there an epidemic of HIV Infection in the US ESRD program? *J Am Soc Nephrol* 15, 2477-85.

Eitner, F., Cui, Y., Hudkins, K. L., Anderson, D. M., Schmidt, A., Morton, W. R. and Alpers, C. E. (1998). Chemokine receptor (CCR5) expression in human kidneys and in the HIV infected macaque. *Kidney Int* 54, 1945-54.

Eitner, F., Cui, Y., Hudkins, K. L., Stokes, M. B., Segerer, S., Mack, M., Lewis, P. L., Abraham, A. A., Schlondorff, D., Gallo, G. et al. (2000). Chemokine receptor CCR5 and CXCR4 expression in HIV-associated kidney disease. *J Am Soc Nephrol* 11, 856-67.

Ellerbrock, T. V., Lennox, J. L., Clancy, K. A., Schinazi, R. F., Wright, T. C., Pratt-Palmore, M., Evans-Strickfaden, T., Schnell, C., Pai, R., Conley, L. J. et al. (2001). Cellular replication of human immunodeficiency virus type 1 occurs in vaginal secretions. *J Infect Dis* 184, 28-36.

Fagard, C., Bandelier, C. Y., Ananworanich, J., Le Braz, M., Gunthard, H., Perneger, T., Garcia, F. and Hirschel, B. (2005). Biphasic decline of CD4 cell count during scheduled treatment interruptions. *AIDS* 19, 439-41.

Falk, R. (2008). UNC Kidney Center. Available in http://www.unckidneycenter.org/kidneyhealthlibrary/glomerulardisease.html#Nephron_Parts [accessed 23 July 2008], vol. 2008 (ed.

Fassin, D. and Schneider, H. (2003). The politics of AIDS in South Africa: beyond the controversies. *BMJ* 326, 495-7.

Fauci, A. S. (1999). The AIDS epidemic--considerations for the 21st century. *N Engl J Med* 341, 1046-50.

Faul, C., Asanuma, K., Yanagida-Asanuma, E., Kim, K. and Mundel, P. (2007). Actin up: regulation of podocyte structure and function by components of the actin cytoskeleton. *Trends Cell Biol* 17, 428-37.

Ferrara, N. (2004). Vascular endothelial growth factor as a target for anticancer therapy. *Oncologist* 9 Suppl 1, 2-10.

Finzi, D., Blankson, J., Siliciano, J. D., Margolick, J. B., Chadwick, K., Pierson, T., Smith, K., Lisziewicz, J., Lori, F., Flexner, C. et al. (1999). Latent infection of CD4+ T cells provides a mechanism for lifelong persistence of HIV-1, even in patients on effective combination therapy. *Nat Med* 5, 512-7.

Gallo, S. A., Finnegan, C. M., Viard, M., Raviv, Y., Dimitrov, A., Rawat, S. S., Puri, A., Durell, S. and Blumenthal, R. (2003). The HIV Env-mediated fusion reaction. *Biochim Biophys Acta* 1614, 36-50.

Gardenswartz, M. H., Lerner, C. W., Seligson, G. R., Zabetakis, P. M., Rotterdam, H., Tapper, M. L., Michelis, M. F. and Bruno, M. S. (1984). Renal disease in patients with AIDS: a clinicopathologic study. *Clin Nephrol* 21, 197-204.

Gelderblom, H. R. (1991). Assembly and morphology of HIV: potential effect of structure on viral function. *AIDS* 5, 617-37.

George, M. D., Sankaran, S., Reay, E., Gelli, A. C. and Dandekar, S. (2003). High-throughput gene expression profiling indicates dysregulation of intestinal cell cycle mediators and growth factors during primary simian immunodeficiency virus infection. *Virology* 312, 84-94.

Gerntholz, T. E., Goetsch, S. J. W. and Katz, I. (2006). HIV-related nephropathy:A South African Perspective. *Kidney Int* 69, 1885-1891.

Gibellini, D., Vitone, F., Schiavone, P., Ponti, C., La Placa, M. and Re, M. C. (2004). Quantitative detection of human immunodeficiency virus type 1 (HIV-1) proviral DNA in peripheral blood mononuclear cells by SYBR green real-time PCR technique. *J Clin Virol* 29, 282-9.

Goldsmith, J. M., Deutsche, J., Tang, M. and Green, D. (1991). CD4 cells in HIV-1 infected hemophiliacs: effect of factor VIII concentrates. *Thromb Haemost* 66, 415-9.

Grimwood, J., Mineo, J. R. and Kasper, L. H. (1996). Attachment of Toxoplasma gondii to host cells is host cell cycle dependent. *Infect Immun* 64, 4099-104.

Grone, H. J., Cohen, C. D., Grone, E., Schmidt, C., Kretzler, M., Schlondorff, D. and Nelson, P. J. (2002). Spatial and temporally restricted expression of chemokines and chemokine receptors in the developing human kidney. *J Am Soc Nephrol* 13, 957-67.

Gupta, P., Leroux, C., Patterson, B. K., Kingsley, L., Rinaldo, C., Ding, M., Chen, Y., Kulka, K., Buchanan, W., McKeon, B. et al. (2000). Human immunodeficiency virus type 1 shedding pattern in semen correlates with the compartmentalization of viral Quasi species between blood and semen. *J Infect Dis* 182, 79-87.

Hadley, T. J. and Peiper, S. C. (1997). From malaria to chemokine receptor: the emerging physiologic role of the Duffy blood group antigen. *blood* 89, 3077-91.

Hahn, B. H., Shaw, G. M., Taylor, M. E., Redfield, R. R., Markham, P. D., Salahuddin, S. Z., Wong-Staal, F., Gallo, R. C., Parks, E. S. and Parks, W. P. (1986). Genetic variation in HTLV-III/LAV over time in patients with AIDS or at risk for AIDS. *Science* 232, 1548-53.

Hamano, Y., Grunkemeyer, J. A., Sudhakar, A., Zeisberg, M., Cosgrove, D., Morello, R., Lee, B., Sugimoto, H. and Kalluri, R. (2002). Determinants of vascular permeability in the kidney glomerulus. *J Biol Chem* 277, 31154-62.

Han, T. M., Naicker, S., Ramdial, P. K. and Assounga, A. G. (2006a). A cross-sectional study of HIV-seropositive patients with varying degrees of proteinuria in South Africa. *Kidney Int* 69, 2243-50.

Han, T. S., Schwartz, M. M. and Lewis, E. J. (2006b). Association of glomerular podocytopathy and nephrotic proteinuria in mesangial lupus nephritis. *Lupus* 15, 71-5.

Hansen, G. H., Niels-Christiansen, L. L., Immerdal, L., Hunziker, W., Kenny, A. J. and Danielsen, E. M. (1999). Transcytosis of immunoglobulin A in the mouse enterocyte occurs through glycolipid raft- and rab17-containing compartments. *Gastroenterology* 116, 610-22.

Hayashi, M. (1998). Physiology and pathophysiology of acid-base homeostasis in the kidney. *Intern Med* 37, 221-5.

Henics, T. and Wheatley, D. N. (1999). Cytoplasmic vacuolation, adaptation and cell death: a view on new perspectives and features. *Biol Cell* 91, 485-98.

Herman, E. S. and Klotman, P. E. (2003). HIV-associated nephropathy: Epidemiology, pathogenesis, and treatment. *Semin Nephrol* 23, 200-8.

Hernandez, J. I., Gomez-Roman, J., Rodrigo, E., Olmos, J. M., Gonzalez-Vela, C., Ruiz, J. C., Val, J. F. and Riancho, J. A. (1997). Bronchiolitis obliterans and IgA nephropathy. A new cause of pulmonary-renal syndrome. *Am J Respir Crit Care Med* 156, 665-8.

Heuer, T. S. and Brown, P. O. (1997). Mapping features of HIV-1 integrase near selected sites on viral and target DNA molecules in an active enzyme-DNA complex by photo-cross-linking. *Biochemistry* 36, 10655-65.

Hirakawa, M., Tsuruya, K., Yotsueda, H., Tokumoto, M., Ikeda, H., Katafuchi, R., Fujimi, S., Hirakata, H. and Iida, M. (2006). Expression of synaptopodin and GLEPP1 as markers of steroid responsiveness in primary focal segmental glomerulosclerosis. *Life Sci* 79, 757-63.

Hiura, T., Yamazaki, H., Saeki, T., Kawabe, S., Ueno, M., Nishi, S., Miyamura, S. and Gejyo, F. (2006). Nephrotic syndrome and IgA nephropathy in polycystic kidney disease. *Clin Exp Nephrol* 10, 136-9.

Hladik, F. and McElrath, M. J. (2008). Setting the stage: host invasion by HIV. *Nat Rev Immunol* 8, 447-57.

Ho, D. D. and Zhang, L. (2000). HIV-1 rebound after anti-retroviral therapy. *Nat Med* 6, 736-7.

Hogg, R. J. and Kokko, J. P. (1979). Renal countercurrent multiplication system. *Rev Physiol Biochem Pharmacol* 86, 95-135.

Holdsworth, S. R., Thomson, N. M., Glasgow, E. F. and Atkins, R. C. (1979). The effect of defibrination on macrophage participation in rabbit nephrotoxic nephritis: studies using glomerular culture and electronmicroscopy. *Clin Exp Immunol* 37, 38-43.

Holdsworth, S. R. and Tipping, P. G. (1985). Macrophage-induced glomerular fibrin deposition in experimental glomerulonephritis in the rabbit. *J Clin Invest* 76, 1367-74.

Honda, N. (1984). [Ultrafiltration of the kidney glomerulus and permeability of macromolecular substances]. *Nippon Rinsho* 42, 1258-64.

Horinouchi, I., Nakazato, H., Kawano, T., Iyama, K., Furuse, A., Arizono, K., Machida, J., Sakamoto, T., Endo, F. and Hattori, S. (2003). In situ evaluation of podocin in normal and glomerular diseases. *Kidney Int* 64, 2092-9.

Huang, L., Quartin, A., Jones, D. and Havlir, D. V. (2006). Intensive care of patients with HIV infection. *N Engl J Med* 355, 173-81.

Ichikawa, I. and Fogo, A. (1996). Focal segmental glomerulosclerosis. *Pediatr Nephrol* 10, 374-91.

Ichimura, K., Kurihara, H. and Sakai, T. (2003). Actin filament organization of foot processes in rat podocytes. *J Histochem Cytochem* 51, 1589-600.

Ichiyama, K. and Yamamoto, N. (2002). [Replication inhibitors targeting early events in the HIV-1 life cycle]. *Nippon Rinsho* 60, 784-9.

Ihalmo, P., Schmid, H., Rastaldi, M. P., Mattinzoli, D., Langham, R. G., Luimula, P., Kilpikari, R., Lassila, M., Gilbert, R. E., Kerjaschki, D. et al. (2007). Expression of filtrin in human glomerular diseases. *Nephrol Dial Transplant* 22, 1903-9.

Imai, M., Taniguchi, J. and Tabei, K. (1987). Function of thin loops of Henle. *Kidney Int* 31, 565-79.

Ingulli, E., Tejani, A., Fikrig, S., Nicastri, A., Chen, C. K. and Pomrantz, A. (1991). Nephrotic syndrome associated with acquired immunodeficiency syndrome in children. *J Pediatr* 119, 710-6.

Izzedine, H., Francois, M. and Deray, G. (1999). Severe nephrotic syndrome without oedema in a patient with HIV associated nephropathy. *Nephrol Dial Transplant* 14, 2522-3.

Jarad, G., Cunningham, J., Shaw, A. S. and Miner, J. H. (2006). Proteinuria precedes podocyte abnormalities inLamb2-/- mice, implicating the glomerular basement membrane as an albumin barrier. *J Clin Invest* 116, 2272-9.

Jennette, J. C. and Falk, R. J. (1997). Diagnosis and management of glomerular diseases. *Med Clin North Am* 81, 653-77.

Kala U, Petersen K, Faller G and Goetsch S. (2007). Spectrum of severe renal disease in children with HIV/Aids at Chris Hani Baragwanath Hospital, Johannesburg [abstract]. *Pediatr Nephrol* 22, 301.

Kaluza, G., Willems, W. R., Lohmeyer, J., Altmannsberger, M., Bohle, R. M. and Lubke, S. (1992). A monoclonal antibody that recognizes a formalin-resistant epitope on the p 24 core protein of HIV-1. *Pathol Res Pract* 188, 91-6.

Katzenstein, T. L. (2003). Molecular biological assessment methods and understanding the course of the HIV infection. *APMIS Suppl*, 1-37.

Kaufman, L., Collins, S. E. and Klotman, P. E. (2010). The pathogenesis of HIV-associated nephropathy. *Adv Chronic Kidney Dis* 17, 36-43.

Kaufman, R. J. (2002). Orchestrating the unfolded protein response in health and disease. *J Clin Invest* 110, 1389-98.

Kaushic, C. (2011). HIV-1 infection in the female reproductive tract: role of interactions between HIV-1 and genital epithelial cells. *Am J Reprod Immunol* 65, 253-60.

Kawachi, H., Miyauchi, N., Suzuki, K., Han, G. D., Orikasa, M. and Shimizu, F. (2006). Role of podocyte slit diaphragm as a filtration barrier. *Nephrology (Carlton)* 11, 274-81.

Kerjaschki, D. (2001). Caught flat-footed: podocyte damage and the molecular bases of focal glomerulosclerosis. *J Clin Invest* 108, 1583-7.

Key, G., Becker, M. H., Baron, B., Duchrow, M., Schluter, C., Flad, H. D. and Gerdes, J. (1993). New Ki-67-equivalent murine monoclonal antibodies (MIB 1-3) generated against bacterially expressed parts of the Ki-67 cDNA containing three 62 base pair repetitive elements encoding for the Ki-67 epitope. *Lab Invest* 68, 629-36.

Kharsany, A. B. M. and Karim, Q. A. (2011). HIV Epidemiology and Prevention. In *HIV-infection - Impact, Awareness and Social Implications of living with HIV/AIDS*, (ed. E. Barros), pp. 1-24. Croatia: Janeza Trdine.

Khedun, S. M., Naicker, T., Moodley, J., Naidoo, S. and Bhoola, K. D. (1997). Changes in urinary tissue kallikrein excretion in black African women with hypertensive disorders of pregnancy. *Immunopharmacology* 36, 243-7.

Kimmel, P. L., Barisoni, L. and Kopp, J. B. (2003). Pathogenesis and treatment of HIV-associated renal diseases: lessons from clinical and animal studies, molecular pathologic correlations, and genetic investigations. *Ann Intern Med* 139, 214-26.

Kimmel, P. L., Ferreira-Centeno, A., Farkas-Szallasi, T., Abraham, A. A. and Garrett, C. T. (1993a). Viral DNA in microdissected renal biopsy tissue from HIV infected patients with nephrotic syndrome. *Kidney Int* 43, 1347-52.

Kimmel, P. L., Phillips, T. M., Ferreira-Centeno, A., Farkas-Szallasi, T., Abraham, A. A. and Garrett, C. T. (1992). Brief report: idiotypic IgA nephropathy in patients with human immunodeficiency virus infection. *N Engl J Med* 327, 702-6.

Kimmel, P. L., Phillips, T. M., Ferreira-Centeno, A., Farkas-Szallasi, T., Abraham, A. A. and Garrett, C. T. (1993b). HIV-associated immune-mediated renal disease. *Kidney Int* 44, 1327-40.

Kiryluk, K., Martino, J. and Gharavi, A. G. (2007). Genetic susceptibility, HIV infection, and the kidney. *Clin J Am Soc Nephrol* 2 Suppl 1, S25-35.

Klotman, P. E. (1999). HIV-associated nephropathy. *Kidney Int* 56, 1161-76.

Kopp, J. B., Nelson, G. W., Sampath, K., Johnson, R. C., Genovese, G., An, P., Friedman, D., Briggs, W., Dart, R., Korbet, S. et al. (2011). APOL1 genetic variants in focal segmental glomerulosclerosis and HIV-associated nephropathy. *J Am Soc Nephrol* 22, 2129-37.

Kopp, J. B., Smith, M. W., Nelson, G. W., Johnson, R. C., Freedman, B. I., Bowden, D. W., Oleksyk, T., McKenzie, L. M., Kajiyama, H., Ahuja, T. S. et al. (2008). MYH9 is a major-effect risk gene for focal segmental glomerulosclerosis. *Nat Genet* 40, 1175-84.

Kopp, J. B. and Winkler, C. (2003). HIV-associated nephropathy in African Americans. *Kidney Int Suppl*, S43-9.

Kosaka, T. and Kosaka, K. (2005). Structural organization of the glomerulus in the main olfactory bulb. *Chem Senses* 30 Suppl 1, i107-8.

Kriz, W. (2003). Progression of chronic renal failure in focal segmental glomerulosclerosis: consequence of podocyte damage or of tubulointerstitial fibrosis? *Pediatr Nephrol* 18, 617-22.

Kumar, A., Lifson, J. D., Li, Z., Jia, F., Mukherjee, S., Adany, I., Liu, Z., Piatak, M., Sheffer, D., McClure, H. M. et al. (2001). Sequential immunization of macaques with two differentially attenuated vaccines induced long-term virus-specific immune responses and conferred protection against AIDS caused by heterologous simian human immunodeficiency Virus (SHIV(89.6)P). *Virology* 279, 241-56.

Kurokawa, K. (1993). [Structure and function of the kidney]. *Nippon Naika Gakkai Zasshi* 82, 1313-7.

Lachgar, A., Jaureguiberry, G., Le Buenac, H., Bizzini, B., Zagury, J. F., Rappaport, J. and Zagury, D. (1998). Binding of HIV-1 to RBCs involves the Duffy antigen receptors for chemokines (DARC). *Biomed Pharmacother* 52, 436-9.

Lacy, E. R., Castellucci, M. and Reale, E. (1987). The elasmobranch renal corpuscle: fine structure of Bowman's capsule and the glomerular capillary wall. *Anat Rec* 218, 294-305.

Lahdenkari, A. T., Kestila, M., Holmberg, C., Koskimies, O. and Jalanko, H. (2004). Nephrin gene (NPHS1) in patients with minimal change nephrotic syndrome (MCNS). *Kidney Int* 65, 1856-63.

Lahdenkari, A. T., Suvanto, M., Kajantie, E., Koskimies, O., Kestila, M. and Jalanko, H. (2005). Clinical features and outcome of childhood minimal change nephrotic syndrome: is genetics involved? *Pediatr Nephrol* 20, 1073-80.

Lai, K. W., Wei, C. L., Tan, L. K., Tan, P. H., Chiang, G. S., Lee, C. G., Jordan, S. C. and Yap, H. K. (2007). Overexpression of interleukin-13 induces minimal-change-like nephropathy in rats. *J Am Soc Nephrol* 18, 1476-85.

Lapham, C. K., Ouyang, J., Chandrasekhar, B., Nguyen, N. Y., Dimitrov, D. S. and Golding, H. (1996). Evidence for Cell-Surface Association Between Fusin and the CD4-gp120 Complex in Human Cell Lines. *Science* 274, 602-605.

Laradi, A., Mallet, A., Beaufils, H., Allouache, M. and Martinez, F. (1998). HIV-associated nephropathy: outcome and prognosis factors. Groupe d' Etudes Nephrologiques d'Ile de France. *J Am Soc Nephrol* 9, 2327-35.

Lasky, L. A., Nakamura, G., Smith, D. H., Fennie, C., Shimasaki, C., Patzer, E., Berman, P., Gregory, T. and Capon, D. J. (1987). Delineation of a region of the human immunodeficiency virus type 1 gp120 glycoprotein critical for interaction with the CD4 receptor. *Cell* 50, 975-85.

Lerner, P., Guadalupe, M., Donovan, R., Hung, J., Flamm, J., Prindiville, T., Sankaran-Walters, S., Syvanen, M., Wong, J. K., George, M. D. et al. (2011). The gut mucosal viral reservoir in HIV-infected patients is not the major source of rebound plasma viremia following interruption of highly active antiretroviral therapy. *J Virol* 85, 4772-82.

Lescure, F. X., Flateau, C., Pacanowski, J., Brocheriou, I., Rondeau, E., Girard, P. E., Ronco, P., Pialoux, G. and Plaisier, E. (2011). HIV-associated kidney glomerular diseases: changes with time and HAART. *Nephrol Dial Transplant* 0, 1–6.

Levidiotis, V. and Power, D. A. (2005). New insights into the molecular biology of the glomerular filtration barrier and associated disease. *Nephrology (Carlton)* 10, 157-66.

Liu, B. L., Viljoen, G. J., Clarke, I. N. and Lambden, P. R. (1999). Identification of further proteolytic cleavage sites in the Southampton calicivirus polyprotein by expression of the viral protease in E. coli. *J Gen Virol* 80 (Pt 2), 291-6.

Lu, T. C., He, J. C. and Klotman, P. E. (2007). Podocytes in HIV-associated nephropathy. *Nephron Clin Pract* 106, c67-71.

Mannucci, P. M., Brettler, D. B., Aledort, L. M., Lusher, J. M., Abildgaard, C. F., Schwartz, R. S. and Hurst, D. (1994). Immune Status of Human Immunodeficiency Virus Seropositive and Seronegative Hemophiliacs Infused for 3.5 Years With Recombinant Factor VI11. *blood* 83: , 1958-1962.

Markowitz, G. S., Lin, J., Valeri, A. M., Avila, C., Nasr, S. H. and D'Agati, V. D. (2002). Idiopathic nodular glomerulosclerosis is a distinct clinicopathologic entity linked to hypertension and smoking. *Hum Pathol* 33, 826-35.

Marras, D., Bruggeman, L. A., Gao, F., Tanji, N., Mansukhani, M. M., Cara, A., Ross, M. D., Gusella, G. L., Benson, G., D'Agati, V. D. et al. (2002). Replication and compartmentalization of HIV-1 in kidney epithelium of patients with HIV-associated nephropathy. *Nat Med* 8, 522-6.

Marshall, C. B. and Shankland, S. J. (2006). Cell cycle and glomerular disease: a minireview. *Nephron Exp Nephrol* 102, e39-48.

Matsuo, N., Tsuchiya, Y., Cho, H., Nagai, T. and Tsuji, A. (1986). Proximal renal tubular acidosis in a child with type 1 glycogen storage disease. *Acta Paediatr Scand* 75, 332-5.

Maurer, K. J., Marini, R. P., Fox, J. G. and Rogers, A. B. (2004). Polycystic kidney syndrome in New Zealand White rabbits resembling human polycystic kidney disease. *Kidney Int* 65, 482-9.

McCulloch, M. I. and Ray, P. E. (2008). Kidney disease in HIV-positive children. *Semin Nephrol* 28, 585-94.

McCutchan, F. E., Viputtigul, K., de Souza, M. S., Carr, J. K., Markowitz, L. E., Buapunth, P., McNeil, J. G., Robb, M. L., Nitayaphan, S., Birx, D. L. et al. (2000). Diversity of envelope glycoprotein from human immunodeficiency virus type 1 of recent seroconverters in Thailand. *AIDS Res Hum Retroviruses* 16, 801-5.

McGraw, H. (2008). HIV Replication**. [Online]. Available**. In *http://www.cegep-ste-foy.qc.ca/profs/gbourbonnais/pascal/nya/genetique/hiv_reproduction.swf [8 June 2008]*, vol. 2008 (ed.

Measday, V., Moore, L., Ogas, J., Tyers, M. and Andrews, B. (1994). The PCL2 (ORFD)-PHO85 cyclin-dependent kinase complex: a cell cycle regulator in yeast. *Science* 266, 1391-5.

Melikyan, G. B., Markosyan, R. M., Hemmati, H., Delmedico, M. K., Lambert, D. M. and Cohen, F. S. (2000). Evidence that the transition of HIV-1 gp41 into a six-helix bundle, not the bundle configuration, induces membrane fusion. . *J Cell Biol* 151, 413-423.

Mitsuya, H., Weinhold, K. J., Furman, P. A., St Clair, M. H., Lehrman, S. N., Gallo, R. C., Bolognesi, D., Barry, D. W. and Broder, S. (1985). 3'-Azido-3'-deoxythymidine (BW A509U): an antiviral agent that inhibits the infectivity and cytopathic effect of human T-lymphotropic virus type III/lymphadenopathy-associated virus in vitro. *Proc Natl Acad Sci U S A* 82, 7096-100.

Moeller, M. J. and Holzman, L. B. (2006). Imaging podocyte dynamics. *Nephron Exp Nephrol* 103, e69-74.

Moore, J. P. and Doms, R. W. (2000). HIV: much at stake with kidneys? *J Am Soc Nephrol* 11, 2138-40.

Morel, F. (1999). The loop of Henle, a turning-point in the history of kidney physiology. *Nephrol Dial Transplant* 14, 2510-5.

Moro, O. S., Pani, S. and Misra, N. (2007). HIV Nephropathy. *eMedicine* 1, 1-5.

Moudgil, A., Nast, C. C., Bagga, A., Wei, L., Nurmamet, A., Cohen, A. H., Jordan, S. C. and Toyoda, M. (2001). Association of parvovirus B19 infection with idiopathic collapsing glomerulopathy. *Kidney Int* 59, 2126-33.

Mundel, P., Gilbert, P. and Kriz, W. (1991). Podocytes in glomerulus of rat kidney express a characteristic 44 KD protein. *J Histochem Cytochem* 39, 1047-56.

Mundel, P., Heid, H. W., Mundel, T. M., Kruger, M., Reiser, J. and Kriz, W. (1997a). Synaptopodin: an actin-associated protein in telencephalic dendrites and renal podocytes. *J Cell Biol* 139, 193-204.

Mundel, P. and Reiser, J. (1997). New aspects of podocyte cell biology. *Kidney Blood Press Res* 20, 173-6.

Mundel, P., Reiser, J., Zuniga Mejia Borja, A., Pavenstadt, H., Davidson, G. R., Kriz, W. and Zeller, R. (1997b). Rearrangements of the cytoskeleton and cell contacts induce process formation during differentiation of conditionally immortalized mouse podocyte cell lines. *Exp Cell Res* 236, 248-58.

Mundel, P. and Shankland, S. J. (1999). Glomerular podocytes and adhesive interaction with glomerular basement membrane. *Exp Nephrol* 7, 160-6.

Nagata, M., Tomari, S., Kanemoto, K., Usui, J. and Lemley, K. V. (2003). Podocytes, parietal cells, and glomerular pathology: the role of cell cycle proteins. *Pediatr Nephrol* 18, 3-8.

Naicker, S., Fabian, J., Naidoo, S., Wadee, S., Paget, G. and Goetsch, S. (2007). Infection and glomerulonephritis. *Semin Immunopathol* 29, 397-414.

Naicker, S., Han, T. M. and Fabian, J. (2006). HIV/AIDS--dominant player in chronic kidney disease. *Ethn Dis* 16, S2-56-60.

Naicker, T., Randeree, I. G., Moodley, J., Khedun, S. M., Ramsaroop, R. and Seedat, Y. K. (1997). Correlation between histological changes and loss of anionic charge of the glomerular basement membrane in early-onset pre-eclampsia. *Nephron* 75, 201-7.

Nazli, A., Chan, O., Dobson-Belaire, W. N., Ouellet, M., Tremblay, M. J., Gray-Owen, S. D., Arsenault, A. L. and Kaushic, C. (2010). Exposure to HIV-1 directly impairs mucosal epithelial barrier integrity allowing microbial translocation. *PLoS Pathog* 6, e1000852.

Nelson, P. W., Mittler, J. E. and Perelson, A. S. (2001). Effect of drug efficacy and the eclipse phase of the viral life cycle on estimates of HIV viral dynamic parameters. *J Acquir Immune Defic Syndr* 26, 405-12.

Ng, Y. Y., Huang, T. P., Yang, W. C., Chen, Z. P., Yang, A. H., Mu, W., Nikolic-Paterson, D. J., Atkins, R. C. and Lan, H. Y. (1998). Tubular epithelial-myofibroblast transdifferentiation in progressive tubulointerstitial fibrosis in 5/6 nephrectomized rats. *Kidney Int* 54, 864-76.

NIAID. (2010). National Institute of Allergy and Infectious Diseases. Avaiable in http://www.niaid.nih.gov/topics/HIVAIDS/Understanding/Biology/pages/hivreplicationcycle.aspx   Acessed [2 December 2011], vol. 2011 (ed.

Nochy, D., Glotz, D., Dosquet, P., Pruna, A., Guettier, C., Weiss, L., Hinglais, N., Idatte, J. M., Mery, J. P., Kazatchkine, M. et al. (1993a). Renal disease associated with HIV infection: a multicentric study of 60 patients from Paris hospitals. *Nephrol Dial Transplant* 8, 11-9.

Nochy, D., Glotz, D., Dosquet, P., Pruna, A., Lemoine, R., Guettier, C., Weiss, L., Hinglais, N., Idatte, J. M., Mery, J. P. et al. (1993b). Renal lesions associated with human immunodeficiency virus infection: North American vs. European experience. *Adv Nephrol Necker Hosp* 22, 269-86.

Noel, J. C., Fayt, I., Fernandez-Aguilar, S., Buxant, F. and Boutemy, R. (2006). Proliferating activity in columnar cell lesions of the breast. *Virchows Arch* 449, 617-21.

Nora, T., Bouchonnet, F., Labrosse, B., Charpentier, C., Mammano, F., Clavel, F. and Hance, A. J. (2008). Functional diversity of HIV-1 envelope proteins expressed by contemporaneous plasma viruses. *Retrovirology* 5, 23.

Novitsky, V., Rybak, N., McLane, M. F., Gilbert, P., Chigwedere, P., Klein, I., Gaolekwe, S., Chang, S. Y., Peter, T., Thior, I. et al. (2001). Identification of human immunodeficiency virus type 1 subtype C Gag-, Tat-, Rev-, and Nef-specific elispot-based cytotoxic T-lymphocyte responses for AIDS vaccine design. *J Virol* 75, 9210-28.

Nurse, P. (1991). Cell cycle. Checkpoints and spindles. *Nature* 354, 356-8.

O'Regan, S. (1979). Glomerular localization of preformed immune complexes in nephrotoxic serum nephritis. *Virchows Arch A Pathol Anat Histol* 384, 103-7.

Oh, J., Reiser, J. and Mundel, P. (2004). Dynamic (re)organization of the podocyte actin cytoskeleton in the nephrotic syndrome. *Pediatr Nephrol* 19, 130-7.

Ojeda, J. L., Icardo, J. M. and Domezain, A. (2003). Renal corpuscle of the sturgeon kidney: an ultrastructural, chemical dissection, and lectin-binding study. *Anat Rec A Discov Mol Cell Evol Biol* 272, 563-73.

Okera, A., Serutoke, J., Madraa, E. and Namagala, E. (2003). Scaling up antiretroviral therapy Ugandan experience. 1-11.

Osho, A. and Olayinka, B. A. (1999). Sexual practices conducive to HIV transmission in Southwest Nigeria. *The Continuing African HIV/AIDS Epidemic*, 85-91.

Pakasa, N. M. and Binda, P. M. (2011). HIV-associated immune complex glomerulonephritis with "lupus-like" features. *Saudi J Kidney Dis Transpl* 22, 769-73.

Pandit, S. D. and Li, K. C. (2004). A primer on molecular biology for imagers: IV. concepts and basic methods in molecular biology. *Acad Radiol* 11, 686-97.

Papeta, N., Chan, K. T., Prakash, S., Martino, J., Kiryluk, K., Ballard, D., Bruggeman, L. A., Frankel, R., Zheng, Z., Klotman, P. E. et al. (2009). Susceptibility loci for murine HIV-associated nephropathy encode trans-regulators of podocyte gene expression. *J Clin Invest* 119, 1178-88.

Paranjape, R. S. (2005). Immunopathogenesis of HIV infection. *Indian J Med Res* 121, 240-55.

Pardo, V., Aldana, M., Colton, R. M., Fischl, M. A., Jaffe, D., Moskowitz, L., Hensley, G. T. and Bourgoignie, J. J. (1984). Glomerular lesions in the acquired immunodeficiency syndrome. *Ann Intern Med* 101, 429-34.

Pardo, V., Meneses, R., Ossa, L., Jaffe, D. J., Strauss, J., Roth, D. and Bourgoignie, J. J. (1987). AIDS-related glomerulopathy: occurrence in specific risk groups. *Kidney Int* 31, 1167-73.

Patrakka, J., Lahdenkari, A. T., Koskimies, O., Holmberg, C., Wartiovaara, J. and Jalanko, H. (2002). The number of podocyte slit diaphragms is decreased in minimal change nephrotic syndrome. *Pediatr Res* 52, 349-55.

Peraldi, M. N., Maslo, C., Akposso, K., Mougenot, B., Rondeau, E. and Sraer, J. D. (1999). Acute renal failure in the course of HIV infection: a single-institution retrospective study of ninety-two patients anad sixty renal biopsies. *Nephrol Dial Transplant* 14, 1578-85.

Peters, P. J., Moore, D. M., Mermin, J., Brooks, J. T., Downing, R., Were, W., Kigozi, A., Buchacz, K. and Weidle, P. J. (2008). Antiretroviral therapy improves renal function among HIV-infected Ugandans. *Kidney Int* 74, 925-929.

Pines, J. (1997). Cyclin-dependent kinase inhibitors: the age of crystals. *Biochim Biophys Acta* 1332, M39-42.

Pitts, T. O. and Van Thiel, D. H. (1986). Disorders of the serum electrolytes, acid-base balance, and renal function in alcoholism. *Recent Dev Alcohol* 4, 311-39.

Popper, S. J., Sarr, A. D., Gueye-Ndiaye, A., Mboup, S., Essex, M. E. and Kanki, P. J. (2000). Low plasma human immunodeficiency virus type 2 viral load is independent of proviral load: low virus production in vivo. *J Virol* 74, 1554-7.

Prins, M., Meyer, L. and Hessol, N. A. (2005). Sex and the course of HIV infection in the pre- and highly active antiretroviral therapy eras. *AIDS* 19, 357-70.

Rajpoot, D., Kaupke, C. J., Vaziri, N. D., Rao, T. K., Pomrantz, A. and Fikrig, S. (1996). Childhood AIDS nephropathy: a 10-year experience. *J Natl Med Assoc* 88, 493-8.

Ramsuran, D., Bhimma, R., Ramdial, P. K., Naicker, E., Adhikari, M., Deonarain, J., Sing, Y. and Naicker, T. (2011a). The spectrum of HIV-related nephropathy in children. *Pediatr Nephrol*.

Ramsuran, D., Moodley, J., Dauth, T. and Naicker, T. (2011b). The role of podocytes in the early detection of pre-eclampsia. *Pregnancy Hypertension: An International Journal of Women's Cardiovascular Health* 2, 43–47.

Rao, T. K., Filippone, E. J., Nicastri, A. D., Landesman, S. H., Frank, E., Chen, C. K. and Friedman, E. A. (1984). Associated focal and segmental glomerulosclerosis in the acquired immunodeficiency syndrome. *N Engl J Med* 310, 669-73.

Rao, T. K., Friedman, E. A. and Nicastri, A. D. (1987). The types of renal disease in the acquired immunodeficiency syndrome. *N Engl J Med* 316, 1062-8.

Raulin, J. (2002). Human immunodeficiency virus and host cell lipids. Interesting pathways in research for a new HIV therapy. *Prog Lipid Res* 41, 27-65.

Ray, P. E. (2009). Taking a hard look at the pathogenesis of childhood HIV-associated nephropathy. *Pediatr Nephrol* 24, 2109-19.

Ray, P. E., Rakusan, T., Loechelt, B. J., Selby, D. M., Liu, X. H. and Chandra, R. S. (1998). Human immunodeficiency virus (HIV)-associated nephropathy in children from the Washington, D.C. area: 12 years' experience. *Semin Nephrol* 18, 396-405.

Ray, P. E., Xu, L., Rakusan, T. and Liu, X. H. (2004). A 20-year history of childhood HIV-associated nephropathy. *Pediatr Nephrol* 19, 1075-92.

Rebouche, C. J. (2004). Kinetics, pharmacokinetics, and regulation of L-carnitine and acetyl-L-carnitine metabolism. *Ann N Y Acad Sci* 1033, 30-41.

Reeves, J. D., Gallo, S. A., Ahmad, N., Miamidian, J. L., Harvey, P. E., Sharron, M., Pohlmann, S., Sfakianos, J. N., Derdeyn, C. A., Blumenthal, R. et al. (2002). Sensitivity of HIV-1 to entry inhibitors correlates with envelope/coreceptor affinity, receptor density, and fusion kinetics. *Proc Natl Acad Sci USA* 99, 16249-16254.

Remuzzi, G., Ruggenenti, P. and Benigni, A. (1997). Understanding the nature of renal disease progression. *Kidney Int* 51, 2-15.

Reynolds, E. S. (1963). The use of lead citrate at high pH as an electron-opaque stain in electron microscopy. *J Cell Biol* 17, 208-12.

Rietveld, A. and Simons, K. (1998). The differential miscibility of lipids as the basis for the formation of functional membrane rafts. *Biochim Biophys Acta* 1376, 467-79.

Ross, M. J. and Klotman, P. E. (2002). Recent Progress in HIV-Associated Nephropathy. *Journal of the American Society of Nephrology* 13, 2997-3004.

Ross, M. J., Klotman, P. E. and Winston, J. A. (2000). HIV-associated nephropathy: case study and review of the literature. *AIDS Patient Care STDS* 14, 637-45.

Sagar, M., Kirkegaard, E., Long, E. M., Celum, C., Buchbinder, S., Daar, E. S. and Overbaugh, J. (2004). Human immunodeficiency virus type 1 (HIV-1) diversity at time of infection is not restricted to certain risk groups or specific HIV-1 subtypes. *J Virol* 78, 7279-83.

Saleem, M. A., O'Hare, M. J., Reiser, J., Coward, R. J., Inward, C. D., Farren, T., Xing, C. Y., Ni, L., Mathieson, P. W. and Mundel, P. (2002). A conditionally immortalized human podocyte cell line demonstrating nephrin and podocin expression. *J Am Soc Nephrol* 13, 630-8.

Salifu. M, O. (2010). HIV-Associated Nephropathy. Available in http://emedicine.medscape.com/article/246031-overview#showall [accessed 14 november 2011], vol. 2011 (ed.

Sands, J. M. (2003). Urine-concentrating ability in the aging kidney. *Sci Aging Knowledge Environ* 2003, PE15.

Schnabel, E., Anderson, J. M. and Farquhar, M. G. (1990). The tight junction protein ZO-1 is concentrated along slit diaphragms of the glomerular epithelium. *J Cell Biol* 111, 1255-63.

Schrier, R. W., Gardenswartz, M. H. and Burke, T. J. (1981). Acute renal failure: pathogenesis, diagnosis and treatment. *Adv Nephrol Necker Hosp* 10, 213-40.

Segerer, S., Mac, K. M., Regele, H., Kerjaschki, D. and Schlondorff, D. (1999). Expression of the C-C chemokine receptor 5 in human kidney diseases. *Kidney Int* 56, 52-64.

Seney, F. D., Burns, D. K., Silva, F. G. and Baker, B. (1989). Renal and electrolyte disorders in 50 patients with AIDS in Dallas (abstract). *Kidney Int* 35, 212.

Shankland, S. J. (1999). Cell cycle regulatory proteins in glomerular disease. *Kidney Int* 56, 1208-15.

Sheerin, N. S., Abe, K., Risley, P. and Sacks, S. H. (2006). Accumulation of immune complexes in glomerular disease is independent of locally synthesized c3. *J Am Soc Nephrol* 17, 686-96.

Sigve. (2008). HIV. Avaiable in http://en.wikipedia.org/wiki/HIV Acccessed [12 November 2011], vol. 2011 (ed.

Simm, M., Pekarskaya, O. and Volsky, D. J. (1996). Synthesis of full-length viral DNA in CD4-positive membrane vesicles exposed to HIV-1. A model for studies of early stages of the hiv-1 life cycle. *J Biol Chem* 271, 28266-70.

Simmonds, P., Balfe, P., Ludlam, C. A., Bishop, J. O. and Brown, A. J. (1990). Analysis of sequence diversity in hypervariable regions of the external glycoprotein of human immunodeficiency virus type 1. *J Virol* 64, 5840-50.

Simons, K. and van Meer, G. (1988). Lipid sorting in epithelial cells. *Biochemistry* 27, 6197-202.

Singh, H. K., Baldree, L. A., McKenney, D. W., Hogan, S. L. and Jennette, J. C. (2000). Idiopathic collapsing glomerulopathy in children. *Pediatr Nephrol* 14, 132-7.

Skalka, A. M. (1999). Advances in virus research. Seminars in virology: retroviral DNA intergration. 52, Academic Press.

Sladen, R. N. and Landry, D. (2000). Renal blood flow regulation, autoregulation, and vasomotor nephropathy. *Anesthesiol Clin North America* 18, 791-807, ix.

Smeets, B., Dijkman, H. B., Wetzels, J. F. and Steenbergen, E. J. (2006). Lessons from studies on focal segmental glomerulosclerosis: an important role for parietal epithelial cells? *J Pathol* 210, 263-72.

Smoyer, W. E., Mundel, P., Gupta, A. and Welsh, M. J. (1997). Podocyte alpha-actinin induction precedes foot process effacement in experimental nephrotic syndrome. *Am J Physiol* 273, F150-7.

Somlo, S. and Mundel, P. (2000). Getting a foothold in nephrotic syndrome. *Nat Genet* 24, 333-5.

Starcich, B. R., Hahn, B. H., Shaw, G. M., McNeely, P. D., Modrow, S., Wolf, H., Parks, E. S., Parks, W. P., Josephs, S. F., Gallo, R. C. et al. (1986). Identification and characterization of conserved and variable regions in the envelope gene of HTLV-III/LAV, the retrovirus of AIDS. *Cell* 45, 637-48.

Stebbing, J., Gazzard, B. and Douek, D. C. (2004). Where does HIV live? *N Engl J Med* 350, 1872-80.

Steffens, C. M. and Hope, T. J. (2004). Mobility of the human immunodeficiency virus (HIV) receptor CD4 and coreceptor CCR5 in living cells: implications for HIV fusion and entry events. *J Virol* 78, 9573-8.

Strauss, J., Abitbol, C., Zilleruelo, G., Scott, G., Paredes, A., Malaga, S., Montané, B., Mitchell, C., Parks, W. and Pardo, V. (1989). Renal Disease in Children with the Acquired Immunodeficiency Syndrome. *New England Journal of Medicine* 321, 625-630.

Strauss, J., Zilleruelo, G., Abitbol, C., Montane, B. and Pardo, V. (1993). Human immunodeficiency virus nephropathy. *Pediatr Nephrol* 7, 220-5.

Sun, S. X. and Wirtz, D. (2006). Mechanics of enveloped virus entry into host cells. *Biophys J* 90, L10-2.

Sunamoto, M., Husain, M., He, J. C., Schwartz, E. J. and Klotman, P. E. (2003). Critical role for Nef in HIV-1-induced podocyte dedifferentiation. *Kidney Int* 64, 1695-701.

Suzuki, K., Honda, K., Tanabe, K., Toma, H., Nihei, H. and Yamaguchi, Y. (2003). Incidence of latent mesangial IgA deposition in renal allograft donors in Japan. *Kidney Int* 63, 2286-94.

Symeonidou, C., Standish, R., Sahdev, A., Katz, R. D., Morlese, J. and Malhotra, A. (2008). Imaging and histopathologic features of HIV-related renal disease. *Radiographics* 28, 1339-54.

Szczech, L. A. (2001). Renal diseases associated with human immunodeficiency virus infection: epidemiology, clinical course, and management. *Clin Infect Dis* 33, 115-9.

Takata, A., Kikuchi, H., Fukuzawa, R., Ito, S., Honda, M. and Hata, J. (2000). Constitutional WT1 correlate with clinical features in children with progressive nephropathy. *J Med Genet* 37, 698-701.

Tang, W. W., Feinstein, E. l. and Massey, S. G. (1988). Hyponatremia in patients with acquired immune deficiency syndrome and the AIDS related complex (abstract). *Kidney Int* 3, 211.

Tapia, R., Guan, F., Gershin, I., Teichman, J., Villegas, G. and Tufro, A. (2008). Semaphorin3a disrupts podocyte foot processes causing acute proteinuria. *Kidney Int* 73, 733-40.

Tenstad, O., Heyeraas, K. J., Wiig, H. and Aukland, K. (2001). Drainage of plasma proteins from the renal medullary interstitium in rats. *J Physiol* 536, 533-9.

Thomas, L. and Huber, A. R. (2006). Renal function--estimation of glomerular filtration rate. *Clin Chem Lab Med* 44, 1295-302.

Thomson, N. M., Simpson, I. J. and Peters, D. K. (1975). A quantitative evaluation of anticoagulants in experimental nephrotoxic nephritis. *Clin Exp Immunol.* 19, 301-308.

Thorner, P. S., Ho, M., Eremina, V., Sado, Y. and Quaggin, S. (2008). Podocytes contribute to the formation of glomerular crescents. *J Am Soc Nephrol* 19, 495-502.

Tipping, P. G. and Holdsworth, S. R. (1986). The participation of macrophages, glomerular procoagulant activity, and factor VIII in glomerular fibrin deposition. Studies on anti-GBM antibody-induced glomerulonephritis in rabbits. *Am J Pathol* 124, 10-7.

Trkola, A., Dragic, T., Arthos, J., Binley, J. M., Olson, W. C., Allaway, G. P., Cheng-Mayer, C., Robinson, J., Maddon, P. J. and Moore, J. P. (1996). CD4-dependent, antibody-sensitive interactions between HIV-1 and its co-receptor CCR-5. . *Nature* 384, 184-187.

Trump, B. F. (1970). Kidney structure and function. *Birth Defects Orig Artic Ser* 6, 8-9.

Truong, L. D., Petrusevska, G., Yang, G., Gurpinar, T., Shappell, S., Lechago, J., Rouse, D. and Suki, W. N. (1996). Cell apoptosis and proliferation in experimental chronic obstructive uropathy. *Kidney Int* 50, 200-7.

Tryggvason, K., Patrakka, J. and Wartiovaara, J. (2006). Hereditary proteinuria syndromes and mechanisms of proteinuria. *N Engl J Med* 354, 1387-401.

Tryggvason, K., Reiser, J. and Mundel, P. (2004). Dynamic (re)organization of the podocyte actin cytoskeleton in the nephrotic syndrome. *Pediatr Nephrol* 19, 130-137.

Tucker, J. K. (2002). Focal segmental glomerulosclerosis in African Americans. *Am J Med Sci* 323, 90-3.

Turner, M. E., Kher, K., Rakusan, T., D'Angelo, L., Kapur, S., Selby, D. and Ray, P. E. (1997). A typical hemolytic uremic syndrome in human immunodeficiency virus-1-infected children. *Pediatr Nephrol* 11, 161-3.

Umareddy, I., Pluquet, O., Wang, Q. Y., Vasudevan, S. G., Chevet, E. and Gu, F. (2007). Dengue virus serotype infection specifies the activation of the unfolded protein response. *Virol J* 4, 91.

UNAIDS. (2010). Global report: UNAIDS report on the global AIDS epidemic 2010. Avaiable in http://www.unaids.org/globalreport/Global_report.htm. Accessed [8 December 2011], vol. 2011 (ed.

UNAIDS. (2011). Global HIV/AIDS response - Epidemic update and health sector progress towards Universal Access 2011. Avaiable in http://www.unaids.org/en/resources/unaidspublications/2011/ Accessed [8 December 2011], vol. 2011 (ed.

Urreizti, R., Asteggiano, C., Vilaseca, M. A., Corbella, E., Pinto, X., Grinberg, D. and Balcells, S. (2007). A CBS haplotype and a polymorphism at the MSR gene are associated with cardiovascular disease in a Spanish case-control study. *Clin Biochem* 40, 864-8.

Valeri, A. and Neusy, A. J. (1991). Acute and chronic renal disease in hospitalized AIDS patients. *Clin Nephrol* 35, 110-8.

Varbanov, M., Espert, L. and Biard-Piechaczyk, M. (2006). Mechanisms of CD4 T-cell depletion triggered by HIV-1 viral proteins. *AIDS Rev* 8, 221-36.

Vaughn-Jones, S. A., Palmer, I., Bhogal, B. S., Eady, R. A. and Black, M. M. (1995). The use of Michel's transport medium for immunofluorescence and immunoelectron microscopy in autoimmune bullous diseases. *J Cutan Pathol.* 22, 365-70.

Vaziri, N. D., Barbari, A., Licorish, K., Cesario, T. and Gupta, S. (1985). Spectrum of renal abnormalities in acquired immune-deficiency syndrome. *J Natl Med Assoc* 77, 369-75.

Verkade, P., Harder, T., Lafont, F. and Simons, K. (2000). Induction of caveolae in the apical plasma membrane of Madin-Darby canine kidney cells. *J Cell Biol* 148, 727-39.

Verkman, A. S., Shi, L. B., Frigeri, A., Hasegawa, H., Farinas, J., Mitra, A., Skach, W., Brown, D., Van Hoek, A. N. and Ma, T. (1995). Structure and function of kidney water channels. *Kidney Int* 48, 1069-81.

Vitone, F., Gibellini, D., Schiavone, P. and Re, M. C. (2005). Quantitative DNA proviral detection in HIV-1 patients treated with antiretroviral therapy. *J Clin Virol* 33, 194-200.

Vivette, D. A. (2003). Pathologic classification of focal segmental glomerulosclerosis. *Seminars in Nephrology* 23, 117-134.

Vogler, C., Eliason, S. C. and Wood, E. G. (1999). Glomerular membranopathy in children with IgA nephropathy and Henoch Schonlein purpura. *Pediatr Dev Pathol* 2, 227-35.

Wang, C., Hou, X., Mohapatra, S., Ma, Y., Cress, W. D., Pledger, W. J. and Chen, J. (2005). Activation of p27Kip1 Expression by E2F1. A negative feedback mechanism. *J Biol Chem* 280, 12339-43.

Wareing, M. and Green, R. (1994). Effect of formate and oxalate on fluid reabsorption from the proximal convoluted tubule of the anaesthetized rat. *J Physiol* 477 (Pt 2), 347-54.

Wharram, B. L., Goyal, M., Wiggins, J. E., Sanden, S. K., Hussain, S., Filipiak, W. E., Saunders, T. L., Dysko, R. C., Kohno, K., Holzman, L. B. et al. (2005). Podocyte depletion causes glomerulosclerosis: diphtheria toxin-induced podocyte depletion in rats expressing human diphtheria toxin receptor transgene. *J Am Soc Nephrol* 16, 2941-52.

Winking, H., Gerdes, J. and Traut, W. (2004). Expression of the proliferation marker Ki-67 during early mouse development. *Cytogenet Genome Res* 105, 251-6.

Winston, J. A., Bruggeman, L. A., Ross, M. D., Jacobson, J., Ross, L., D'Agati, V. D., Klotman, P. E. and Klotman, M. E. (2001). Nephropathy and establishment of a renal reservoir of HIV type 1 during primary infection. *N Engl J Med* 344, 1979-84.

Winston, J. A., Klotman, M. E. and Klotman, P. E. (1999). HIV-associated nephropathy is a late, not early, manifestation of HIV-1 infection. *Kidney Int* 55, 1036-40.

Wu, L. and Kewalramani, V. N. (2006). Dendritic-cell interactions with HIV: infection and viral dissemination. *Nat Rev Immunol* 6, 859-68.

Wyatt, C. M. and Klotman, P. E. (2007). HIV-1 and HIV-Associated Nephropathy 25 Years Later. *Clin J Am Soc Nephrol* 2 Suppl 1, S20-4.

Wyatt, C. M., Klotman, P. E. and D'Agati, V. D. (2008). HIV-associated nephropathy: clinical presentation, pathology, and epidemiology in the era of antiretroviral therapy. *Semin Nephrol* 28, 513-22.

Yahi, N., Baghdiguian, S., Moreau, H. and Fantini, J. (1992). Galactosyl ceramide (or a closely related molecule) is the receptor for human immunodeficiency virus type 1 on human colon epithelial HT29 cells. *J Virol* 66, 4848-54.

Yanagida-Asanuma, E., Asanuma, K., Kim, K., Donnelly, M., Young Choi, H., Hyung Chang, J., Suetsugu, S., Tomino, Y., Takenawa, T., Faul, C. et al. (2007). Synaptopodin protects against proteinuria by disrupting Cdc42:IRSp53:Mena signaling complexes in kidney podocytes. *Am J Pathol* 171, 415-27.

Yilmaz, G. (2001). Diagnosis of HIV infection and laboratory monitoring of its therapy. *J Clin Virol* 21, 187-96.

Yoshikawa, N., Nakamura, H. and Ito, H. (1994). IgA nephropathy in children and adults. *Springer Semin Immunopathol* 16, 105-20.

Yuan, H., Takeuchi, E. and Salant, D. J. (2002). Podocyte slit-diaphragm protein nephrin is linked to the actin cytoskeleton. *Am J Physiol Renal Physiol* 282, F585-91.

Zhang, L., Chung, C., Hu, B. S., He, T., Guo, Y., Kim, A. J., Skulsky, E., Jin, X., Hurley, A., Ramratnam, B. et al. (2000). Genetic characterization of rebounding HIV-1 after cessation of highly active antiretroviral therapy. *J Clin Invest* 106, 839-45.

Zhang, L. Q., MacKenzie, P., Cleland, A., Holmes, E. C., Brown, A. J. and Simmonds, P. (1993). Selection for specific sequences in the external envelope protein of human immunodeficiency virus type 1 upon primary infection. *J Virol* 67, 3345-56.

Zuo, Y., Matsusaka, T., Zhong, J., Ma, J., Ma, L. J., Hanna, Z., Jolicoeur, P., Fogo, A. B. and Ichikawa, I. (2006). HIV-1 genes vpr and nef synergistically damage podocytes, leading to glomerulosclerosis. *J Am Soc Nephrol* 17, 2832-43.

ADDENDUM I

THE SPECTRUM OF HIV-RELATED NEPHROPATHY IN CHILDREN

ADDENDUM II

THE ROLE OF PODOCYTES IN THE EARLY DETECTION OF PRE-ECLAMPSIA

ADDENDUM III

PODOCYTURIA IN THE EARLY DECTION OF PRE-ECLAMPSIA-A PILOT STUDY

ADDENDUM IV

STAGING OF HIV RELATED NEPHROPATHY PATIENTS

STAGING OF HIV RELATED NEPHROPATHY PATIENTS

Stage I	Lymphadenopaty
	Asymptomatic
Stage II	Hepatosplenomegaly
	Papular Pruritic eruptions
	Seborrhoeic dermatitis
	Extensive human papilloma virus infection
	Extensive molluscum contagiosum
	Fungal nail infections
	Recurrent oral ulceration
	Linear gingival erythema
	Angular Chellitis
	Parotid enlargement
	Herpes zoster
	Recurrents or chronic RTIs (otitis media, otorrhoea, sinusitis)
Stage III	Moderate unexplained malnutrition
	Unexplained persistent diarrhea
	Unexplained persistent fever
	Oral Candidiasis
	Oral hairy leukoplakia
	Acute necrotizing ulcerative gingivitis / periodontitis
	Pulmonary TB
	Tuberculous lymphadenopathy(axillary, cervical or inguinal)
	Severe recurrent presumed bacterial pneumonia
	Unexplained anaemia (<8gm/dl), and/or thrombocytopenia (<50 000/mm^3) for more than one month
	Chronic HIV-associated lung disease including bronchiectasis
	Symptomatic Lymphoid interstitial pneumonitis (LIP)
Stage IV	Unexplained sever wasting or sever malnutrition not adequately
	Pneumocystis Pneumonia
	Recurrent sever presumed bacterial infection

Chronic herpes simplex infection (orolabial or cutaneous of more then one months duration)

Extrapulmonary TB

Kaposi's sarcoma

Oesophageal candidiasis

CNS toxoplasmosis (out side the neonatal period)

HIV encephalopathy

CMV infection

Extrapulmonary cryptococcosis including meningitis

Any disseminated endemic mycosis (e.g. Extrapulmonary histoplasmosis, coccidiomycosis, penicilliosis)

Cryptosporidiosis

Isosporiasis

Disseminated non-tuberculous mycobacterial infection

Candida of trachea, bronchi or lungs

Visceral herpes simplex infection

Cerebral or B cell non-Hodgkin's lymphoma

Progressive multifocal leukoencephalopathy

HIV-associated cardiomyopathy or HIV-associated nephropathy

ADDENDUM V

POST-GRADUATE APPROVAL

ADDENDUM VI

ETHICS APPROVAL

Research Office
BIOMEDICAL RESEARCH ETHICS ADMINISTRATION
Research Office
Room N40 - Govan Mbeki Building
University Road, WESTVILLE CAMPUS
KwaZulu-Natal, SOUTH AFRICA
Tel: 27 31 2604769 - Fax: 27 31 2604609
Email: - Website:

19 March 2008

Mr D Ramsuran
Optics & Imaging Centre
DDMRI
Nelson R Mandela School of Medicine
University of KwaZulu-Natal

Dear Mr Ramsuran

PROTOCOL: The Spectrum of HIV related nephropathy in Kwazulu-Natal: A pathogenetic appraisal and impact of HAART. Optics & Imaging Centre. Mr. Duram Ramsuram. RE:BF149/07

The Biomedical Research Ethics Committee considered the abovementioned application and the protocol was approved by a **full sitting of the committee** at a meeting held on **11 December 2007** pending appropriate responses to queries raised. Your responses received on 12 March 2008 to queries raised on 07 February 2008 have been noted by a sub-committee of the Biomedical Research Ethics Committee. The conditions have now been met and the study is given full ethics approval and may begin as at **19 March 2008.**

This approval is valid for one year from **19 March 2008.** To ensure continuous approval, an application for recertification should be submitted a couple of months before the expiry date. In addition, when consent is a requirement, the consent process will need to be repeated annually.

I take this opportunity to wish you everything of the best with your study. Please send the Biomedical Research Ethics Committee a copy of your report once completed.

Yours sincerely

PROFESSOR D WASSENAAR
Chair: Biomedical Research Ethics Committee

215

ADDENDUM VII

IALCH MANAGERS APPROVAL

PERMISSION TO CONDUCT A RESEARCH STUDY/TRIAL

This must be completed and submitted to the Medical Superintendent/s / Hospital Manager/s for signature.

For King Edward VIII Hospital (KEH) and Inkosi Albert Luthuli Central Hospital (IALCH) studies please submit the document together with the following:

1. Research proposal and protocol.
2. Letter giving provisional ethical approval.
3. Details of other research presently being performed by yourself if in the employ of KEH (individually or as a collaborator).
4. Details of any financial or human resource implications to KEH, including all laboratory test EEGs, X-rays, use of nurses, etc. (See Addendum 1)
5. Declaration of all funding applications / grants, please supply substantiating documentation.
6. Complete the attached KEH Form - "Research Details"

Once the document has been signed it should be returned to Mrs S Buccas: Biomedical Research Ethics Administrator, Room 840, Gavin Wheel Building, Westville Campus, University of KwaZulu-Natal.

To: Chief Medical Superintendent / Hospital Manager

Permission is requested to conduct the above research study on the hospital's indicated below.

Site 1 address:

I.A.L.C.H.

Investigator/s:

Principal: __BANSURAN__

Co-investigator: _____

Co-investigator: _____

Signature of Chief Medical Superintendent/Hospital Manager

Date: __07/03/08__

Site 2 address:

Investigator/s

Principal: _____

Co-investigator: _____

Co-investigator: _____

Signature of Chief Medical Superintendent / Hospital Manager

Date: _____

NB: Medical Superintendent/s / Hospital Manager/s to send a copy of this document to Natalia

ADDENDUM VIII

KEH VIII MANAGERS APPROVAL

PERMISSION TO CONDUCT A RESEARCH STUDY/TRIAL

This must be completed and submitted to the Medical Superintendent/s / Hospital Manager/s for signature.

For King Edward VIII Hospital (KEH) and Inkosi Albert Luthuli Central Hospital (IALCH) studies please submit the document together with the following:

1. Research proposal and protocol.
2. Letter giving provisional ethical approval.
3. Details of other research presently being performed by yourself if in the employ of KEH, (individually or as a collaborator).
4. Details of any financial or human resource implications to KEH, including all laboratory tests, EEGs, X-rays, use of nurses, etc. (See Addendum 1)
5. Declaration of all funding applications / grants, please supply substantiating documentation.
6. Complete the attached KEH Form - *"Research Details"*
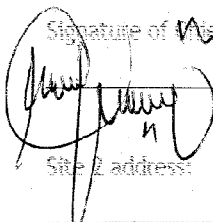
Once the document has been signed it should be returned to Mrs S Buccas: Biomedical Research Ethics Administrator, Room N40, Govan Mbeki Building, Westville Campus, University of KwaZulu-Natal.

To: Chief Medical Superintendent / Hospital Manager

Permission is requested to conduct the above research study at the hospitals indicated below:

Site 1 address: Investigator/s:

_____   Principal: _____

_____   Co-Investigator: _____

_____   Co-Investigator: _____

Signature of Chief Medical Superintendent /Hospital Manager:

Date: 18/02/08

Site 2 address: Investigator/s

_____   Principal: _____

_____   Co-Investigator: _____

_____   Co-Investigator: _____

Signature of Chief Medical Superintendent / Hospital Manager:

_____   Date: _____

NB: Medical Superintendent/s / Hospital Manager/s to send a copy of this document to Natalia

ADDENDUM IX

EXAMPLE OF INFORMED CONSENT

SECTION 4: INFORMATION GIVEN TO PARTICIPANTS (an example follows): INFORMATION DOCUMENT

Study title: The spectrum of HIV related nephropathy in KwaZulu-Natal: A pathogenetic appraisal and impact of HAART.

Good day Miss/ Mrs _____. My name is Duran Ramsuran. Thank you for giving me the time to speak to you.

We, R Bhimma, T Naicker, and D Ramsuran from the Department of Paediatrics and Child Health, University of KwaZulu-Natal., are carrying out research on kidney diseases in children, from which one of the investigators will obtain an academic degree. As you know HIV may affect the kidney, if we can pick up kidney involvement early and treat, the child may do much better. Kidney biopsies are standard of care in patients presenting with persistent proteinuria. This study will determine the effect of highly active anti-retroviral therapy. It will also help us to study the mechanism of injury by the HIV virus on the kidney and the way this is altered by treatment.

We are asking for your permission to include you or your child in our research study. We require your permission to take a sample of blood, urine and a kidney biopsy so that we may study it. There will be a repeat biopsy after a year to assess the how good the treatment was.

The general purpose of the study is to learn more about how genes influence kidney disease, particularly nephrotic syndrome. Genes are the parts of the body's cells that carry the coded information (DNA) that determine how all the body parts function. To date there have been few studies have been carried out in Africa which address how genes influence kidney disease. The specific purpose of the study is to determine how genes influence kidney disease

When your child undergoes the kidney biopsy mentioned above, we request your permission to take a small portion of the kidney biopsy sample for research studies. We will study which genes are expressed (active) in the kidney. In patients who show persistent proteinuria and/or deterioration in renal function this second biopsy is clinically indicated to evaluate progression or regression of disease following HAART and ACEI therapy. As your child will undergo a kidney biopsy that is part of routine medical care, this study also requires a small sample for research purposes post highly active anti-retroviral therapy.

We plan to recruit 30 subjects to participate in the present study all of whom must be South African citizens. We will be collecting blood, urine and kidney biopsies from 30 patients who are HIV positive and have renal disease. You will be followed-up for life or until you are cured following diagnosis and appropriate treatment to assess kidney function. All these samples are being collected and will be studied at the Nelson Mandela Medical School. We treat the specimens chemically, and store them at the Medical School so we can analyse them over the next three years. We will require your permission prior to specimen collection to do this.

Blood letting may result in mild pain and discomfort. A single tube of blood is required, for research studies to learn whether your child's genes are slightly different from those

individuals who do not have kidney disease. All preventions will be taken to ensure this will be done under sterile conditions to prevent infection. You will not have any immediate benefit from participating in this study. Participation in this study will not alter the management of your disease. However, if we show that the treatment works man children in the future will benefit.

You will be given pertinent information on the study while involved in the project and after the results are available.

Alternatives: Your participation is voluntary/optional. Refusal to participate will involve no penalty or loss of benefits to you. You may discontinue participation at any time without penalty/loss of benefits to which you are otherwise entitled. You will not be given any reimbursement for participating in the study.

Personal information will be kept confidential. Personal information may only be disclosed if required by law. Records of your child's information will not be added in, have your child's name recorded but only a number. Organizations that may inspect and/or copy your research records for quality assurance and data analysis include groups such as the Research Ethics Committee and the Medicines Control Council (where appropriate).

You may contact the researchers at any time. Their contact details are as follows:
Prof R Bhimma   -   Tel.:   031-2604351   or   031-2604345
Duran Ramsuran-   031-2604274   0735821636
Prof T Naicker-   031-2604435 or   031-2604746

Contact details of BREC Administrator – for reporting of complaints/ problems:
MRS S BUCCAS, Nelson R Mandela School of Medicine, Private Bag 7, Congella 4013
Telephone: +27 (0) 31 260 4769
Fax: +27 (0) 31 260 4609   email: buccas@ukzn.ac.za

ISAHLUKO 4: ULWAZI OLUNIKEZWA ABATHATHA INXEXHEBA

INCWADI YESAZISO

Isihloko socwaningo: Isandulela ngculazi esinobudlelwano nezifo zezinso kwisiFundazwe saKwaZulu-Natal; Ucwaningo nobungozi besifo iHAART.

Ukubingelela: Sawubona Nks./Nkz. …………………………………… Igama lami ngingu Duran Ramsuran. Ngiyabonga isikhathi ongiphe sona ukuba ngikhulume nawe.

Isandulelo: Into eyenza ngifise ukukhuluma nawe namhlanje yingoba mina nalabo esisebenza nabo o-R Bhimma, T Naicker kanye nami uD Ramsuran boMnyango wokunakekela impilo yezingane, ewuphiko lweNyuvesi yaKwaZulu-Natal senza ucwaningo ngezifo eziphathelene nezinso zezingane lapho omunye wabacwaningi ezothola iziqu eziphakeme ngalokhu. Ukutholakala nokwelashwa kwegciwane lengculazi elihambisana nezinso kuyisidingo ukuze kuvimbeleke kumbe kunqande ukubhebhetheka kwesifo sezinso. Lolucwaningo luzothola ukusebenza nokwelapha kwezivusi zamasosha i-anti-retroval.   Luzophinde lusisize ukuthi sifunde ngokuphazamiseka kwezinso ziphazanyiswa isifo sesandulela ngculazi.

Isicelo sokuzimbandakanya: Sicela imvume yakho yokuba wena noma ingane yakho nibe yingxenye yalolucwaningo oluzokwenziwa. Sicela imvume yakho ukuba sithathe igazi, umchamo kanye nokuhlolwa kwezinso ukuze sikwazi ukukucwaninga. Lolucwaningo luyophindwa esikhathini esingangonyaka ukuze kutholakale ukuthi ezokwelapha zibe nempumelelo kangakanani.

Inhloso yalesisifundo: Inhloso yalesisifundo ukufunda nokewazi kabanzi ukuthi ama Genes athintana kanjani nesifo sezinso, kahle kahle kwi Nephrotic Syndrome. Ama Genes ayenye yezicubu zomzimba esithola kuwona ulwazi oluphathelene nama DNA okuyiwona atshengisayo ukuthi zonke izicubu zomzimba zisebenza kahle na. Kuze kube inamhlanje kunezifundo eziyidlanzana ezilokhu zenziwa lapha e Africa ezichaza kahle ukuthi ama Genes athintana kanjani nesifo sezinso. Inhloso ukwazi kabanzi nokuningi ngokuthi ama Genes athintana kanjani nesifo sezinso.

Uma umntwana wakho eba ingxenye ekwenzeni I Biopsy njengoba kuchaziwe ngenhla, siyaye sicele imvume yakho njengomzali ukuba sithathe isicubu esincane nje esizoba isibonelo kulesisifundo. Siyobeke sesibheka ukuthi iyiphi I Genes esebenzisana kahle nenso yakhe. Umntwana wakho uma ethathe ingxenye kukhona nokunakekeleka okuthile akutholayo, abukho ubungozi noma ukungaphatheki kahle angase abe nacho ngokuthi kusetshenziswe isicubu sakhe.

Okuphathelene nocwaningo: Sizodingo abangamashumi ayisithupha abazoba yingxenye yalolucwaningo bonke okumele kube abalapha eMzansi Afrika.   Siyothatha igazi, umchamo kanye nokuhlolwa kwezinso kwiziguli ezingamashumi amathathu ezinesifo sezinso.   Uyobhekwa njalo impilo yakho yonke noma kuze kutholakale ukuthi sewelaphekile ukuthola ukuthi amakhambi owasebenzisayo ayasebenza yini ezinsweni zakho.   Konke okuyothathwa kuwe kuyocwaningwa esikhungweni sokufundela

ubudokotela esaziwa ngokuthi iNelson R Mandela School of Medicine. Konke okuyobe kuthathwe kuwe kuyolashwa ngamakhemikhali bese kugcinwa kuso lesisikhungo ukuze bakwazi ukukucubungula esikhathini esingangeminyaka emithathu esizayo. Siyodinga imvume yakho ngaphambi kokuba sithathe konke lokhu.

Ukuthathwa kwegazi kungaholela ebuhlungwini obuncane nje nokungakhululeki. Ibhodlela elincane nje legazi elidingekayo eliqondene nalesisifundo sezophenyo ukuze sazi ukuthi amaGenes omntwana wakho ahlukile yini nawalabo abangenayo inkinga yesifo yezinso.

Ingozi engabakhona: Ukuthathwa kwegazi kungaholela ezinhlungwini ezincane ngokunjalo nokungaphatheki kahle. Sidinga ishubhana elilodwa legazi. Konke lokhu kuyokwenziwa ngokuba kuqinisekiswe ukuthi akukho magciwane angenayo.

Ukuzimbandakanya akuphoqiwe: Sicela ukukwazisa ukuthi ukuzimbandakanya kululucwaningo akuphoqelekile neze, kanti futhi uma ukhetha ukunqaba, lokhu angeke kuthikameze impatho yakho esibhedlela. Uyokwaziswa ngocwaningo ngesikhathi useyingxenye yocwaningo nangesikhathi sekuphume imiphumela. Kuyilungelo lakho ukuba uyeke ukuba yingxenye yocwaningo noma ngasiphi isikhathi phakathi nocwaningo futhi akukho nhlawulo kumbe inzuzo eyokulahlekela ngalokho. Akukho nkokhelo eyonikezwa abayoba yingxenye yocwaningo. Izingane eziningi ziyozuza ngokuthola ukwelashwa kweqophelo elifanele.

Imfihlo: Imininingwane yakho izohlala iyimfihlo. Abantu abangafunyana lolulwazi yilabo abasemakomitini nezinyunyana zocwaningo.

Imibuzo: Kungabe unayo yini imibuzo?

Imininingwane yocwaningo: Uma udinga olunye ulwazi noma kukhona ongagculisekile ngakho, mayelana nocwaningo, ungaxhumana nalaba abalandelayo:

Prof R Bhimma	031-260 4351	noma	031-260 4345
Prof T Naicker	031-260 4435	noma	031-260 4746
Duran Ramsuran	031-260 4274	noma	031-260 4746

SECTION 5: INFORMED CONSENT (an example follows)

This document must be written in language understandable to the subject

CONSENT DOCUMENT

Study Title:

The spectrum of HIV related nephropathy in KwaZulu-Natal: A pathogenetic appraisal and impact of HAART.

Consent to Participate in Research

You have been asked to grant permission for your child/yourself
_____ to participate in a research study.

You have been informed about the study by _____

You may contact R Bhimma / D Ramsuran at 2604351/4274 (cell- 0735821636) any time if you have questions about the research or if you are injured as a result of the research.

You may contact the **Biomedical Research Office** at the Nelson R Mandela School of Medicine at **031-260 4769** if you have questions about your rights as a research subject.

Your participation in this research is voluntary, and you will not be penalized or lose benefits if you refuse to participate or decide to stop.

If you agree to participate, you will be given a signed copy of this document and the participant information sheet which is a written summary of the research.

The research study, including the above information, has been described to me orally. I understand what my involvement in the study means and I voluntarily agree to participate.

_____   _____
Signature of Participant   **Date**

_____   _____
Signature of Witness   **Date**
(Where applicable)

_____   _____
Signature of Translator   **Date**
(Where applicable)

ISAHLUKO 5: ULWAZI OLUNIKEZWA ABATHATHA INXEXHEBA
INCWADI YOLWAZI

Isihloko socwaningo:
Isandulela ngculazi esinobudlelwano nezifo zezinso kwisiFundazwe saKwaZulu-Natal; Ucwaningo lwesibalo nobungozi besifo iHAART

Imvume yokuzimbandakanya nocwaningo
Uyacelwa ukuba unikeze imvume yengane yakho noma wena uqobo _____ ukuba uzimbandakanye ocwaningweni olwenziwayo.

Ulwazi ngocwaningo uluthole ngo _____

Ungathintana no R Bhimma / D Ramsuran kwinombolo yocingo u031-260 4351/4274 (umakhalekhukhwini – 073 582 1636) ngazozonke izikhathi uma unemibuzo mayelana nocwaningo noma uthole ukulimala ngezizathu zoqhutshwa kocwaningo.

Ungathintana nehovisi le**Biomedical Research Office** esikoleni sokufundela ubudokotela iNelson R Mandela kulenombolo yocingo **031-260 4769** uma unemibuzo ngamalungela akho maqondana nocwaningo.

Uba yingxenye yocwaningo ngokusothandweni lakho futhi uma ungenaso isifiso sokuba yingxenye kumbe unesifiso sokuyeka phakathi nocwaningo akukho nhlawulo oyoyikhokha kumbe nzuzo eyokulahlekela.

Uma uvuma ukuba yingxenye yocwaningo, uyonikezwa ikhophi esayiniwe yalencwadi kanye nepheshana leminininingwane yozinikele okuyincwadi yocwaningo ebekwe ngamafuphi.

Ucwaningo kanye nolwazi olungenhla, luchaziwe kimina ngomlomo. Ngiyaqonda ukuthi ukuba yingxenye yaloolucwaningo kusho ukuthini futhi ngiyavuma ukuzinikela ukuthi ngibe yingxenye.

_____   _____
Isishicilelo Sozinikele   Usuku

_____   _____
Isishicilelo Sofakazi   Usuku
(Uma kunesidingo)

_____   _____
Isishicilelo Sikatolika   Usuku
(Uma kunesidingo)

ADDENDUM X

ETHICS APPROVAL FOR CONTROL SAMPLE

ADDENDUM XI

SOLUTION PREPARATION

SOLUTION PREPARATION

Mayer's Haematoxylin

- 4g Haematoxylin

- 4g Citric acid

- 1g Sodium Iodate

- 200g Chloral Hydate

- 200g Aluminium Ammonium Sulphate

- 4000ml distilled water

0.5% Alcoholic Eosin

- 20g Eosin

-4000ml Absolute Alcohol

- 20ml Acetic Acid

Weigert's Iron Haematoxylin

Working Solution: (1:1) Weigerts Solution A: Weigerts Solution B

Weigerts Solution A:

- 1g Haematoxylin

- 100ml 95% alcohol

Weigerts Solution B:

- 4ml 29% Ferric Chloride

- 100ml Distilled water

- 1ml concentrated hydrochloric Acid

Biebrich Scarlet-Acid Fuchsin Solution

- 90ml 1% Aqueous Biebrich Scarlet

- 10ml 1% Aqueous Acid Fuchsin

- 1ml Acetic Acid, glacial

0.5% Potassium Permanganate

- 10g Potassium Permanganate

- 2000ml distilled water

- 3m Sulphuric Acid

Elastic Stain

- 1g Victoria Blue 4R

- 1g Basic Fuchsin

- 1g Crystal Violet

- Dissolved in 200ml distilled water (warm)

- 4g Resorcin

- 1g Dextrin

- 50ml 30% Aqueous ferric Chloride

- Filter

- 200ml 95% Alcohol

- Filter

- Make up to 200ml with 95% Alcohol

- 2ml concentrated Hydrochloric Acid

Methenamine Silver Solution

- 50ml 3% Hexamine solution

- 2.5ml 5% Silver Nitrate solution

-Filter 40ml of solution

 -5ml 5% Borax

4% Glutaraldehyde

- 25ml 0.2M Cacodylate buffer

- 8ml 25% Glutaraldehyde

Cacodylate buffer (0.2M)

- 21.4g Sodium Cacodylate in 250ml distilled water

- 40ml 0.2M Hydrochloric Acid

- Make up to 500ml with distilled water

Palades Fixative (Osmium tetroxide)

- 2ml Osmium tetroxide

- 3ml Cacodylate buffer

- 2.8ml distilled water

Araldite

- 10g Epoxy resin

- 10g DDSA

- 1g Dibutylphthalate

- 0.5g DMP 30

1% Toluidine blue

- 1% Sodium Bicarbonate

- 1g Toluidine blue

- filter

- 40ml Glycerine to 60ml of above solution